

UNIVERSITÀ
DEGLI STUDI
DI PADOVA

Sede Amministrativa: Università degli Studi di Padova

Dipartimento di Ingegneria Civile, Edile ed Ambientale

SCUOLA DI DOTTORATO DI RICERCA IN SCIENZE DELL'INGEGNERIA CIVILE ED AMBIENTALE

CICLO XXVIII

INSIGHT INTO SEISMIC BEHAVIOUR OF TIMBER SHEAR-WALL SYSTEMS

Direttore della Scuola: Ch.mo Prof. **STEFANO LANZONI**

Supervisore: Ch.mo Prof. **ROBERTO SCOTTA**

Controrelatore: Ch.mo Prof. **MASSIMO FRAGIACOMO**

Dottorando: **DAVIDE TRUTALLI**

Gennaio 2016

Summary

This Ph.D. dissertation is the result of a three-year research activity focused on structural and seismic engineering applied to innovative timber constructive systems. The main purpose is to give a contribution to international scientific research and current design practice about the seismic behaviour of timber shear-wall systems, which still represent an innovation in the construction industry and are being developed due to their favourable characteristics.

An initial overview on the use of main timber structural systems in seismic-prone areas for low- and medium-rise buildings is provided, within the context of current European seismic code.

The theme of the seismic design of timber shear-wall systems is discussed in the first part, giving close attention to linear and non-linear modelling criteria: various strategies are proposed and main characteristics are highlighted. Basic definitions and concepts proper of the seismic analysis of timber structures are provided. A particular attention is paid to the definition and application of the capacity design approach and the close link with the concept of behaviour factor is emphasized. Finally, the definition of behaviour factor, as product between an “intrinsic” capacity of the structure and a design over-strength value is proposed. This definition allows to characterize the structural systems with their proper dissipative capacity and to evaluate separately the safety reserve introduced by design.

The second part analyses the structural behaviour of the cross-laminated timber (CLT) technology, which represents one of the most common timber structural systems. The concepts of ductility, dissipative capacity, regularity and irregularity applied to CLT system are provided. The seismic response and the dissipative capacity of this system are firstly evaluated via an experimentally based procedure. Then, the evaluation of its intrinsic dissipative capacity is determined via non-linear numerical modelling with the aim of studying the correlation with the construction variables. Results show that the construction design decisions affect the seismic response and dissipative capacity of buildings, as opposed to apply a single behaviour factor value to the whole CLT technology. A statistical analysis applied to numerical results allowed also to propose analytical formulations for the computation of the suitable behaviour factor value for regular buildings. Then, the same analyses carried out on in-elevation non-regular buildings returned a correction factor to account for the reduction in dissipative capacity due to irregularity.

The application of the CLT technology to realize high-rise buildings is presented in the third part, analysing the behaviour of slender buildings with seismic resisting core and perimeter shear walls. The major limitations and drawbacks in realizing these structures in areas characterized by high seismic intensity and their implication in the design are reported.

The final part presents three novel structural systems as alternative to more common technologies, as CLT or platform frame. These innovative systems are characterized mainly by a diffuse dissipative and deformation capacity when subjected to seismic loads, while in CLT system such capacity is concentrated in connection elements. This different response is studied via quasi-static tests and numerical simulations. In detail, two non-glued massive timber shear walls and a mixed steel-timber wall with an innovative bracing system are presented.

Keywords: *timber structures; structural engineering; seismic engineering; seismic design; timber constructive systems; timber shear-wall systems; massive timber shear walls; cross-laminated timber; CLT; X-Lam; light-frame system; platform-frame system; behaviour factor; q-factor; q_0 -factor; design over-strength; numerical modelling; FEM; experimental tests; innovative systems; novel systems; mixed systems; hybrid structures; connections; hysteresis behaviour; dissipative capacity; tall buildings; regularity.*

Sommario

Questa tesi di dottorato è il risultato di tre anni di attività di ricerca in ambito ingegneristico strutturale applicato allo studio di sistemi costruttivi innovativi in legno. Il principale obiettivo è quello di fornire un contributo alla ricerca scientifica internazionale e ai metodi attuali di progettazione in merito alla risposta sismica di sistemi in legno a pareti sismo-resistenti, i quali rappresentano tutt'ora un'innovazione nel settore delle costruzioni e si stanno diffondendo grazie alle loro caratteristiche favorevoli.

Una panoramica iniziale sull'utilizzo dei principali sistemi strutturali in legno in zone sismiche per la realizzazione di edifici bassi o di media altezza viene fornita e contestualizzata nella vigente normativa sismica europea.

La prima parte della tesi affronta il tema della progettazione sismica di sistemi a pareti in legno, con particolare attenzione ai criteri di modellazione lineare e non lineare, proponendo diverse strategie ed evidenziandone le caratteristiche. In questa parte vengono forniti inoltre definizioni e concetti fondamentali propri dell'analisi sismica di strutture in legno. Un'attenzione particolare è riservata alla definizione e applicazione del "capacity design", sottolineandone lo stretto legame con il concetto di fattore di struttura. Viene proposta infine una definizione del fattore di struttura come prodotto tra una parte intrinseca alla struttura e una sovreresistenza di progetto. Tale definizione permette di caratterizzare i sistemi strutturali con la propria capacità dissipativa e di valutare separatamente la riserva di sicurezza introdotta dalla progettazione.

La seconda parte della tesi analizza il comportamento strutturale della tecnologia X-Lam (CLT), che rappresenta uno dei più comuni sistemi strutturali in legno. In questa parte vengono approfonditi i concetti di duttilità, capacità dissipativa, regolarità e irregolarità applicati al sistema X-Lam. La risposta sismica e la capacità dissipativa di questo sistema sono state preliminarmente valutate tramite una procedura analitico-sperimentale. Modelli numerici non-lineari hanno quindi permesso di valutarne la capacità dissipativa intrinseca in funzione delle variabili costruttive proprie del sistema. I risultati mostrano come le decisioni costruttive in fase di progettazione influenzino la risposta sismica dell'edificio; ciò è in contrasto all'applicazione di un unico valore del fattore di struttura per l'intera tecnologia X-Lam. Un'analisi statistica applicata a tali risultati numerici ha consentito di proporre formulazioni analitiche per il fattore di struttura per edifici regolari in funzione delle caratteristiche dell'edificio stesso. Infine, le stesse analisi condotte su edifici non regolari in altezza hanno fornito un coefficiente per tenere in conto della riduzione di capacità dissipativa a causa dell'irregolarità.

Nella terza parte viene presentata un'applicazione della tecnologia X-Lam per costruire edifici alti, analizzando il comportamento di edifici snelli con nucleo sismo-resistente e pareti aggiuntive

perimetrali. Vengono riportati inoltre le principali limitazioni e inconvenienti nel realizzare tali strutture in aree caratterizzate da elevata intensità sismica e le loro implicazioni nella progettazione.

La parte finale descrive e analizza tre sistemi strutturali in legno innovativi, come alternative a tecnologie più comuni, quali X-Lam o platform-frame. Questi sistemi, soggetti ad azioni sismiche, sono caratterizzati da una capacità deformativa e dissipativa diffusa, al contrario del sistema X-Lam in cui tale capacità è concentrata principalmente negli elementi di connessione. Questa risposta differente è studiata attraverso test sperimentali quasi statici e simulazioni numeriche. In dettaglio, sono presentati e analizzati due sistemi a pareti massicce stratificate; realizzate senza l'uso di colla tra gli strati e una parete ibrida acciaio-legno con un sistema innovativo di controvento.

Parole chiave: Strutture in legno; ingegneria strutturale; ingegneria sismica; progettazione sismica; sistemi costruttivi in legno; sistemi a pareti in legno; pareti massicce in legno; cross-laminated timber; CLT; X-Lam; sistema a telaio leggero; sistema platform-frame; fattore di struttura; fattore q ; fattore q_0 ; sovrarresistenza di progetto; modellazione numerica; FEM; test sperimentali; sistemi innovativi; sistemi misti; strutture ibride; connessioni; comportamento isteretico; capacità dissipativa; edifici alti; regolarità.

Acknowledgments

My deepest gratitude goes to my supervisor prof. Roberto Scotta, for his dedication in this research experience that allowed me to achieve objectives and satisfactions and for conveying to me not only a passion for the scientific research but also a positive attitude in dealing with problems and commitments.

I wish to thank all my colleagues at University of Padova known during these years and with whom I worked: Luca P. (with special thanks for the important collaboration in the development of this research), Luca M., Laura, Lorenzo, Paolo, Davide, Michela, Enrico and all the other colleagues of the research group.

Special thanks to Prof. A. Ceccotti for his valuable suggestions and his fundamental support in the research on the seismic behaviour of timber structures and to Dr. A. Polastri for successful cooperation in various research activities and scientific papers.

I would like also to thank Prof. M. Fragiaco for his external and independent evaluation of this research and for his valuable suggestions to improve this work.

I gratefully thank Martina, Francesco, Dario and Meri for having always supported me.

Table of contents

Introduction.....	1
I.1 Earthquake-resistant buildings with timber shear walls	1
I.1.1 Seismic behaviour of timber structures: basic concepts	1
I.1.2 Seismic-resistant timber wall systems: massive walls and light frames	3
I.2 Overview on European seismic standards and codes on timber structures	5
I.3 Objectives and scope of this dissertation.....	7
References - Introduction	8
Chapter 1 Seismic design of timber shear-wall systems	11
1.1 Introduction, definitions and state of the art.....	12
1.2 Fundamentals of seismic design and modelling of timber shear-wall systems based on connection stiffness	14
1.2.1 Evaluation of connection stiffness	16
1.2.2 Linear and non-linear modelling strategies.....	17
1.3 Evaluation and application of the fundamental seismic-design factors: the behaviour factor and the design over-strength	21
1.4 Conclusions	23
References – Chapter 1.....	24
Chapter 2 Seismic behaviour of CLT system	27
2.1 Introduction and state of the art	28
2.1.1 Advantages in the use of CLT	28
2.1.2 Current research on the seismic behaviour of CLT system.....	29
2.2 Evaluation of the seismic response with an experimentally-based procedure.....	32
2.2.1 Tested specimens and results	32
2.2.2 Analytical evaluation of CLT shear-wall capacity.....	37
2.2.2.1 Design calculation of lateral-load resistance	37
2.2.2.2 Proposed procedure for estimation of q-factor	39
2.2.2.3 Computation of q_0 and Ω	39
2.3 Evaluation of the seismic response with non-linear numerical analyses	41
2.3.1 Evaluation of q_0 -factor for CLT shear walls.....	42
2.3.1.1 Calibration of numerical models and validation	42
2.3.1.2 Computation of q_0 -factor.....	47
2.3.2 Evaluation of q_0 -factor for CLT buildings	49
2.3.2.1 Definition and design of case-study configurations	51

2.3.2.2	Numerical models for case-study configurations	52
2.3.2.3	Non-linear analyses and q_0 -factor evaluation	53
2.4	Updating of analytical formulations for the computation of the q_0 -factor for regular buildings.....	56
2.4.1	Analyses of results by indexes.....	56
2.4.2	Proposed analytical formulations	58
2.5	Study of the behaviour of in-elevation non-regular buildings	61
2.5.1	Definition of irregularity in elevation for CLT buildings.....	61
2.5.2	Q-factor reduction for in-elevation irregular CLT buildings.....	64
2.6	Conclusions.....	67
	Acknowledgments.....	68
	References – Chapter 2.....	68
Chapter 3	Application of the CLT system for high-rise buildings	73
3.1	Introduction and state of the art	74
3.2	Structural characterization of buildings with CLT cores and perimeter shear walls	77
3.2.1	Case-study buildings and seismic design	77
3.2.2	Numerical modelling of case-study buildings.....	79
3.2.2.1	Finite element models.....	79
3.2.2.2	Stiffness of connections.....	79
3.2.3	Analysis of numerical results	80
3.2.4	Numerical simulations with varied q -factor.....	82
3.3	Major limits in the use of CLT to realise tall structures and design implication	83
3.4	Conclusions.....	84
	References – Chapter 3.....	85
Chapter 4	Development and analyses of novel timber shear-wall systems.....	89
4.1	Introduction and state of the art	90
4.2	Evaluation of the seismic response of non-glued massive timber shear walls.....	91
4.2.1	Description of the systems and experimental tests.....	91
4.2.1.1	Description of the specimens.....	91
4.2.1.2	Test results and comparison with CLT.....	93
4.2.2	Numerical modelling of not-glued CLT shear walls and evaluation of q_0 -factor.....	95
4.2.2.1	Description and calibration of the models.....	95
4.2.2.2	Evaluation of the q_0 -factor.....	97
4.3	Evaluation of the seismic performance of a new mixed steel-timber solution with an innovative bracing system.....	103
4.3.1	Description of the system.....	103
4.3.2	Experimental tests	107

4.3.2.1	Analysis of test results	109
4.3.3	Numerical modelling and simulations	110
4.3.3.1	Simulation of quasi-static test and validation of the model	110
4.3.3.2	Evaluation of the q_0 -factor for a case-study building	112
4.4	Conclusions	114
	Acknowledgments.....	115
	References – Chapter 4.....	115
Chapter 5	Conclusions and future works.....	119
	List of Figures.....	123
	List of Tables	126
	List of Publications	127

List of notations

B	Base dimension of the wall
CLT	Cross-laminated timber
d	Diameter of fastener
DLS	Damage Limitation State
d_u	Ultimate displacement
d_y	Yielding displacement
EEEEP	Equivalent Elastic-Plastic Energy method
EEEEH	Equivalent Energy method with post-elastic hardening branch
F_A	Shear resistance of angle-bracket connections
$F_{ax,Rk}$	Characteristic withdrawal capacity of fastener
F_d	Design shear strength
FE	Finite Element
FEM	Finite Element Method
F_e	Maximum base shear strength achieved when behaviour of structure is assumed to be perfectly elastic
$f_{h,k}$	Characteristic embedment strength in timber member
F_{HD}	Uplift resistance of hold-down connections
F_{max}	Maximum base shear strength
FMD	Force Modification Design method
F_o	Maximum spectral amplification factor
$F_{v,Rk}$	Characteristic single shear capacity per nail
F_y	Yielding shear strength
H	Height of the wall
k_{conn}	Connection stiffness
K_e	Elastic stiffness of bi-liner response
K_{pl}	Post-elastic stiffness of bi-liner response
k_{mod}	Modification factor adjusted from reference to design situations of combined influences of duration of loading and moisture
k_R	Reduction coefficient of the behaviour factor for in-elevation irregularity
k_{ser}	Connection stiffness derived from code (slip modulus)
k_{test}	Connection stiffness derived from tests
I	Base dimension of the wall
l_1	Position of hold-down
LVL	Laminated Veneer Lumber
m	Amount of vertical joints per storey
M	Seismic mass
$M_{y,Rk}$	Characteristic yield moment of fastener
NLDA	Non-linear dynamic analysis
NLSA	Non-linear static analysis
OSB	Oriented strand board
P	Summation of connection-line lengths
P_0	Perimeter of the façade
PGA	Peak ground acceleration

PGA_d	Design peak ground acceleration
PGA_y	Yielding peak ground acceleration
PGA_u	Near-collapse peak ground acceleration
q	Behaviour factor
q_0	Intrinsic behaviour factor
R	Seismic Force Modification Factor
$R_{0.05}$	5 th percentile of resistance
$R_{0.95}$	95 th percentile of resistance
R_d	Design resistance
R_k	Characteristic resistance
S	Soil factor
SD	Standard deviation
$SFRS$	Seismic Force Resisting System
T	Fundamental elastic period of the system
T_B	Lower limit of the period of the constant spectral acceleration branch
T_C	Upper limit of the period of the constant spectral acceleration branch
T_D	Beginning of the constant displacement response range of the spectrum
t_1	Depth of penetration of fastener into timber member
ULS	Ultimate Limit State
W	Vertical load
$X-Lam$	Cross-laminated timber
α	Index to account for the joint density of the building
α_0	Reference configuration of a hypothetical façade without any intermediate vertical joint
β	Joint-density index
γ_m	Partial coefficient of material
γ_{Rd}	Over-strength factor in the capacity design
λ	Slenderness
λ	Correction factor
μ	Ductility ratio
ρ_k	Characteristic value of panel density
Ω	Design over-strength

Introduction

I.1 Earthquake-resistant buildings with timber shear walls

I.1.1 Seismic behaviour of timber structures: basic concepts

The effectiveness of the use of timber to realize seismic-resistant buildings is intrinsic in some of its properties. In particular, the use of timber when loaded parallel to the grain demonstrated to be very efficient if compared with traditional construction materials, as steel or concrete. One criterion to quantify its efficiency can be computed as the ratio between a resistance parameter f , as compressive strength parallel to the grain, and density of material ρ (Table I.1). This comparison shows that this ratio is about 5 times higher than concrete and similar to steel. Therefore, timber allows to realize lightweight and resistant structures, with clear advantages for the use in seismic areas.

Table I.1 – Effectiveness of the use of timber, comparison with traditional materials (data from [I.1])

Material	f/ρ [m ² /s ²]
Timber (Glulam GL24 [I.2])	~ 63.000
Concrete (R_{ck} 30MPa [I.3])	~ 10.400
Steel (S275 [I.4])	~ 55.000

Many examples of highly efficient timber buildings, in terms not only of seismic resistance and lightness but also of durability are available. Interesting examples are the Japanese Pagodas, which have been survived against numerous strong earthquakes ([I.5]-[I.6]). Fig. I.1 shows the 5-storey pagoda in Horyu-ji Temple founded in 607; this pagoda, realized entirely of wood, stands at about 32.5 meters in height and is one of the oldest building in the world. This suggests that if correctly conceived, designed and realized, timber structures can overcome they possible drawbacks, i.e., intrinsic brittle behaviour of wood (with the only exception of compression perpendicular to the grain) and exposure to natural degradation of the material.



Fig. 1.1 – 5-storey pagoda in Horyu-ji Temple (Japan). [1.7]

Four important mechanical parameters have to be optimized in seismic-resistant structures with respect to horizontal loads: strength, stiffness, ductility and dissipation capacity [1.8]. These four parameters can coexist in a timber structure only if timber elements are designed to remain in the elastic field and to fail never before ductile elements, as semi-rigid metal joints. These connections are therefore “fuse” elements and confer to the entire structure an hysteretic dissipative behaviour when loaded over their yielding limit.

The hysteretic behaviour of these connection elements is mainly characterized by two mechanisms, which can coexist during shear deformation of the joint: wood embedment near fasteners and formation of one or two plastic hinges in the connector ([1.9]-[1.11]). These two phenomena are responsible of the ductility and energy dissipation capacity of a connector, clearly explained in Fig. 1.2: the deformation of a correctly designed joint with slender fasteners is given both by plastic deformation of steel and by wood embedment, whereas large-diameter connectors are too stiff to deform plastically and total deformation is given only by wood embedment. In the first case, pinching effect (i.e., the reduction of dissipative capacity measured by the area within an hysteretic force-displacement cycle in the repeated cycles) is moderate and hysteresis curves maintain a sufficient amplitude also after the first cycle, Fig. 1.2a. In the second case, the pinching phenomenon is amplified and energy dissipation capacity decays for repeated loading cycles, Fig. 1.2b. The best solution in terms of energy dissipation could be obtained ensuring the localization of deformations in steel plates, limiting deformation on the wooden side (Fig. 1.2c), but this requires the use of ductile connectors rigidly fixed to the wooden parts. Another phenomenon that characterizes connection elements in timber structures is the strength degradation for repeated loading cycles, which can cause oligo-cyclic failure of connections subjected to seismic action before the actual ultimate displacement achievable with monotonic loading.

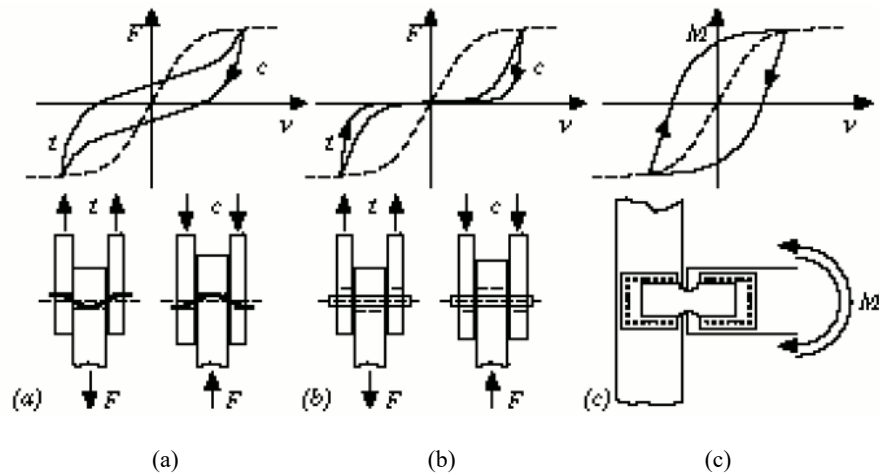


Fig. 1.2 – Typical hysteresis behaviour of a connection with metal fasteners. [1.12]

All these basic properties influence the whole seismic behaviour of a seismic-resistant timber structure and are the main responsible of its resulting seismic performance.

1.1.2 Seismic-resistant timber wall systems: massive walls and light frames

Buildings with timber structure constitute an important portion in the residential construction industry, not only in North America but also in Japan and Europe [1.9], as shown in Fig. 1.3. In particular, various timber structural systems have been developed to work properly if subjected to seismic action, paying close attention to strength, stiffness, ductility and connection details.

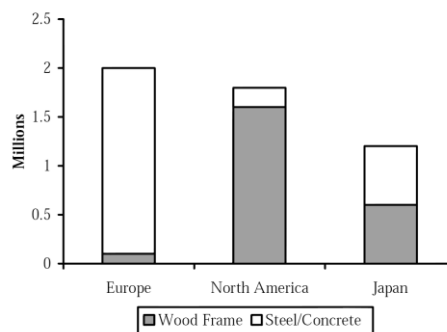


Fig. 1.3 – Comparison between residential buildings in 1999 in millions of m^3 . [1.13]

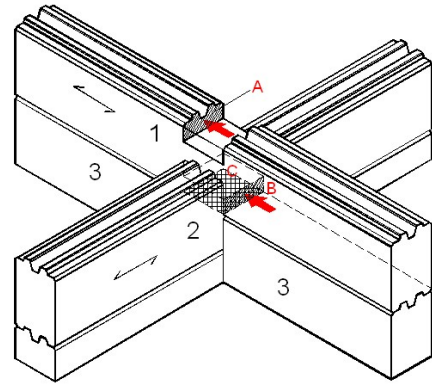
A good seismic performance can be reached using timber shear-wall systems. Shear walls are elements of the seismic force resisting system: they can be realized with massive timber elements or with light timber frames. In the first case, layers of massive timber can be oriented horizontally (e.g., log-house, Fig. 1.4), vertically, or cross-wise (e.g., cross-laminated timber, Fig. 1.5) and have to be connected among them to confer in-plane shear stiffness and strength to the resulting panel. In the second case, frames have to be braced with timber studs or with timber-based panels (e.g., platform frame, Fig. 1.6).

In log-house system (Fig. 1.4), shear walls are realized overlaying horizontal timber logs, generally shaped with carpentry connections. The stability of the building and the resistance against lateral

loads are generally obtained with joints between orthogonal walls (Fig. 1.4b). These structures are realized with few on-site metal joints and their ductility is mainly due to friction between layers, which confers to the wall an high elastic stiffness and high ultimate displacements, until reaching failure (e.g., due to out-of-plane instability of walls orthogonal to the seismic direction). However, friction cannot be considered in the design: this structural system has to be considered as not dissipative and strength capacity should be entirely assigned to joints with orthogonal walls.



(a)



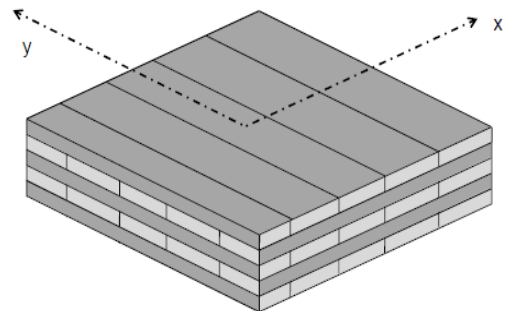
(b)

Fig. 1.4 – Log-house system. (a) Example of building [I.14]; (b) assembly of orthogonal walls [I.15]

The cross-laminated timber (CLT) panel (Fig. 1.5) is realized with massive timber boards stacked cross-wise and glued together at 90 degrees (Fig. 1.5b). This technique allows to obtain a strength and stiff large panel that can be used as floor of shear-wall element, orienting the panel with external layers parallel to axial loading direction. Regarding resistance to vertical loads, this technique allows to overcome limitations of log-house system, in which timber elements are subjected to compression perpendicular to the grain. Moreover, if the panels are anchored at the base and among them with ductile and correctly designed metal connections, this system shows a good seismic response characterized by a box-like behaviour, good energy dissipation capacity and high redundancy.



(a)



(b)

Fig. 1.5 – Cross-laminated timber system. (a) Example of building [I.16]; (b) cross-lamination technique [I.17].

In light timber-frame system, known also as platform-frame system or two by four (Fig. 1.6), shear walls are realized with massive timber posts with section dimension normally 2 x 4" (38 x 89 mm) placed at a distance variable from 40 to 60 cm and timber beams placed above and underneath [I.9]. The modern light frame is normally braced on the outer side with Oriented-Strand-Board

(OSB) panels fastened to the frame with ductile metal nails or staples. The inner side can be braced with another OSB sheet and the wall is normally finished with a gypsum panel. These walls are anchored to foundations with hold-downs and wood screws. Buildings realized with this system can show an highly dissipative behaviour if subjected to seismic actions, thanks to the diffused plasticization in nailing between frames and panels.



Fig. 1.6 – Platform-frame system. (a) Example of building [I.18]; (b) bracing of light frame [I.19].

In this dissertation, an overview on general seismic design methods for timber shear-wall systems is given in Chapter 1. The following chapters analyse the seismic response of three specific structural systems. An in-depth study refers to CLT structural system, because it currently represents an important constructive system, which is widely spreading in seismic-prone areas, thanks to its high potential for medium- and high-rise buildings. Other two massive structural systems, which represent an innovation and an alternative to CLT, are studied and their seismic response is assessed. These innovative systems are realized without the use of glue and are characterized by a dissipative capacity diffused in the joints between layers. Finally, an innovative light-frame system is presented and studied. This system derives from the platform-frame concept but its response is improved thanks to the coupling with an additional plastic bracing system and steel columns, which resist to vertical loads.

1.2 Overview on European seismic standards and codes on timber structures

The broad implementation of newly developed principles requires their proper transition into rules and regulations that constitute the basis for the daily work of practicing engineers. Thus, rules and regulations as structural design codes constitute the mayor interface between structural engineering research and practical application and it is of utmost importance that structural design codes are up to date with the best scientific information [I.20].

The reference European codes for timber structures are: EN 1995 – Eurocode 5 [I.11], which provides common rules for the static design; and chapter 8 of EN 1998 – Eurocode 8 [I.21], which is complementary to Eurocode 5 and gives specific rules for seismic design of timber buildings. The purpose of Eurocode 8 is to ensure that in the event of earthquakes: (1) human lives are

protected (i.e., ultimate limit state (ULS) is verified); (2) damage is limited (i.e., damage limitation state (DLS) is verified); and (3) structures important for civil protection remain operational. The first criterion relates to seismic actions with a reference probability of exceedance of 10% in 50 years or with a return period of 475 years. The second criterion refers to seismic actions with larger probability of occurrence, i.e., with a probability of exceedance of 10% in 10 years or a return period of 95 years. Third criterion implies the adoption of lower probability of exceedance that is an increased design return period.

EN 1998 – Eurocode 8 [I.21] provides definitions and methods to compute the seismic action, as function of the elastic spectrum, the main elastic period of the structure, its regularity, its seismic mass and its ductility and dissipative behaviour (summarized in the behaviour factor value, i.e., q -factor). Then, verifications are performed in terms of resistance to seismic action (ULS) and maximum compatible inter-storey drift (DLS).

The specific rules for timber structures at chapter 8, subdivide structural systems in low-dissipative (belonging to DCL low ductility class) or dissipative (belonging to DCM medium or DCH high ductility classes). In the first case, buildings have to be computed elastically, applying Eurocode 5 definitions, with a q -factor not greater than 1.5. In the second case, the q -factor ranges from 2.0 to 5.0 and specific rules and details are given to design the dissipative zones (i.e., metal joints) and brittle parts (i.e., timber or timber-based materials). In order to ensure that given q -factors may be used, verifications with cyclic-loading tests can also be performed: static ductility ratio has to be equal to 4 for DCM and of 6 for DCH, with less than a 20% strength reduction after three fully reversed cycles.

The reference European Standard for cyclic-loading tests of joints with mechanical fasteners for timber structures or of entire timber structural systems is EN 12512 [I.22]. These tests consist of the application of cyclic loads in displacement control with increasing amplitude, up to failure of the specimen. Displacements are recorded with various transducers positioned at significant points of the specimen. Fig. I.7 shows the setup of a quasi-static test of a connection element for CLT system (Fig. I.7a) and the setup of a test of a timber shear-wall system with a full-scale wall (Fig. I.7b). These tests allow to evaluate fundamental parameters for the seismic characterization of timber structures, such as stiffness, strength, failure, ductility, strength reduction and equivalent viscous damping.

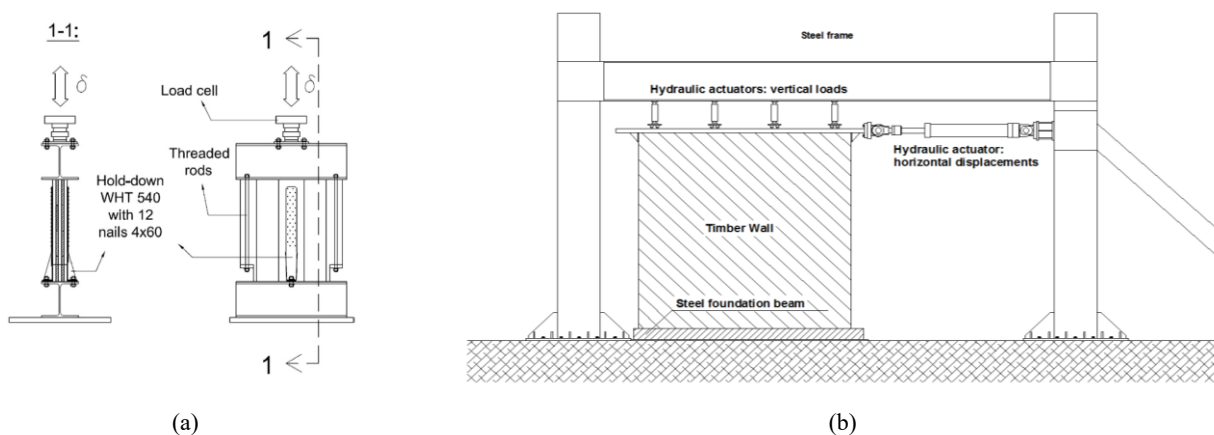


Fig. I.7 – Quasi-static tests according to EN 12512 [I.22]. (a) Setup of a test of a connection element for CLT structures [I.23]; (b) setup of a test of a timber structural system [I.24].

I.3 Objectives and scope of this dissertation

The main scope of this thesis work is to give a contribution to international scientific research and current design practice about the seismic response and design of timber shear-wall systems, with particular focus on the cross-laminated timber (CLT) system and on three innovative structural systems.

- (1) The first target is to clarify basic definitions and methods for seismic design and modelling of timber shear-wall systems.
- (2) A large part is dedicated to CLT system, with the aim to provide information on its energy dissipation capacity and the applicable behaviour factor value, as function of geometrical and mechanical characteristics of the building. A review of definitions of regularity in European seismic code and a proposal for amendments is given, in order to fit better with CLT technology.
- (3) The final part has the aim of evaluating the seismic response of three innovative timber shear-wall systems. This part allows also to focus on procedures and steps for a suitable seismic characterization of novel timber structural systems with currently available tools, as full-scale tests and non-linear numerical simulations.
- (4) Another target is to present non-linear modelling techniques applicable to timber structures and main steps for a correct calibration based on experimental tests.

The main tools used to obtain the results presented in this dissertation are:

- (1) Experimental data from cyclic-loading tests on connection elements or full-scale wall specimens representative of the structural system studied;
- (2) Analytical methods based on code provisions or on literature;
- (3) Numerical dynamic simulations of linear and non-linear models calibrated on results from tests or on code provisions.

This thesis presents original data, results and conclusions based both on novel research activities, which started in the period between 2013 and 2015, and on the continuation of research activities presented in ([I.25]-[I.28]), which have been further developed and extended.

References - Introduction

- [I.1] Piazza, M., Tomasi, R., and Modena, R. (2005). "Strutture in legno. Materiale, calcolo e progetto secondo le nuove normative europee." Hoepli, Milano.
- [I.2] EN 14080 (2002). "Timber structures - Glued laminated timber and glued solid timber – Requirements." CEN. Brussels, Belgium.
- [I.3] EN 206 (2013). "Concrete - Specification, performance, production and conformity." CEN. Brussels, Belgium.
- [I.4] EN 10025-2 (2004). "Hot rolled products of structural steels - Part 2: Technical delivery conditions for non-alloy structural steels." CEN. Brussels, Belgium.
- [I.5] Nakahara, K., Hisatoku, T., Nagase, T., and Takahashi, Y. (2000). "Earthquake response of ancient five-story pagoda structure of horyu-ji temple in japan." In proceedings of 12th World Conference on Earthquake Engineering (WCEE), Auckland, New Zealand.
- [I.6] Fujita, K., Hanazato, T., and Sakamoto, I. (2004). "Earthquake response monitoring and seismic performance of five-storied timber pagoda." In proceedings of the 13th World Conference on Earthquake Engineering (WCEE). Vancouver, Canada.
- [I.7] <https://aehistory.wordpress.com>.
- [I.8] Elnashai, A.S., and Di Sarno, L. (2008). "Fundamentals of Earthquake Engineering". Wiley, UK.
- [I.9] Ceccotti, A., Follesa, M., and Lauriola, M.P. (2007). "Le strutture di legno in zona sismica. Criteri e regole per la progettazione ed il restauro". C.L.U.T. Editrice, Torino.
- [I.10] Johansen, K.W. (1949). Theory of timber connections. International Association of bridge and structural Engineering, Bern, p. 249-262.
- [I.11] EN 1995-1-1 Eurocode 5 (2004). "Design of timber structures, Part 1-1, General: Common rules and rules for buildings". CEN. Brussels, Belgium.
- [I.12] Ceccotti, A. (2003). "Il manuale del legno strutturale Vol. II". Mancosu Editore, Roma.
- [I.13] Cohen, D., Gaston, C., and Kozak, R. (2001). "Influences on Japanese demand for wood products." ECE/FAO Forest Products Annual Market Review.
- [I.14] Kontio Loghouse. Available online: <http://www.kontio.net>.
- [I.15] Promo_legno website. Available online: <http://www.promolegno.com>.
- [I.16] Website of KLH UK. Available online: <http://www.klhuk.com>.
- [I.17] Bernasconi, A. (2010). "Il materiale XLAM: caratteristiche e prestazioni". Available online: <http://www.promolegno.com>.
- [I.18] Woodlab website. Available online: <http://www.woodlab.info>.
- [I.19] Schickhofer, G., Bernasconi, A., and Traetta, G. "Costruzione di edifici di legno." Promo_legno website. Available online: www.promolegno.com.
- [I.20] Kohler, J., and Fink, G. (2015). "Aspects of Code Based Design of Timber Structures." In proceedings of 2nd International Network on Timber Engineering Research (INTER), Šibenik, Croatia.

- [I.21] EN 1998-1-1 Eurocode 8 (2004). "Design of structures for earthquake resistance, part 1: general rules, seismic actions and rules for buildings". CEN. Brussels, Belgium.
- [I.22] EN 12512 (2001). "Timber structures—test methods—cyclic testing of joints made with mechanical fasteners". CEN. Brussels, Belgium.
- [I.23] Gavric, I., Fragiaco, M., and Ceccotti, A. (2015). "Cyclic behaviour of typical metal connectors for cross-laminated (CLT) structures". *Materials and Structures*, 48:1841-1857.
- [I.24] Pozza, L., Scotta, R., Trutalli, D., Pinna, M., Polastri, A., and Bertoni, P. (2014). "Experimental and Numerical Analyses of New Massive Wooden Shear-Wall Systems." *Buildings* 4(3):355-374. MDPI. DOI: 10.3390/buildings4030355.
- [I.25] Pozza, L. (2013). "Ductility and behaviour factor of wood structural systems". Ph.D. Thesis, University of Padova, Italy.
- [I.26] Pozza, L., Trutalli, D., Polastri, A., and Ceccotti, A. (2013). "Seismic design of CLT buildings: definition of the suitable q-factor by numerical and experimental procedures." In proceedings of the Second International Conference ICSEA, 24-26 July, Guimaraes, Portugal. *Structures and Architecture* 9:90–97. DOI: 10.1201/b15267-13.
- [I.27] Pozza, L., Scotta, R., Trutalli, D., Ceccotti, A., and Polastri, A. (2013). "Analytical formulation based on extensive numerical simulations of behavior factor q for CLT buildings." In proceedings of meeting 46 of the Working Commission W18-Timber Structures, CIB, Vancouver, Canada. Paper CIB-W18/46-15-5.
- [I.28] Pozza, L., Scotta, R., Trutalli, D., Polastri, A., and Ceccotti, A. (2015). "Concrete-Plated Wooden Shear Walls: Structural Details, Testing, and Seismic Characterization." *Journal of Structural Engineering*. ASCE. DOI 10.1061/(ASCE)ST.1943-541X.0001289.

Chapter 1 Seismic design of timber shear-wall systems

Abstract

The theme of the seismic design of timber shear-wall systems is discussed in this part giving close attention to linear and non-linear modelling criteria: various strategies are proposed and the main advantages and disadvantages are highlighted. The basic definitions and concepts proper of the seismic analysis of timber structures are provided. An overview on the application of the hierarchy of resistances to apply correctly the capacity design approach is reported and the close link with the chosen behaviour factor value is emphasized. Moreover, the definition of the behaviour factor value, as product between an “intrinsic” capacity of the structure and a design over-strength value is proposed. This definition allows to characterize the structural systems with their proper dissipative capacity (intrinsic factor) and to evaluate separately the safety reserve introduced by the design and code provisions (over-strength).

1.1 Introduction, definitions and state of the art

The advantages in the use of timber to realize multi-storey buildings has led to the development of numerous innovative construction systems. In seismic-prone areas, a great interest has been addressed in the development and optimization of shear-wall systems, realized with light frames or cross-laminated timber panels (CLT), due to their resistance and ductility if subjected to seismic actions. However, this development was not followed by an adequate update of codes and design criteria. The still unresolved main issues are:

- No clear design methods are available for novel timber structural systems;
- No exhaustive indications are provided by codes;
- No clear indications are given on modelling strategies of timber shear-wall buildings.

The seismic design of timber shear-wall systems according to the force-based method requires the determination of type, number and spacing of metal connectors loaded in shear and/or tension and type and thickness of wooden panels subjected to in-plane shear forces, based on the resistance of each component. This method requires the application of a suitable behaviour factor value q (≥ 1.00), henceforth called q -factor, which allows to reduce the seismic forces obtained from elastic methods, implicitly taking into account the post-elastic behaviour and energy dissipation capacity of the structural system. Therefore, it can be correctly applied only if the structure is designed to dissipate energy before failure, according to the capacity design approach.

The application of the capacity design approach, originally developed for RC structures [1.1], has already been studied for timber structures and its definition is available in literature [1.2]. This approach is based on the hierarchy of resistance applied to the design of ductile components (i.e., connections), whose resistance has to be always less than that of brittle elements (i.e., timber members) and fragile components. The importance of the correct application of this method is crucial: if not applied, brittle components can fail before yielding of ductile parts. Consequently, the structure is not able to dissipate energy and should be designed elastically, with a q -factor equal to 1.00. Typical examples of brittle failures of timber shear walls are shown in Fig. 1.1.

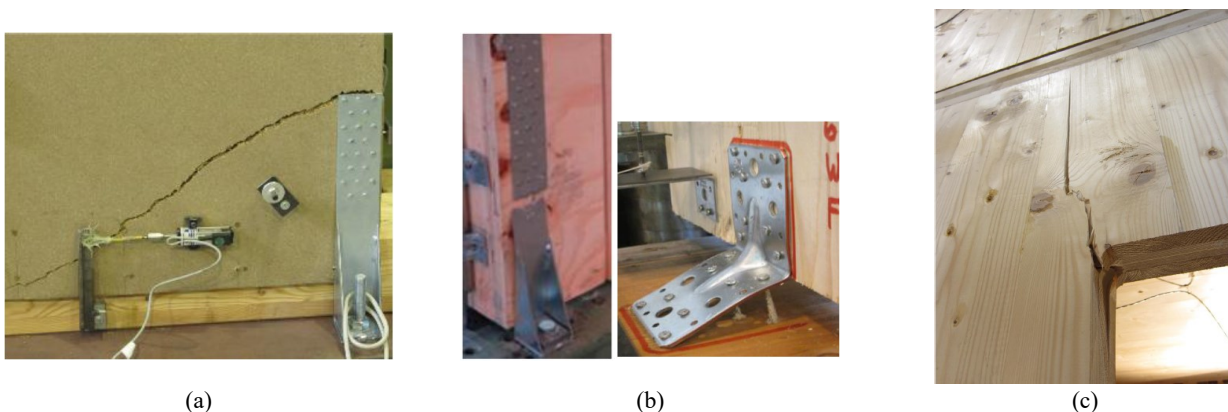


Fig. 1.1 – Example of brittle failures in timber shear-wall systems. (a) Failure of bracing panel in light-frame system [1.3]; (b) brittle failure of an hold-down and an angle bracket in CLT system [1.4]; (c) failure of timber lintel in CLT system [1.5].

The capacity design approach is based on the application of an over-strength factor γ_{Rd} defined as the minimal ratio to be assured between design strength of a brittle component ($R_{B,d}$) and of a

ductile component ($R_{D,d}$). It depends on statistical strength-capacity distribution according to test results (i.e., 5th and 95th percentile of resistance, $R_{0.05}$ and $R_{0.95}$) and on design coefficients used to shift from characteristic R_k to design R_d resistances according to a specific code. The concept of capacity design and the procedure to evaluate γ_{Rd} value by means of tests are shown in Fig. 1.2.

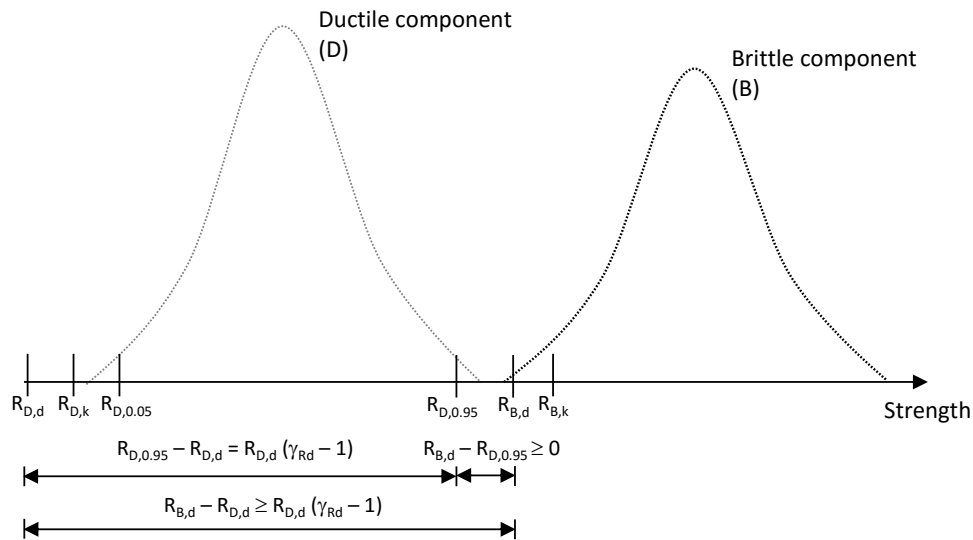


Fig. 1.2 – Definition of capacity design and over-strength factor.

This approach is characterized by some differences if applied to design light-frame or CLT structures. In timber-frame buildings, ductility and energy dissipation are normally diffused in connectors (as staples or nails) between bracing panels (nowadays mostly realized with OSB or multi-layered sheets) and timber frame. Recent works were conducted with the aim of developing analytical models to evaluate the load-bearing capacity and deformation of timber frame shear-walls subjected to lateral loads ([1.6]-[1.8]). In timber frame systems, connections at the base (hold-downs and angle brackets) are normally over-designed and their resistance should be determined applying the capacity design approach. Conversely, in CLT systems the energy dissipation capacity is entirely concentrated in connections at the base and along vertical joints, which have to be the weakest (and possibly dissipative) components of system. Analytical methods to compute the load-bearing capacity has been provided also for CLT system (e.g., [1.9]), together with specific rules for the application of the capacity design approach ([1.4];[1.10]-[1.12]) and values of suitable over-strength factor, obtained from tests of typical metal connectors [1.13] and typical screwed connections [1.14]. However, such studies are uncompleted and their results still not incorporated into seismic code, also for the difficulties arising from the excessive value of γ_{Rd} to be assured.

The European seismic code (Eurocode 8 [1.15]) is currently incomplete with regard to classification of timber structures, seismic design rules and constructive details. Moreover, this code provides the q-factor only for standard building typologies. For CLT systems a value $q=2$ is safely given based on few results from tests on specific buildings or shear walls. Finally, no clear indications are given about the correct application of the capacity design approach. Recently, a proposal for a new background document of Chapter 8 of Eurocode 8 has been studied and proposed ([1.16]). This proposal relates in particular to three issues: clear identification of the structural type and relative q-factor; design according to the capacity based design and detailing provisions; adoption of over-strength factors for the over-design of brittle components.

Another important issue regards the design of complex timber shear-wall buildings by means of FE modelling. In literature, various advanced non-linear models have been performed to predict or simulate the behaviour of complex structures (e.g., [1.17]-[1.21]) but no provisions are available regarding the correct modelling criteria of timber buildings, even if by means of linear dynamic analyses. In particular, the correct evaluation and modelling of connection stiffness are fundamental to obtain a reliable model.

1.2 Fundamentals of seismic design and modelling of timber shear-wall systems based on connection stiffness

A fundamental issue in the seismic design of complex timber shear-wall buildings is the definition of suitable inputs in a FE model for the correct evaluation of forces on each component. Such inputs are mainly the stiffness and distribution of connections, which influence the building fundamental period T , the distribution of seismic forces and the displacement and drift of each storey. The vibration period depends on the mass distribution and on the global stiffness of the building, which is highly sensitive to deformability of the connection elements. The distribution of seismic forces is function of stiffness of the shear-walls, which on its own depends on stiffness of seismic-resisting connections. Displacements and inter-storey drifts depend on the deformation of the shear walls, which can be a rocking, sliding and/or shear deformation, according to Fig. 1.3. These three deformation mechanisms depend on connection stiffness and strength. Consequently, for a precise modelling of a building the definition of the stiffness of each connection is crucial. For example, in platform-frame buildings the correct modelling of panel-to-frame connections or of equivalent shear stiffness of each shear wall is fundamental (predominant shear behaviour). Conversely, in CLT buildings the most important elements to be modelled are angle brackets, hold-downs and panel-to-panel joints (predominant rocking and sliding mechanisms).

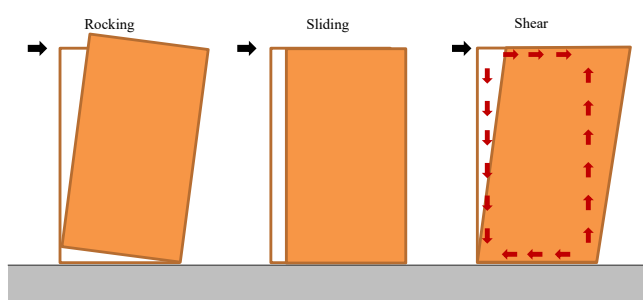


Fig. 1.3 – Deformability of a timber shear wall.

Even in a linear-elastic design process, engineers are therefore required to solve an iterative scheme (Fig. 1.4). (1) The connection stiffness influences the fundamental period of the building, the distribution of forces and drifts; (2) the external force in each connection induced by earthquake is a function of the period and of the connection stiffness; (3) the load bearing capacity of the connections has to be compatible with the external force (Ultimate Limit State verification – ULS [1.15]) and the drift of each storey has to be compatible with the limitation of damage of non-structural elements (Damage Limitation State verification – DLS [1.15]); (4) the strength and the stiffness of the connections are linked through the effective number of fasteners.

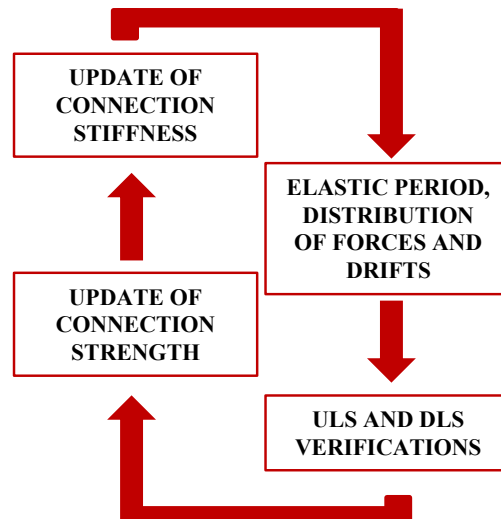


Fig. 1.4 – Iterative scheme for the seismic design of connection elements.

An efficient approach to design a timber shear-wall building starts from a preliminary definition of the external force induced by earthquake in each shear wall according to the equivalent linear static analysis [1.15]. In this preliminary step the definition of fundamental period T according to global stiffness of the building can use a simplified formulation based on the height of the building, assuming $C_t=0.05$ [1.15]. Once lateral forces on each shear wall are determined, analytical methods (e.g., [1.6]-[1.9]) can be applied to design each connection element (type and number of fasteners, thickness of steel parts) compatible with the external seismic force. For the CLT system, a simplified and efficient analytical method to compute the lateral-load resistance of a shear wall is presented in section 2.2.2.

This first step allows to estimate roughly the connection elastic stiffness and to obtain a preliminary model. Then, the frequency and spectral-response analyses allow to estimate a more realistic period and to calculate the effective forces induced in connections by earthquake. The procedure ends with ULS and DLS verifications. If one of them is not verified, it means that forces and/or drifts are not compatible with connection strength and/or stiffness. Therefore, it is necessary to redesign connections and update stiffness values in the model. The iterative process continues up to convergence, i.e., connection strength compatible with ULS and DLS verification and stiffness in the model congruent with strength. This iterative scheme is illustrated in Fig. 1.5.

Therefore, two key points have to be correctly assessed for the application of this procedure: (1) suitable values of connection stiffness and (2) suitable modelling of connections.

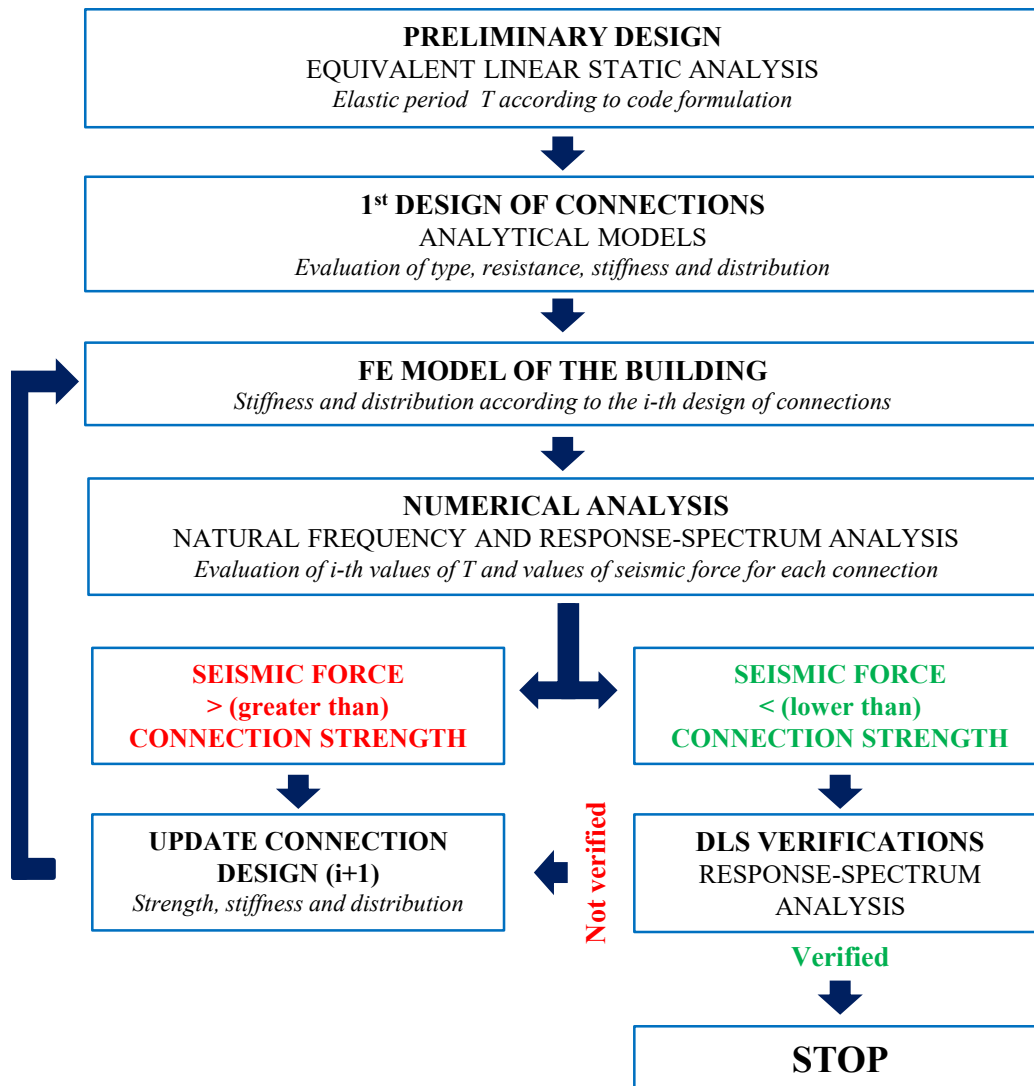


Fig. 1.5 – Seismic-design procedure for timber shear-wall buildings based on linear modelling.

1.2.1 Evaluation of connection stiffness

With reference to the first point, it is clear that connection stiffness (k_{conn}) can be derived from tests on single elements ($k_{\text{conn}}=k_{\text{test}}$). In this case, monotonic- or cyclic-loading tests have to be performed, both in tension and in shear, and the elastic slope of the backbone curve, according to a bi-linearization method (e.g., EEEP method [1.22] or others [1.23]-[1.24]) can be adopted as k_{test} , Fig. 1.6. This approach is consistent and it is the most accurate and correct estimate of how connections actually behave. However, this approach has some limitations: it depends on adopted bi-linearization method and on the characteristics of the tested connection. Moreover, it normally under-estimates stiffness of full shear walls, in particular when depending on base shear connections, because of the neglecting of friction and other secondary phenomena. Consequently, the approach based on tests on single components leads to an un-realistic overestimation of period T that is normally not in side of safety. Conversely, for the same reasons it normally underestimates dissipative capacities. An alternative approach consists in deriving stiffness from tests on full-scale specimens or full-scale buildings, if available, but in this case the dependence on specimen's characteristics increases.

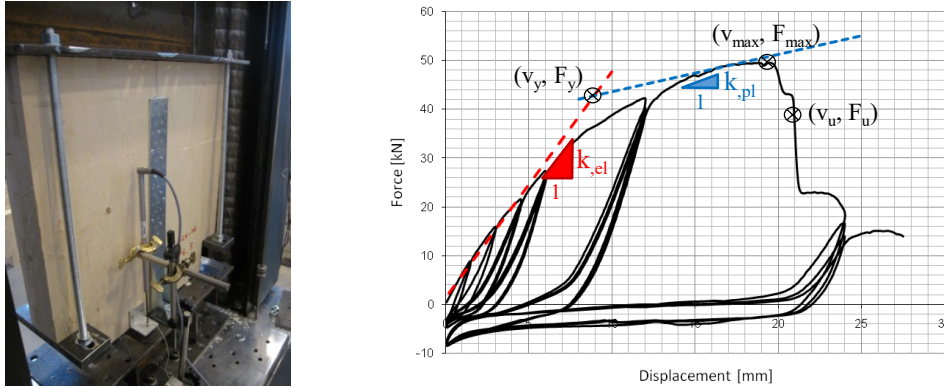


Fig. 1.6 – Estimation of connection stiffness from cyclic tests of single elements [1.25].

A simple way to estimate connection stiffness is based on information in Eurocode 5 [1.26] or similar international codes, assuming elastic stiffness equal to the slip modulus k_{ser} (i.e. $k_{conn} = k_{ser}$). Fig. 1.7 shows formulations to obtain k_{ser} for a timber-to-timber fastener. For a steel-to-timber connection, values obtained in Fig. 1.7 may be multiplied by 2.0 [1.26]. The extreme approximation given by the expression for k_{ser} has to be underlined: it cannot keep into account of the several parameters of the connection and consequently the obtained values of stiffness are seldom close to experimental ones. The total stiffness of a connection element can be obtained multiplying this value by the number of fasteners in the connection. The simplification of this approach is to assume the connection stiffness proportional to the stiffness of fasteners, neglecting all other deformability of the connection. This leads to much higher values of stiffness and lower values of periods. The problem in this case is the marked under-estimation of displacements and drifts, which can provide not-fully consistent results in DLS verification.

The optimal solution could be the performing of two separate models and comparing the results: a model with $k_{conn}=k_{test}$ and a model with $k_{conn}=k_{ser}$.

Fastener type	K_{ser}
Dowels Bolts with or without clearance ^a Screws Nails (with pre-drilling)	$\rho_m^{1,5} d^{1/23}$
Nails (without pre-drilling)	$\rho_m^{1,5} d^{0,8}/30$
Staples	$\rho_m^{1,5} d^{0,8}/80$
Split-ring connectors type A according to EN 912 Shear-plate connectors type B according to EN 912	$\rho_m d_c/2$
Toothed-plate connectors:	
– Connectors types C1 to C9 according to EN 912	$1,5 \rho_m d_c/4$
– Connectors type C10 and C11 according to EN 912	$\rho_m d_c/2$
^a The clearance should be added separately to the deformation.	

Fig. 1.7 – Table 7.1 of Eurocode 5 [1.26]. Slip modulus k_{ser} per shear plane per fastener in N/mm in timber-to-timber and wood-based panel-to-timber connections.

1.2.2 Linear and non-linear modelling strategies

Concepts discussed above emphasize the importance of paying close attention to connection modelling. Timber shear walls can be modelled with linear and/or non-linear elements. In the

design practice, linear elastic models are sufficient to estimate the elastic period of the structure and to design all components. This type of modelling requires only the evaluation of the elastic stiffness of the components and allows to perform linear static and dynamic analyses. Conversely, to simulate correctly the behaviour of these structures and predict their response in terms of displacement and energy dissipation capacity, the non-linear behaviour of the components has to be correctly reproduced. In particular, the definition of monotonic curves is sufficient for non-linear static analysis (pushover), whereas non-linear dynamic analysis (time history) requires the complete hysteresis behaviour of each inelastic component.

Three modelling strategies can be used to simulate the actual non-linear behaviour of a timber shear wall, which can be then extended to entire buildings:

1. Shear walls modelled with all non-linear deformations diffused in the bracing system and fixed restraints at the base (examples in [1.27]-[1.28]), Fig. 1.8a;
2. Shear walls modelled with high in-plane stiffness of the timber panel and non-linear springs representing the single connection elements (modelling for components) (examples in [1.19];[1.29]-[1.30]), Fig. 1.8b;
3. Shear walls modelled with non-linear elements simulating the shear deformation of the bracing system and non-linear springs representing the connection elements (modelling for components) (examples in [1.20]-[1.21]), Fig. 1.8c.

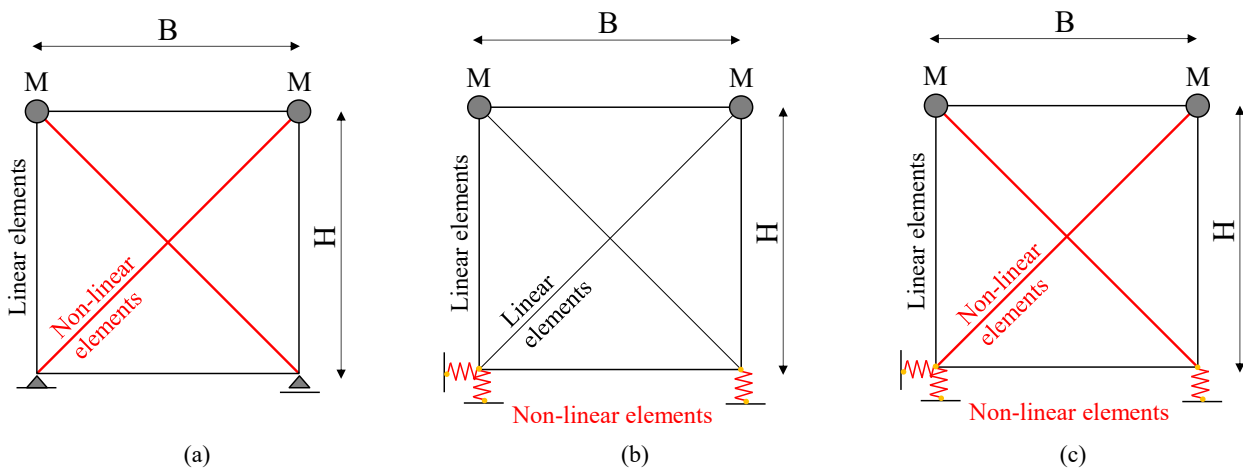


Fig. 1.8 – Numerical models of timber shear walls: (a) diffused non-linearity; (b) modelling for components (suitable for stiff panels as CLT); (c) modelling for components (suitable for deformable panels as light-frame system).

According to the first modelling strategy, all the nonlinearities due to the base connections and specific composition of the panel are concentrated in the diagonal elements. The modelling of non-linear effects exclusively in the shear deformation of the panel instead of introducing the hysteretic behaviour of each connection is possible for simple case studies. This modelling strategy is more appropriate for walls, whose deformation is mainly due to shear deformation of the wooden panel, whereas base connections are over-resistant and undergo negligible displacements. An application of this approach is presented in Chapter 4 to study the response of massive shear walls characterized by predominant shear deformability.

The second model is more appropriate for walls, whose deformation is mainly concentrated in connection elements. This model conforms to the classical design assumption for rigid wall panels, as CLT: the non-linear behaviour is concentrated in the connections, whereas panels remain in the elastic field. This approach allows to obtain models that are more accurate and to study not only

the global behaviour of the wall but also the response of each connection. Furthermore, this approach allows to extend the analysis of simple shear walls to more complex systems, as multi-storey buildings with panel-to-panel and panel-to-floor joints. This strategy is adopted in Chapter 2 to study the hysteretic behaviour of CLT shear walls and of entire CLT buildings.

The third model is the most complex and allows to simulate all the possible deformations of a timber shear wall, shown in Fig. 1.3. This strategy is appropriate when all components of a shear wall (connections at bracing system and at the base) yield during earthquake, and their contribution is fundamental. An example of the adoption of this strategy is given in Chapter 4 to study the response of a novel hybrid system.

The models shown in Fig. 1.8 are realized with truss elements. This does not preclude the use of other finite elements to simulate the behaviour of the timber panel: shell elements with equivalent shear stiffness of bracing system (Fig. 1.9a); rotational springs at the corner of the perimeter frame (Fig. 1.9b) or diffused springs simulating connections between panel and frame (Fig. 1.9c).

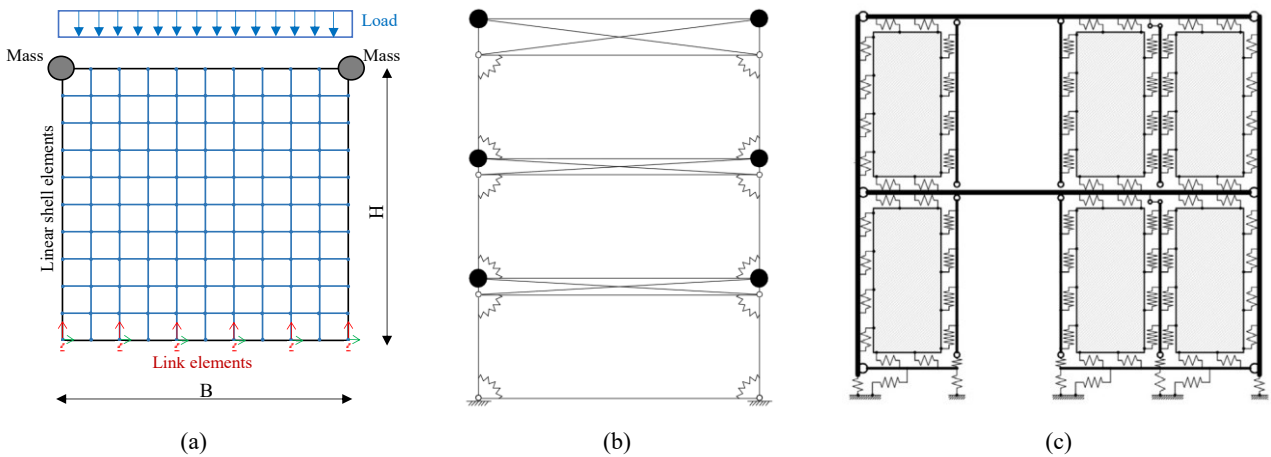


Fig. 1.9 – Other strategies to model the in-plane behaviour of a timber wall: (a) linear shell elements [1.25]; (b) rotational springs [1.28]; (c) diffused springs [1.21].

Linear models can be obtained with the same strategies presented above, modelling each component with its elastic stiffness. In this case, shell elements are normally used to model the panels and spring elements with suitable shear and axial stiffness are used to connect panels among them and with the basement.

To switch from a simple model of a shear wall to a complex building, each shear-wall model has to be assembled with rigid or deformable elements. Various models can be obtained with different complexity, depending on modelling of horizontal and vertical panel-to-panel connections, and modelling of walls and floors. Table 1.1 illustrates various strategies with different complexity and efficiency. The most efficient strategy is to model the deformable connections with their actual stiffness (or equivalent stiffness if connections are diffused in the wall or floor), while the over-resistant connections can be assumed as rigid, and their deformability can be neglected. This criterion complies with building-level capacity design approach, as shown in Fig. 1.10 for the case of CLT system. Following this criterion, all connections which provide a box-like behaviour to the building have to be over-designed with respect to the other ductile elements [1.4]. Examples of FE models of building superstructures carried out with two different software are shown in Fig. 1.11.

Table 1.1 – Modelling strategies for complete building superstructures.

	MODEL 1	MODEL 2	MODEL 3
Connections at the base	Rigid	Actual stiffness	Actual stiffness
Connections between floors and walls above	Rigid	Actual stiffness	Actual stiffness
Connections between floors and walls underneath	Rigid	Rigid	Actual stiffness
Vertical panel-to-panel joints	Rigid	Actual stiffness	Actual stiffness
Connections between perpendicular walls (corners and T-joints)	Rigid	Rigid	Actual stiffness
Connections at bracing system (only for light frame)	Stiffness of timber panel	Equivalent stiffness	Equivalent stiffness
Connections between adjacent floor panels	Rigid	Equivalent stiffness	Actual stiffness
Lintels	Rigid	Actual stiffness	Actual stiffness
SUITABILITY	WRONG	CORRECT	CORRECT
EFFICIENCY	SIMPLE	EFFICIENT	COMPLEX

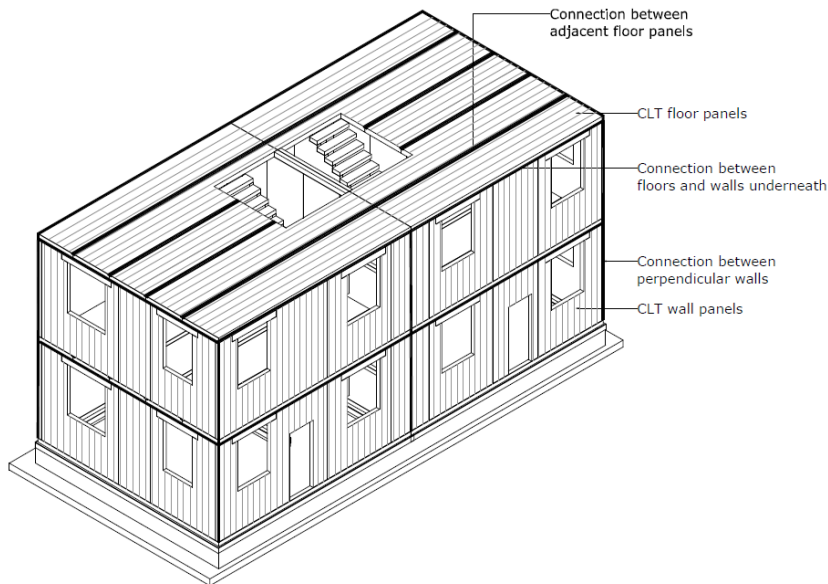


Fig. 1.10 – Example of a CLT building: connections designed with over-strength, which can be modelled as rigid [1.16].

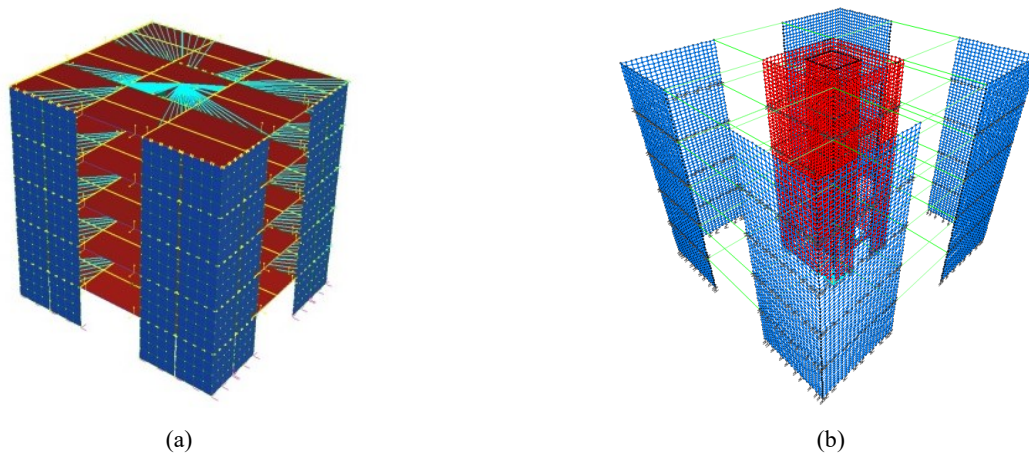


Fig. 1.11 – Examples of linear FE models of CLT buildings. (a) 5-storey building with vertical joints; (b) 5-storey building without vertical joints [1.25].

1.3 Evaluation and application of the fundamental seismic-design factors: the behaviour factor and the design over-strength

As mentioned above, available seismic codes which allow linear design methods, as alternatives to non-linear static or dynamic analysis on building superstructures, follow the approach commonly called Force Modification Design or FMD [1.31]. In these cases, each structural system requires the suitable choice of a “seismic force modification factor” or “behaviour factor”, called “R” in North America and “q” in Europe, which makes overall corrections to estimate design forces, accounting for all simplifications embedded within equivalent elastic design practice. Design codes specify R- or q-factors applicable to many types of superstructure walls and frameworks realized with various materials ([1.15];[1.32];[1.33]). With reference to timber shear-wall systems, different R- or q-factor values are provided, depending on expected ductility of the structural system. Eurocode 8 [1.15] defines some structural types and provides the q-factor for each one (Fig. 1.12), together with some criteria that have to be respected to use the proposed q-factor. This code considers three typologies of shear-wall systems: glued wall panels with glued diaphragms; nailed wall panels with glued diaphragms, nailed wall panels with nailed diaphragms. Considering this classification, normally CLT system is assigned a low value of behaviour factor, equal to 2.0, whereas nailed shear-wall systems (e.g., light frames) can be classified as high-ductility systems and a q-factor of 3.0 or 5.0 can be assigned, depending on the type of diaphragm and nailing.

Design concept and ductility class	q	Examples of structures
Low capacity to dissipate energy - DCL	1,5	Cantilevers; Beams; Arches with two or three pinned joints; Trusses joined with connectors.
Medium capacity to dissipate energy - DCM	2	Glued wall panels with glued diaphragms, connected with nails and bolts; Trusses with doweled and bolted joints; Mixed structures consisting of timber framing (resisting the horizontal forces) and non-load bearing infill.
	2,5	Hyperstatic portal frames with doweled and bolted joints (see 8.1.3(3)P).
High capacity to dissipate energy - DCH	3	Nailed wall panels with glued diaphragms, connected with nails and bolts; Trusses with nailed joints.
	4	Hyperstatic portal frames with doweled and bolted joints (see 8.1.3(3)P).
	5	Nailed wall panels with nailed diaphragms, connected with nails and bolts.

Fig. 1.12 – Table 8.1 of Eurocode 8 [1.15]. Behaviour factor values for timber structures.

Recent studies and tests have obtained higher q-factors than 2.0 for CLT system (e.g., [1.19];[1.34]-[1.36]) but lower q-factor than 5.0 for nailed shear-wall systems (e.g., [1.21];[1.37]-[1.38]). The evaluation of the suitable q-factor for timber shear-wall buildings is therefore still an open issue.

Q-factor can be expressed as the product between two sub-factors taking into account respectively of the “intrinsic” energy dissipation capacity proper of the structural system and of all “external” contributes to over-strength. This leads to the definition of separate sub-factors, which can be called “intrinsic q-factor” and “design over-strength” [1.27]. The first sub-factor, henceforth called

q_0 , takes into account the dissipative capacity of the system, given by its ductility and hysteresis dissipation, and all intrinsic over-resistances (e.g. due to post-elastic hardening behaviour). The design over-strength, henceforth called Ω , is used to quantify the difference between the required and the actual strength of a material, a component or a structural system [1.39]. As emphasised by Boudreault et al. [1.40], the design over-strength factor depends on all components which give rise to over-sizing of the structure, e.g., choice of member size, rounding and factored resistances, partial resistance coefficient γ_m and load duration coefficient k_{mod} , to change from the characteristic 5% resistance to the design value (e.g., computation of design capacity for fasteners and nails) [1.26]. In other words, the q-factor is not only an “intrinsic” property of the structure, but it is also strictly related to the adopted seismic design code and the safety level assumed by designers. A precise estimation of design over-strength is difficult, in particular for complex structures, because of many factors of uncertainty [1.41], whereas the definition of “intrinsic” q-factor requires many tests and simulations on components or entire buildings with different geometric characteristics.

Codes generally refer to a unique factor that takes into account energy dissipation, intrinsic over-resistances and design over-strength, since the design acceleration is typically lower than yield acceleration [1.42]. The Eurocode 8 definition [1.15] of the q-factor for timber structures does not explicitly explain strength reserve [1.41]. Conversely, other codes clearly define two sub-factors. The most general definition is that proposed by Canadian standards. Its assigned value is the same as the product of two sub-factors: R_d = ductility related force modification factor, accounting for deviation from ideal linear-elastic behaviour; and R_o = over-strength related force modification factor, accounting for the capacity of the system to redistribute forces after damage [1.33]. According to this definition, R_d represents the extent to which the structure dissipates energy, i.e., it is “intrinsic” to its behaviour factor. In US codes [1.43], R values explain both strength reserve and ductility [1.32].

The definition of these two sub-factors is therefore fundamental for the seismic characterization of a structural system and a correct seismic design. A definition can be given, referring to monotonic- or cyclic-loading tests of simple shear-wall specimens. As shown in Fig. 1.13a, q_0 -factor, for a shear wall or any other type of substructure, is defined as the ratio between the maximum base shear strength achieved when the behaviour of the structure is assumed to be perfectly elastic (F_e) and the yielding base shear strength (F_y), obtained from real non-linear behaviour. Ultimate elastic force F_e can be obtained by applying the principle of equal energy between the elastic response and the bi-linear envelope response, fitting the real non-linear response of the structure. Directly from the definition of ductility ratio μ - obtained as the ratio between ultimate displacement d_u of the structure and yielding displacement d_y , Fig. 1.13a - the method of Newmark and Hall [1.44] allows to obtain the q_0 -factor, according to period T of the structure (equations (1.1) to (1.3)):

$$\begin{array}{l} \textit{Principle of equal displacement} \\ q_0 = \mu \qquad \qquad \qquad \text{for } T > 0.5 \text{ s} \end{array} \qquad (1.1)$$

$$\begin{array}{l} \textit{Principle of equal energy} \\ q_0 = \sqrt{2\mu - 1} \qquad \qquad \text{for } 0.1 \text{ s} < T < 0.5 \text{ s} \end{array} \qquad (1.2)$$

$$\begin{array}{l} \textit{Principle of equal acceleration} \\ q_0 = 1 \qquad \qquad \qquad \text{for } T < 0.03 \text{ s} \end{array} \qquad (1.3)$$

As shown in Fig. 1.13b, design over-strength value Ω can be defined for a substructure as the ratio between the yielding force and design force F_d , which, in shear-wall systems, is normally a function of the design procedure of metal connectors.

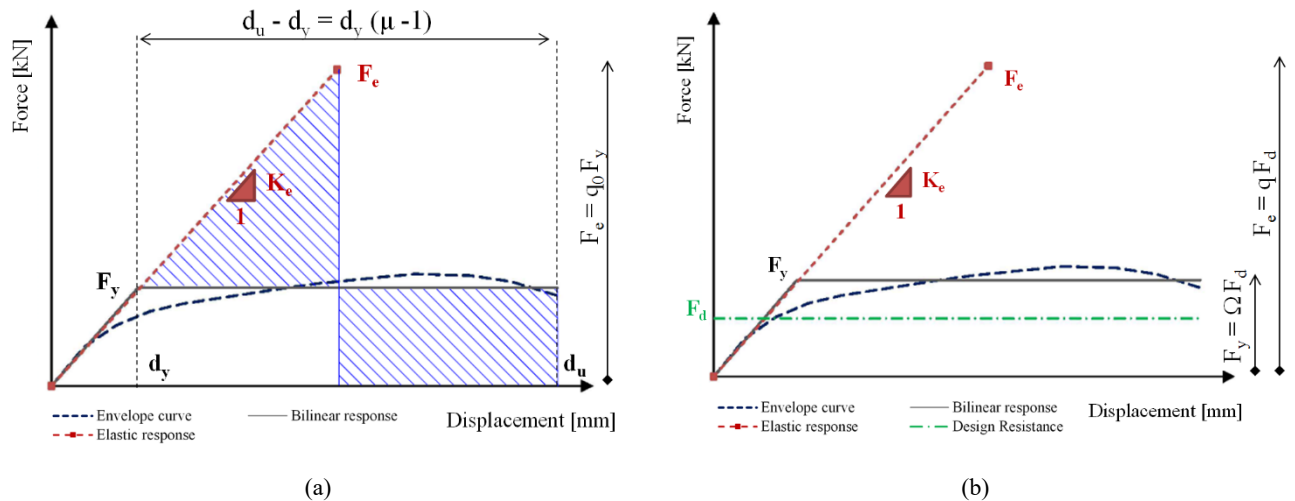


Fig. 1.13 – (a) Bi-linearization of envelope curve and estimation of q_0 ; (b) bi-linearization of envelope curve and estimation of Ω and q . [1.45]

Studies and results reported in the following chapters have the aim of providing information on the q_0 -factor for three massive shear-wall systems (CLT and two typologies of non-glued walls) and a novel hybrid light-frame system. Numerical and analytical methods are used, referring to Eurocode 5 [1.26] and Eurocode 8 [1.15]. According to this code, the q -factor value should be further reduced by a k_R coefficient, equal to 0.8, if the building suffers of in-elevation irregularity. Analyses presented in Chapter 2 will allow to verify this coefficient for CLT system and to provide information on the applicability of the regularity criteria.

Globally, the q -factor is henceforth defined as product between two sub-factors and a reduction coefficient (Fig. 1.14).

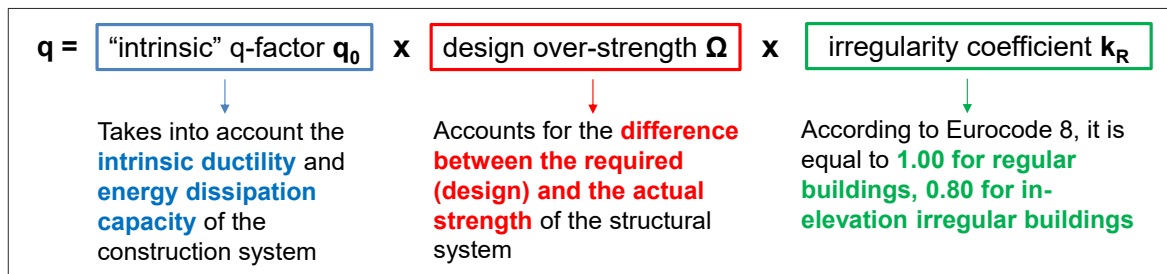


Fig. 1.14 – Definition of q -factor.

1.4 Conclusions

This chapter presented the main definitions and methods, according to European codes, for the seismic design of timber shear-wall systems, with main focus on current open issues, as modelling strategies to represent correctly the seismic-resisting components (i.e., connections) and definition and evaluation of the behaviour factor as product of three sub-factors, which account for energy dissipation capacity, design over-strength and elevation regularity.

The primary finding is that the design of complex timber structures can be inaccurate if proper attention is not paid to represent the connection stiffness. This can lead to incorrect sizing of

seismic-resisting elements and inaccurate predictions of inter-storey drifts. For these reasons, it is important that design standards give specific guidance related to determination of initial stiffness as well as capacities of connections.

An original aspect is the definition of a design approach based on an iterative method to perform reliable models, in which stiffness, strength, required resistance and limitation of drifts are consistent each other. This leads to the definition of modelling strategies for the correct evaluation of the building deformability with linear models, representing the main ductile components, i.e., base connections, inter-storey connections, vertical joints and bracing system.

References – Chapter 1

- [1.1] Pauley, T., and Priestley, M.J.N (1992). “Seismic design of reinforced concrete and masonry buildings”. Wiley Ed.
- [1.2] Jorissen, A., and Fragiaco, M. (2011). “General notes on ductility in timber structures”. *Engineering Structures*, 33:2987-2997.
- [1.3] Gattesco, N., Boem, I., and Gratton, L. (2015). “Analysis of the behavior of nailed timber frame shear walls through experimental tests and numerical simulations.” In proceedings of ANIDIS, L’Aquila, Italy.
- [1.4] Gavric, I., Fragiaco, M., and Ceccotti, A. (2013). “Capacity seismic design of X-LAM wall systems based on connection mechanical properties.” In proceeding of Meeting 46 of the Working Commission W18-Timber Structures, CIB, Vancouver, Canada, paper CIB-W18/46-15-2.
- [1.5] Popovski, M., and Gavric, I. (2015). “Performance of a 2-Story CLT House Subjected to Lateral Loads”. *Journal of Structural Engineering*, ASCE. DOI 10.1061/(ASCE)ST.1943-541X.0001315.
- [1.6] Källsner, B., and Girhammar, U.A. (2009). “Analysis of fully anchored light-frame timber shear walls—elastic model”. *Materials and Structures*, 42:301–320.
- [1.7] Casagrande, D., Rossi, S., Sartori, T., and Tomasi, R. (2015). “Proposal of an analytical procedure and a simplified numerical model for elastic response of single-storey timber shear-walls”. *Construction and Building Materials*, DOI: 10.1016/j.conbuildmat.2014.12.114.
- [1.8] Casagrande, D., Rossi, S., Tomasi, R., and Mischi, G. (2015). “A predictive analytical model for the elasto-plastic behaviour of a light timber-frame shear-wall”. *Construction and Building Materials*, DOI: 10.1016/j.conbuildmat.2015.06.025.
- [1.9] Gavric, I., Fragiaco, M., and Ceccotti, A. (2015). “Cyclic behaviour of CLT wall systems: experimental tests and analytical prediction models”. *Journal of Structural Engineering*, ASCE. DOI: 10.1061/(ASCE)ST.1943-541X.0001246.
- [1.10] Fragiaco, M., Dujic, B., and Sustersic, I. (2011). “Elastic and ductile design of multi-storey crosslam massive wooden buildings under seismic actions”. *Engineering Structures*, 33:3043-3053.
- [1.11] Sustersic, I., Fragiaco, M., and Dujic, B. (2011). “Influence of connection properties on the ductility and seismic resistance of multi-storey cross-lam buildings”. In proceeding of Meeting 44 of the Working Commission W18-Timber Structures, CIB, Alghero, Italy, paper CIB-W18/44-15-9.
- [1.12] Fragiaco, M. (2013). “Seismic behaviour of Cross-laminated timber buildings: numerical modelling and design provisions”. *European Conference on Cross Laminated Timber (CLT), COST Action*

FP1004, Graz. Edited by Harris, R., Ringhofer, A., and Schickhofer, G.

- [1.13]Gavric, I., Fragiaco, M., and Ceccotti, A. (2015). "Cyclic behaviour of typical metal connectors for cross-laminated (CLT) structures". *Materials and Structures*, 48:1841-1857.
- [1.14]Gavric, I., Fragiaco, M., and Ceccotti, A. (2014). "Cyclic behaviour of typical screwed connections for cross-laminated (CLT) structures". *Eur. J. Wood Prod.*, DOI 10.1007/s00107-014-0877-6.
- [1.15]EN 1998-1-1 Eurocode 8 (2004). "Design of structures for earthquake resistance, part 1: general rules, seismic actions and rules for buildings". CEN. Brussels, Belgium.
- [1.16]Follesa, M., Fragiaco, M., Vassallo, D., Piazza, M., Tomasi, R., Rossi, S., and Casagrande, D. (2015). "A proposal for a new Background Document of Chapter 8 of Eurocode 8". In proceedings of 2nd International Network on Timber Engineering Research (INTER), Šibenik, Croatia.
- [1.17]Dujic, B., Strus, K., Zarnic, R., and Ceccotti, A. (2010). Prediction of dynamic response of a 7-storey massive XLam wooden building tested on a shaking table". In proceedings of the 11th World Conference on Timber Engineering WCTE, Riva del Garda, Italy.
- [1.18]Pei, S., van de Lindt, J.W., and Popovski, M. (2013). "Approximate R-Factor for Cross-Laminated Timber Walls in Multistory Buildings". *Journal of Architectural Engineering* **19(4)**:245–255. ASCE.
- [1.19]Pozza, L., Scotta, R., Trutalli, D., Ceccotti, A., and Polastri, A. (2013). "Analytical formulation based on extensive numerical simulations of behavior factor q for CLT buildings." In proceedings of meeting 46 of the Working Commission W18-Timber Structures, CIB, Vancouver, Canada. Paper CIB-W18/46-15-5.
- [1.20]Pozza, L., Scotta, R., Trutalli, D., Polastri, A., and Ceccotti, A. (2015). "Concrete-Plated Wooden Shear Walls: Structural Details, Testing, and Seismic Characterization." *Journal of Structural Engineering*. ASCE. DOI 10.1061/(ASCE)ST.1943-541X.0001289.
- [1.21]Gattesco, N., and Boem, I. (2015). "Seismic performances and behavior factor of post-and-beam timber buildings braced with nailed shear walls". *Engineering Structures* **100**:674–685.
- [1.22]Foliente, G.C. (1996). "Issues in seismic performance testing and evaluation of timber structural systems". *Proceedings of the International Timber Engineering Conference*. Vol. **1**:29–36.
- [1.23]EN 12512 (2001). "Timber structures—test methods—cyclic testing of joints made with mechanical fasteners". CEN. Brussels, Belgium.
- [1.24]Muñoz, W., Mohammad, M., Salenikovich, A., and Quenneville, P. (2008). "Need for a harmonized approach for calculations of ductility of timber assemblies". In *Proceedings of Meeting 41 of the Working Commission W18-Timber Structures*, St Andrews, Canada, paper CIB-W18/41-15-1.
- [1.25]Polastri, A., Pozza, L., Trutalli, D., Scotta, R., and Smith, I. (2014). "Structural characterization of multi-storey buildings with CLT cores." In proceedings of the World Conference on Timber Engineering (WCTE), 10-14 August 2014, Quebec City, Canada.
- [1.26]EN 1995-1-1 Eurocode 5 (2004). "Design of timber structures, Part 1-1, General: Common rules and rules for buildings". CEN. Brussels, Belgium.
- [1.27]Pozza, L., Scotta, R., Trutalli, D., and Polastri, A. (2015). "Behaviour factor for innovative massive timber shear walls". *Bulletin of Earthquake Engineering*, **13(11)**:3449-3469. DOI 10.1007/s10518-015-9765-7.
- [1.28]Schädle P., and Blaß, H.J. (2010). "Earthquake behaviour of modern timber construction systems". In *Proceedings of the 11th World Conference on Timber Engineering WCTE*, Riva del Garda, Italy.

- [1.29]Ceccotti, A. (2008). "New technologies for construction of medium-rise buildings in seismic regions: the XLAM case". *Structural Engineering International* **18(2)**:156-165.
- [1.30]Rinaldin, G., Amadio, C., and Fragiaco, M. (2013). "A component approach for the hysteretic behaviour of connections in cross-laminated wooden structures". *Earthquake Engineering and Structural Dynamics* **42**:2023-2042.
- [1.31]Chopra, A.K. (1995). "Dynamics of Structures - Theory and Applications to Earthquake Engineering". Upper Saddle River, NJ, Prentice Hall.
- [1.32]ASCE (2010). "Minimum design loads for buildings and other structures". ASCE 7-10, Washington, DC.
- [1.33]NBCC (2010). "National Building Code of Canada". Institute for Research in Construction, National Research Council of Canada, Ottawa, Ontario.
- [1.34]Ceccotti, A., Follesa, M., Lauriola, M.P., Sandhaas, C., Minowa, C., Kawai, N., and Yasumura, M. (2006b). "Which seismic behaviour factor for multi-storey buildings made of cross-laminated wooden panels?" In proceedings of Meeting 39 of the Working Commission W18-Timber Structures, Florence, Italy, paper CIB 39-15-2.
- [1.35]Pozza, L., and Scotta, R. (2014). "Influence of wall assembly on behaviour of cross-laminated timber buildings". *Proceedings of the ICE - Structures and Buildings* **168(4)**:275-286.
- [1.36]Pei, S., van de Lindt, J.W., and Popovski, M. (2013). "Approximate R-Factor for Cross-Laminated Timber Walls in Multistory Buildings". *Journal of Architectural Engineering* **19(4)**:245-255. ASCE.
- [1.37]Germano, F., Metelli, G., and Giuriani, E. (2015). "Experimental results on the role of sheathing-to-frame and base connections of a European timber framed shear wall". *Construction and Building Materials* **80**:315-328.
- [1.38]Follesa, M. (2015). "Seismic design of timber structures - A proposal for the revision of Chapter 8 of Eurocode 8". Phd Thesis, Università degli Studi di Cagliari, Italy.
- [1.39]Elnashai, A.S., and Di Sarno, L. (2008). "Fundamentals of Earthquake Engineering". Wiley, UK.
- [1.40]Boudreault, F.A., Blais, C., and Rogers, C.A. (2007). "Seismic force modification factors for light-gauge steel-frame - wood structural panel shear walls". *Can. J. Civ. Eng.* **34(1)**: 56-65.
- [1.41]Elnashai, A.S., and Mwafy, A.M. (2002). "Overstrength and force reduction factors of multi-storey reinforced-concrete buildings". *Struct. Des. Tall Build.* **11**:329-351.
- [1.42]Fajfar, P. (2000). "A nonlinear analysis method for performance based seismic design". *Earthq. Spectra*, **16(3)**:573-592.
- [1.43]Uniform Building Code (UBC). (1997). "International Conference of Building Officials", Whittier, CA.
- [1.44]Newmark, N.M., and Hall, W.J. (1982). "Earthquake Spectra and Design". Earthquake Engineering Research Institute, Berkeley, CA.
- [1.45]Pozza, L., Scotta, R., Trutalli, D., Polastri, A., and Smith, I. (2016). "Experimentally based q-factor estimation of cross-laminated timber walls". *Proceedings of the ICE - Structures and Buildings*. DOI: 10.1680/jstbu.15.00009.

Chapter 2 Seismic behaviour of CLT system

Abstract

The structural behaviour of the cross-laminated timber technology, which represents one of the most common timber structural systems, is analysed. The concepts of ductility, dissipative capacity, regularity and irregularity applied to CLT system are provided. The seismic response and the dissipative capacity of this system are evaluated via an experimentally based procedure. Then, the evaluation of its intrinsic dissipative capacity in function of construction variables is determined via non-linear numerical modelling. The results show that the construction design decisions strongly affect the seismic response of buildings. Hence, a single behaviour-factor cannot be representative indistinctly of all CLT buildings. A statistical analysis applied to numerical results allowed to propose analytical formulations for the proper intrinsic behaviour factor value for regular buildings. Then, the same analyses carried out on in-elevation irregular buildings returned a single modification factor k_R to account for the reduction of seismic capacity due to irregularity.

2.1 Introduction and state of the art

2.1.1 Advantages in the use of CLT

The cross-laminated timber panel represents a new technology and an effective construction material, with significant potential for use in multi-storey earthquake-resistant buildings. In recent years, the CLT structure has become quite widely employed to realize multi-storey residential and non-residential buildings.

This product was introduced in the late 1990s in Austria and Germany and has been gaining popularity in Europe, North America and Australasia, thanks to the advantages in the use as wall or floor system. The strength and stiffness capacities of CLT panels have been analysed by various researches: these panels can be loaded effectively in plane and/or out of plane, as floor, walls, shear walls or beams (e.g., [2.1]-[2.8]). The load carrying capacity of joints in CLT panels has also been studied (e.g., [2.9]-[2.11]) in order to apply the Johansen's yield theory [2.12]. In seismic-prone countries, like Italy – where CLT is better known as X-Lam – its application is particularly advantageous due to its good weight-to-strength ratio, especially if compared with traditional use of concrete, masonry or steel. However, knowledge and code development about the seismic response of this structural system are still limited and research activities are fundamental to provide the necessary background.

Various advantages make CLT an excellent construction material and competitive with traditional constructive systems. CLT panels consist of multiple layers of massive timber boards stacked crosswise and glued together. The cross-section has at least three layers but it can have up to eleven layers, for thickness up to 500mm. Length and width of the panel can be up to 24.0 m and 4.80 m respectively, depending on production site [2.13]. The first advantage regards therefore the realization of large plane elements of massive timber that is favourable both for static and seismic conditions. Other important advantages can be listed:

- The crossed layers improve dimensional stability, restraining the transversal deformation due to variation in moisture content. This phenomenon permits to realize floors with large CLT panels and few expansion joints;
- The cross-laminating process is favourable also for the resulting strength and stiffness of the panel, if subjected to in-plane loads;
- The high thickness allows to realize floors with high spans or, if used as wall elements, to realize high-rise buildings;
- The large plane elements permit to overcome the disadvantages of the use of light frames, thanks to a better stress distribution from roof to foundation;
- The large plane elements are favourable also for fire resistance, because only one face is exposed to fire and the material insulates the compartments nearby [2.14].

The CLT panels are used also as shear walls, to resist efficiently to seismic actions. The considerable advantages in the use of this material as seismic force resisting system (SFRS) are mainly due to the high in-plane strength and stiffness of the panel itself and the possibility of realizing stiff panel-to-panel joints at floors, walls and between them, obtaining a box-like behaviour.

2.1.2 Current research on the seismic behaviour of CLT system

The seismic behaviour of CLT technology has been widely studied through experimental tests and numerical simulations. The most comprehensive experimental research on the seismic behaviour of low- and medium-rise CLT buildings has been carried out by CNR-IVALSA at San Michele all'Adige (Trento, Italy) during the SOFIE Project ([2.14]-[2.18]) that also addressed fire, acoustical and non-structural performance of such system. The performed shake-table tests on a three-storey and a seven-storey building demonstrated that, after a series of destructive earthquakes with high values of PGAs, *not only does this construction system help to avoid loss of human lives but the infrastructural losses can also be kept smaller and observed damage can be easily repaired if accessible* [2.18]. In Canada, Slovenia, Macedonia, Portugal and Japan other tests were performed to determine the structural properties, failure mechanisms and seismic resistance of CLT shear walls and 3-D structures ([2.19]-[2.26]), Fig. 2.1.

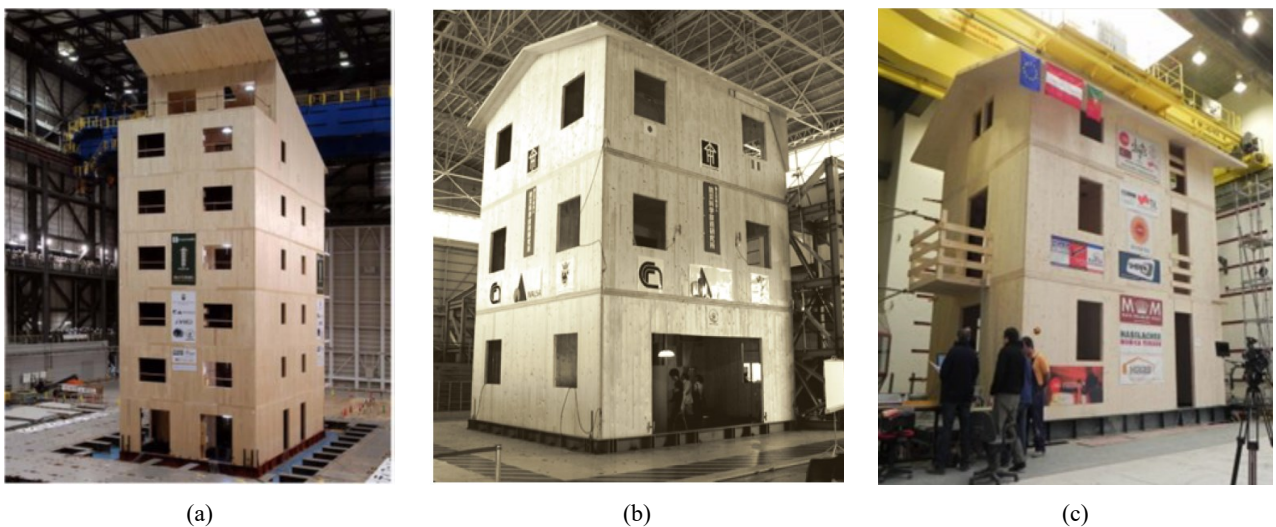


Fig. 2.1 - Shake-table tests: (a)(b) SOFIE project [2.14][2.17] and (c) Timber Buildings project [2.26].

The aforementioned tests of full-scale shear walls and buildings showed that timber panels remain elastic with limited damage, whereas connections undergo high deformation and fail. Therefore, the primary basic concept is that the seismic performance of CLT buildings is related to the capability of connections to do plastic work if loaded over yielding, whereas timber elements have limited capability to deform inelastically [2.27]. However, this favourable behaviour is not always ensured ([2.20];[2.28]) and CLT structures might have low ductility and dissipative capacity if failure occurs before the complete plasticization of ductile components, i.e., connections. This possible brittle behaviour is mainly due to typology, arrangement and design of connection system.

Tests of connectors typically used in CLT buildings (angle brackets, hold-downs, screws and nails – Fig. 2.2) have defined their behaviour (e.g., [2.29]-[2.35]). Then, their non-linear behaviour was modelled numerically, in order to simulate the earthquake effects on buildings and define their seismic behaviour and proper seismic design rules of connections (e.g., [2.36]-[2.43]). These traditional connections are mainly characterized by:

- ductile and dissipative behaviour concentrated in nailing;
- brittle behaviour of the steel plates and of the anchorage to foundation;
- a preferable uniaxial load application;
- a reduction in dissipative capacity for repeated loading cycles due to wood-embedment phenomenon caused by nail deformation (pinching behaviour).

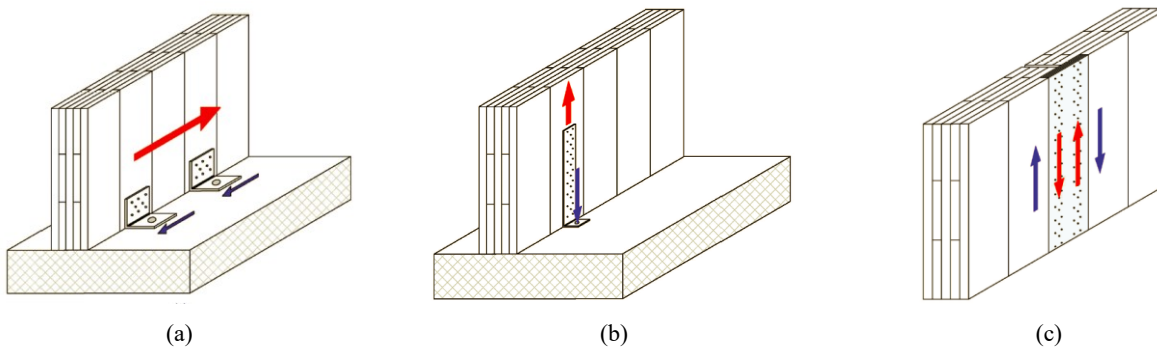


Fig. 2.2 - Traditional connections for CLT structures: (a) angle brackets loaded in shear; (b) hold-down loaded in tension; (c) panel-to-panel vertical joint loaded in shear. [2.42]

To optimize the seismic response of CLT structures and to overcome one or more unfavourable characteristics of traditional connections, homemade devices have also been proposed in literature ([2.44]-[2.48]), Fig. 2.3.

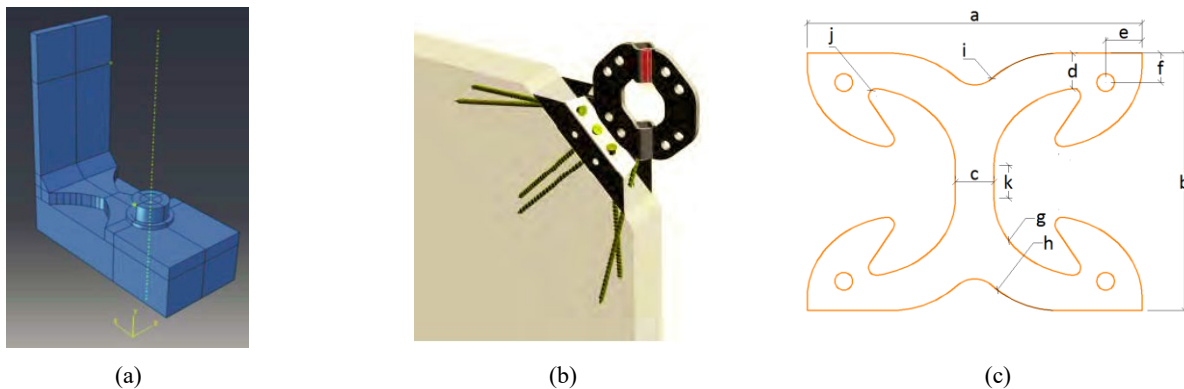


Fig. 2.3 - Innovative connections for CLT structures: (a) [2.44]; (b) [2.46]; (c) [2.48].

Aforementioned tests are necessary to quantify the most important parameters for the seismic characterization of a CLT structure, as strength, stiffness and ductility, that can be fully assessed with quasi-static cyclic-loading tests, according to EN12512 [2.49]. However, extensive analyses of test data are required to obtain provisions for the seismic design of these structures, e.g., to assess the correct value of the behaviour factor and its possible variability. These analyses could require also complex numerical models, as those discussed in section 1.2.2.

According to current seismic standards and codes (e.g., Eurocode 8 [2.50]) CLT structures with regular geometry can be designed for the effects of seismic loadings based on equivalent static force design criteria, applying a suitable q -factor to take account of non-linear behaviour and dissipative capacity of the structural system. However, as no R or q values have yet been specified in any codes for buildings with CLT panel walls, those factors must currently be assigned very conservative values. Moreover, a single value is prescribed by codes for CLT structures, independently from design decisions, building configuration and expected ductility due to correct application of the capacity design (see section 1.1).

Actually, the considerable development of CLT panels as building material has been flanked by the development of several construction methods, differing mainly in the dimensions and arrangement of the panels used to assemble the walls. In detail, walls may be composed of a single CLT panel or by proper assembly of narrow panels. From the construction viewpoint, it would be preferable to use CLT panels as large as possible to minimise the number of on-site joints. Recently, however, it

has become more common to use small modular CLT panels, which have other advantages, e.g., easier lifting and handling, simpler modularisation and minimal material waste. Structurally, the change is important, because smaller panels require increasing the number of on-site joints, which greatly affect the displacement capacity and therefore the seismic behaviour of CLT buildings. It is therefore highly reasonable to expect that appropriate values of R or q should be higher than those applicable to walls exhibiting brittle characteristics and that these values could vary with the chosen construction method.

The q -factor of a CLT building could be defined as a function of various parameters. (1) If the building is correctly designed, the number of storeys has a direct effect on the seismic response: the number of panel-to-floor connections, which are responsible of the dissipative capacity of the system, increases with storey number, therefore, also the overall dissipative capacity of the building could increase. (2) The number of panel-to-panel joints strongly influences the building dissipative and displacement capacities and its resulting ductility. (3) Slenderness - defined as the ratio between the height and base dimensions of the building - determines its response: squat buildings are more prone to shear failure mechanisms, whereas greater slenderness induces flexural and rocking behaviour. All these characteristics are directly influenced by the criterion used to design the connections: only if a correct capacity design approach – that allows to avoid brittle failure – is applied [2.38] and the largest number of connections can achieve the post-elastic behaviour, the SFRS guarantees the maximum dissipative capacity. No criteria are given by codes to take account for these three parameters.

Another parameter directly correlates with CLT-building seismic response is the regularity. In-plan regularity influences the distribution of the horizontal seismic forces among the shear walls of the structure. This phenomenon can be controlled with the use of 3D models of the structure. In-elevation regularity affects the transmission of seismic forces through each storey, down to the building foundations. Eurocode 8 [2.50] provides some criteria for regularity in elevation applicable to all structural materials and prescribes to reduce the reference q -factor value by 20%. No additional provisions are given for timber structures.

Past experimental evidence about CLT shear-wall behaviour has been collected on single case studies and therefore does not provide information fully generalizable to the system. Moreover, the criteria for regularity in elevation and their applicability to CLT structures are not fully exhaustive yet. In this chapter, tests are analysed to clarify how the characteristics of the walls themselves can influence a building response during a seismic event and to study the effects of construction variables on the behaviour factor. The following aspects are discussed:

- An experimentally-based method is used to compute a preliminary estimation of the behaviour factor as the product between the intrinsic part q_0 and the design over-strength Ω , computed from the design lateral strength of CLT;
- A numerical campaign on various CLT-building configurations is presented to analyse the variability of their seismic response;
- The criteria for regularity in elevation are clarified and additional numerical simulations are presented with the aim to verify the reduction of the behaviour factor value.

2.2 Evaluation of the seismic response with an experimentally-based procedure

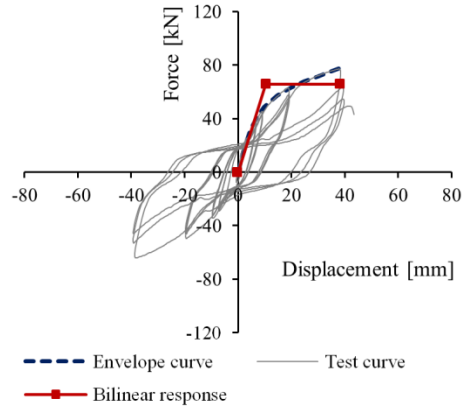
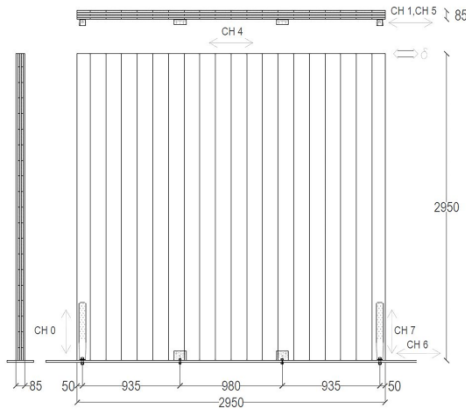
Research results presented in this section are partially available at ICE virtual library via <http://dx.doi.org/10.1680/jstbu.15.00009> [2.51]. *Journal Structures and Buildings – Proceedings of the ICE* is acknowledged as the original source of publication.

2.2.1 Tested specimens and results

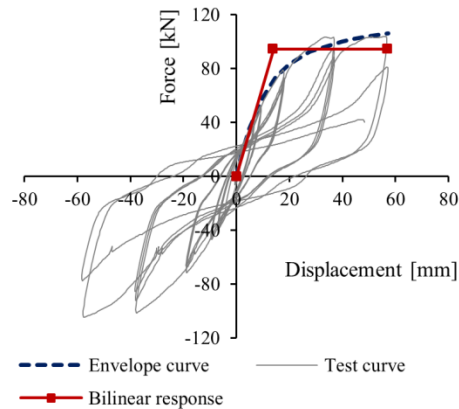
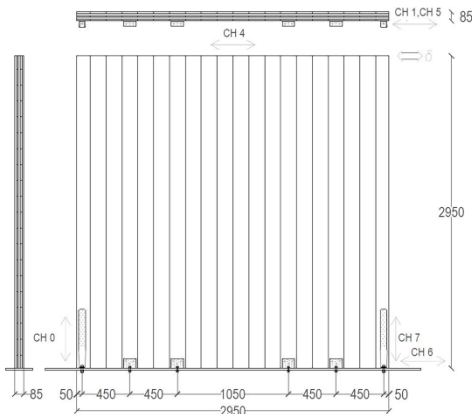
Five CLT wall specimens with different panel and connection configurations (A-1, A-2, B-1, B-2, C), were tested during the SOFIE project [2.35] with quasi-static cyclic loading protocol, according to EN 12512 [2.49]. Fig. 2.4 shows the geometrical characteristics and fastener arrangements of the tested walls. All panels are composed of 5 layers of 17-mm thick timber boards, resulting in a total panel thickness of 85 mm. Each specimen is anchored to foundations with commercial connections (hold-downs and angle brackets) of the types listed in Table 2.1. These steel elements are connected to the panels with 4x60-mm ring shank nails. Specimens A are composed of one CLT panel; specimens B and C had two half-width CLT panels with a vertical panel-to-panel joint. In detail, specimens B-1 and C have a half-lap joint in the middle (Fig. 2.4c and Fig. 2.4e), realized with 8x100-mm screws inclined 35° with respect to the horizontal. Specimen B-2 (Fig. 2.4d) is composed of two CLT panels vertically jointed with a Laminated Veneer Lumber (LVL) strip 175-mm wide, connected to both panels using 8X100-mm screws inclined 35° with respect to the horizontal. The screws used to join the panels of type B specimens have the same spacing, 150 mm; specimen C is made with a weak half-lap joint (screw spacing 500 mm), with two extra hold-downs at the foundation to resist rocking (Fig. 2.4e). An equal vertical load of 18.5 kN/m was applied during tests to all compared specimens. The differences of the specimens enabled therefore the evaluation of the effects of different base anchorage systems and vertical construction joints on the behaviour of walls subjected to in-plane lateral force. For further details on specimen geometry and experimental test procedure, see ([2.35];[2.51];[2.52]).

Fig. 2.4 shows the recorded hysteresis cycles for each specimen obtained during tests, together with fitted non-linear envelope curves defined according to Foschi and Bonac [2.53] and fitted bi-linear envelope responses defined according to Equivalent Elastic-Plastic Energy (EEEP) method [2.54]. The comparison of the hysteresis responses shows that the most obvious difference among arrangements was how they influenced the maximum base shear force (or maximum lateral force) and the maximum horizontal displacement. As expected, increasing the number of shear-resisting angle brackets increased the base shear resistance, as seen by comparing type A walls. Moreover, the pure-sliding behaviour of wall A-1 causes failure for lower ultimate displacement than wall A-2. These results demonstrate that a wall connected at the base with under-designed angle brackets (i.e., failure of the wall is due to sliding) has impaired ductility and resistance. This is because the ultimate resistance and displacement of the wall depend only on the strength and ductility of the angle brackets (i.e., the weakest part of the system for specimen A-1), whereas hold-downs are deformed in shear and do not significantly affect the overall behaviour of the wall, due to their low value of shear stiffness and failure for buckling of the steel part. Applying other methods to obtain the bi-linear response, variations in yielding point estimation and therefore ductility occur (e.g., [2.35]). However, the increase of displacement capacity and resistance for wall A-2 remains valid. Analysis of force-displacement curves of type B specimens showed the

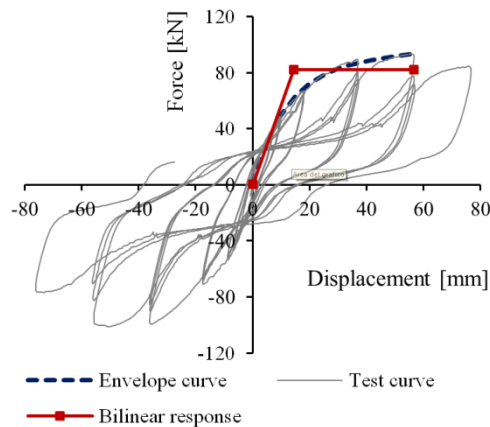
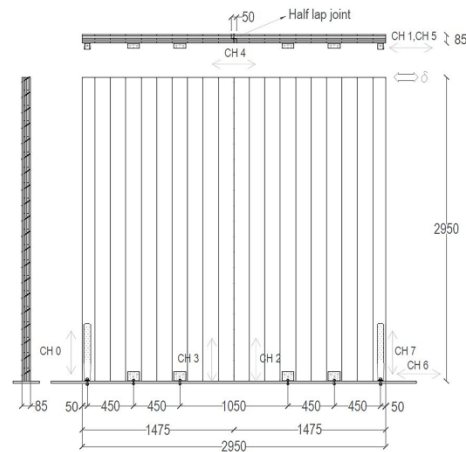
influence of different vertical joints on the overall response of the wall. Comparisons between wall B-1 (with vertical half-lap joint) and wall A-2 showed a slight increase in displacement capacity under cyclic loading, although this increase may be neglected because the wall failed before the end of the first cycle at higher amplitude. Wall B-2 (LVL joint) reached the highest ductility. Therefore, the presence of an LVL joint increases the ultimate top displacement of the wall, due to deformation of the base connections and sliding of two lines of screws at vertical joint. Lastly, wall C (with a weak half-lap joint and two extra hold-downs) showed good behaviour in terms of both ductility and resistance. Therefore, this connection arrangement can be effectively used as alternative to strong panel-to-panel joints



(a)



(b)



(c)

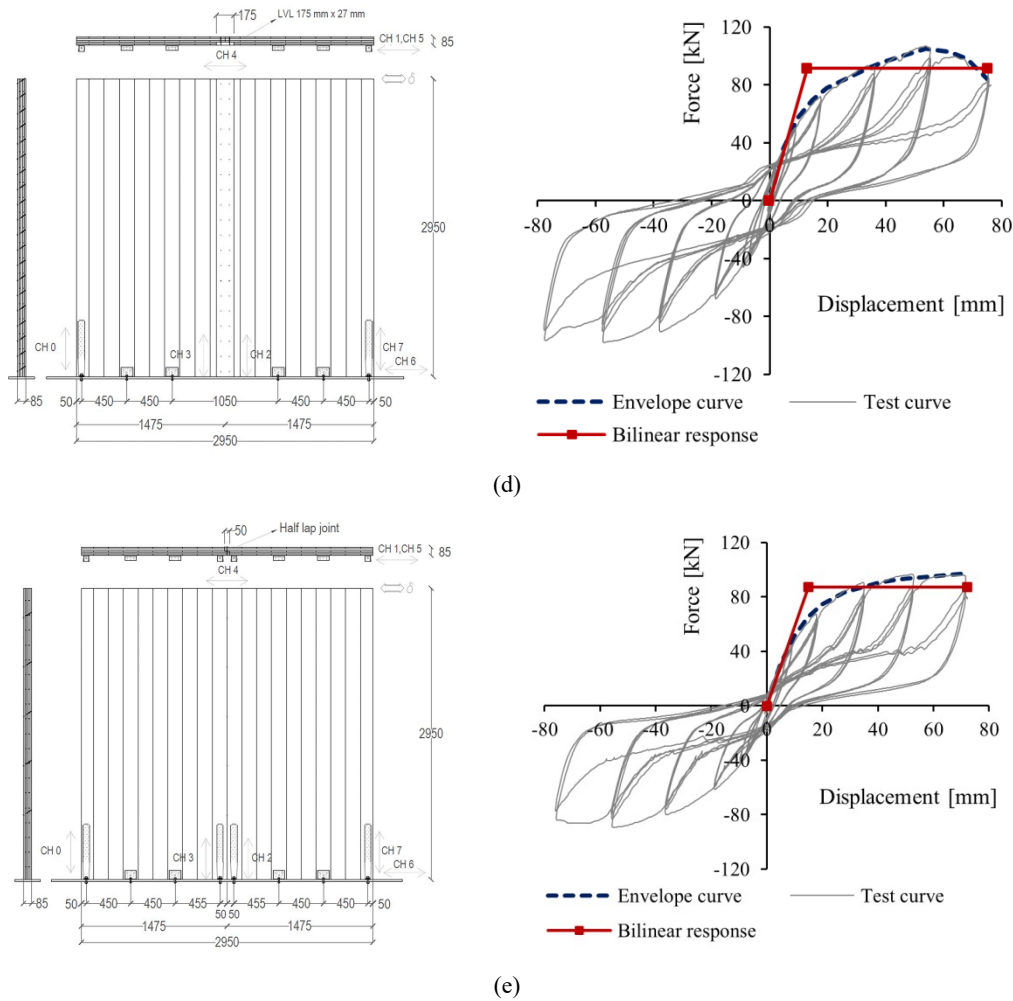


Fig. 2.4 – Geometric arrangement, hysteresis cycles, and envelope and bilinear curves of specimens: (a) A-1; (b) A-2; (c) B-1; (d) B-2; (e) C. [2.51]

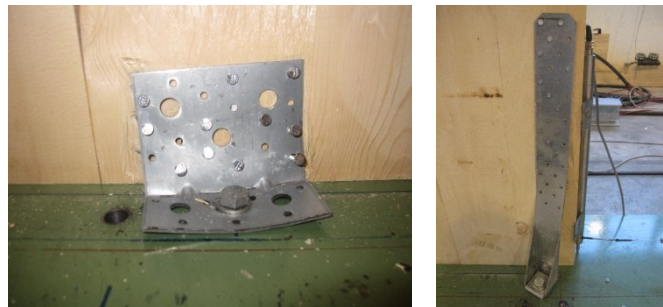
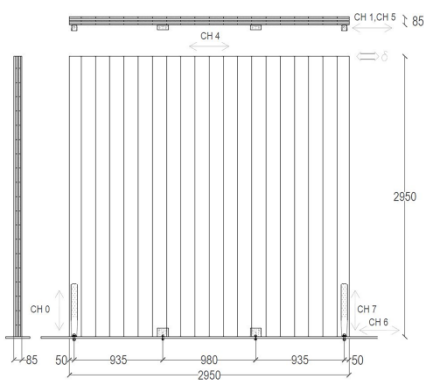
Table 2.1 - Type and number of wall connectors. (see also [2.35];[2.51])

Specimen	Base connectors		Nails		Vertical joint	
	Type	No.	Size	No.		
A-1	Hold-down HTT22	2	4x60	12	No	
	Angle bracket BMF 90x48x3x116	2	4x60	11		
A-2	Hold-down HTT22	2	4x60	12	No	
	Angle bracket BMF 90x48x3x116	4	4x60	11		
B-1	Hold-down HTT22	2	4x60	12	Yes	
	Angle bracket BMF 90x48x3x116	4	4x60	11		
B-2	Hold-down HTT22	2	4x60	12	Yes	
	Angle bracket BMF 90x48x3x116	4	4x60	11		
C	Hold-down HTT22	4	4x60	12	Yes	
	Angle bracket BMF 90x48x3x116	4	4x60	11		
Specimen	Type of fastener	Inclination	Diameter [mm]	Length [mm]	No.	Spacing [mm]
B-1	Screw HBS 8x100	35°	8	100	20	150
B-2	Screw HBS 8x100	35°	8	100	2x20	150
C	Screw HBS 8x100	35°	8	100	5	500

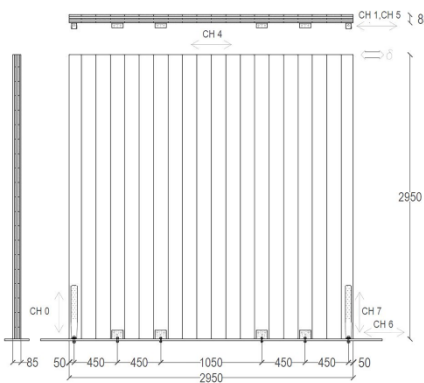
Fig. 2.5 shows specimens after tests. The photographs of the damaged anchorage of specimen A-1 (Fig. 2.5a) show that the base connections underwent extensive sliding and moderate uplift deformation, which was not recoverable. Fig. 2.5b and Fig. 2.5d show that specimens anchored

with four angle brackets underwent rocking deformations, causing higher ultimate displacements. In specimen A-2 (Fig. 2.5b), deformations were concentrated at hold-downs and angle brackets, due to combined rocking and sliding [2.35]. This behaviour was also seen in wall B-1 (Fig. 2.5c), despite the presence of the vertical joint, so that similar results for these two walls are expected. At failure, specimens B-2 and C (Fig. 2.5d and Fig. 2.5e) showed moderate base sliding, extensive uplift, and relative displacement of the two half-width CLT panels. Fig. 2.5e (specimen C) shows failure concentrated in hold-downs and vertical panel-to-panel joint, due to rocking of the two panels and failure of screws and nails (pull-out of a screw and nails missing). Nevertheless, the wall preserved its resistance without marked loss in strength or an evident failure point, up to the top displacement of about 80 mm (maximum applied displacement). Fig. 2.5d shows similar failure modes: pull-out of screws in the middle joint and almost all hold-down nails missing. Since the screws used to join the CLT panels were inclined and had a relatively small slenderness ratio (length 100 mm, diameter 8 mm), the actual failure mode was tensile withdrawal without any plastic deformation in the metal connector.

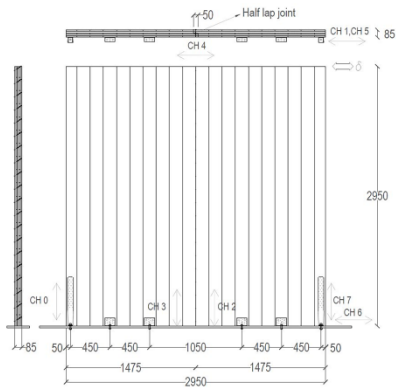
The failure modes described above imply that it is appropriate that q_0 -factor and design over-strength Ω depend on design variables (dimensions of CLT panels, and type, number and position of connections) and on the type of vertical joints. Although not explicitly investigated, q_0 and Ω should also depend on the anchoring systems applied at the tops of walls (storey-to-storey connections).



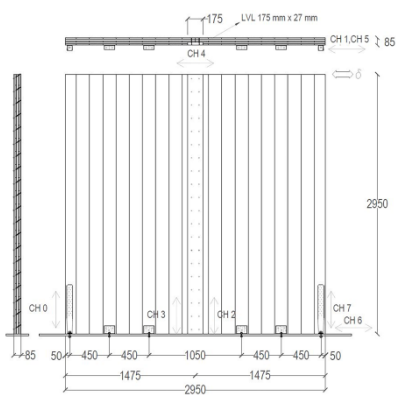
(a)



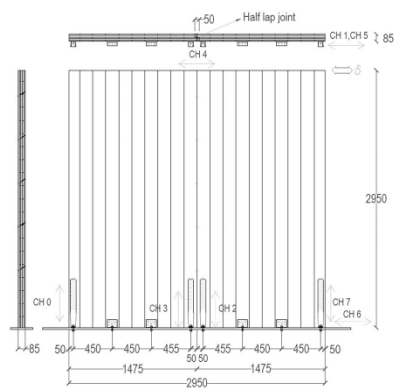
(b)



(c)



(d)



(e)



Fig. 2.5 – (a) Specimen A-1: large deformation of angle brackets, lateral yielding of hold-downs; (b) Specimen A-2: major deformation concentrated at hold-downs, and deformation of angle brackets; (c) Specimen B-1: predominant sliding and uplift of wall; (d) Specimen B-2: sliding, uplift and relative displacement of CLT plates; (e) Specimen C: pull-out of screws and nails missing due to shear failure. [2.51]

2.2.2 Analytical evaluation of CLT shear-wall capacity

As discussed in section 1.3, the definition of q-factor as product between q_0 and Ω depends on the application of a specific design code and method. This is mainly due to the definition of Ω -factor as function of design strength. Similarly, the analytical design procedures for determining the resistance of timber or steel parts and relative safety and corrective factors are based on code provisions (e.g., [2.50];[2.55]). For timber shear walls the design approach is normally based on assigning reference capacity in terms of resistance per unit of length of the wall. Such capacity includes definition of failure, wall geometry, base connection method, duration of loading, and service environment classification to which the design properties refer.

The analytical evaluation of reference shear-wall capacities for CLT walls here proposed is based on the provisions of Eurocode 5 [2.55]. However, this does not preclude the use of these results in non-European jurisdictions, because adjustments can be made for differences among reference conditions applicable in European Union countries and elsewhere.

2.2.2.1 Design calculation of lateral-load resistance

According to current practice, shear resistance is provided by angle-bracket connectors, which anchor wall panels at their bases [2.17]. Conversely, all uplift forces resulting from earthquake or wind are demanded to hold-downs. Although not fully realistic, in sake of simplicity in design practice it is normally assumed that angle brackets do not contribute to the rocking resistance of CLT walls, so that angle bracket tensile contributions are neglected. This leads to the mechanistic concept shown in Fig. 2.6, which is the basis for evaluating the reference shear-wall capacities reported here. This simplification was made in order to obtain results consistent with commonly adopted design assumptions, i.e., the axial strength of angle brackets is neglected due to the uncertainty of their position, since they are normally uniformly distributed along the base of the wall and are designed to resist shear forces. This assumption is also justified, as the experimental results of Gavric et al. [2.30] demonstrate that the axial stiffness and load-bearing capacity of angle brackets loaded in tension are about half that of hold-downs with about the same number of nails (11 for the angle brackets, 12 for the hold-downs). According to the approach shown in Fig. 2.6, the lateral-load resistance of the wall F_d , can be calculated from angle-bracket strength F_A and hold-down resistance F_{HD} .

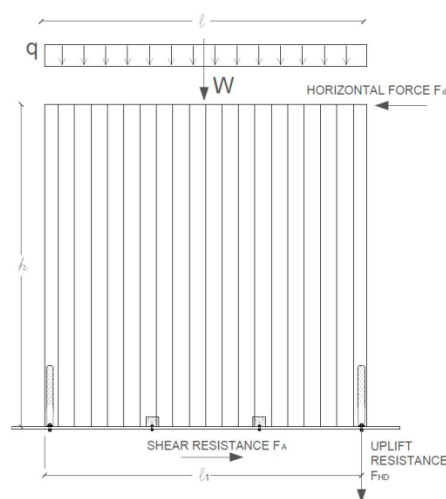


Fig. 2.6 - Definition and calculation of shear resistance F_A and uplift resistance F_{HD} . [2.51]

It follows from the above definition that lateral load resistance F_d of a single-storey wall of the type shown in Fig. 2.6 can be computed according to equation (2.1) as the minimum of the resistances associated with failure of angle brackets and hold-downs.

$$F_d = \min \left\{ F_A; \frac{1}{h} \left(I_1 F_{HD} + \frac{WI}{2} \right) \right\} \quad (2.1)$$

This equation is also valid for evaluating the resistance of jointed walls only if connectors at vertical joints are over-resistant with respect to the failure of base anchors (type B walls). In the case of wall C, the vertical joint was too weak to guarantee sufficient resistance to lateral loads and the continuity of the in-plane shear stiffness between the two panels composing the specimen. This means that the contribution of the vertical joint can be neglected and rocking is prevented by the four hold-downs (Fig. 2.5e). Equilibrium equation (2.1) is therefore still valid, considering each panel of the wall separately.

If F_A and F_{HD} are taken as the shear and hold-down resistance capabilities, the per-fastener resistances of angle brackets and hold-downs can be calculated according to Johansen's yield theory [2.12]. This theory is universally accepted, sometimes with minor modifications, as the basis for estimating the lateral capacity of slender fasteners like nails ([2.55];[2.56]). Here, the Eurocode 5 definition is used to calculate the characteristic single shear capacity per nail, called $F_{v,Rk}$ [2.55]. For the pertinent case of a thick steel plate, the Eurocode 5 lateral-load capacity per nail is (equation (2.2)):

$$F_{v,Rk} = \min \left\{ \begin{array}{l} f_{h,k} t_1 d \left[\sqrt{2 + \frac{4M_{y,Rk}}{f_{h,k} d t_1^2}} - 1 \right] + \frac{F_{ax,Rk}}{4} \\ 2.3 \cdot \sqrt{M_{y,Rk} f_{h,k} d} + \frac{F_{ax,Rk}}{4} \\ f_{h,k} t_1 d \end{array} \right\} \quad (2.2)$$

where:

- $f_{h,k}$ = characteristic embedment strength in the timber member;
- t_1 = depth of penetration of the fastener into the timber member;
- d = diameter of fastener;
- $M_{y,Rk}$ = characteristic fastener yield moment;
- $F_{ax,Rk}$ = characteristic withdrawal capacity of the fastener (associated with pulling the fastener out of the timber member).

In calculations described here, the characteristic embedment strength $f_{h,k}$ was computed according to Eurocode 5 for nails without pre-drilled holes [2.55] (equation (2.3)):

$$f_{h,k} = 0.082 d^{-0.3} \rho_k \quad (2.3)$$

where ρ_k is the characteristic value of panel density.

Fastener yield moment $M_{y,Rk}$ and withdrawal capacity of fastener $F_{ax,Rk}$ are parameters computed according to the manufacturers' technical certifications and are therefore product-specific. The design capacity per fastener/nail is therefore computed according to equation (2.4):

$$F_{d, \text{nail}} = F_{v,Rk} k_{\text{mod}} / \gamma_m \quad (2.4)$$

where k_{mod} is the modification factor which considers the combined influences of duration of loading and moisture; γ_m is the partial coefficient of the materials. In this analysis, $F_{v,Rk} = 2.02$ kN, based on the proprietary fastener information and properties of CLT (assumed values:

$M_{y,Rk} = 6.55 \text{ Nm}$; $F_{ax,Rk} = 1.32 \text{ kN}$; $t_1 = 55.6 \text{ mm}$; $\rho_k = 380 \text{ kg/m}^3$; and $k_{mod} = 1.10$, $\gamma_m = 1.00$, matching values in Eurocode 5 [2.55]. This results in the predicted design values for lateral load resistance F_d , listed in Table 2.2.

Table 2.2 - Design values of lateral load resistance F_d . [2.51]

Specimen	$F_{d,nail}$ [kN]	F_A [kN]	F_{HD} [kN]	F_d [kN]
A-1	2.22	48.84	26.64	48.84
A-2; B-1; B-2; C	2.22	97.68	26.64	54.85

2.2.2.2 Proposed procedure for estimation of q-factor

An experimental-analytical method based on Equivalent Energy Elastic-Plastic (EEEP) analysis of the shear-wall test results is proposed here for the determination of the q-factor. The main steps of the procedure are as follows (see definitions in section 1.3):

- Experimental evaluation of the load vs. displacement response and of the fitted envelope curve of a representative wall specimen with quasi-static monotonic or cyclic-loading tests;
- Bi-linearization of the envelope curve, with definition of the yielding limit (d_y , F_y) and therefore of elastic stiffness K_e and ductility μ , with balancing of strain energy by the EEEP method [2.54];
- Application of the method of Newmark and Hall [2.58], based on the ductility value to define the q_0 -factor;
- Computation of horizontal design force F_d and the corresponding design over-strength factor Ω .

This method can be applied, since pushover procedures are well-known to be able to substitute time-history analyses [2.59] in the case of structures conforming to regularity criteria [2.50].

2.2.2.3 Computation of q_0 and Ω

The bi-linearization of the experimental envelope curves by the EEEP method and consequent application of the procedure of Newmark and Hall [2.58] allow to evaluate the q_0 -factor as function of ductility μ . The evaluation of design over-strength factor Ω is given by the ratio between yielding force F_y obtained with EEEP method and design force F_d defined by code. Table 2.3 and Fig. 2.7 summarise the results obtained from the application of EEEP method, the related q_0 and Ω , and the q-factor estimate. Table 2.3 also shows the value of design force F_d , applied mass M , elastic period of idealised bi-linear system T [2.59], elastic stiffness of bi-linear response K_e and yielding point values, for each specimen.

Table 2.3 - Results of analysis of test data to obtain q_0 and Ω , based on $F_{d,nail} = 2.22 \text{ kN}$. [2.51]

Spec.	Design failure mechanism	Actual failure mechanism	F_y [kN]	d_y [mm]	F_{max} [kN]	d_u [mm]	K_e [kN/mm]	μ	F_d [kN]	M [t]	T [s]	Ω	q_0	q
A-1	Sliding	Sliding	65.64	10.40	77.08	38.40	6.30	3.69	48.84	5.56	0.187	1.34	2.53	3.40
A-2	Rocking	Rocking-sliding	94.13	14.08	104.60	57.20	6.70	4.06	54.85	5.56	0.181	1.72	2.67	4.58
B-1	Rocking	Rocking-sliding	82.08	14.51	93.30	56.60	5.65	3.90	54.85	5.56	0.197	1.50	2.61	3.90
B-2	Rocking	Rocking	91.61	12.96	107.04	75.00	7.05	5.79	54.85	5.56	0.176	1.67	3.25	5.43
C	Rocking	Rocking	87.03	14.87	96.66	72.20	5.85	4.86	54.85	5.56	0.194	1.59	2.95*	4.68

* q_0 value for specimen C underestimated, because experiment was terminated before ultimate capacity and displacement were achieved.

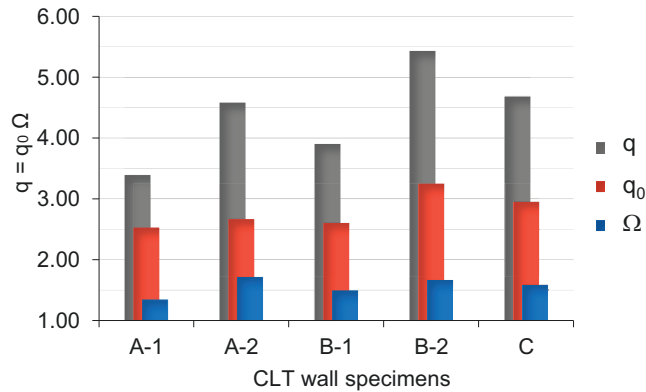


Fig. 2.7 – Results in terms of q , q_0 and Ω .

Comparison of the results in Table 2.3 and Fig. 2.7 for type B vs. type A specimens shows that q_0 -factors for walls A-1, A-2 and B-1 are similar, so that the difference in terms of q is mainly given by Ω , i.e., the design and resistance of the wall. Wall B-2 reaches the highest values of q_0 and q , mainly due to the high ductility value. Wall C has q_0 and q values between those of walls A-2 and B-2.

A first conclusion is that q_0 increases for a CLT wall by incorporating one or more vertical construction joints, if rocking of the two panels composing the wall occurs. The physical explanation is that sliding or combined rocking-sliding failures of an un-jointed wall is replaced by rocking failure, in which the two CLT panels that compose the wall rock and slide relative to one another at the vertical joint. This conclusion is not fully consistent with the behaviour of wall B-1, which behaves and fails like wall A-2, mainly due to the high stiffness of its vertical joint. Therefore, the same results in terms of q_0 -factor were obtained for these two walls, whereas the decrease in Ω for wall B-1 was due to the impairment caused by the vertical joint with inclined screws, which failed, due to pull-out of these connectors.

The obtained values of Ω -factor are consistent with the adopted design method and safety factors used. As shown in Table 2.3, they are quite stable for the five types of shear walls tested. The lowest value within the range ($1.34 \leq \Omega \leq 1.72$) was that of specimen A-1, which has the lowest number of anchorage connectors and the least capability to redistribute forces during application of cyclic horizontal forces. It can be concluded that a Ω -factor of 1.3 would be a reasonable estimate for CLT shear-walls system. In general, appropriate values of Ω should vary according to design method, codes, coefficients, and the safety level adopted. Table 2.4 shows how alteration of design capacity per fastener F_{d_nail} influences the Ω -factor and therefore also q -factor. The consequence is that q -factors may vary between design codes applicable in various countries but, when applied in conjunction with the relevant F_{d_nail} , they should result roughly the same. Similarly, if the design method and hypotheses vary the different F_{d_wall} involves a different Ω and therefore q value.

Although not explicitly clarified in these analyses, the design over-strength value should also be related to the number of shear walls within the critical storey of a building and the ability of horizontal diaphragms to involve all wall segments in the SFRS during a seismic event, whereas the q_0 -factor should also function of the regularity in elevation of the SFRS. Assigning a value of 1.3 to Ω would be associated with buildings in which the SFRS consists of two parallel shear walls, without vertical joints and fixed at the base by correctly designed angle brackets and hold-downs.

From a code development perspective, a primary question should be therefore how to create reliable rules for recognising that q_0 and Ω depend on the number, arrangement and characteristics of connection elements in any CLT SFRS.

Table 2.4 - Dependence of q-factor on F_{d_nail} . [2.51]

Wall	F_{d_nail} [kN]	F_{d_wall} [kN]	F_y [kN]	d_y [mm]	d_u [mm]	μ	Ω	q_0	q
A-1	2.22	48.84	65.64	10.40	38.40	3.69	1.34	2.53	3.40
	3.38*	68.54					0.96		2.42
A-2	2.22	54.85	94.13	14.08	57.20	4.06	1.72	2.67	4.58
	3.38*	68.54					1.37		3.67
B-1	2.22	54.85	82.08	14.51	56.60	3.90	1.50	2.61	3.90
	3.38*	68.54					1.20		3.12
B-2	2.22	54.85	91.61	12.96	75.00	5.79	1.67	3.25	5.43
	3.38*	68.54					1.34		4.35
C	2.22	54.85	87.03	14.87	72.20	4.86	1.59	2.95	4.68
	3.38*	68.54					1.27		3.75

* F_{d_nail} according to [2.17]

2.3 Evaluation of the seismic response with non-linear numerical analyses

Results discussed in the previous section are based on the application of the pushover procedure to the capacity curve obtained directly from tests of representative shear-wall systems. This procedure is useful to obtain a preliminary estimate of the q_0 -factor and to provide a suitable value of the Ω -factor, which depend on the bi-linearization method used, on the design resistance assumed for fasteners and on the code applied. This method provides reliable results in terms of q_0 -factor, with the only exception of neglecting two specific properties of timber structures subjected to cyclic loading: the pinching behaviour due to wood-embedment phenomenon and the strength degradation for high amplitude of hysteresis cycles. These two phenomena can be taken into account only by means of non-linear dynamic analyses (NLDA) performed with advanced numerical models, which allow to calibrate correctly the non-linear elements according to the hysteresis cycles obtained by tests. Conversely, these limitations of the pushover procedure do not influence the Ω -factor values.

Using NLDA, the q -factor can be estimated with the PGA approach ([2.17];[2.37]). This method starts performing experimental cyclic-loading tests on single wall specimens suitable to characterize the constructive system, recording applied lateral force vs. displacement of wall and connections. Then, linear and non-linear hysteretic springs representing connection elements and bracing system in suitable numerical FE models, are calibrated based on equivalence of hysteresis cycles and dissipated energy and assembled to model the wall specimen and to simulate the cyclic-loading test. Finally, the earthquake action on shear-wall systems or sample buildings can be simulated using NLDA. According to this method, the definition of q -factor refers to the design condition, defined by the design PGA (PGA_d), and the ultimate condition, defined by near-collapse PGA (PGA_u): the former can be analytically or experimentally evaluated, the latter is numerically obtained. Q -factor values are calculated as ratio between PGA_u and PGA_d . Therefore, q_0 -factor can be defined as the ratio between PGA_u and PGA_y , obtained directly from the yielding force (F_y)

of the wall. Ω -factor can be computed in addition, as ratio between yielding and design force (see section 1.3).

2.3.1 Evaluation of q_0 -factor for CLT shear walls

The q_0 -factor for typical CLT wall systems is here calculated using NLDA. The most representative walls (A-1, A-2 and B-2) among those already analysed in section 2.2 have been modelled numerically, using the component approach, illustrated in section 1.2.2. Then, eight earthquakes artificially generated have been applied to the model to simulate the seismic response of these walls, characterized by the same mass listed in Table 2.3 and the same hysteretic behaviour obtained from tests [2.35], Fig. 2.4. The q_0 -factor is finally obtained applying the PGA method and averaging results from the eight simulations.

2.3.1.1 Calibration of numerical models and validation

Numerical simulations were carried out with open-source research FEM code “Open System for Earthquake Engineering Simulation–OPENSEES” [2.60] with hysteresis material model Pinching4 [2.61]. This model provides a polygonal scheme of the hysteretic curve with four slopes and the possibility of reproducing softening branch, pinching, strength degradation and stiffness degradation phenomena. It requires the calibration of sixteen parameters for stress and strain on the positive and negative response envelopes, six parameters for pinching cycles and four parameters for strength degradation. Stiffness degradation was not considered.

The examined walls were modelled with non-linear elements calibrated on the results of experimental tests of full-scale shear-wall specimens ([2.35];[2.52]). These tests are representative of the actual behaviour of connections commonly used in construction practice and of their interaction with CLT panel. The hysteretic cycles considered for the calibration of each connection element were obtained directly from these tests, with reference to the cycles recorded from transducers placed at connections. In particular, the calibration of springs simulating shear-resisting connections was based on a specimen with predominant sliding behaviour (wall 1.1 in [2.52]); the calibration of springs representing uplift-resisting connections was based on a specimen with predominant rocking behaviour (wall 1.3 in [2.52]). In this way, secondary phenomena as friction of the panel with the basement have been implicitly taken into account. Moreover, both shear and axial resistances of angle brackets and hold-downs are implicitly considered. Such model is hereafter referred as phenomenological model.

To validate the calibration, numerical cyclic analyses were conducted to replicate the experimental tests with the same loading protocol [2.49] and to compare the results in terms of hysteretic behaviour and energy dissipation capacity.

The applied modelling criteria allow to obtain a model consistent with the reality and to consider all the contributions of the connection elements to the overall strength of the wall. A scheme of the calibration process is shown in Fig. 2.8. The reliability of the numerical model is demonstrated by Fig. 2.9, which shows for each specimen the numerical cycles (top displacement vs. applied lateral force) superimposed on test data.

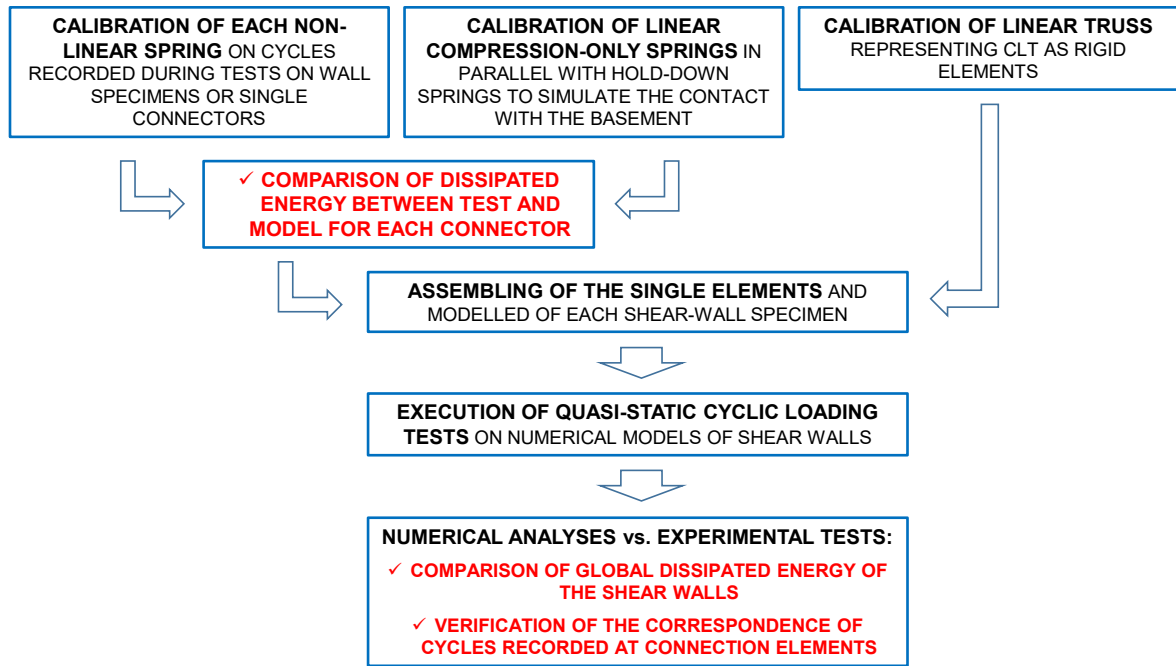
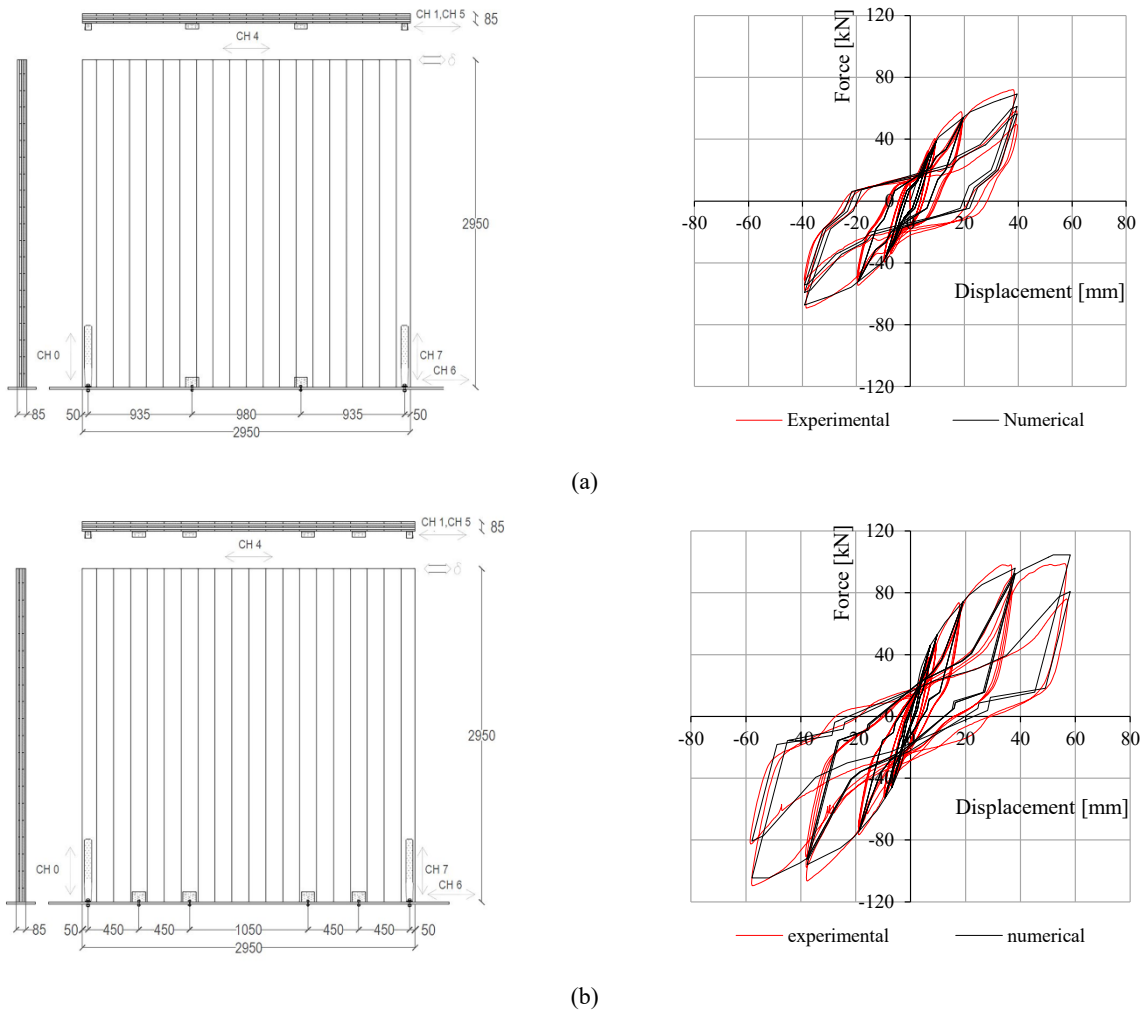
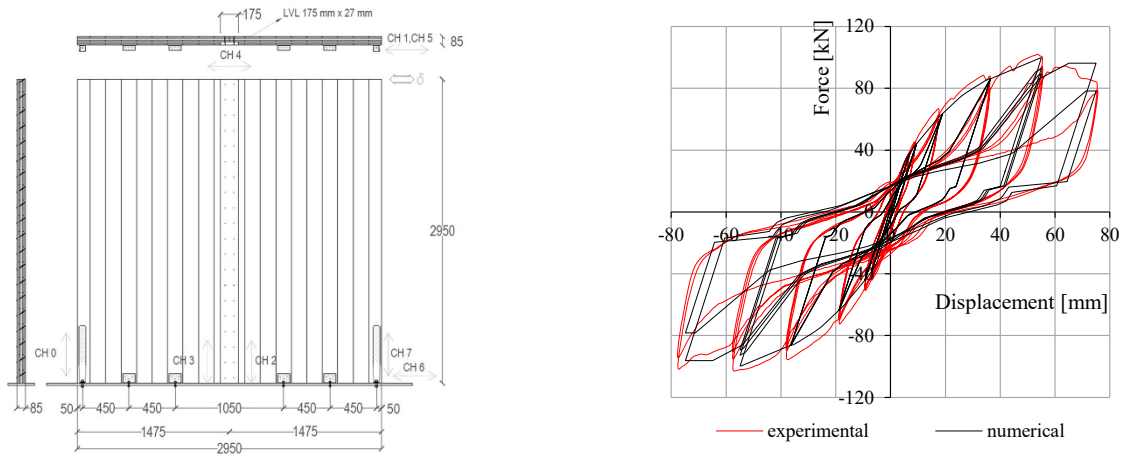


Fig. 2.8 – Calibration process adopted for modelling of the CLT shear walls.

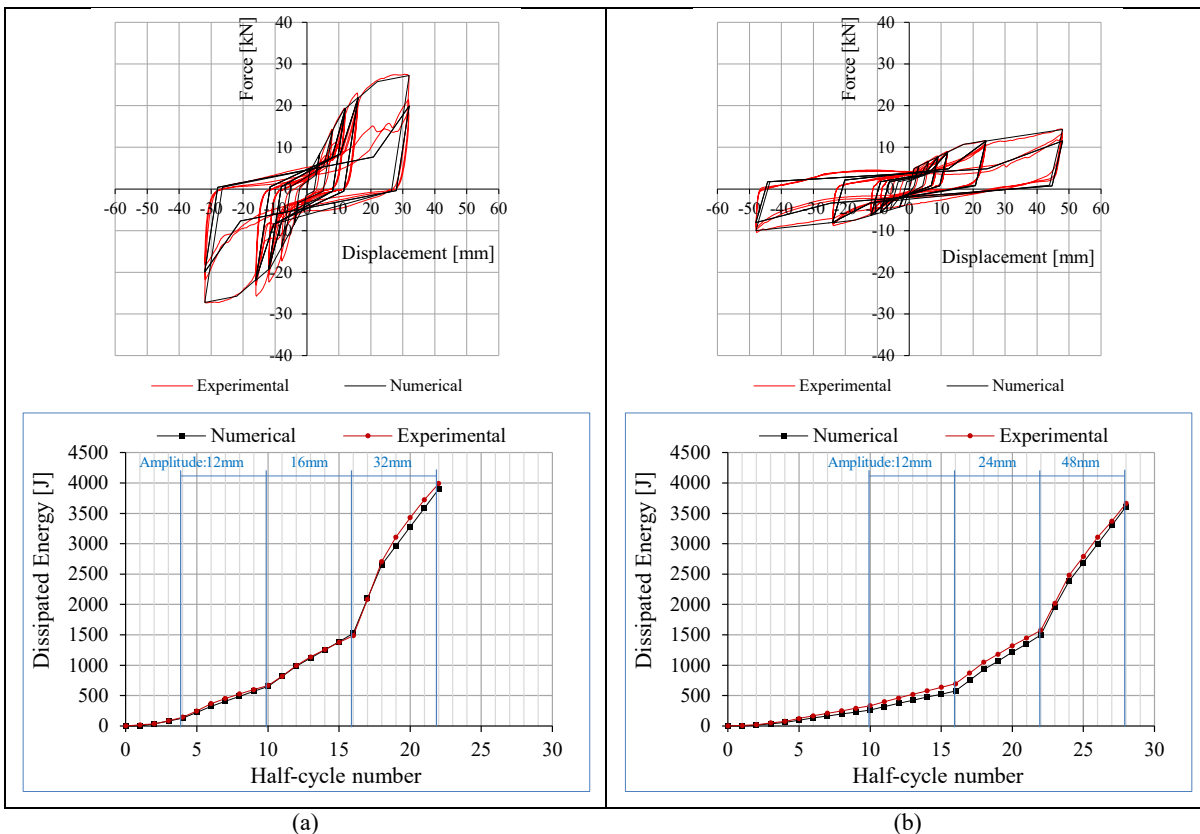




(c)

Fig. 2.9 – Top displacement vs. lateral force: (a) Wall A-1; (b) wall A-2; (c) wall B-2.

The consistency of the applied modelling strategy has been also verified performing additional analyses using a different approach, where each connection is described by its specific cyclic behaviour (detailed model). The calibration of non-linear springs is based on results from tests on the single connection element loaded in shear or tension (tests of angle brackets and hold-downs in ([2.30];[2.34])). For each single connection, both shear and tension response has been considered. Simplification is assumed since the two responses are un-coupled. Fig. 2.10 shows the numerical calibration of non-linear springs based on results from tests on an angle bracket and a hold-down loaded in shear or tension (detailed model). It can be noted that the numerical model is able to simulate correctly the hysteretic behaviour of the connections, the strength degradation and the energy dissipation capacity.



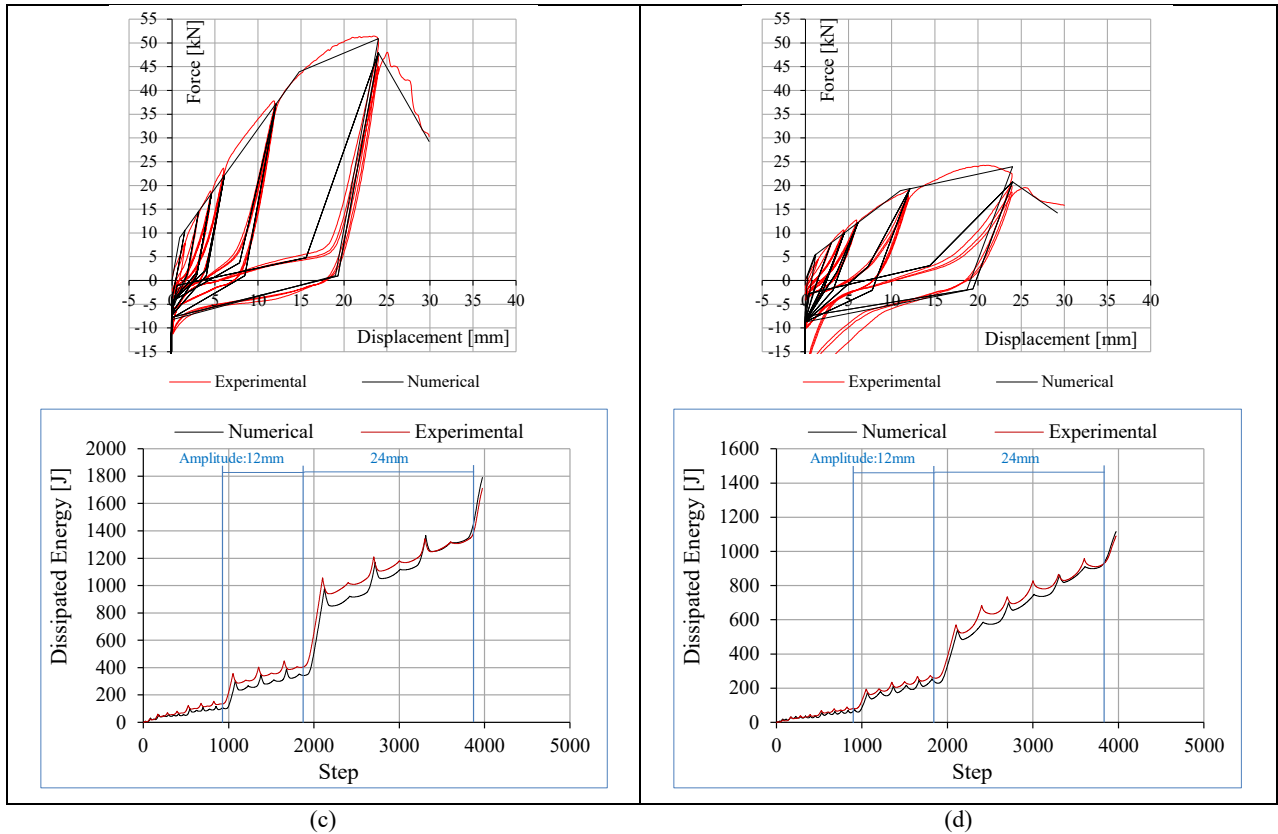


Fig. 2.10 – Calibration of non-linear springs: (a) angle bracket loaded in shear; (b) hold-down loaded in shear; (c) hold-down loaded in tension; (d) angle bracket loaded in tension. (Tests: [2.30];[2.34]).

Both phenomenological and detailed modelling strategies were applied to a case-study wall specimen subjected to predominant rocking behaviour due to a low vertical load applied (9.25 kN/m), (wall 1.3 in [2.52]). The two alternative models are shown in Fig. 2.11. The results of the comparative analyses applying the two modelling approaches are shown in Fig. 2.12 in terms of top displacement vs. lateral force cycles and overall energy dissipation for the case-study wall.

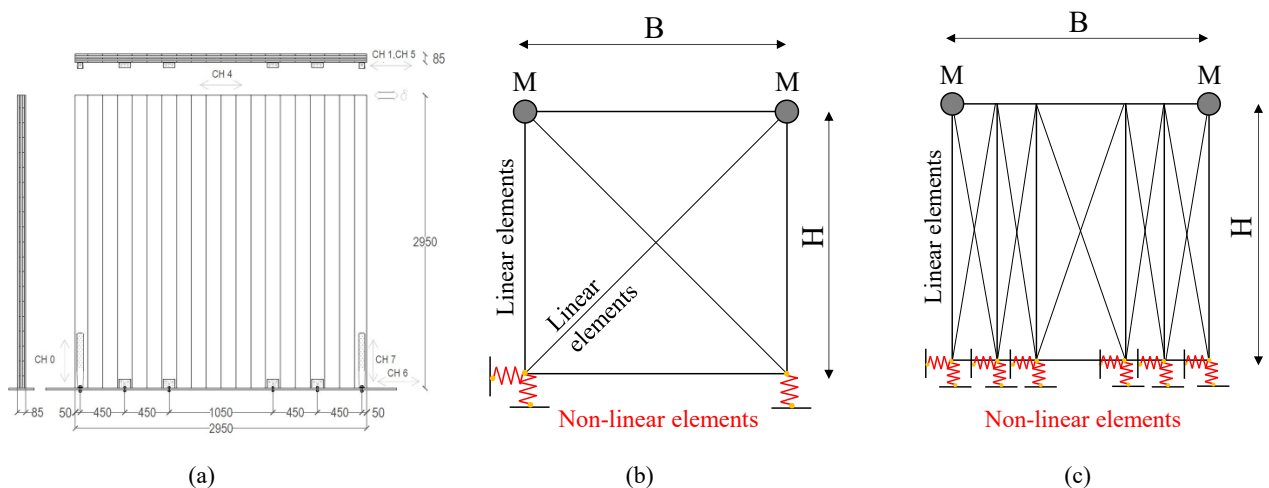


Fig. 2.11 – Comparison of the two modelling strategies: (a) tested specimen; (b) phenomenological model; (c) detailed model.

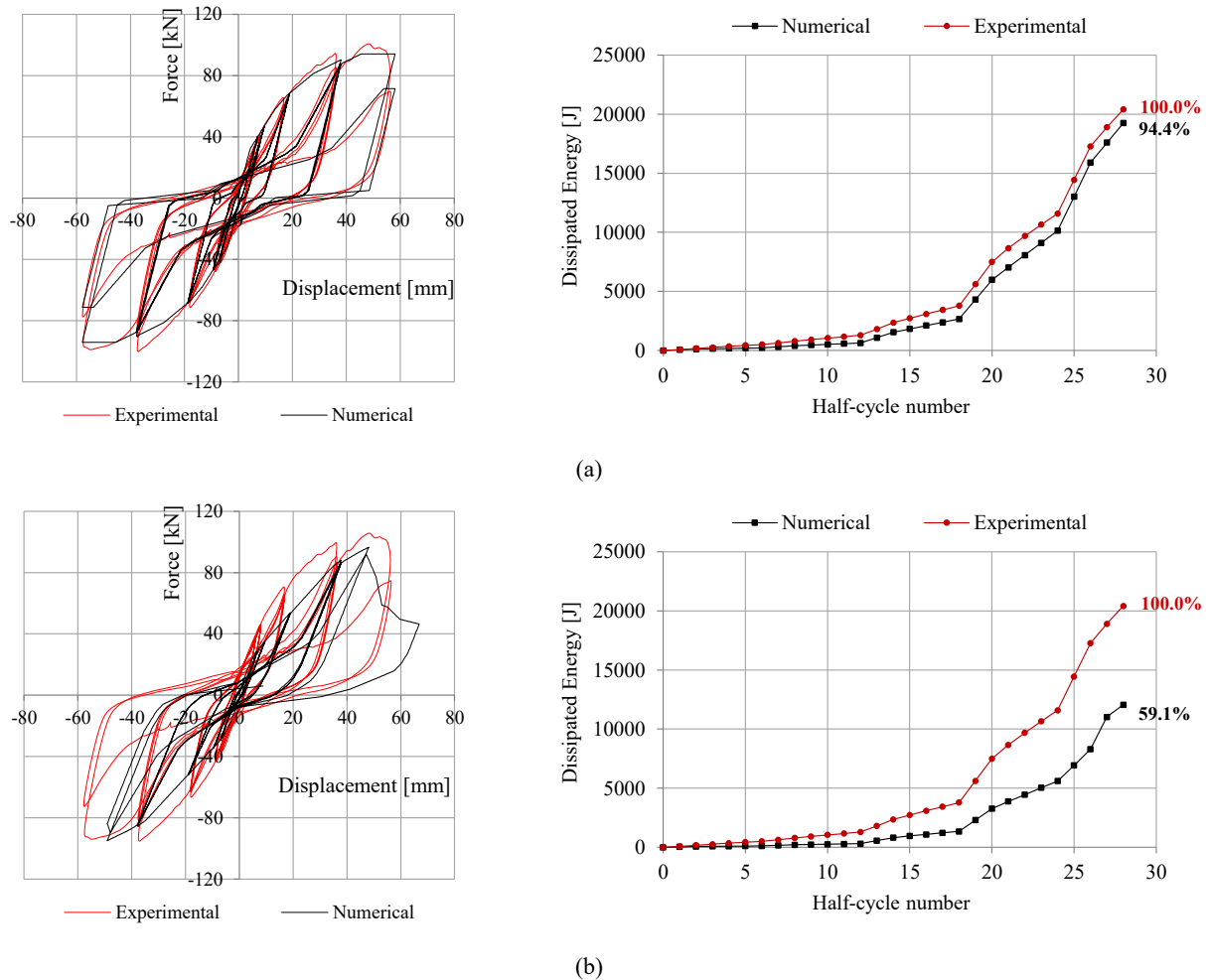


Fig. 2.12 – Simulation of test on case-study wall: (a) phenomenological model; (b) detailed model.

It can be noted that the detailed model underestimates stiffness, strength, displacement capacity and energy dissipation capacity of the wall system. This is because it is unable to consider secondary phenomena proper of the wall, as friction. The total energy dissipation is 5.6% lower than test value with phenomenological model, whereas in detailed model this difference is 40.9%.

As mentioned above, the phenomenological model considers the resistance of all connections in the weak direction implicitly, whereas in the detailed model each contribution has to be considered separately. Further cyclic analyses on the same case-study wall performed with detailed modelling approach have shown how results would change in terms of cyclic response of the wall, neglecting shear resistance of hold-downs or tension resistance of angle brackets. Comparing Fig. 2.12b with Fig. 2.13a (hold-down shear resistance neglected), it can be noted almost no differences: a slight increase of displacement capacity and energy dissipation has been obtained due to a greater sliding displacement. Conversely, the comparison between Fig. 2.12b with Fig. 2.13b (angle-bracket tension resistance neglected) shows that the resulting behaviour is substantially different. In this case, a marked decrease in strength, stiffness and energy dissipation (about 23.6% lower) was obtained. This suggests that tension resistance of angle brackets shall be considered in detailed models for walls with predominant rocking behaviour. Conversely, it can be supposed that for walls with a predominant sliding behaviour (squat or highly loaded walls) hold-down shear resistance gives a greater contribution than angle-bracket tension one.

All these additional analyses demonstrate therefore that numerical results presented in this Chapter are reliable because they have been obtained with phenomenological modelling approach, which allows to simulate the actual behaviour of the wall with sufficient accuracy.

The analytical approach described in section 2.2, in which resistance of connections in the weak direction was neglected according to currently design practice, does not limit results obtained in terms of q_0 -factor because this value has been computed as ratio between PGA_u (from numerical models that take into account all contributions of connections) and PGA_y (from tests). The q_0 -factor therefore is intrinsic to the structural system and is not influenced by design hypotheses. Conversely, the Ω -factors obtained in section 2.2.2 depend on design hypotheses. Accordingly, if other design hypotheses were assumed, it would be sufficient to modify Ω -factors, whereas q_0 -factors would remain the same. However, analytical models that consider the resistance of connections in the weak direction involve some issues, i.e., the actual position of all connections and their coupled shear-tension behaviour have to be known or hypothesized.

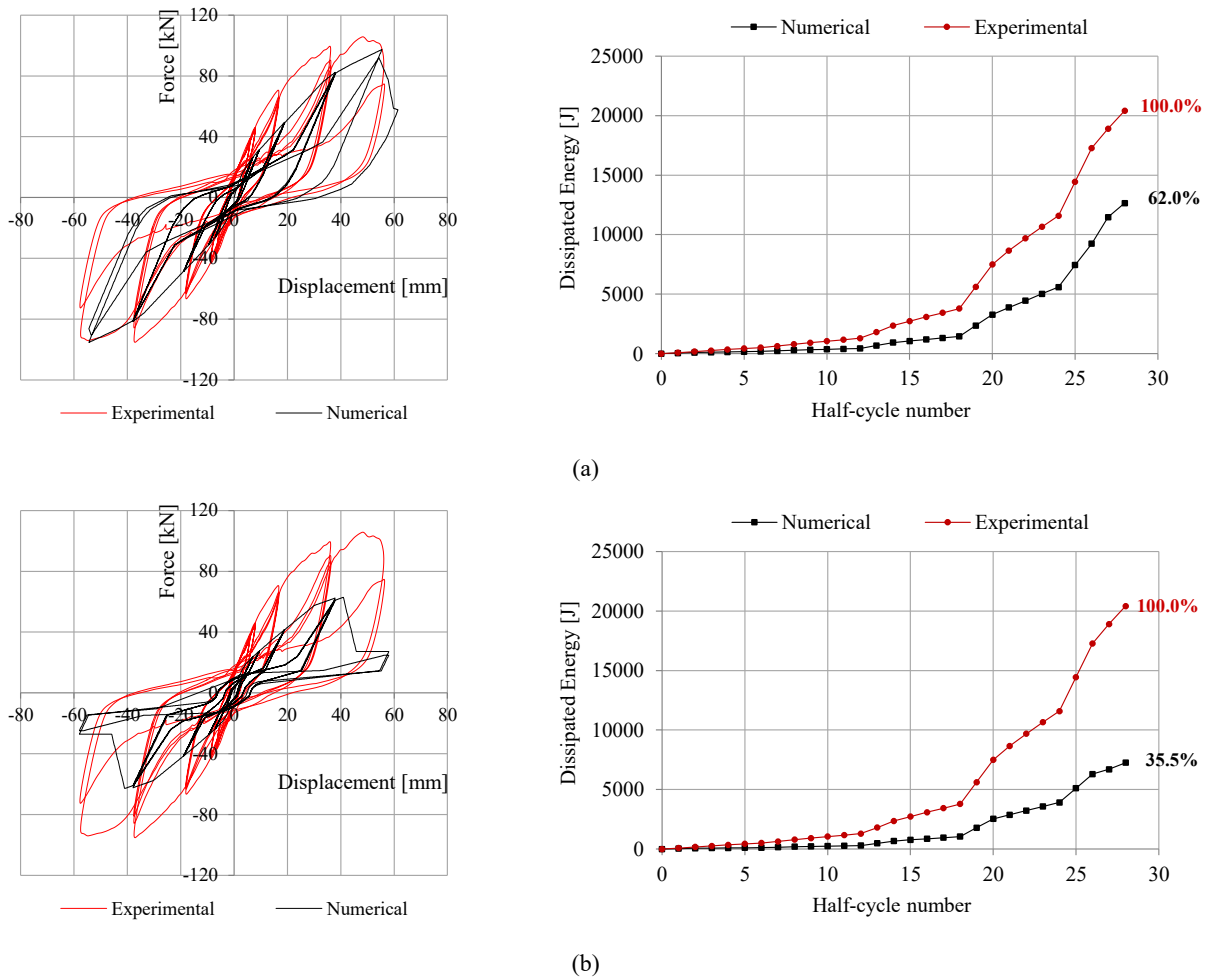


Fig. 2.13 – Simulation of test on case-study wall with detailed model: (a) hold-down shear resistance neglected; (b) angle-bracket tension resistance neglected.

2.3.1.2 Computation of q_0 -factor

The PGA_y for each shear wall was obtained directly from the yielding force (see Table 2.3) as the value compatible with an elastic response spectrum for building foundations resting on type A soil (rock soil, corresponding to $S = 1.0$, $T_B = 0.15$ s, $T_C = 0.4$ s, $T_D = 2.0$ s), behaviour factor $q = 1$, and building importance factor $\gamma_I = 1$, according to Eurocode 8 [2.50]. The maximum spectral

amplification factor F_o was assumed equal to 2.5. The PGA_y compatible with an elastic design of the structure without safety factors applied was finally computed for all walls, assuming the fundamental period of the shear wall within the plateau range. The hypothesis that the first mode period T was in the plateau range was confirmed by the frequency analysis.

The NLDA were performed considering 8 earthquakes, artificially generated with SIMQKE_GR [2.62] in order to meet the spectrum compatibility requirement with the design elastic spectrum. Dynamic equilibrium equations were integrated with a not-dissipative Newton–Raphson scheme and time-steps of 0.001 s, introducing an equivalent Rayleigh viscous damping of 2%, according to Ceccotti [2.17]. By progressively increasing the magnitude of the applied earthquakes, the $PGA_{u,i}$ values, which lead to the near-collapse condition, were evaluated for all signals. Lastly, the q_0 -factors for each signal were evaluated as the ratio between the $PGA_{u,i}$ values and the PGA_y value. Results for each time-history are reported in Table 2.5. PGA_y , T and average results are listed in Table 2.6.

The assumed yielding condition depends on the bi-linearization method adopted, whereas it is independent of the design of the structure. The actual Ω -factor, i.e., the ratio between PGA_y and PGA_d remains the same provided in Table 2.3, as the bi-linearization method adopted is the same. If other methods of bi-linearization of the envelope curve were used, results in terms of q_0 -factor and Ω -factor would vary, but the final values of q -factor would remain the same.

Results obtained from numerical analyses confirm the conclusions given in section 2.2. In particular the conclusion that q_0 can be increased for a CLT wall by incorporating one or more vertical construction joints, is again confirmed. Furthermore, these results show a reduction of the q_0 -factor with respect to results obtained with the experimental-analytical procedure. As mentioned above, this likely could be due to the pinching behaviour and the strength degradation phenomenon that the NLDAs using accurate FE models are able to take into account. This conclusion does not restrict the validity of the analytical-experimental procedure presented above. However, to apply correctly such simplified procedure, q_0 -factor should be reduced by about 25% to 35%, where the minor value was obtained for wall A-1 with less connection elements, the major for wall B-2 with more connections and the presence of the vertical panel-to-panel joint. These reduction factors allow to consider the combined effect of pinching behaviour and strength degradation in the application of the pushover procedure to CLT wall systems.

Table 2.5 – $q_{0,i}$ values from numerical analysis.

SIGNALS	SPECIMENS		
	A-1	A-2	B-2
Earthq.1	1.77	1.70	1.90
Earthq.2	2.14	2.07	2.26
Earthq.3	1.79	1.77	2.01
Earthq.4	1.89	1.85	2.09
Earthq.5	2.24	2.20	2.52
Earthq.6	1.93	1.89	2.06
Earthq.7	1.93	1.82	1.97
Earthq.8	1.73	1.77	2.17
AVERAGE	1.93	1.89	2.12

Table 2.6 – Summary of results from numerical analysis.

Spec.	Design failure mechanism	Actual failure mechanism	T [s]	PGA _y [g]	Ω	average q ₀	average q
A-1	Sliding	Sliding	0.161	0.49	1.34	1.93	2.59
A-2	Rocking	Rocking-sliding	0.154	0.70	1.70	1.89	3.21
B-2	Rocking	Rocking	0.169	0.69	1.65	2.12	3.50

2.3.2 Evaluation of q₀-factor for CLT buildings

The numerical procedure applied in section 2.3.1 to analyse single wall specimens can be extended to 2D plane models of entire CLT building façades, assembling the modelled wall systems with non-linear elements suitable to simulate the behaviour of horizontal and vertical panel-to-panel joints. In this section a parametric study is applied to 24 different CLT building configurations, to define the effects of some construction variables on their seismic response and therefore on appropriate q₀-factor values and to generalize the main conclusions to the overall CLT technology. Data reported here derived from an update and extension of the numerical analyses reported in [2.39].

In detail, this extensive study on CLT construction technology aims to provide information about the relationship between q₀-factor values and some characteristic parameters of CLT buildings: slenderness, number of storeys and number of vertical panel-to-panel joints. The study of the influence of the in-elevation irregularity is addressed in the section 2.5. Accurate definition of the q₀-factor cannot disregard the influence of these parameters, all affecting the seismic behaviour of CLT buildings in terms of displacement capacity, ductility and energy dissipation capacity. The main hypothesis is that the seismic response of CLT system depends on the building geometry (e.g., slenderness) and the number, type, arrangement and design of joints used to assemble the timber panels. In detail:

- The seismic performance of CLT buildings is mainly related to the capability of connections to do plastic work, therefore increasing the number of metal connections, the displacement capability increases, as demonstrated by experimental tests discussed above. Moreover, being the dissipative capacity of a CLT building concentrated in connectors, the intrinsic value of the behaviour factor could increase with their number. This number varies both with the number of storeys and with the number of panels that compose the façade.
- Squat and scarcely jointed CLT buildings realized with large horizontal panels show limited dissipative capacity due to their prevailing sliding behaviour. Conversely, slender and highly jointed buildings, realized with a proper assembling of narrow panels with metal fasteners, can reach higher displacement before failure and higher ductility, due to a prevailing rocking behaviour. Moreover, this behaviour has other advantages: it involves both hold-downs and vertical joints in the global dissipation capacity of the buildings and the building naturally returns to its original position after the earthquake event (self-centring capacity).

In the constructive practice many types of CLT buildings can be found, which differ mainly in the parameters listed above.

- Scarcely jointed buildings realized with large horizontal panels (see Fig. 2.14a) are normally preferred, because adoption of large panels with few joints allows the reduction of time and cost for on-site assembling. Adopting this particular assembling strategy allows to realize doors and windows by cutting directly the panel. The main limitation is the inter-storey

height that depends on the maximum available width dimension of the panel. The floors are realized interrupting the in-height continuity of the façade panels, as shown in Fig. 2.14b. Metal connections are used only at the foundations and at each storey to restrain mainly shear forces.



Fig. 2.14 – Assembling of large horizontal panels [2.63]: (a) façade panel; (b) floor.

- Adoption of narrow jointed panels (Fig. 2.15) could be preferred for the lower weight to be lifted. In this case, windows and doors can be realized fasten CLT or glulam beams to the vertical panels, to realize lintels. The adoption of this assembling strategy allows to maintain the continuity of the panels between storeys, even if this solution is rarely adopted and floors are normally realized as mentioned before (Fig. 2.14b). Therefore, this second assembling strategy allows normally to use a large amount of metal connections, between storeys and as panel-to-panel joints (see Fig. 2.1a-b).






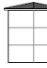
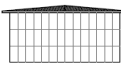

Fig. 2.15 – Assembling of small jointed panels [2.64].

The second strategy is economically disadvantageous, considering that existing codes provide a single behaviour factor value for all CLT buildings. Eurocode 8 [2.50], suggests a quite prudential behaviour factor for seismic design of CLT buildings: $q=2$. Actually, slender or highly jointed buildings have more dissipative and ductility capacities than squat and scarcely jointed buildings and in the first case more generous values of the q -factor could be allowed. The results of the extensive numerical campaign reported here is focused on this issue.

2.3.2.1 Definition and design of case-study configurations

A total of 24 two-dimensional configurations were set, identified as A1N, B1N etc., varying number of storeys, base dimension and wall composition. All configurations were regular in plan and in elevation, so that the dependence of the q_0 -factor on regularity was not taken into account in this phase. Two building configurations with different base dimensions (B) of 17.5 and 8.75m were studied in order to evaluate the effects of slenderness. Four building heights were chosen, corresponding to 1, 3, 5 and 7 storeys, with an inter-storey height of 3.05m. Three construction methodologies were analysed: façades made by a unique CLT panel (No vertical joints), façades subdivided in 4 or 2 CLT panels for configurations with base dimensions of 17.5m and 8.75m respectively (Medium density of vertical joints), and façades made with narrow modular CLT panels 1.25-m wide (High density of vertical joints). Table 2.7 lists the 24 configurations, together with their seismic mass (M).

Table 2.7 – Building configurations studied.

	NO VERTICAL JOINTS		MEDIUM DENSITY OF VERTICAL JOINTS		HIGH DENSITY OF VERTICAL JOINTS	
Storeys	 B = 17.5m	 B = 8.75m	 B = 17.5m	 B = 8.75m	 B = 17.5m	 B=8.75m
1	A 1 N M=18.0 t	B 1 N M=12.0 t	A 1 M M=18.0 t	B 1 M M=12.0 t	A 1 H M=18.0 t	B 1 H M=12.0 t
3	A 3 N M=92.0 t	B 3 N M=60.0 t	A 3 M M=92.0 t	B 3 M M=60.0 t	A 3 H M=92.0 t	B 3 H M=60.0 t
5	A 5 N M=166.0 t	B 5 N M=108.0 t	A 5 M M=166.0 t	B 5 M M=108.0 t	A 5 H M=166.0 t	B 5 H M=108.0 t
7	A 7 N M=240.0 t	B 7 N M=156.0 t	A 7 M M=240.0 t	B 7 M M=156.0 t	A 7 H M=240.0 t	B 7 H M=156.0 t

All examined configurations were designed with the aim to obtain the most suitable estimation of the intrinsic behaviour factor q_0 . The following design hypotheses were made:

1. All the buildings were designed according to Equivalent Linear Static Analysis, with the following data, according to Eurocode 8 [2.50]: type 1 elastic response spectra with type A soil, behaviour factor $q=1$, design PGA equal to 0.35g (the highest value for Italian territory) with a building importance factor of $\gamma_I=1$ and maximum spectral amplification factor equal to 2.5. Therefore, according to the PGA approach described above [2.17], the value of PGA_d for the computation of the q_0 -factor value is equal to 0.35g;
2. The design value of the resistance of angle brackets and hold-downs was assumed equal to yielding of connections obtained in the experimental tests conducted during SOFIE project [2.15]. The same test data were used to calibrate the numerical models and to evaluate the near-collapse condition of the connection elements for the computation of $PGA_{u,i}$ with NLDAs. To switch from experimental resistance to the design one no partial resistance coefficient γ_m or load duration coefficient k_{mod} were used;
3. Neither rounding on sizing of connectors nor introduction of oversizing on the structural elements were imposed, in order to obtain an estimation of the q_0 -factor due only to the dissipative capacity of the structure. The design over-strength Ω was therefore imposed equal to 1.00 (coherently with design assumption);

4. The respect of the exact equivalence between the actual storey resistance and that required by equivalent linear-elastic analysis was imposed to ensure the regularity in elevation [2.50];
5. After the design of angle-bracket and hold-down connections preliminary pushover analyses (NLSA) were conducted to design the vertical panel-to-panel joints in order to guarantee to achieve the maximum displacement capacity of the building before the premature collapse of one or more connections. The correct application of the capacity design approach was therefore verified via NLSAs, because the connections were designed both to resist to seismic action and to ensure the greatest displacement capacity of the building, that can be reached if a combined rocking-sliding behaviour [2.21] is ensured at each storey. This assumption guarantees that each connection element develops plastic deformations before reaching the near-collapse condition due to the diffused failure of all connections in the building. In this way, the maximum shear force and the maximum ductility can be reached together.

It should be evidenced that the hypotheses 4 and 5 led to the highest q_0 -factor achievable from a regular CLT building and with equal-resistant ductile connections. If connections are designed without respecting such hypotheses a reduction of the q_0 -factors here obtained should be imposed. The irregularity in elevation can be taken into account applying a reduction factor, as will be discussed afterwards. The over-strength of the vertical joints with respect to base connections can be taken into account simply considering the q_0 -factors obtained for the configurations without vertical joints.

2.3.2.2 Numerical models for case-study configurations

The examined configurations were modelled with 2D plane models, in which the non-linear elements were calibrated on results from the experimental tests conducted at CNR-IVALSA laboratory during SOFIE project ([2.15];[2.29]). These tests are representative of the actual behaviour of connections commonly used in construction practice. Each connection element was modelled with non-linear springs according to the modelling for components described in section 1.2.2. The hysteretic cycles considered for the calibration of angle brackets and hold-downs were obtained from tests on full-scale walls variously connected to the foundation. The experimental curves obtained from a specimen connected to a steel foundation beam [2.15] were used in the numerical model to simulate the behaviour of the elements at the ground floor, whereas the experimental curves obtained from a specimen connected to a CLT basement [2.15], for the modelling of the elements at the upper floors. To complete the calibration process, numerical cyclic-loading analyses were conducted to replicate the experimental tests and to compare the results in terms of hysteretic behaviour and energy dissipation capacity. The calibration of panel-to-panel LVL joints for the assembling of modelled shear walls was made according to tests on a single element, conducted by Sandhaas et al. [2.29].

Numerical simulations were carried out with open-source research FEM code “Open System for Earthquake Engineering Simulation–OPENSEES” [2.60] with hysteresis material model Pinching4 [2.61]. As an example, Fig. 2.16 shows the numerical model used to assess the seismic response of the three-storey configuration with modular CLT panels 1.25-m wide (A3H). For a detailed description of model calibration, see ([2.65]-[2.67]).

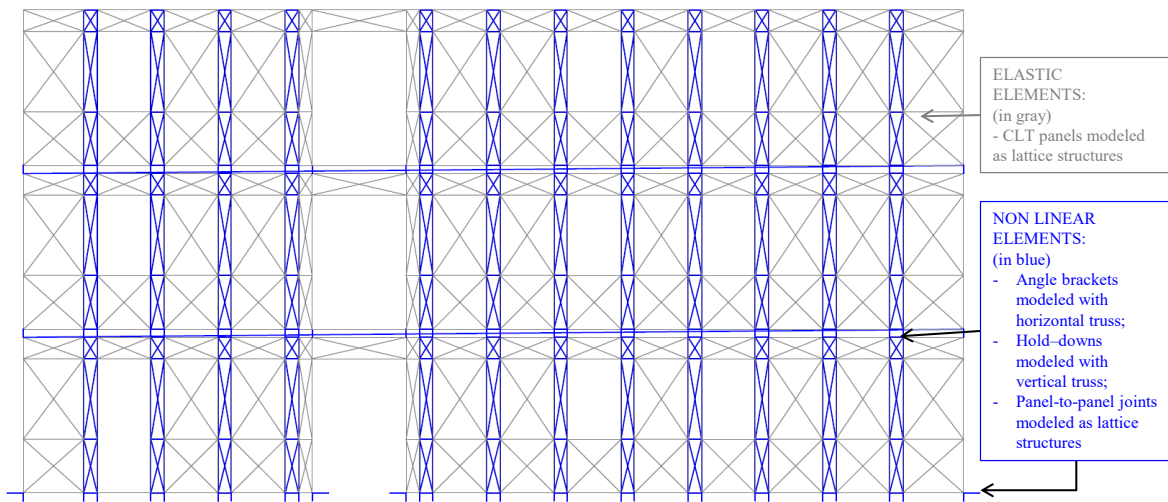


Fig. 2.16 –Scheme of numerical model for case-study A3H.

2.3.2.3 Non-linear analyses and q_0 -factor evaluation

The NLDAs were carried out for each case study with increasing PGA levels, starting from the design value, to define the failure value corresponding to the near-collapse condition. Each case study was analysed considering 7 artificially generated seismic shocks [2.62], so as to respect the spectrum compatibility requirement according to the design elastic spectrum. The application of various seismic signals had the aim of defining the influence of the frequency content of the earthquakes on the building response. The total number of performed NLDAs was therefore 168. The dynamic equilibrium equations were integrated with a time step of 0.001s, by adopting an equivalent viscous damping of 2%, according to the Rayleigh model. The choice of this damping coefficient was made according to Ceccotti [2.17]. The assumed near-collapse condition for the evaluation of the $PGA_{u,i}$ corresponds to the first failure of a connector, defined as maximum admissible displacement reached by a non-linear spring during the applied earthquake. The values of ultimate displacements were assumed according to experimental tests adopted to calibrate the model: 10 mm for angle-bracket sliding and 20 mm for hold-down uplift for the connections at ground floor; 30 mm for angle-bracket sliding and 15 mm for hold-down uplift for the connections at the upper floors.

For the configuration A3M, Fig. 2.17 shows pushover curves, used to design the building, overlapping the NLDA results increasing PGA, i.e., the points representing the average values of maximum top displacements vs. corresponding base shear (NLDA_1) and maximum base shear vs. corresponding top displacements (NLDA_2). Two horizontal force distributions were examined in the NLSAs: one proportional to that of the first modal shape of the building (NLSA_1) and the other proportional to storey masses (NLSA_2). As Fig. 2.17 shows, there is a good fit between NLSAs and NLDAs. The interval between the curves defines the range of possible responses of the building during an earthquake.

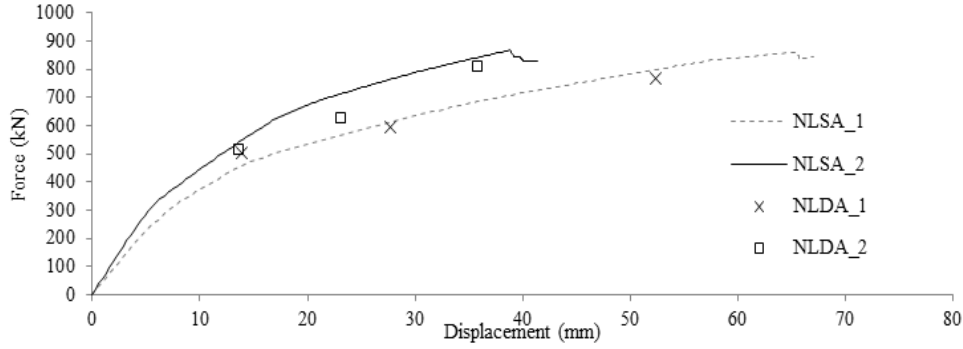


Fig. 2.17 – Comparison of results from NLSA and NLDA for building configuration A3M.

The PGA approach ([2.17];[2.37]) was used to estimate the q_0 -factor as the ratio between $PGA_{u,i}$ and PGA_d . Fig. 2.18, Table 2.8 and Table 2.9 show the q_0 -factor values for each building configuration. Minimum, maximum and average q_0 -factors are listed together with standard deviation and 5th-percentile according to EN 1990 [2.68].

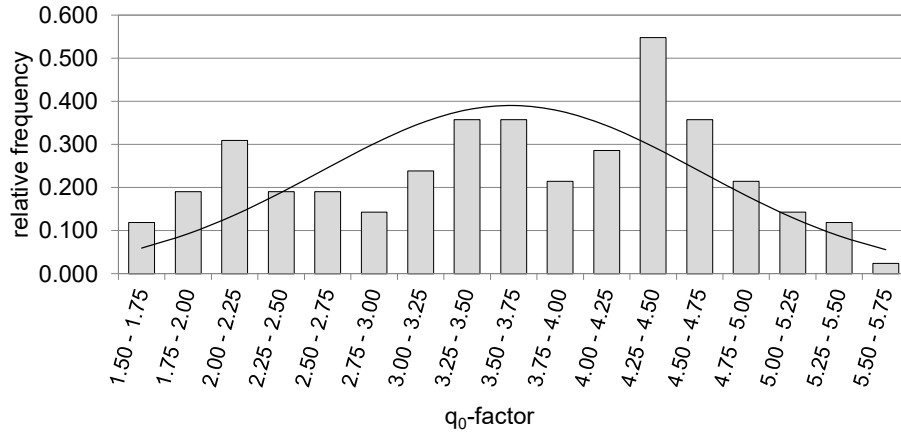


Fig. 2.18 – Obtained q_0 -factor values and normal distribution of results.

Table 2.8 – Obtained q_0 -factor values for case-study building with $B=17.50$ m.

Geometric parameters	Notations	Units	1 STOREY			3 STOREYS			5 STOREYS			7 STOREYS		
			0	3	12	0	3	12	0	3	12	0	3	12
Height dimension	H	m	3.05			9.15			15.25			21.35		
Amount of vertical joints per storey	m	-	0	3	12	0	3	12	0	3	12	0	3	12
Seismic signals	Notations	Units	1 STOREY			3 STOREYS			5 STOREYS			7 STOREYS		
Earthquake 1	q_0	-	1.81	1.97	2.29	2.80	3.12	3.76	2.96	3.66	4.52	3.76	4.41	5.11
Earthquake 2	q_0	-	2.01	2.41	2.61	3.12	3.33	3.93	3.23	4.09	4.84	4.30	4.84	5.38
Earthquake 3	q_0	-	1.69	1.97	2.10	2.69	2.96	3.66	3.07	3.66	4.30	4.03	4.03	5.11
Earthquake 4	q_0	-	1.61	1.97	2.19	2.90	3.39	4.20	4.19	4.26	4.47	4.22	4.52	4.95
Earthquake 5	q_0	-	2.01	2.28	2.42	3.33	3.98	4.72	4.84	4.58	4.73	4.30	4.95	5.29
Earthquake 6	q_0	-	1.57	1.71	2.06	3.23	3.66	3.94	3.50	3.57	5.08	3.01	4.73	5.16
Earthquake 7	q_0	-	1.65	1.97	2.19	3.39	3.44	4.62	4.57	4.44	4.04	4.22	4.09	4.39
Minimum	q_0	-	1.57	1.71	2.06	2.69	2.96	3.66	2.96	3.57	4.04	3.01	4.03	4.39
Average	q_0	-	1.76	2.04	2.27	3.07	3.41	4.12	3.76	4.04	4.57	3.98	4.51	5.06
Maximum	q_0	-	2.01	2.41	2.61	3.39	3.98	4.72	4.84	4.58	5.08	4.30	4.95	5.38
SD	-	-	0.18	0.23	0.19	0.27	0.34	0.41	0.76	0.41	0.35	0.47	0.36	0.33
5 th percentile	q_0	-	1.38	1.56	1.87	2.50	2.71	3.25	2.17	3.18	3.85	3.00	3.76	4.38

Table 2.9 – Obtained q_0 -factor values for case-study building with $B=8.75$ m.

Geometric parameters	Notations	Units	1 STOREY			3 STOREYS			5 STOREYS			7 STOREYS		
Height dimension	H	m	3.05			9.15			15.25			21.35		
Amount of vertical joints per storey	m	-	0	1	5	0	1	5	0	1	5	0	1	5
Seismic signals	Notations	Units	1 STOREY			3 STOREYS			5 STOREYS			7 STOREYS		
Earthquake 1	q_0	-	2.19	2.19	2.29	3.26	3.14	2.86	4.29	4.46	4.86	4.00	4.29	5.03
Earthquake 2	q_0	-	2.74	2.74	2.86	3.71	3.54	3.60	4.69	4.86	4.80	4.17	4.57	5.14
Earthquake 3	q_0	-	2.19	2.19	2.29	3.14	3.43	3.54	4.29	4.57	4.29	4.00	4.46	5.71
Earthquake 4	q_0	-	2.08	2.08	2.17	3.43	3.54	3.54	3.73	3.25	4.25	4.43	4.25	5.26
Earthquake 5	q_0	-	2.58	2.58	2.69	3.43	3.66	4.57	4.22	4.11	4.62	4.39	4.43	5.26
Earthquake 6	q_0	-	1.92	1.87	1.89	3.49	3.43	3.31	3.73	3.20	3.47	4.34	4.57	5.26
Earthquake 7	q_0	-	2.47	2.47	2.57	3.43	3.60	4.00	4.32	3.89	4.39	4.30	4.53	4.75
Minimum	q_0	-	1.92	1.87	1.89	3.14	3.14	2.86	3.73	3.20	3.47	4.00	4.25	4.75
Average	q_0	-	2.31	2.30	2.39	3.41	3.48	3.63	4.18	4.05	4.38	4.23	4.44	5.20
Maximum	q_0	-	2.74	2.74	2.86	3.71	3.66	4.57	4.69	4.86	4.86	4.43	4.57	5.71
SD	-	-	0.29	0.31	0.33	0.18	0.17	0.54	0.34	0.64	0.47	0.18	0.13	0.29
5 th percentile	q_0	-	1.70	1.67	1.70	3.04	3.12	2.51	3.46	2.70	3.41	3.86	4.17	4.59

The obtained values of q_0 -factor depend on the yielding values of resistance of connectors, consistent with test data, and the experimental data used for the calibration of the model, relative to two specimens tested with cyclic-loading tests.

As mentioned above, the case-study buildings were designed with the mean values of strength of materials, without introducing any safety coefficients or modification coefficients, rounded factors or oversizing factors. All factors that influence significantly the value of the near-collapse PGA and therefore the value of the q_0 -factor. To obtain a code-dependent estimation of q -factor an examination of these aspects should be done, in order to evaluate an appropriate design over-strength factor Ω . It should be noted also that these results are applicable only to perfectly regular buildings, which allow to reach the near-collapse condition after reaching the maximum displacement capacity of the building, assured by the ductility of each connection element. Other failure mechanisms might cause the collapse at lower PGA and a consequent reduction of the q_0 -factor.

Results shown in Table 2.8 and Table 2.9 suggest that the q_0 -factor values depend strongly on specific building characteristics and have a great variability. In detail, the q_0 -factor trend increases with number of storeys, number of panels used to compose walls (i.e., with the amount of vertical joints per storey) and slenderness. However, hypothesizing a single value of q -factor for the overall CLT technology – according to current version of Eurocode 8 [2.50] – and not considering the contribution of Ω -factor some conclusions can be obtained directly from the normal distribution of the results shown in Fig. 2.18.

1. The q -factor equal to 2.00, as proposed by Eurocode 8 [2.50], is a conservative value. However, it is suitable for low-rise buildings realized with large horizontal panels and no vertical joints, characterized by predominant or pure sliding behaviour. For these buildings, the behaviour is similar to a single wall specimen subjected to pure sliding deformation. It can be noted that results obtained for these cases are similar to results obtained for wall A-1 in section 2.3.1.2.

2. The q-factor equal to 3.00, as proposed by Ceccotti [2.17] and by Ceccotti and Sandhaas [2.37] is a correct value to summarize the dissipative capacity of the overall CLT technology. This value seems more suitable to represent the behaviour of medium-rise CLT buildings with vertical joints, as the one tested on the shake table within the SOFIE Project [2.17]. Analogous results can be found in [2.42].
3. Q-factors higher than 3.50, can be suitable for high-ductility buildings, as high-rise CLT structures with several and correctly designed vertical joints. Therefore, the application of these high values should be supported by precise design and detail rules.

It seems therefore appropriate to analyse obtained results and to study their statistical variability with the geometrical parameters considered. Preliminary analytical formulations that consider such variability of the behaviour factor can be found in [2.39]. In the following section an update of these formulations is given, considering the results from the additional NLDAs performed.

2.4 Updating of analytical formulations for the computation of the q_0 -factor for regular buildings

2.4.1 Analyses of results by indexes

In CLT structures, the connections are arranged along the interfaces of panels with the foundation, floor, roof, and other panels. A specific index, α , is proposed to account for the joint density of the building, and is defined as the ratio between façade area A and the sum of connection line lengths P . Once wall dimensions (B and H), inter-storey height (h), façade area (A), storey number (n) and number of vertical joints per storey (m) have all been defined, index α can be calculated according to Equation (2.5). The reference configuration of a hypothetical façade without any intermediate vertical joint is characterized by index α_0 , defined as the ratio between area (A) and perimeter (P_0), according to Equation (2.6). Fig. 2.19 shows the specific indexes α and α_0 for a typical wall.

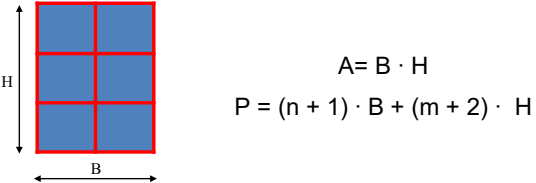
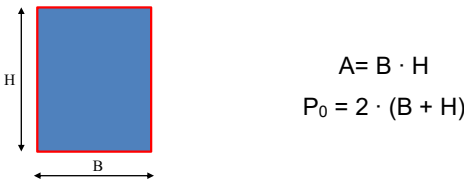
Current configuration	Reference configuration
$\alpha = \frac{A}{P} \quad (2.5)$	$\alpha_0 = \frac{A}{P_0} \quad (2.6)$
 <p style="text-align: center;"> $A = B \cdot H$ $P = (n + 1) \cdot B + (m + 2) \cdot H$ </p>	 <p style="text-align: center;"> $A = B \cdot H$ $P_0 = 2 \cdot (B + H)$ </p>

Fig. 2.19 – Definition of actual (left) and reference (right) joint indexes.

The ratio between the two indexes in Equation (2.7) provides a-dimensional joint density index β , accounting for both number of vertical joints and number of storeys.

$$\beta = \frac{\alpha_0}{\alpha} = \frac{P}{P_0} \quad (2.7)$$

Table 2.10 and Table 2.11 list the values of β index for each configuration, together with q_0 -factor range and average values.

Table 2.10 – Indexes and q_0 -factor values for buildings with $B=17.50$ m.

Geometric parameters	Notations	Units	1 STOREY			3 STOREYS			5 STOREYS			7 STOREYS		
Height dimension	H	m	3.05			9.15			15.25			21.35		
Base dimension	B	m	17.50			17.50			17.50			17.50		
Vertical joint number	m	-	0	3	12	0	3	12	0	3	12	0	3	12
Slenderness	$\lambda = H/B$	-	0.17	0.17	0.17	0.52	0.52	0.52	0.87	0.87	0.87	1.22	1.22	1.22
Façade area	$A = H \cdot B$	m ²	53.4	53.4	53.4	160.1	160.1	160.1	266.9	266.9	266.9	373.6	373.6	373.6
Reference Perimeter	P_0	m	41.1			53.3			65.5			77.7		
Perimeter	P	m	41.1	50.3	77.7	88.3	115.8	198.1	135.5	181.3	318.5	182.7	246.8	438.9
β index	β	-	1.00	1.22	1.89	1.66	2.17	3.72	2.07	2.77	4.86	2.35	3.18	5.65
q_0-factor variability	Notations	Units												
Minimum	q_0	-	1.57	1.71	2.06	2.69	2.96	3.66	2.96	3.57	4.04	3.01	4.03	4.39
Average	q_0	-	1.76	2.04	2.27	3.07	3.41	4.12	3.76	4.04	4.57	3.98	4.51	5.06
Maximum	q_0	-	2.01	2.41	2.61	3.39	3.98	4.72	4.84	4.58	5.08	4.30	4.95	5.38

Table 2.11 – Indexes and q_0 -factor values for buildings with $B=8.75$ m.

Geometric parameters	Notations	Units	1 STOREY			3 STOREYS			5 STOREYS			7 STOREYS		
Height dimension	H	m	3.05			9.15			15.25			21.35		
Base dimension	B	m	8.75			8.75			8.75			8.75		
Vertical joint number	m	-	0	1	5	0	1	5	0	1	5	0	1	5
Slenderness	$\lambda = H/B$	-	0.35	0.35	0.35	1.05	1.05	1.05	1.74	1.74	1.74	2.44	2.44	2.44
Façade area	$A = H \cdot B$	m ²	26.7	26.7	26.7	80.1	80.1	80.1	133.4	133.4	133.4	186.8	186.8	186.8
Reference Perimeter	P_0	m	23.6			35.8			48.0			60.2		
Perimeter	P	m	23.6	26.7	38.9	53.3	62.5	99.1	83.0	98.3	159.3	112.7	134.1	219.5
β index	β	-	1.00	1.13	1.65	1.49	1.74	2.77	1.73	2.05	3.32	1.87	2.23	3.65
q_0-factor variability	Notations	Units												
Minimum	q_0	-	1.92	1.87	1.89	3.14	3.14	2.86	3.73	3.20	3.47	4.00	4.25	4.75
Average	q_0	-	2.31	2.30	2.39	3.41	3.48	3.63	4.18	4.05	4.38	4.23	4.44	5.20
Maximum	q_0	-	2.74	2.74	2.86	3.71	3.66	4.57	4.69	4.86	4.86	4.43	4.57	5.71

The results show how the q_0 -factor increases with index β . It can be noted also that for a given β value, a slender building has a higher q_0 -factor, i.e., building slenderness λ also influences the q_0 -factor. Accordingly, it may be expressed the q_0 -factor as a function of indexes β and λ . Their relationship with q_0 -factor can be studied by means of frequency distribution curves. Fig. 2.20 and Fig. 2.21 show the frequency histograms of the q_0 -factor grouped with a class amplitude of 0.25. The corresponding normal distributions overlap the frequency histograms. A first representation may be made by separating the values corresponding to two ranges of slenderness λ : $0 < \lambda \leq 1$ and $\lambda > 1$. Fig. 2.20 clearly shows that configurations with higher slenderness have higher q_0 -factor values.

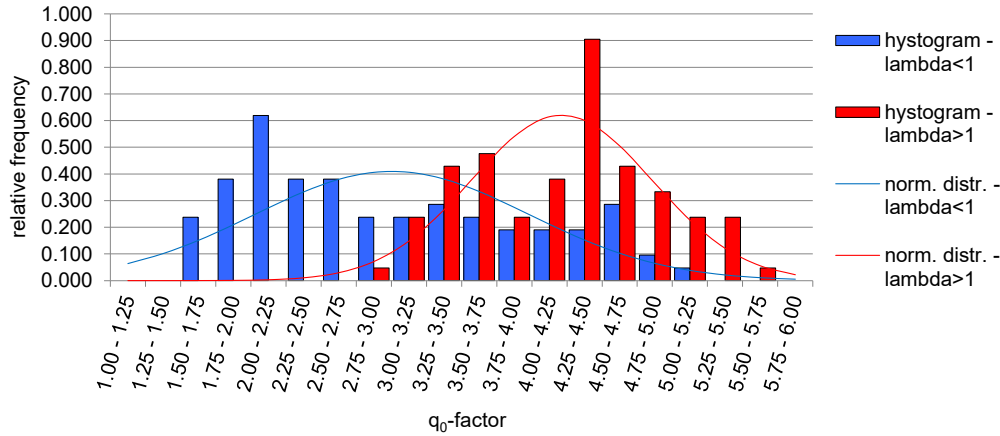


Fig. 2.20 – Histograms and normal distributions of q_0 -factors for two ranges of slenderness.

The frequency histograms for increasing levels of coefficient β can also be calculated. Three ranges were examined: $1 \leq \beta \leq 2$; $2 < \beta \leq 3$; $\beta > 3$. Fig. 2.21 shows the histograms and corresponding normal distributions. The normal distributions show that the q_0 -factor strongly depends on index β .

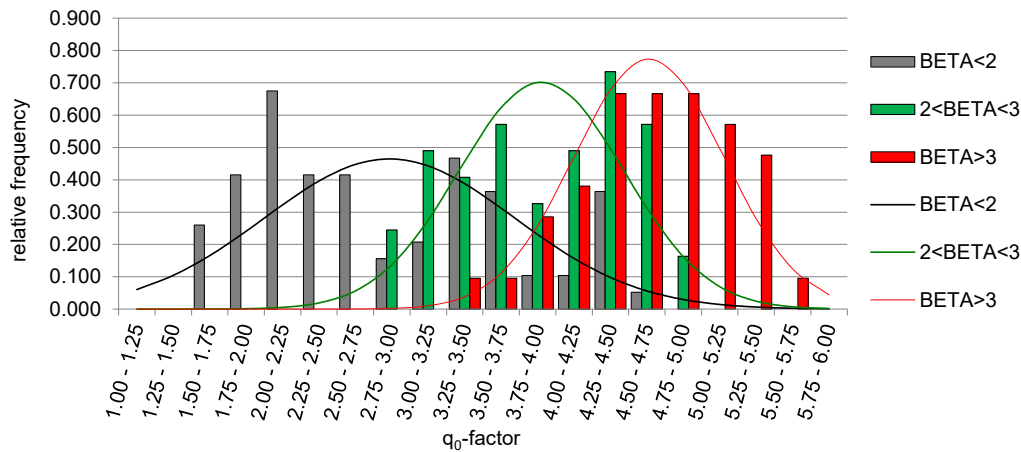


Fig. 2.21 – Histograms and normal distributions of q_0 -factors for three ranges of β .

2.4.2 Proposed analytical formulations

Two analytical formulas for the computation of q_0 -factor with suitable correlation between λ and β are proposed here. The first formulation correlates the q_0 -factor values with β and λ by means of four coefficients, as shown by Equation (2.8):

$$q_0(\beta, \lambda) = k_1 \lambda^{k_2} + k_3 \beta^{k_4} \quad (2.8)$$

The second formulation proposes a function according to Equation (2.9).

$$q_0(\beta, \lambda) = (q_{0,\text{ref}} + k_1 \lambda) \beta^{k_2} \quad (2.9)$$

In both formulations, the coefficients were calibrated to minimize the summation of the square difference between analytical values and numerical average values of the q_0 -factor. It was adopted the average value for the calibration of the empirical coefficients, because of the use of seven

seismic signals to obtain the results. According to this minimization procedure, the parameters which guarantee the best fit are $k_1=2.259$, $k_2=0.367$, $k_3=0.791$, $k_4=0.725$, (first formulation) and $k_1=0.554$, $k_2=0.355$, $q_{0,ref}=2.118$ (second formulation).

As a final remark, the proposed analytical laws do not pose any limit on the q_0 -factor for high values of λ and β . An upper limit of $q_{max}=5$ should be assumed.

The analytical formulations in Equations (2.8) and (2.9) lead to the abacus representations shown in Fig. 2.22, which allow immediate estimation of the appropriate q_0 -factor for a CLT building with specific slenderness λ and joint density β .

The good accuracy of the formulations is certified by comparing the analytical results and the numerical average values with scatter plots (Fig. 2.23) and with residual plots (Fig. 2.24). It can be seen that a maximum relative error of $\pm 20\%$ (Fig. 2.23) or a maximum absolute error of q_0 equal to ± 0.5 (Fig. 2.24) has been obtained with both formulations. In particular, formulation 1 shows minor errors (absolute of ± 0.3) thanks to the high number of empirical coefficients used.

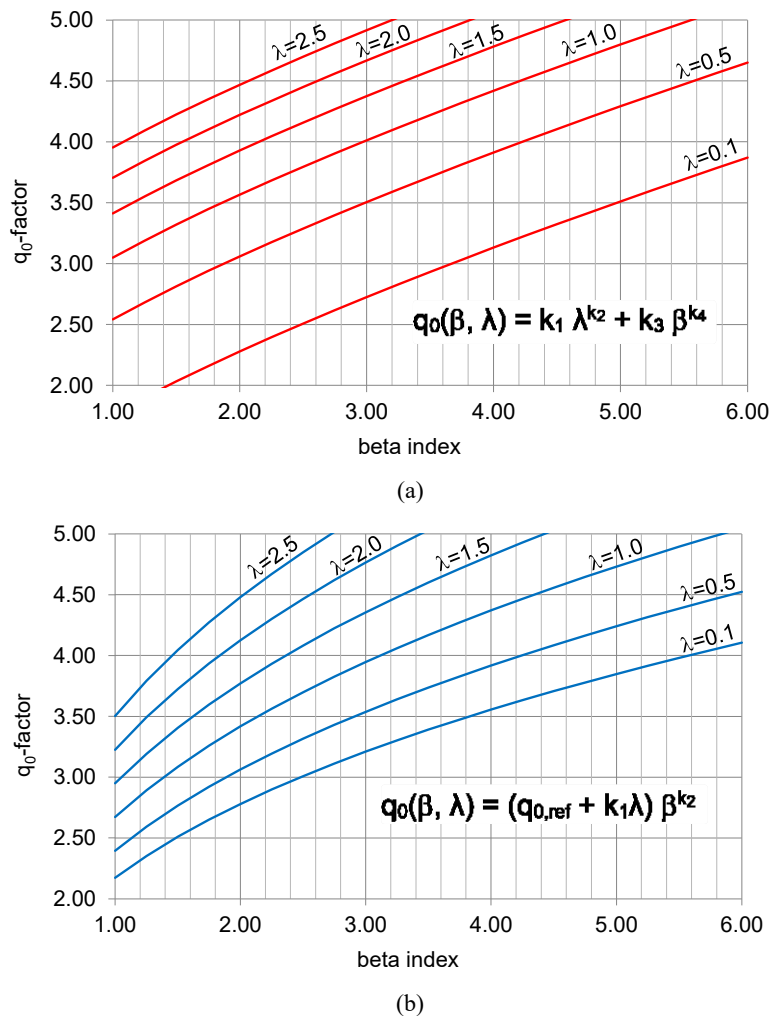


Fig. 2.22 – Abacus representations for q_0 -factor estimation: (a) first formulation; (b) second formulation.

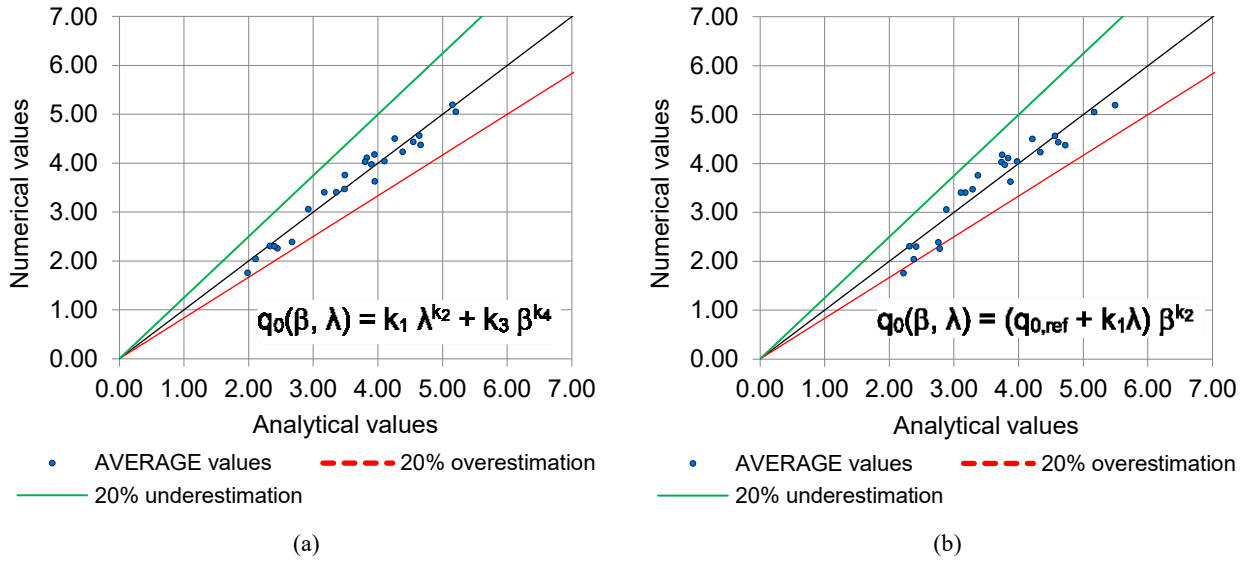


Fig. 2.23 – Comparison between average numerical results and analytical prediction with scatter plots: (a) first formulation; (b) second formulation.

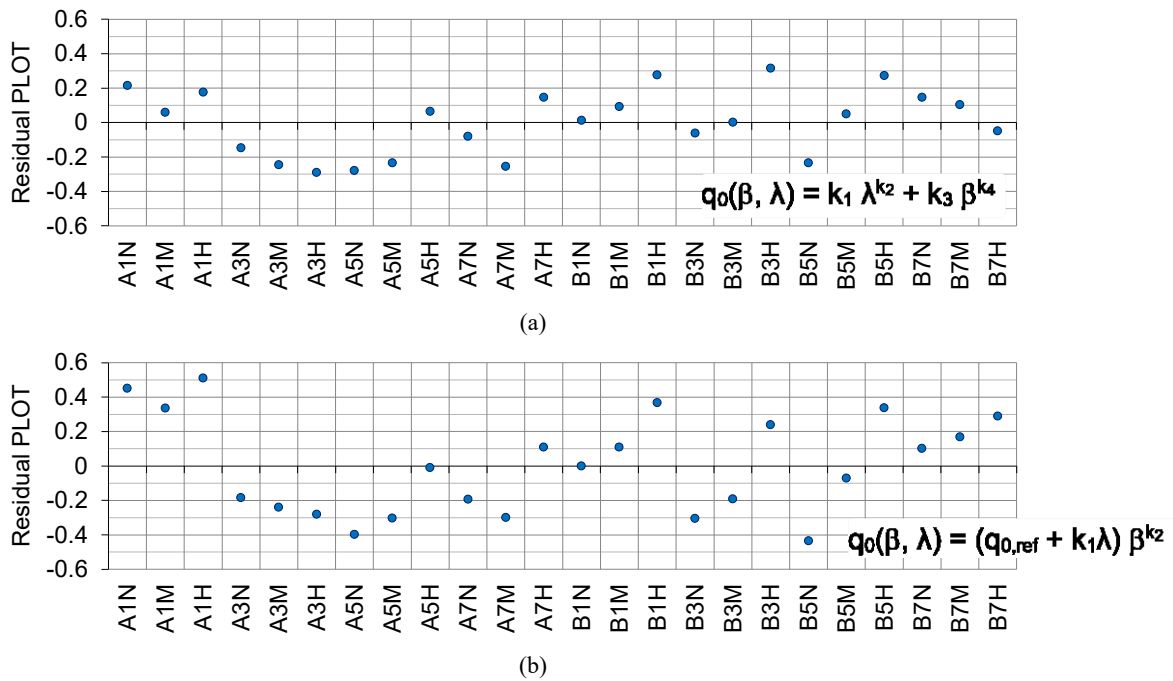


Fig. 2.24 – Comparison among average numerical results and analytical prediction with residual plots: (a) first formulation; (b) second formulation.

A simpler and conservative formulation, which allows also to reduce positive residuals, could be obtained from formulation 2, imposing $q_{0,ref} = 2.00$ and rounding the proposed factors, equation (2.10). The abacus representation is shown in Fig. 2.25

$$q_0(\beta, \lambda) = \left(2.00 + \frac{\lambda}{2} \right) \cdot \sqrt[3]{\beta} \quad (2.10)$$

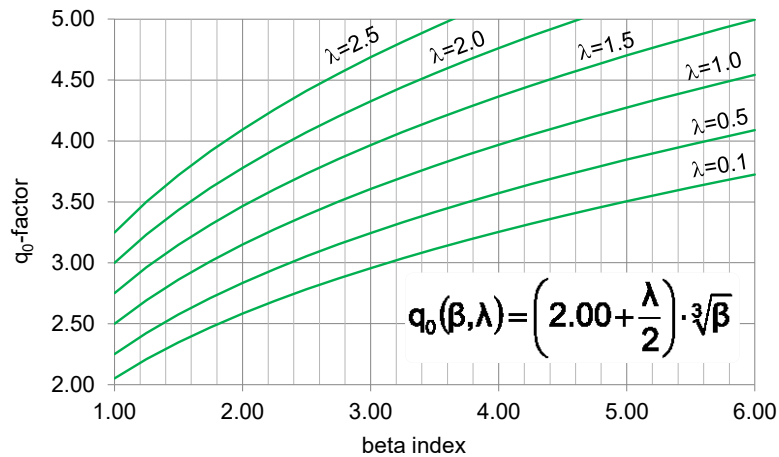


Fig. 2.25 – Abacus representation for the approximate formulation.

This formulation provides the q_0 -factor for in-plane and in-elevation regular buildings. Additional coefficients should be multiplied in order to consider also irregularities ($k_R \leq 1.00$) and design over-strength ($\Omega \geq 1.00$). Furthermore, suitable safety coefficients could be applied in order to change from the average test behaviour obtained from a unique experimental test to a 5% characteristic one.

2.5 Study of the behaviour of in-elevation non-regular buildings

2.5.1 Definition of irregularity in elevation for CLT buildings

The regularity of a building is an important factor that has to be taken into account in its seismic design. In-plan regularity improves the response of a building, reducing some drawbacks, e.g., the eccentricity between centre of mass and stiffness; the importance of torsional modes; and the differences in terms of unitary lateral loads among the shear walls of the building. The in-elevation irregularity affects the transmission of the seismic loads from the roof to the building foundation and makes possible the presence of soft-storey mechanisms, which involve the collapse of the building due to the failure of the weakest storey (normally the ground floor). Collapse mechanisms imputable to irregularities often took place under seismic events, even for timber structures. Many multi-storey wood-frame buildings have been identified as susceptible to collapse at the first storey during earthquakes [2.69]. This type of collapse for timber-frame buildings was analysed with full-scale tests performed during NEES-Soft project [2.70], Fig. 2.26. No test evidences regarding CLT structures are currently available yet, but it is evident that also CLT buildings are more exposed to failures if irregular in elevation.



Fig. 2.26 – NEES-Soft project. Collapse of a wood-frame building due to “soft-storey” mechanism. [2.71]

The European seismic code Eurocode 8 [2.50] recognises these issues and recommends that “to the extent possible, structures should have simple and regular forms both in plan and elevation. If necessary this may be realised by subdividing the structure by joints into dynamically independent units”. The same code provides the criteria for structural regularity and the methods to design the irregular structures, summarized in Fig. 2.27.

Regularity		Allowed Simplification		Behaviour factor
Plan	Elevation	Model	Linear-elastic Analysis	(for linear analysis)
Yes	Yes	Planar	Lateral force ^a	Reference value
Yes	No	Planar	Modal	Decreased value
No	Yes	Spatial ^b	Lateral force ^a	Reference value
No	No	Spatial	Modal	Decreased value

^a If the condition of 4.3.3.2.1(2)a) is also met.

^b Under the specific conditions given in 4.3.3.1(8) a separate planar model may be used in each horizontal direction, in accordance with 4.3.3.1(8).

Fig. 2.27 – Consequences of structural regularity in seismic analysis and design [2.50].

A specific definition of in-elevation regularity is not given in Eurocode 8 [2.50] for timber structures. In this section, the applicability of the generic definitions of in-elevation regularity to CLT structures is investigated by means of numerical analyses of irregular case-study buildings. Conversely, being the general in-plan regularity criteria clearly applicable also to CLT structures, no specific studies were conducted about these. Therefore, the word *irregularity* hereafter means *in-elevation irregularity*.

In literature no researches on in-elevation regularity of CLT buildings have been found, therefore the only reference is again Eurocode 8 [2.50]. In section eight, specific rules for timber buildings are given. The only reference to in-elevation irregularity recommends to reduce the value of the behaviour factor for irregular buildings and refers to the generic definitions of irregularity. “If the building is non-regular in elevation the q -values should be reduced by 20%, but need not be taken less than $q=1.5$ ” [2.50]. The obvious implication for CLT buildings is to assume a behaviour factor $q=1.6$ for irregular buildings instead of $q=2$ for regular “glued wall panels with glued diaphragms, connected with nails and bolts” [2.50]. The section 4.2.3.3 of Eurocode 8 provides the general

criteria for regularity in elevation applicable to all structures. Below, each criterion is partially taken from this code and the application to CLT buildings is discussed.

1. *“All lateral load resisting systems, such as cores, structural walls, or frames, shall run without interruption from their foundations to the top of the building or, if setbacks at different heights are present, to the top of the relevant zone of the building”.*

This criterion is clearly applicable to CLT structural walls and is normally satisfied for CLT buildings.

2. *“Both the lateral stiffness and the mass of the individual storeys shall remain constant or reduce gradually, without abrupt changes, from the base to the top of a particular building”.*

It is well known that in CLT structures stiffness is mainly linked to connections. If such criterion is applied, an in-elevation regular CLT building should be characterized either by the same mass and the same connections at each storey, or by a proportional gradually decreased mass and number of connections from the base to the top of the building. Therefore, the fulfilment of this criterion would involve a localized failure of the connections at ground floor where the seismic shear is maximum (i.e. “soft-storey” failure).

3. *“In framed buildings the ratio of the actual storey resistance to the resistance required by the analysis should not vary disproportionately between adjacent storeys. Within this context the special aspects of masonry infilled frames are treated in 4.3.6.3.2”.*

This criterion is restricted to framed buildings only, however if applied in design of connections in CLT structures, a seismic failure with simultaneous crisis of connections at each storey would be assured, i.e. the achievement of the maximum global ductility and dissipative capacity. Therefore, this criterion seems consistent for CLT structures and should be extended to these structures as well, but is contradictory with the previous one.

4. *“When setbacks are present, the following additional conditions apply:*
 - a. *for gradual setbacks preserving axial symmetry, the setback at any floor shall be not greater than 20 % of the previous plan dimension in the direction of the setback;*
 - b. *for a single setback within the lower 15 % of the total height of the main structural system, the setback shall be not greater than 50 % of the previous plan dimension. In this case the structure of the base zone within the vertically projected perimeter of the upper storeys should be designed to resist at least 75% of the horizontal shear forces that would develop in that zone in a similar building without the base enlargement;*
 - c. *if the setbacks do not preserve symmetry, in each face the sum of the setbacks at all storeys shall be not greater than 30 % of the plan dimension at the ground floor above the foundation or above the top of a rigid basement, and the individual setbacks shall be not greater than 10 % of the previous plan dimension”.*

The application of these last criteria to CLT shear-wall buildings is clear and does not require any discussion.

According to previous principles both two following criteria could define a regular CLT building, assuming that the seismic masses are constant at each storey:

1. The number of angle brackets and hold-downs remains the same for each storey and equal to that assumed at ground floor, i.e., the lateral stiffness remains constant;

2. The number of angle brackets and hold-downs decreases from the foundation to the roof to maintain constant among storeys the ratio of the actual storey resistance to the resistance required by the analysis.

However, these two criteria imply a marked different seismic response of a building.

1. Applying the first criterion:
 - a. The building fails always due to failure of connections at ground floor, whereas connections at upper floors remain elastic or almost elastic. This could be favourable to replace connections after seismic events but reduces significantly the ductility and the energy dissipation, which are assured only by the connections at foundations;
 - b. The lateral top displacement of the building is mainly due to base sliding and base rocking and the storey drift is maximum at the ground floor;
 - c. The building is characterized by higher global lateral stiffness and lower fundamental period. This is favourable for the damage limitation state (DLS) verification but unfavourable for ultimate limit state (ULS) verification for buildings with $T > T_c$.
2. Applying the second criterion:
 - a. The building is characterized by lower lateral stiffness;
 - b. The building tends to fail with contemporary failure of connections at each floor; all connections in the building are yielded and the building fails achieving the maximum available ductility and dissipation capacity;
 - c. The top displacement is given by sliding and rocking of all storeys. The storey drift (summation of sliding and rocking contributes) increases from the foundation to the roof. The DLS verification becomes fundamental, in particular for slender buildings.

In conclusion, the application of the first criterion implies a reduction of dissipative capacity, which implies a decreased value of the behaviour factor. Therefore, the regularity for CLT buildings can be obtained only applying the second criterion. Below, numerical analyses demonstrate this evidence and provide a reduction value for the q-factor applicable to CLT buildings designed with the first criterion, i.e., irregular buildings, to be compared with the reduction factor for in-elevation irregular buildings proposed by Eurocode 8 (see Fig. 2.27).

2.5.2 Q-factor reduction for in-elevation irregular CLT buildings

The case-study buildings presented in section 2.3.2 were regular in elevation because they were designed according to the second criterion discussed above, i.e., at each storey the ratio between the resistance capacity to the resistance demand was set equal to 1.00.

The same set of NLDAs has been performed on the same case-study buildings, now non-regular in elevation. The irregularity in elevation means that the connections designed for the ground floor are kept constant along the entire height of the buildings. Therefore, the ratio of the actual storey resistance to the resistance required by the design is equal to 1.00 for the connections at the base, whereas it increases for each upper storey and is maximum for the highest storey. These buildings are therefore non-regular in elevation. All the numerical analyses have been replicated for all case-study buildings, except of the one-storey buildings.

Results in terms of q-factor obtained for irregular buildings are hereafter compared with the same for regular buildings. Such comparison allows to verify the decrease of the behaviour factor for the irregular buildings and to estimate the consequent reduction coefficient k_R , as ratio between the q_0 -factors obtained from numerical analyses of irregular buildings and those already computed in section 2.3.2.3 for regular buildings, according to Fig. 2.27. Table 2.12 and Table 2.13 list all the obtained k_R coefficients, which are summarized in Fig. 2.28 by means of normal distribution.

The preliminary evidences are:

- In the irregular buildings the total amount of metal connections has increased significantly;
- The connections at upper storeys undergo displacements always less than connections at ground floor, therefore all the irregular buildings fail with a total top displacement lower than that reached by the regular buildings.

Table 2.12 – Obtained k_R coefficients for case-study building with $B=17.50$ m.

Geometric parameters	Notations	Units	3 STOREYS			5 STOREYS			7 STOREYS		
Height dimension	H	m	9.15			15.25			21.35		
Amount of vertical joints per storey	m	-	0	3	12	0	3	12	0	3	12
Vertical joint index			NVJ	MVJ	HVJ	NVJ	MVJ	HVJ	NVJ	MVJ	HVJ
Seismic signals	Notations	Units									
Earthquake 1	k_R	-	0.67	0.64	0.64	0.67	0.81	0.77	0.66	0.55	0.89
Earthquake 2	k_R	-	0.84	0.89	0.68	0.73	0.86	0.94	0.91	0.89	0.95
Earthquake 3	k_R	-	0.70	0.62	0.74	0.63	0.78	0.84	0.71	0.80	0.86
Earthquake 4	k_R	-	0.93	0.78	0.75	0.51	0.80	0.75	0.61	0.79	0.91
Earthquake 5	k_R	-	0.87	0.70	0.89	0.84	0.88	0.89	0.80	0.67	0.86
Earthquake 6	k_R	-	0.67	0.76	0.64	0.74	0.64	0.75	0.89	0.77	0.88
Earthquake 7	k_R	-	0.73	0.63	0.59	0.64	0.75	0.88	0.64	0.81	0.77
Average	k_R	-	0.77	0.72	0.70	0.68	0.79	0.83	0.75	0.75	0.88

Table 2.13 – Obtained k_R coefficients for case-study building with $B=8.75$ m.

Geometric parameters	Notations	Units	3 STOREYS			5 STOREYS			7 STOREYS		
Height dimension	h	m	9.15			15.25			21.35		
Amount of vertical joints per storey	m	-	0	1	5	0	1	5	0	1	5
Vertical joint index			NVJ	MVJ	HVJ	NVJ	MVJ	HVJ	NVJ	MVJ	HVJ
Seismic signals	Notations	Units									
Earthquake 1	k_R	-	0.67	0.65	0.78	0.47	0.68	0.65	0.50	0.88	0.91
Earthquake 2	k_R	-	0.65	0.73	0.65	0.67	0.76	0.87	0.67	0.94	0.89
Earthquake 3	k_R	-	0.58	0.52	0.61	0.57	0.73	0.80	0.67	0.53	0.88
Earthquake 4	k_R	-	0.65	0.68	0.74	0.77	0.85	0.75	0.79	0.75	0.73
Earthquake 5	k_R	-	0.83	0.73	0.73	0.86	0.87	0.92	0.72	0.77	0.96
Earthquake 6	k_R	-	0.66	0.73	0.81	0.65	0.86	0.92	0.72	0.81	0.83
Earthquake 7	k_R	-	0.70	0.60	0.69	0.40	0.76	0.73	0.69	0.62	0.82
Average	k_R	-	0.68	0.66	0.72	0.63	0.79	0.81	0.68	0.76	0.86

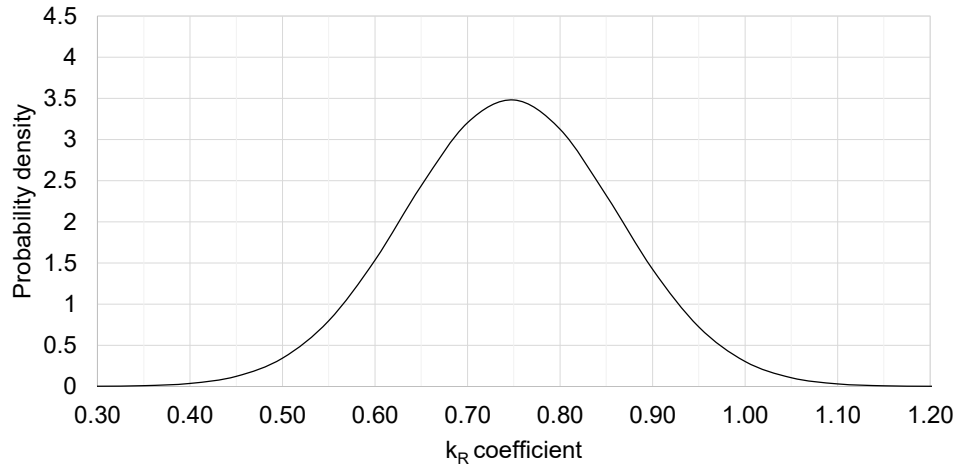


Fig. 2.28 – Normal distribution of obtained k_R coefficients.

The obtained values of k_R coefficient are always less than 1.00. This demonstrates that the design criterion consisting in replicating at each storey the connections designed for the ground floor leads to a non-regular building. As shown by Fig. 2.28, the average k_R coefficient is about 0.75, which is very similar to coefficient 0.8 proposed by Eurocode 8 [2.50]. This means that the in-elevation irregularity of a CLT building can be taken into account reducing the reference q-factor and that the coefficient 0.8 is a suitable value to account for this phenomenon.

An analysis of results listed in Table 2.12 and Table 2.13 show a relatively high dispersion, because they range from 0.40 to 0.96 considering all signals, or from 0.63 to 0.88 considering average values. Grouping results among three categories, i.e., buildings without vertical joints (NVJ), with medium density of vertical joints (MVJ) and with high density of vertical joints (HVJ) it is possible to reduce slightly the dispersion of results, as shown by Fig. 2.29. It can be noted that the average coefficient varies for the three configurations: approximately 0.70 for NVJ, 0.75 for MVJ and 0.8 for HVJ. This leads to the further conclusion that the presence of vertical joints affects positively the effects of in-elevation irregularity thanks to a more diffuse energy dissipation.

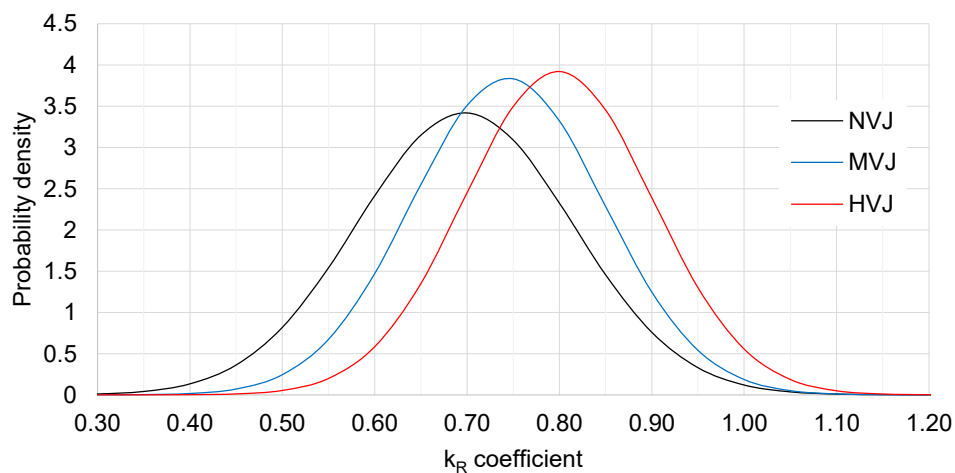


Fig. 2.29 – Normal distribution of obtained k_R coefficients, grouped according to vertical joint density.

It is clear that the definition given by Eurocode 8 [2.50] of in-elevation regularity for a CLT building remains not fully exhaustive. Application of first criterion (section 2.5.1) could lead to classify an irregular building as regular.

It has to be noted that these results do not preclude that also the in-plan regularity could reduce the dissipative capacity and therefore the q_0 -factor for CLT buildings. As proposed for other structural systems (e.g., [2.72]) the overall irregularity reduction can be considered multiplying $k_{R,p}$ accounting for in-plan regularity and $k_{R,h}$ accounting for in-elevation regularity, according to the following equation (2.11):

$$k_R = k_{R,p} \cdot k_{R,h} \quad (2.11)$$

In this work the in-plan regularity has not been studied ($k_{R,p}=1$) therefore k_R coincides with $k_{R,h}$. To extend results to in-plan irregular buildings, 3D models have to be performed and analyses on different case-study buildings can provide a suitable $k_{R,p}$ value also for in-plane irregular CLT buildings.

2.6 Conclusions

This chapter presented two methods for deriving the q -factor applicable to the seismic design of CLT buildings, based on definition of sub-factors q_0 and Ω , which account for energy dissipation capacity and design over-strength. The first method is based on the analysis of the experimental data obtained from standardized cyclic-loading tests on wall specimens. The second method is based on numerical simulations of earthquakes by means of dynamic analyses applied to non-linear models.

An original point here is the combined use of data generated by physical and numerically simulated case studies to characterise suitable values of q and its sub-factors according to wall and building configurations. Another original aspect discussed in this chapter is that due attention must be paid to evaluate how design decisions influence ductility and energy dissipation capacity of shear walls or entire buildings. In detail, a different response has to be expected, depending on: design (methods, codes and coefficients); presence of vertical joints; number of storeys; slenderness of the building; irregularity (adopted criterion and coefficient). These parameters led to different values of the q_0 -factor applicable to CLT building systems. Analytical formulations for q_0 -factor for regular buildings have been given.

Obtained results demonstrated that it is fundamental to give to designers clear rules for a safe seismic design of CLT structures. These rules should clarify the methods to compute the lateral resistance of CLT shear walls and the correct evaluation of the irregularity.

Obtained results demonstrated also that the definitions provided by Eurocode 8 for the structural regularity do not fit with CLT buildings. In particular, it was demonstrated that two definitions are contradictory if applied to CLT and that the most correct definition between these is limited to framed buildings. Therefore, a proposal of modification of these two definitions can be provided as follows:

1. "The mass of the individual storeys shall remain constant or reduce gradually, without abrupt changes, from the base to the top of the building".

2. “The ratio of the actual storey resistance to the resistance required by the analysis should remain constant from the base to the top of a particular building”.

However, it has to be highlighted that the application of the second definition implies an increase of deformability of the building and a marked increase of inter-storey drift at higher storeys, due to summation of drifts given by rocking at each lower storey. Therefore, it is necessary to recommend to apply always a DLS verification.

In conclusion, as anticipated in section 1.3, the behaviour factor for a CLT building can be written as:

$$q = q_0 \cdot \Omega \cdot k_R \quad (2.12)$$

Where:

- q_0 is the intrinsic q -factor, evaluated according to equation (2.10), as function of β and λ ;
- Ω is the design over-strength, that can be assumed in the range between 1.00 and 1.30 in function of design method and applied standard code;
- $k_R = k_{R,p} \cdot k_{R,h}$ accounts for overall irregularity, where $k_{R,h}$ can be taken equal to a value in the range between 0.7 and 0.8.

Acknowledgments

The experimental tests presented in this chapter have been carried out by CNR-IVALSA within the SOFIE project. CNR-IVALSA is acknowledged for test data kindly provided.

References – Chapter 2

- [2.1] Bogensperger, T., Moosbrugger, T., and Silly, G. (2010). “Verification of CLT-plates under loads in plane”. In proceedings of 11th World Conference on Timber Engineering WCTE, Riva del Garda, Italy.
- [2.2] Brandner, R., Bogensperger, T., and Schickhofer, G. (2013). “In Plane Shear Strength of Cross Laminated Timber (CLT): Test Configuration, Quantification and Influencing Parameters”. In proceeding of Meeting 46 of the Working Commission W18-Timber Structures, CIB, Vancouver, Canada, paper CIB-W18/46-12-2.
- [2.3] Flaig, M., and Blass, H.J. (2013). “Shear strength and shear stiffness of CLT-beams loaded in plane”. In proceeding of Meeting 46 of the Working Commission W18-Timber Structures, CIB, Vancouver, Canada, paper CIB-W18/46-12-3.
- [2.4] Karacabeyli, E., and Douglas, B. (2013). “CLT Handbook”. FPIInnovations, U.S. Edition.
- [2.5] Thiel, A., Zimmer, S., Augustin, M., and Schickhofer, G. (2013). “CLT and floor vibrations: A comparison of design methods”. In proceeding of Meeting 46 of the Working Commission W18-Timber Structures, CIB, Vancouver, Canada, paper CIB-W18/46-20-1
- [2.6] Thiel, A. (2013). “ULS and SLS design of CLT and its implementation in the CLTdesigner”. European

Conference on Cross Laminated Timber (CLT), COST Action FP1004, Graz. Edited by Harris, R., Ringhofer, A., and Schickhofer, G.

- [2.7] Brandner, R., and Schickhofer, G. (2014). "Properties of Cross Laminated Timber (CLT) in Compression Perpendicular to Grain". In proceedings of 1st International Network on Timber Engineering Research (INTER), Bath, United Kingdom, paper INTER/47-12-5.
- [2.8] Flaig, M. (2014). "Design of CLT Beams with Rectangular Holes or Notches". In proceedings of 1st International Network on Timber Engineering Research (INTER), Bath, United Kingdom, paper INTER/47-12-4.
- [2.9] Zarnani, P., and Quenneville, P. (2014). "Resistance of Connections in Cross-Laminated Timber (CLT) Under Block Tear-Out Failure Mode". In proceedings of 1st International Network on Timber Engineering Research (INTER), Bath, United Kingdom, paper INTER/47-7-3.
- [2.10] Uibel, T., and Blass, H.J. (2006). "Load Carrying Capacity of Joints with Dowel Type Fasteners in Solid Wood Panels". In proceeding of Meeting 39 of the Working Commission W18-Timber Structures, CIB, Florence, Italy, paper CIB-W18/39-7-5
- [2.11] Uibel, T., and Blass, H.J. (2007). "Edge Joints with Dowel Type Fasteners in Cross Laminated Timber". In proceeding of Meeting 40 of the Working Commission W18-Timber Structures, CIB, Bled, Slovenia, paper CIB-W18/40-7-2
- [2.12] Johansen, K.W. (1949). Theory of timber connections. International Association of bridge and structural Engineering, Bern, p. 249-262.
- [2.13] Bernasconi, A. (2010). "Il materiale XLAM: caratteristiche e prestazioni". Available online: www.promolegno.com.
- [2.14] SOFIE PROJECT. Available online: www.ivalsa.cnr.it.
- [2.15] Ceccotti, A., Lauriola, M.P., Pinna, M., and Sandhaas, C. (2006a). "SOFIE project – cyclic tests on cross-laminated wooden panels." In proceedings of the 9th World Conference on Timber Engineering (WCTE), Portland, USA.
- [2.16] Ceccotti, A., Follesa, M., Lauriola, M.P., Sandhaas, C., Minowa, C., Kawai, N., and Yasumura, M. (2006b). "Which seismic behaviour factor for multi-storey buildings made of cross-laminated wooden panels?" In proceedings of Meeting 39 of the Working Commission W18-Timber Structures, Florence, Italy, paper CIB 39-15-2.
- [2.17] Ceccotti, A. (2008). "New technologies for construction of medium-rise buildings in seismic regions: the XLAM case". Structural Engineering International **18(2)**:156-165.
- [2.18] Ceccotti, A., Sandhaas, C., Okabe, M., Yasumura, M., Minowa, C. and Kawai, N. (2013). "SOFIE project – 3D shaking table test on a seven-storey full-scale cross-laminated timber building". Earthquake Engineering & Structural Dynamics **42(13)**: 2003-2021.
- [2.19] Popovski, M., Schneider, J. and Schweinsteiger, M. (2010). "Lateral load resistance of Cross-Laminated wood panels". In proceeding of the 11th World Conference on Timber Engineering (WCTE), Riva del Garda, Italy.
- [2.20] Popovski, M., and Gavric, I. (2015). "Performance of a 2-Story CLT House Subjected to Lateral Loads". Journal of Structural Engineering. ASCE. DOI 10.1061/(ASCE)ST.1943-541X.0001315.
- [2.21] Gavric, I., Fragiaco, M., Popovski, M. and Ceccotti, A. (2014) "Behaviour of cross-laminated timber panels under cyclic loads". Materials and Joints in Timber Structures **9**:689-702.

- [2.22] Yasumura, M. (2012). "Determination of failure mechanism of CLT shear walls subjected to seismic action". In proceedings of Meeting 45 of the Working Commission W18-Timber Structures, Växjö, Sweden, paper CIB 45-15-3.
- [2.23] Yasumura, M., Kobayashi, K., Okabe, M., Miyake, T., and Matsumoto, K. (2015). "Full-Scale Tests and Numerical Analysis of Low-Rise CLT Structures under Lateral Loading". *Journal of Structural Engineering*. ASCE. DOI 10.1061/(ASCE)ST.1943-541X.0001348.
- [2.24] Hristovski, V., Dujic, B., Stojmanovska, M., and Mircevska, V. (2013). "Full-Scale Shaking-Table Tests of XLam Panel Systems and Numerical Verification: Specimen 1". *Journal of Structural Engineering*, **139(11)**:2010-2018. ASCE.
- [2.25] Flatscher, G., and Schickhofer, G. (2015). "Shaking-table test of a cross-laminated timber structure". *Proceedings of the ICE - Structures and Buildings* **168(11)**:878-888. DOI 10.1680/stbu.13.00086.
- [2.26] TIMBER BUILDINGS PROJECT – Final report. Available online: http://www.series.upatras.gr/TIMBER_BUILDINGS.
- [2.27] Smith, I., Landis, E. and Gong, M. (2003). "Fracture and fatigue in wood". John Wiley and Sons, Chichester, UK.
- [2.28] Gavric, I., Fragiaco, M., and Ceccotti, A. (2013): "Capacity seismic design of X-LAM wall system based on connection mechanical properties." In proceedings of meeting 46 of the Working Commission W18-Timber Structures, CIB, Vancouver, Canada, paper CIB-W18/46-15-2.
- [2.29] Sandhaas, C., Boukes, J., van de Kuilen, J.W.G., and Ceccotti, A. (2009). "Analysis of X-lam panel-to-panel connections under monotonic and cyclic loading." In proceedings of Meeting 42 of the Working Commission W18-Timber Structures, CIB, Dübendorf, Switzerland, Paper CIB-W18/42-12-2.
- [2.30] Gavric, I., Ceccotti, A., and Fragiaco, M. (2011). "Experimental cyclic tests on cross-laminated timber panels and typical connections". In proceedings of ANIDIS, Bari, Italy.
- [2.31] Piazza, M., Polastri, A., and Tomasi, R. (2011). "Ductility of timber joints under static and cyclic loads". *Proceedings of the ICE - Structures and Buildings* **164(2)**:79–90.
- [2.32] Tomasi, R., and Smith, I. (2014). "Experimental characterization of monotonic and cyclic loading responses of CLT panel-to-foundation angle bracket connections". *Journal of Materials in Civil Engineering*, ASCE. DOI: 10.1061/(ASCE)MT.1943-5533.0001144.
- [2.33] Gavric, I., Fragiaco, M., and Ceccotti, A. (2015). "Cyclic behavior of typical screwed connections for cross-laminated (CLT) structures". *Eur. J. Wood Prod.* DOI 10.1007/s00107-014-0877-6.
- [2.34] Gavric, I., Fragiaco, M., and Ceccotti, A. (2015). "Cyclic behaviour of typical metal connectors for cross-laminated (CLT) structures". *Materials and structures* **48**:1841-1857.
- [2.35] Gavric, I., Fragiaco, M., and Ceccotti, A. (2015). "Cyclic behaviour of CLT wall systems: experimental tests and analytical prediction models". *Journal of Structural Engineering*, ASCE. DOI: 10.1061/(ASCE)ST.1943-541X.0001246.
- [2.36] Dujic, B., Strus, K., Zarnic, R., and Ceccotti, A. (2010). Prediction of dynamic response of a 7-storey massive XLam wooden building tested on a shaking table". In proceedings of the 11th World Conference on Timber Engineering WCTE, Riva del Garda, Italy.
- [2.37] Ceccotti, A., and Sandhaas, C. (2010). "A proposal for a standard procedure to establish the seismic behaviour factor q of timber buildings." In proceedings of the 11th World Conference on Timber Engineering WCTE, Riva del Garda, Italy.

- [2.38]Fragiacomo, M., Dujic, B., and Sustersic, I. (2011). "Elastic and ductile design of multi-storey crosslam massive wooden buildings under seismic actions". *Engineering Structures* **33**:3043-3053.
- [2.39]Pozza, L., Scotta, R., Trutalli, D., Ceccotti, A., and Polastri, A. (2013). "Analytical formulation based on extensive numerical simulations of behavior factor q for CLT buildings." In proceedings of meeting 46 of the Working Commission W18-Timber Structures, CIB, Vancouver, Canada. Paper CIB-W18/46-15-5.
- [2.40]Rinaldin, G., Amadio, C., and Fragiaco, M. (2013). "A component approach for the hysteretic behaviour of connections in cross-laminated wooden structures". *Earthquake Engineering and Structural Dynamics* **42**:2023-2042.
- [2.41]Pei, S., van de Lindt, J.W., and Popovski, M. (2013). "Approximate R-Factor for Cross-Laminated Timber Walls in Multistory Buildings". *Journal of Architectural Engineering* **19**(4):245–255. ASCE.
- [2.42]Pozza, L., and Scotta, R. (2014). "Influence of wall assembly on behaviour of cross-laminated timber buildings". *Proceedings of the ICE - Structures and Buildings* **168**(4):275-286.
- [2.43]Popovski, M., Pei, S., van de Lindt, J.W., and Karacabeyli, E. (2014). "Force Modification Factors for CLT Structures for NBCC". *Materials and Joints in Timber Structures* **9**:543-553.
- [2.44]Latour, M., and Rizzano, G. (2015). "Cyclic Behavior and Modeling of a Dissipative Connector for Cross-Laminated Timber Panel Buildings". *Journal of Earthquake Engineering*, **19**(1):137-171, DOI: 10.1080/13632469.2014.948645.
- [2.45]Loo, W.Y., Kun, C., Quenneville, P. and Chouw, N. (2014). "Experimental testing of a rocking timber shear wall with slip-friction connectors". *Earthquake Engineering and Structural Dynamics*, **43**(11):1621-1639.
- [2.46]Polastri, A., Angeli, A., and Dal Ri, G. (2014). "A new construction system for CLT structures". In proceedings of World Conference on Timber Engineering WCTE, Quebec City, Canada.
- [2.47]Sarti, F., Palermo, A., and Pampanin, S. (2015). "Quasi-Static Cyclic Testing of Two-Thirds Scale Unbonded Posttensioned Rocking Dissipative Timber Walls". *Journal of Structural Engineering*, ASCE. DOI: 10.1061/(ASCE)ST.1943-541X.0001291.
- [2.48]Scotta, R., Pozza, L., Trutalli, D., Marchi, L., and Ceccotti, A. (2015). "Dissipative connections for squat or scarcely jointed CLT buildings. Experimental tests and numerical validation." In proceedings of 2nd International Network on Timber Engineering Research (INTER), Šibenik, Croatia.
- [2.49]EN 12512 (2001). "Timber structures—test methods—cyclic testing of joints made with mechanical fasteners". CEN. Brussels, Belgium.
- [2.50]EN 1998-1-1 Eurocode 8 (2004). "Design of structures for earthquake resistance, part 1: general rules, seismic actions and rules for buildings". CEN. Brussels, Belgium.
- [2.51]Pozza, L., Scotta, R., Trutalli, D., Polastri, A., and Smith, I. (2016). "Experimentally based q-factor estimation of cross-laminated timber walls". *Proceedings of the ICE - Structures and Buildings*. DOI: 10.1680/jstbu.15.00009.
- [2.52]Gavric, I. (2013). "Seismic behaviour of cross-laminated timber buildings". Ph.D. thesis, University of Trieste, Italy.
- [2.53]Foschi, R.O., and Bonac, T. (1977). "Load slip characteristic for connections with common nails". *Wood. Sci. Technol.* **9**(3):118-123.
- [2.54]Foliente, G.C. (1996). "Issues in seismic performance testing and evaluation of timber structural

systems". Proceedings of the International Timber Engineering Conference. Vol. 1:29–36.

- [2.55]EN 1995-1-1 Eurocode 5 (2004). "Design of timber structures, Part 1-1, General: Common rules and rules for buildings". CEN. Brussels, Belgium.
- [2.56]Canadian Standards Association (2009). "Engineering design in wood". Standard O86-09, CSA, Toronto, Canada.
- [2.57]Institute for Research in Construction (2010). "National Building Code". National Research Council of Canada, Ottawa, Ontario.
- [2.58]Newmark, N.M., and Hall, W.J. (1982). "Earthquake Spectra and Design". Earthquake Engineering Research Institute, Berkeley, CA.
- [2.59]Fajfar, P. (1996). "Design spectra for the new generation of codes". In proceedings of the 11th World Conference on Earthquake Engineering, Acapulco, Mexico.
- [2.60] "OpenSees. Open System for Earthquake Engineering Simulation" (2009). Pacific Earthquake Engineering Research Center, University of California, Berkeley. Available at <http://opensees.berkeley.edu>.
- [2.61]Lowes, L.N., and Altoontash, A. (2003). "Modeling reinforced-concrete beam-column joints subjected to cyclic loading". Journal of Structural Engineering, **129**:1686–1697.
- [2.62]Gelfi, P. (2012). "SIMQKE_GR", Version 2.7. University of Brescia, Italy. Available online: <http://dicata.ing.unibs.it/gelfi>.
- [2.63]Assembly and installation manual of KLH Massivholz GmbH. Available online: www.klh.at.
- [2.64]AHC group website. Available online: www.ahc1893.com.
- [2.65]Tonellato, D. (2012). "Seismic response of multi-storey buildings made with cross laminated timber panels – First part". Master Thesis, University of Padova, Italy.
- [2.66]Trutalli, D. (2012). Seismic response of multi-storey buildings made with cross laminated timber panels – Second part". Master Thesis, University of Padova, Italy.
- [2.67]Pozza, L. (2013). "Ductility and behaviour factor of wood structural systems". Ph.D. Thesis, University of Padova, Italy.
- [2.68]EN 1990 Eurocode (2002). "Basis of structural design". CEN, Brussels, Belgium.
- [2.69]Van de Lindt, J.W., Symans, M.D., Pang, W., Shao, X., and Gershfeld, M. (2012). "The NEES-Soft Project: Seismic Risk Reduction for Soft-Story Woodframe Buildings". In proceedings of the 15th WCEE, Lisboa.
- [2.70]Van de Lindt, J.W., Bahmani, P., Gershfeld, M., Mochizuki, G., Shao, X., Pryor, S.E., Pang, W., Symans, M.D., Tian, J., Ziaei, E., Jennings, E.N., Rammer, D. (2014). "Seismic risk reduction for soft-story wood-frame buildings: test results and retrofit recommendations from the NEES-Soft project". In proceedings of WCTE, Quebec City, Canada.
- [2.71]NEES website. Available online: <https://nees.org/home>.
- [2.72]Girardini, D. (2015). "Static and seismic performances of R.C. shear walls cast into wood chip and cement formworks - Experimental tests, theoretical interpretation and numerical validations". Ph.D. Thesis, University of Padova, Italy.

Chapter 3 Application of the CLT system for high-rise buildings

Abstract

The possibility of using CLT technology to build high-rise structures is explored in this chapter. The behaviour of various 3-dimensional configurations of slender buildings with seismic resisting cores and additional perimeter shear walls has been analysed with linear numerical models. Two model calibrations, based on parameters that characterise the connections used, are proposed according to codes and experimental test data respectively. Results are presented in terms of principal elastic periods, and base shear and up-lift forces. The discussion addresses primary issues associated with modelling and response of such systems. The major limitations and drawbacks concerning the realization of tall CLT structures in seismic areas and design implications are reported.

3.1 Introduction and state of the art

In recent years CLT panels have become quite widely employed in Europe and elsewhere to realize multi-storey residential, directional and commercial buildings. Mostly, traditional timber buildings employed post-and-beam structures to resist to gravity loads, while lateral loads are resisted by moment-resisting connections, cross-bracing, wood-based sheathings or non-timber frame infill materials (e.g., 3)-[3.5]).

An exhaustive description and summary of researches on traditional low and medium-rise CLT buildings have been given in Chapter 2 and their seismic response have been studied with extensive analyses.

Realization of high-rise buildings and/or buildings with large open spaces represents still an unexplored potential application for CLT. Normally, the adopted construction technologies use beams and columns for gravity loads, and CLT cores and shear walls for lateral loads generated by earthquakes or wind storms ([3.6]-[3.9]). Although examples of this new typology have been already built [3.10], their structural behaviour has not been fully investigated yet. There is no clear understanding of optimal structural configurations, dimensional limitations of spans, minimum number of columns or feasible maximum number of storeys. The most crucial aspects that have to be studied concern the construction method for CLT building cores (examples are given in [3.11];[3.12]). Other structural performance issues not fully studied are related to usage of CLT panels in place of concrete or masonry cores. Other open issues are about vertical continuity between storeys, core-to-floor connections, and core-to-foundation connections. The in-plane deformability of floors is also a factor that greatly influences the global response of buildings subjected to lateral loads ([3.13];[3.14]).

Examples of high-rise CLT structures (intended here with number of storeys equal or greater than seven) have already been realized. However, these buildings have limited height (with respect to height studied in literature) and are normally realized in low- or moderate-intensity seismic areas, Fig. 3.1.



(a)



(b)

Fig. 3.1 – (a) Murray Grove, 9 storeys, London, 2009 ([3.15];[3.16]). (b) Bridport House, 8 storeys, London, 2011 [3.17].



Fig. 3.2 – Forte Living, 10 storeys, Melbourne, 2012 ([3.18];[3.19]).

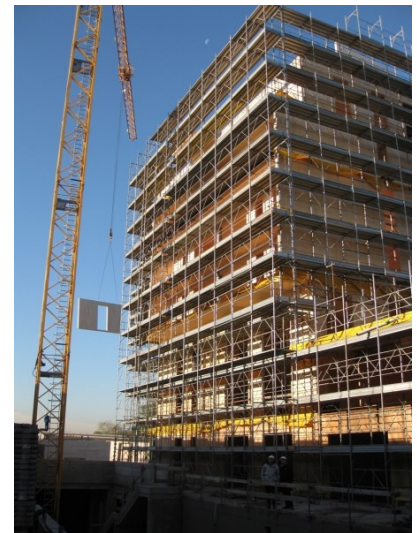


Fig. 3.3 – Cenni di cambiamento, 9 storeys, Milano, 2013 ([3.19];[3.20]).

Currently, various researches have studied different proposals to resist efficiently high seismic loads like those occurring in tall CLT buildings (up to tens of storeys) in high seismic areas. The main problem is that traditional connection elements and their anchorage with foundation and/or with timber panels are not able to resist very high loads, in particular axial loads due to rocking.

CNR-IVALSA [3.21] developed special high-strength hold-downs with ultimate resistance of about 200 kN to realize the 7-storey building tested on the shaking table, and arranged them in parallel (see Fig. 3.4). Furthermore, these hold-downs were connected to a steel foundation.

Pei et al. [3.22] proposed a “Resilient System concept”, in which *multiple resilient energy dissipation layers are distributed along the height of a tall CLT building, keeping other parts of the building relatively rigid and damage free during seismic excitation. The added “soft” layers will elongate the system natural period and increase damping.* Three innovative energy dissipative systems were proposed: “deformable floor diaphragm, single-story pre-stressed re-centering walls, multi-story segmental rocking walls”.



Fig. 3.4 – High-strength IVALSA hold-downs [3.21].

Chapman [3.23] studied a 20-storey CLT building with a central CLT core and long panels disposed vertically. This building is characterized by three main structural aspects: integrating CLT panels to form elements that are much larger; vertical panels placed end on end to ensure that gravity loads are transferred only parallel to grain; load between CLT panels transferred in direct bearing. The energy dissipation capacity is controlled with fuses at base connections.

Van de Kuilen et al. [3.24] proposed “a wood-concrete skyscraper” in the range up to 150 m but for more than 80% made of timber products. This building is realized with the use of CLT walls in combination with a concrete core and rigid structural outrigger storeys. The concept makes use of integrated steel tension bars.

Bhat et al. [3.25] conducted an experimental and numerical investigation on the steel-timber system called FFTT. *It consists of CLT panels that are anchored down using ductile hold downs or dampers and rigid (elastic) shear connectors. Steel beams are partially embedded into the panel faces that hold the walls together across openings.* The main concept is a strong-column weak-beam failure mechanism that occurs with formations of plastic hinges in steel beams that act as a ductile weak link of the system. Four options were proposed for heights up to 30 storeys [3.26].

Liu and Lam [3.27] studied a six-storey prototype of CLT shear walls continuous along the height with traditional base connections. Coupling beams with energy dissipation devices are used to decrease deformation and internal forces of walls.

Other researches proposed dissipative devices to improve the seismic energy dissipation capability ([3.28]-[3.31]) or strong connections to improve the resistance of the building [3.32].

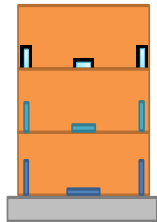
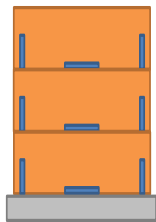
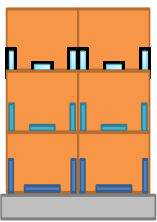
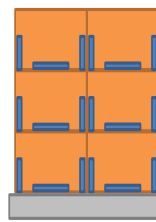
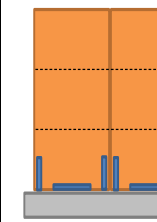
The aim of the work discussed in this chapter is to study the behaviour of complete high-rise CLT buildings, with traditional connections. Results presented below are from numerical analyses of various 3-dimensional configurations, based on connection parameters calculated according to Eurocode 5 [3.33] or experimental cyclic-loading test data.

3.2 Structural characterization of buildings with CLT cores and perimeter shear walls

3.2.1 Case-study buildings and seismic design

In this section, the behaviour of different configurations of multi-storey CLT structures characterized by the presence of a central CLT core and perimeter shear walls, is studied. This configuration allows to realize high-rise buildings (8 storeys) with large interior space. This configuration was applied also to low- (3 storeys) and medium-rise (5 storeys) buildings. Differences in geometry were also introduced to evaluate the effects of varying design parameters, which are (Table 3.1): number of storeys (3-5-8), construction methodology (A-B-C), and regularity of the building (R-I) according to definitions given in section 2.6. These differences allow to assess the optimal configuration for high-rise CLT buildings and the main limitations and troubles in the design. An insight into modelling criteria is also given.

Table 3.1 – Scheme of the studied configurations.

Case-study	3(5-8) A R	3(5-8) A I	3(5-8) B R	3(5-8) B I	3(5-8) C R
Graphical schematization (example: 3-storey building)					
Panel assembly	No vertical panel-to-panel joints		Jointed wall panels with additional hold-downs		No horizontal panel-to-floor joints (multi-storey panels)
Regularity in elevation	Regular	Irregular	Regular	Irregular	Regular
Construction methodology	"Platform"				"Balloon"

Numerical modal response spectrum analyses [3.34] were conducted for all case-study buildings having plan dimensions of 17.1 m (direction X) by 15.5 m (direction Y). Seismic Force Resisting Systems (SFRSs) include a central core 5.5 by 5.5 m and partial perimeter CLT shear walls with base length of 6 m. Storey heights are 3 m, resulting in total superstructure heights of 9, 15 and 24 m. All CLT panels in the core walls have a thickness of 200 mm. CLT panels of perimeter shear walls are 154 mm thick, except for those in the lowest four storeys of the eight storey SFRS which are 170 mm thick. Floor diaphragms are composed of 154-mm CLT panels in all cases, and are anchored to beams or directly to walls. These beams have only static functions because joints with walls do not transfer moment. Fig. 3.5 shows the modelled case-study buildings. Horizontal and vertical continuity in force flows between storeys is achieved at discrete positions of shear connectors and tie-down anchors respectively, except for configurations C. Connectors are located at both faces of CLT panels and twinned hold-downs are anchored at ends of panels. The anchoring to foundation is realized with traditional angle brackets and hold-downs.

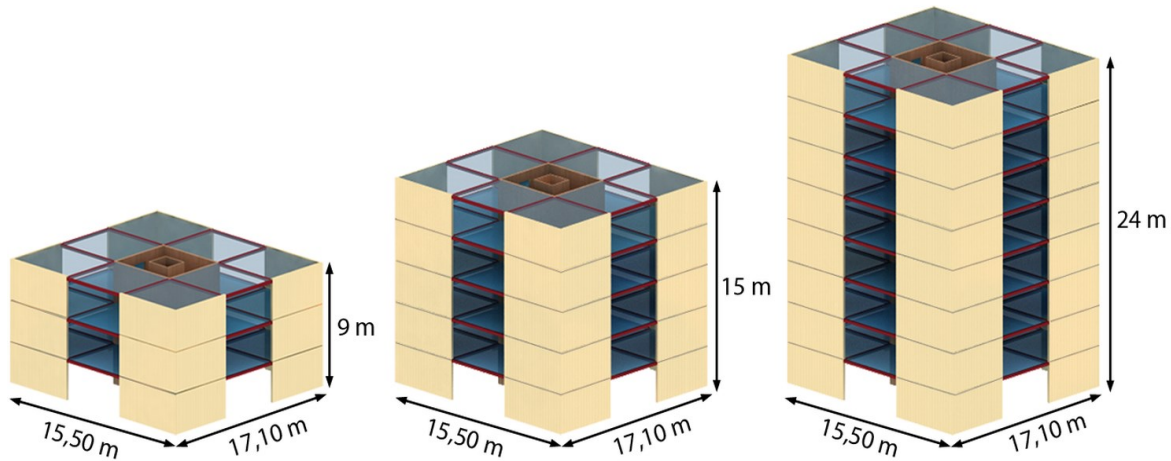
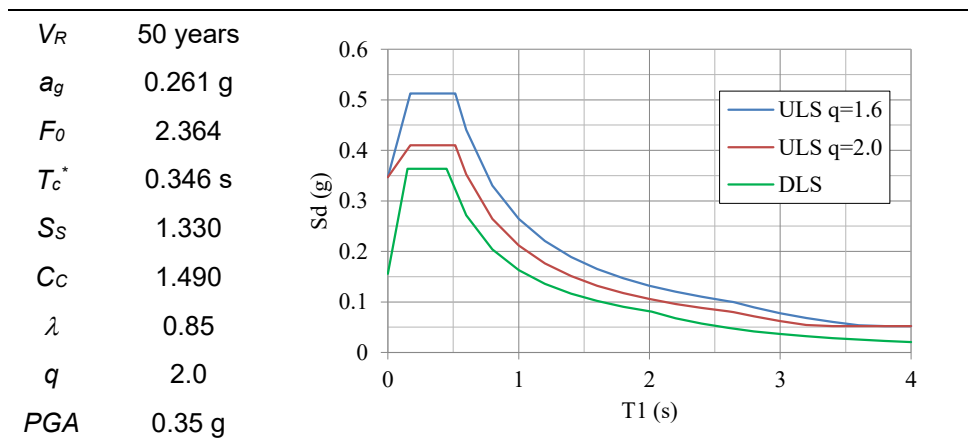


Fig. 3.5 – Modelled case-study buildings [3.9].

The earthquake action for these case-study buildings was calculated according to Eurocode 8 [3.34] and Italian Regulation [3.35], using design response spectra for building foundations resting on ground type C (Deep deposits of dense or medium dense sand, gravel or stiff clay with thickness from several tens to many hundreds of meters). The chosen site location of L'Aquila in the region of Abruzzo (Italy) is characterised by the seismic frequency spectra and parameters show in Table 3.2. This corresponds to the highest seismic zone classification for Italy. The design seismic action was calculated with a q -factor of 2.00 [3.34]. The coefficient k_R was taken equal to 1.0 for regular configurations and 0.8 for irregular configurations [3.34]. The correction factor λ was taken equal to 0.85 for all three buildings, which have more than 2 storeys [3.34].

Table 3.2 – Design spectra for L'Aquila (Italy) according to Italian Regulation [3.35].



Connections and CLT panels were first designed using the force pattern obtained applying equivalent linear elastic analysis and the seismic action corresponding to the fundamental period from the simplified formulation reported in Eurocode 8 [3.34]. Connection design was then refined according to the iterative method described in Chapter 1.

3.2.2 Numerical modelling of case-study buildings

3.2.2.1 Finite element models

Numerical models of the investigated buildings were realized using the finite-element code Strand 7 [3.36]. Fig. 3.6 shows three examples of the modelled case-study buildings. CLT panels were modelled with linear elastic 2-D shell elements. Assumptions made to simplify the models were:

- 1) Horizontal slabs for floors and roof behave as rigid diaphragms;
- 2) The vertical joints between CLT panels at corners of the building core or perimeter shear walls behave as rigid connections, assuming them over-resistant with respect to other deformable connection elements (see section 1.2.2).

Connections between SFRSs and foundation, between storeys and along vertical joints, were modelled with linear link elements with the actual elastic stiffness of connectors. Beam elements with bending moment end releases (hinge joints) were used to represent beam members interconnecting perimeter shear walls and shear walls of the central core at the top of each storey.

A comparison was made between results from numerical models having link stiffness calculated according to European code [3.33] (analytical stiffness k_{ser}), and models having link elements calibrated from experimental data (experimental stiffness k_{test}). This enabled evaluation of the effects of modelling hypotheses on results like elastic periods, base shear and up-lift forces.

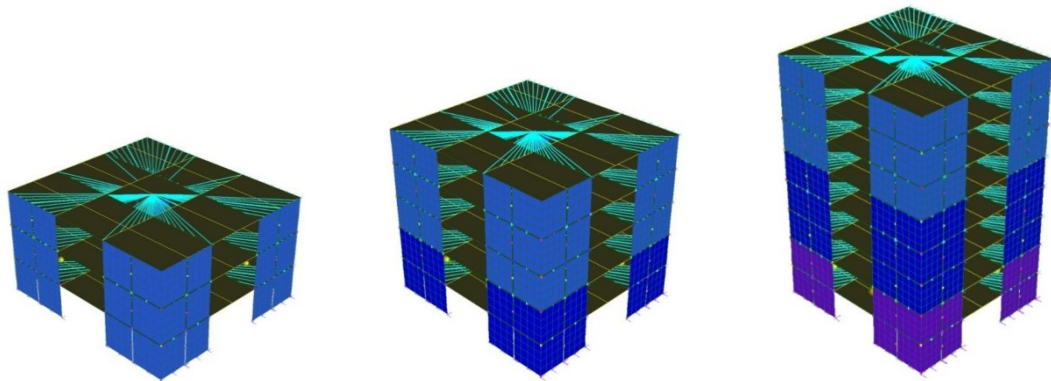


Fig. 3.6 – Numerical models of case-study buildings (3B, 5B and 8B).

3.2.2.2 Stiffness of connections

As reported in section 1.2, the fundamental parameter for a reliable linear modelling of CLT buildings is the elastic stiffness of the connections. Two independent models have been implemented to take into account the variability of the buildings' responses using analytical values or experimental data to compute the elastic stiffness.

The analytical stiffness of connectors was calculated taking into account the stiffness of the steel-to-timber nailed joints in shear and hold-down connections. Deformation of steel parts within the connections are very small compared to deformation of nails and was therefore neglected. The analytic elastic stiffness of a connection was therefore assumed equal to the slip modulus k_{ser} of a single nail according to Eurocode 5 [3.33] multiplied by the number of nails necessary to resist to seismic action, assuming angle brackets resistant only to shear loading and hold-downs to axial

loading, as explained exhaustively in section 2.2.2. Nails are subjected only to shear and their resistance is obtained with Johansen's theory [3.37].

The experimental-based evaluation of the connections' stiffness is based on tests conducted at CNR-IVALSA. The connections used for these buildings and implemented in the FE models are hold-downs Rothoblaas WHT340, WHT440, WHT620 [3.38] and angle brackets TITAN TTF200 [3.39] fastened to CLT panels made of C24 timber boards using 4x60 Anker nails. Table 3.3 lists the assumed values for the angle brackets and hold-downs, which have been used in almost all cases. The values of stiffness are also in producer's catalogues.

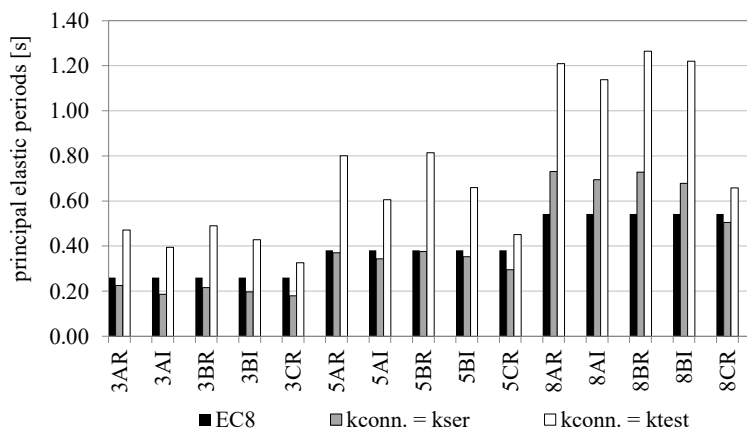
Table 3.3 – Analytical and experimental values of connection stiffness [3.9].

Connection type	Elastic stiffness (kN/mm)	
	Test (k_{test})	EC5 (k_{ser})
TITAN TTF 200	8.2	23.1
WHT 620	12.1	24.8

It can be noted immediately from Table 3.3 that analytical stiffness k_{ser} is higher than experimental evidence. This can be explained considering that real deformation of connections is not given only by shear deformation of nails, especially for angle brackets, for which the divergence is the highest (Table 3.3). This difference on stiffness values involves strong differences in numerical results, especially for tall buildings, for which the period T is normally out of the plateau range.

3.2.3 Analysis of numerical results

Results presented hereafter were obtained from modal response spectrum analyses of all case-study buildings. Fig. 3.7 shows the main mechanical parameters for the seismic characterization of all buildings and the comparison among them: principal elastic period T ; maximum unitary base shear forces recorded at the base of perimeter shear walls (resisted by angle brackets); maximum axial forces at the base corners of shear walls (resisted by hold-downs); maximum displacement in term of inter-storey drift and top displacement. Results obtained with both values of the connection stiffness (k_{conn}) are shown: analytical value (k_{ser}) and experimental value (k_{test}). The principal elastic period is evaluated also from simplified formulation provided by Eurocode 8 (EC8) [3.34].



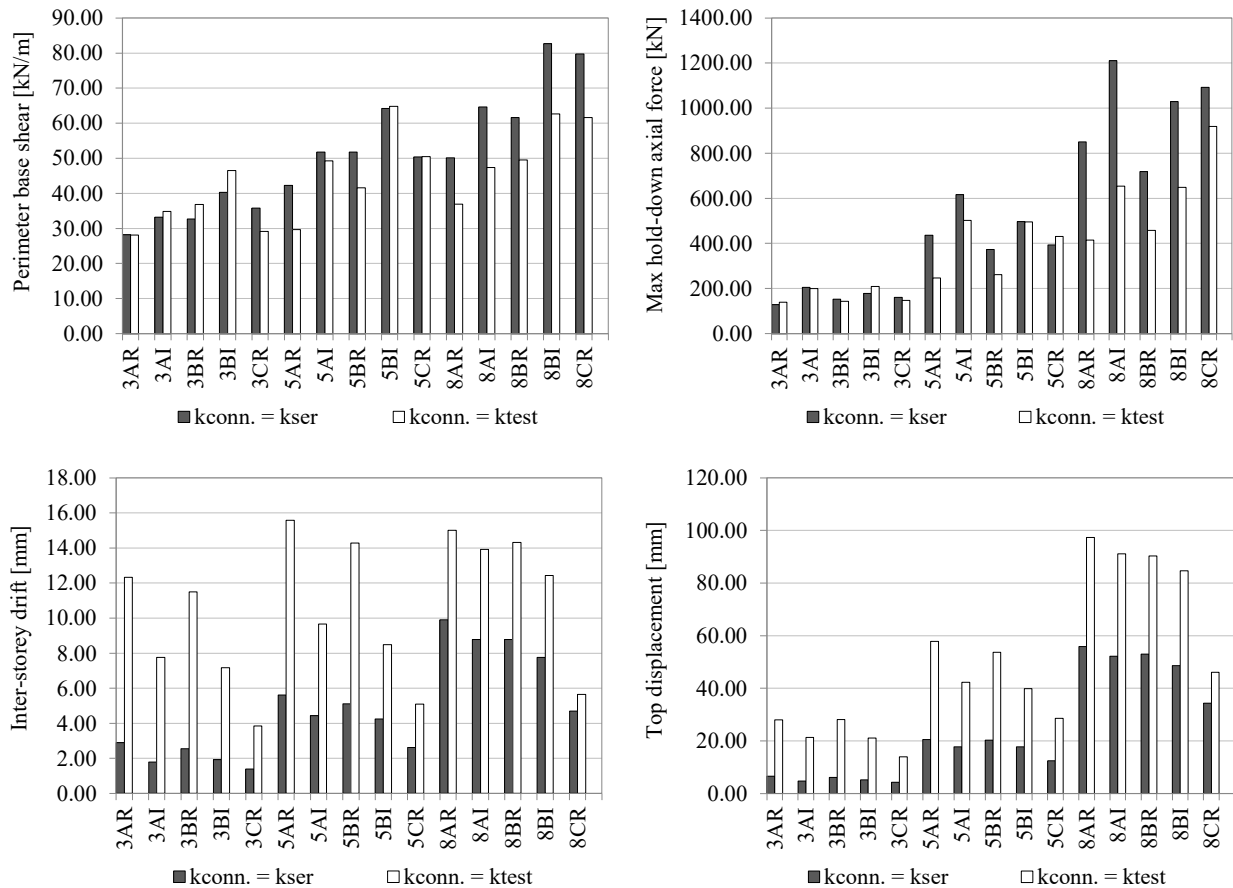


Fig. 3.7 – Main numerical results and comparisons.

Analysing the results some conclusions can be drawn, which are of particular relevance for the high-rise buildings studied (8 storeys).

1. The use of k_{test} leads to much larger T values than the use of k_{ser} , which provides values similar to those obtained from simplified formulation of Eurocode 8. Therefore, results suggest that neither of these two approaches (i.e., $k_{conn}=k_{ser}$ or $T=T_{EC8}$) are reliable ways of estimating principal natural periods of buildings having SFRSs consisting of CLT cores and perimeter shear walls. Perhaps, experimental values of connection stiffness are normally unknown or available for just a few connection typologies.
2. The use of k_{ser} to evaluate the connection stiffness implies an over-estimation of forces, but an under-estimation of displacements and drifts. This means that it results normally a conservative approach for ULS verification but not conservative for DLS verification.
3. The design of high-rise buildings (8 storeys) in medium/high-seismicity areas, involves very high up-lift forces at corner of CLT shear walls (about 900 kN with $k_{conn}=k_{test}$ in configuration 8CR). These high forces cannot be resisted with traditional CLT constructive technology: not only by hold-downs and their anchoring to foundation, but also because of localized over-tensioning in CLT panels.
4. Differences in terms of forces between in-elevation regular and irregular buildings are mainly due to the different q-factor used. The differences in terms of displacements are more marked. As reported in section 2.5, buildings considered regular in-elevation according to the definition given in this dissertation, are subjected to high inter-storey drift and the DLS verification may be determinant. This has been demonstrated also by these analyses, comparing I with R cases. However, for almost all these cases (with exception of

8AR and 8BR with $k_{\text{conn.}}=k_{\text{test}}$) the ULS verification was determinant, because of the use of a conservative value for behaviour factor, which implies an high number of connections and, therefore, high stiffness of the buildings.

3.2.4 Numerical simulations with varied q-factor

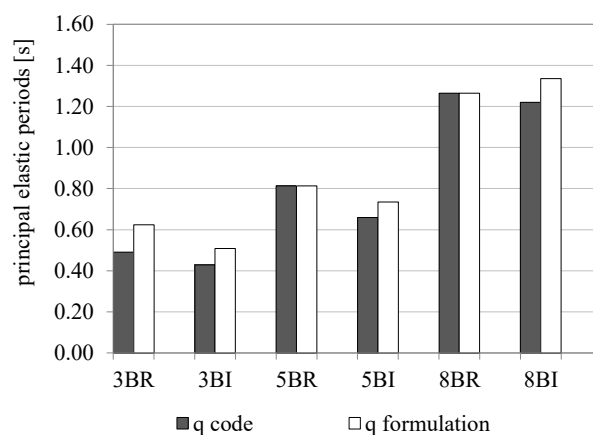
Obtained results demonstrated that the major limitation in the use of CLT to build tall structures in high-seismicity areas is due to the very high axial forces at the base. These high forces are due to the slenderness of the building and the low q-factor value used.

To obtain a comparison of how results would change if higher q-factor values were applied, the most significant case-study buildings (i.e., BR and BI configurations) have been re-analysed applying equation (2.10) proposed in section 2.4.2, to compute the q-factor for the various case studies. k_R coefficient was assumed again equal to 0.8, according to Eurocode 8 [3.34] and to results obtained in section 2.5.2. The design over-strength value was assumed equal to 1.00, according to Eurocode 8 [3.34]. Table 3.4 shows the evaluation of the q-factor with the proposed analytical formulation.

Table 3.4 – Computation of q-factor according to equation (2.10).

		3BR	3BI	5BR	5BI	8BR	8BI
beta coefficient	β (-)	2.34	2.34	3.00	3.00	3.62	3.62
slenderness	λ (-)	0.53	0.53	0.88	0.88	1.40	1.40
q ₀ -factor	q_0 (-)	3.01	3.01	3.52	3.52	4.15	4.15
assumed q ₀ -factor	q_0 (-)	3.00	3.00	3.50	3.50	4.00	4.00
design over-strength	Ω (-)	1.00	1.00	1.00	1.00	1.00	1.00
reduction coefficient	k_R (-)	1.00	0.80	1.00	0.80	1.00	0.80
Assumed q-factor	q (-)	3.00	2.40	3.50	2.80	4.00	3.20

The application of these q-factor values (q formulation) leads to the results shown in Fig. 3.8 that provides a comparison with values obtained applying the q-factor equal to 2.00 for regular buildings and 1.6 for irregular buildings, according to Eurocode 8 [3.34] (q code).



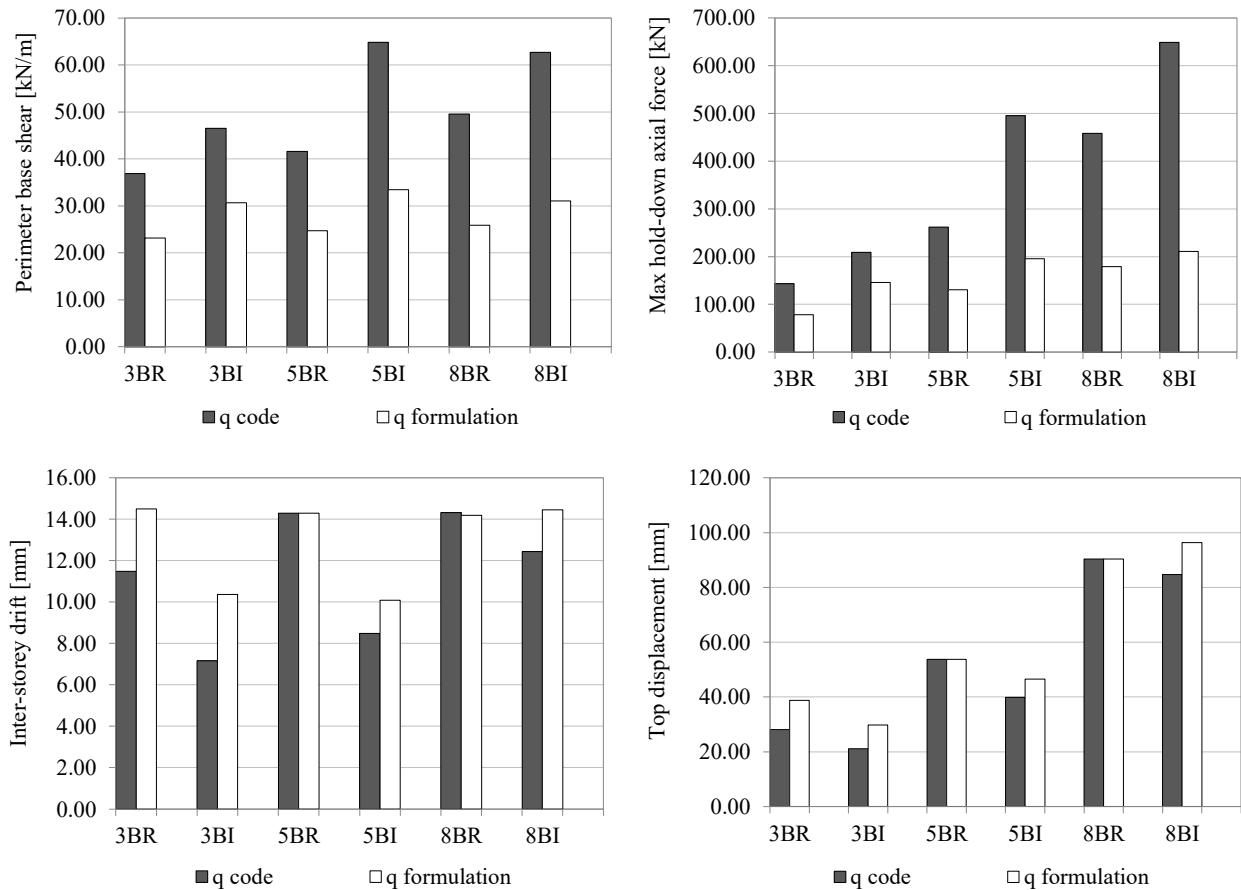


Fig. 3.8 – Comparison between results obtained with q -factor from code and from proposed formulation.

Some conclusions can be obtained from these results.

1. Axial and shear forces have been clearly reduced for all case-study buildings.
2. Only for the cases of 3BR-3BI-5BI-8BI an effective reduction of the number of connections was obtained. For the cases 5BR and 8BR, i.e., medium and high-rise regular buildings, the number of connections remained the same, as shown comparing the principal elastic periods (i.e., the stiffness remains the same). This is because, applying higher q -factor values, the DLS verification (drift limited to 5‰) for 5BR and 8BR resulted determinant due to the rocking behaviour of each storey. Clearly, the irregular configurations with over-designed connections at upper storeys do not show this phenomenon.
3. A final comparison with shear forces due to wind action shows also that the application of the proposed q -factor values could make seismic shear lower than wind shear for the cases of the eight-storey buildings (8BR and 8BI).

3.3 Major limits in the use of CLT to realise tall structures and design implication

Results in this chapter showed large variation in the elastic lateral vibration periods due to alteration of the connection stiffness, i.e., between k_{ser} obtained from codes and k_{test} obtained from experiments. In particular, the periods obtained with the code formulation were up to about 55%

lower than those with the experimentally based approach. This evidences the importance of properly modelling the contributions of connections to the dynamic response of CLT buildings. Given that the vibration period for the fundamental mode is a primary parameter for the application of linear design methods, the correct estimation of the connection stiffness is very important. It is clear also that T values should be estimated by means of realistic analytical methods or experimental tests rather than from approximate formulas. Use of approximate formulas should be restricted to initial sizing of structural elements.

Variation of the connection stiffness does not cause large variation in the unitary base shear forces and uplift forces for the 3- and 5-storey buildings. Differences among cases are greater, in relative terms, for the 8-storey buildings. Therefore, the implication for tall buildings is that numerical modelling could be not fully realistic if the stiffness of all connections is not accurately estimated. Moreover, the stiffness of the connections must be always consistent with the assumed strength for verifications, i.e., the iterative process described in section 1.2 has to be continued until convergence.

Obtained results suggest therefore that testing of connections intended to be used in high-rise buildings constructed partially or completely from CLT wall panels should be preferably required. These tests should characterize both initial stiffness and capacities of such connections.

The utilization of greater q -factors evaluated according to relationships formulated in section 2.4 results in values of up-lift forces, which can be resisted with existing technologies. Differently, utilization of $q=2.00$ according to Eurocode 8 [3.34] produces forces that hardly can be sustained with feasible solutions.

3.4 Conclusions

Analyses of relatively tall and slender CLT buildings demonstrate the importance of a realistic numerical representation of the resisting structure. Attention has to be paid to the actual stiffness of base and inter-storey connections. If such attention is not paid, inaccurate prediction of the fundamental lateral vibration period, and therefore inappropriate sizing of structural elements can occur. Moreover, a careful and iterative design of connections is mandatory to assure consistency between strength and stiffness of connections.

It has also to be observed that up-lift forces due to seismic overturning moments can be very large. Given that the tallest building considered here has a quite modest height of 24 m, the base anchoring could be a limiting factor on the realization of taller CLT buildings in high-seismicity areas. Resisting such forces can be beyond the resistance capabilities of conventional hold-down anchors and would require the use of many hold-downs in parallel, with the result that brittle failures could be concentrated in timber side or at anchoring with foundation.

The application of higher q -factors reduces the uplift forces and hold-downs needed. This makes the DLS verification more important, but does not restrict the feasibility of slender and high-rise CLT buildings in medium/high seismic areas, if the number of storeys is up to 10. For higher buildings, the high uplift forces become the main limitation if standard connections are used.

References – Chapter 3

- [3.1] Buchanan, A., Deam, B., Fragiaco, M., Pampanin, S., and Palermo, A. (2008). "Multi-Storey Prestressed Timber Buildings in New Zealand". *Structural Engineering International*, 18(2):166-173.
- [3.2] Smith, T., Fragiaco, M., Pampanin, S., and Buchanan, A.H. (2009). "Construction time and cost for post-tensioned timber buildings". *Proceedings of the ICE - Construction Materials* 162(4):141-149.
- [3.3] Tlustochowicz G., Kermani, A., and Johnsson H. (2010). "Beam and post system for non-residential multi-storey timber buildings – conceptual framework and key issues". In *Proceedings of the 11th World Conference on Timber Engineering WCTE*, Riva del Garda, Italy.
- [3.4] Tlustochowicz G., Johnsson H., and Girhammar U.A. (2010). "Beam and post system for non-residential multi-storey timber buildings – horizontal stabilising system". In *Proceedings of the 11th World Conference on Timber Engineering WCTE*, Riva del Garda, Italy.
- [3.5] Gattesco, N., and Boem, I. (2015). "Seismic performances and behavior factor of post-and-beam timber buildings braced with nailed shear walls". *Engineering Structures* **100**:674–685.
- [3.6] Polastri, A., Pozza, L., Trutalli, D., Scotta, R., and Smith, I. (2014). "Structural characterization of multi-storey buildings with CLT cores." In *proceedings of the World Conference on Timber Engineering (WCTE)*, 10-14 August 2014, Quebec City, Canada.
- [3.7] Dunbar, A., Moroder, D., Pampanin, S., and Buchanan, A.H. (2014). "Timber core-walls for lateral load resistance of multi-storey timber buildings". In *proceedings of the World Conference on Timber Engineering (WCTE)*, 10-14 August 2014, Quebec City, Canada.
- [3.8] Fairhurst, M., Zhang, X., and Tannert, T. (2014). "Non-linear dynamic analyses of novel timber-steel hybrid system". In *proceedings of the World Conference on Timber Engineering (WCTE)*, 10-14 August 2014, Quebec City, Canada.
- [3.9] Polastri, A., Pozza, L., Loss, C., and Smith, I. (2015). "Structural characterization of multi-storey CLT buildings braced with cores and additional shear walls". In *proceedings of 2nd International Network on Timber Engineering Research (INTER)*, Šibenik, Croatia.
- [3.10] Zumbrennen, P., and Fovargue, J. (2012). "Mid rise CLT buildings – The UK's experience and potential for AUS and NZ". In *proceedings of the World Conference on Timber Engineering WCTE*, 15-19 July, Auckland, NZ.
- [3.11] Dunbar, A., Pampanin, S., Palermo, A., and Buchanan, A.H. "Seismic design of core-walls for multi-storey timber buildings". In *Proceedings of NZSEE Conference*.
- [3.12] Dunbar, A., Pampanin, S., and Buchanan, A.H. (2014). "Seismic performance of core-walls for multi-storey timber buildings". I: *Proceedings of NZSEE Conference*.
- [3.13] Smith, I., and Frangi, A. (2014). "Use of timber in tall multi-storey buildings". *Struct. Eng. Doc. 13*, Int. Assoc. Bridge & Struct. Eng., Zurich, Switzerland, 2014.
- [3.14] Asiz, A., and Smith, I. (2011). "Connection System of Massive Timber Elements Used in Horizontal Slabs of Hybrid Tall Buildings". *Journal of Structural Engineering*, ASCE. DOI: 10.1061/(ASCE)ST.1943-541X.0000363.
- [3.15] Website of KLH UK. Available online: www.klhuk.com.
- [3.16] TRADA Technology. Stadthaus, Murray Grove, London – Case Study. 2009. Available online:

<http://www.trada.co.uk>.

- [3.17]Karakusevic Carson Architects. Available online: <http://karakusevic-carson.com/work/bridport-house>.
- [3.18]World's tallest timber building 'tops out' in Melbourne. Available online: www.architectureanddesign.com.au.
- [3.19]Promo_legno website. Available online: www.promolegno.com.
- [3.20]Cenni di cambiamento. Available online: <http://www.cennidicambiamento.it>.
- [3.21]Ceccotti, A., Sandhaas, C., Okabe, M., Yasumura, M., Minowa, C. and Kawai, N. (2013). "SOFIE project – 3D shaking table test on a seven-storey full-scale cross-laminated timber building". *Earthquake Engineering & Structural Dynamics* **42(13)**: 2003-2021.
- [3.22]Pei, S., Berman, J., Dolan, D., van de Lindt, J., Ricles, J., Sause, J., Blomgren, H-E, Popovski, M., and Rammer, D. (2014). "Progress on the development of seismic resilient tall CLT buildings in the pacific northwest." In proceedings of the World Conference on Timber Engineering (WCTE), 10-14 August 2014, Quebec City, Canada.
- [3.23]Chapman, J. (2014). "Integrating cross-laminated timber panels to construct buildings to 20 levels." In proceedings of the World Conference on Timber Engineering (WCTE), 10-14 August 2014, Quebec City, Canada.
- [3.24]Van de Kuilen, J.W.G., Ceccotti, A., Xia, Z., and He, M. (2011). "Very tall wooden buildings with cross laminated timber." In proceedings of the Twelfth East Asia-Pacific Conference on Structural Engineering and Construction, *Procedia Engineering* 14:1621-1628.
- [3.25]Bhat, P., Azim, R., Popovski, M., and Tannert, T. (2014). "Experimental and numerical investigation of novel steel-timber-hybrid system". In proceedings of the World Conference on Timber Engineering (WCTE), 10-14 August 2014, Quebec City, Canada.
- [3.26]Fairhurst, M., Zhang, X., and Tannert, T. (2014). "Nonlinear dynamic analyses of novel timber-steel hybrid system". In proceedings of the World Conference on Timber Engineering (WCTE), 10-14 August 2014, Quebec City, Canada.
- [3.27]Liu, J., and Lam, F. (2014). "Numerical simulation for the seismic behaviour of mid-rise CLT shear walls with coupling beams". In proceedings of the World Conference on Timber Engineering (WCTE), 10-14 August 2014, Quebec City, Canada.
- [3.28]Latour, M., and Rizzano, G. (2015). "Cyclic Behavior and Modeling of a Dissipative Connector for Cross-Laminated Timber Panel Buildings". *Journal of Earthquake Engineering*, **19(1)**:137-171, DOI: 10.1080/13632469.2014.948645.
- [3.29]Loo, W.Y., Kun, C., Quenneville, P. and Chouw, N. (2014). "Experimental testing of a rocking timber shear wall with slip-friction connectors". *Earthquake Engineering and Structural Dynamics*, **43(11)**:1621-1639.
- [3.30]Sarti, F., Palermo, A., and Pampanin, S. (2015). "Quasi-Static Cyclic Testing of Two-Thirds Scale Unbonded Posttensioned Rocking Dissipative Timber Walls". *Journal of Structural Engineering*, ASCE. DOI: 10.1061/(ASCE)ST.1943-541X.0001291.
- [3.31]Scotta, R., Pozza, L., Trutalli, D., Marchi, L., and Ceccotti, A. (2015). "Dissipative connections for squat or scarcely jointed CLT buildings. Experimental tests and numerical validation." In proceedings of 2nd International Network on Timber Engineering Research (INTER), Šibenik, Croatia.
- [3.32]Polastri, A., Angeli, A., and Dal Ri, G. (2014). "A new construction system for CLT structures". In proceedings of World Conference on Timber Engineering WCTE, Quebec City, Canada.

- [3.33]EN 1995-1-1 Eurocode 5 (2004). "Design of timber structures, Part 1-1, General: Common rules and rules for buildings". CEN. Brussels, Belgium.
- [3.34]EN 1998-1-1 Eurocode 8 (2004). "Design of structures for earthquake resistance, part 1: general rules, seismic actions and rules for buildings". CEN. Brussels, Belgium.
- [3.35]DM Infrastrutture 14 gennaio 2008 - Norme Tecniche per le Costruzioni - NTC (Italian National Regulation for Construction) (2008). Ministero delle Infrastrutture e dei Trasporti, Rome, Italy.
- [3.36]Strand 7 (2005). "Theoretical Manual – Theoretical background to the Strand 7 finite element analysis system". Available online: http://www.strand7.com/html/docu_theoretical.htm.
- [3.37]Johansen, K.W. (1949). Theory of timber connections. International Association of bridge and structural Engineering, Bern, p. 249-262.
- [3.38]European Organisation for Technical Assessment (EOTA) (2011). Rotho Blaas WHT hold-downs, European Technical Approval ETA-11/0086, Charlottenlund, Denmark.
- [3.39]European Organisation for Technical Assessment (EOTA) (2011). Rotho Blaas TITAN Angle Brackets, European Technical Approval ETA-11/0496, Charlottenlund, Denmark.

Chapter 4 Development and analyses of novel timber shear-wall systems

Abstract

This chapter presents three novel structural systems, alternative to standard shear-wall technologies (CLT and light frame). In detail, two non-glued massive timber shear walls and a hybrid steel-timber wall with an innovative bracing system are presented. The details of the constructive systems and of performed tests and simulations are given. These systems are characterized by a diffuse yielding and deformation when subjected to seismic loads, as opposed to CLT system whose deformation is concentrated in connection elements. Their structural responses are investigated via quasi-static tests and numerical simulations. Main results in terms of mechanical parameters and suitable behaviour factor values are illustrated and discussed. This chapter provides also an overview on test and analysis methods suitable to characterize novel structural systems for which no provisions are given in structural codes.

4.1 Introduction and state of the art

Newly developed construction technologies based on timber have been introduced into the market. They have been used to realize buildings although their structural behaviour, especially under seismic action, still needs to be fully assessed in terms of resistance, stiffness, ductility and dissipative properties. The main issue to be studied in a novel timber shear-wall system is related to the in-plane shear behaviour.

CLT panels are characterized by an almost rigid behaviour in their plane due to glued interfaces that transfer shear stress among layers with small elastic deformations. Shear walls realized with CLT panels rock and slide when subjected to lateral loads. Plastic deformations and energy dissipation are exclusively demanded to the connections. However, massive timber panels can deform in shear and dissipate energy if glued connections among layers are not adopted. Not-glued massive wooden shear walls alternative to CLT technology have been proposed and developed, but few research activities can be found in scientific literature (e.g., [4.1]-[4.4]). Two different technologies are discussed hereafter. They differ in the connection system used between adjacent layers and consequently in the in-plane shear resistance mechanism.

In this work also results of quasi-static cyclic tests on an innovative hybrid light timber frame are reported and interpreted.

Structural systems based on light timber-frame technology have been developed before massive wall systems. They originally born in USA but their usage is gaining acceptance worldwide. In seismic-prone regions, e.g., Northern America, Italy, Japan and New Zealand, the application of this wall system as seismic force resisting system (SFRS) proved to be very efficient, thanks to lightness and intrinsic dissipative capacity when correctly designed (e.g., [4.5]). Light-frame systems are normally characterized by high shear deformability and the dissipative capacity is mainly concentrated in nailing between frames and panels.

Hybrid systems are also of great interest in current construction practice. Coupling of different materials allows to take advantage of their intrinsic properties and to reduce their limitations, with the effect of improving the overall behaviour of the building. Steel and wood can be integrated at component and/or at building system level (e.g., steel connections with timber frames or walls, hybrid frames, steel frames and wood diaphragms) ([4.7];[4.8]). Examples of hybrid building systems have already been realized and tested: steel beams or frames combined with CLT panels ([4.9];[4.10]) or with timber-frame shear walls ([4.11];[4.12]) have been studied through experimental tests and numerical modelling. These systems show a relatively high ductility and demonstrate to be reliable as SFRSs.

Innovative platform-frame structural systems are proposed in response to the changing needs of users and construction industry, with the aim of optimizing the performance of traditional buildings [4.6]. The innovation regards mainly the material used as bracing system and the ductile connections used to join the panel to the frame. Normally, bracing panels are realized with timber-base products (usually OSB sheets) and non-wood materials such as gypsum and cement plaster are used as finish materials. The influence of these brittle materials on the performance of wood-frame shear walls is reported in [4.13]. Brick masonry is also frequently used as façade in North America and its contribution to the light-frame wood shear-wall resistance is neglected in the

calculations. Zisi [4.14] and Zisi and Bennett [4.15] studied a system where an anchored brick veneer is tied to the exterior wall face of the wood frame wall. A gypsum wallboard sheathing is added on the interior wall face. Analytical models demonstrated that both brick veneer and wallboard sheathing stiffen significantly the timber frame shear wall.

The use of innovative systems in seismic areas, requires the assessment of mechanical properties through experimental tests, in order to evaluate their seismic performance. In [4.16] a summary of testing and modelling studies on timber shear walls over the last two decades of 20th century is presented. More recently in the United States, the seismic behaviour of typical light-frame wood structural systems has been studied [4.17] to analyse the design and retrofit of existing wooden frame dwellings [4.18].

The innovative hybrid light frame considered in this work consists of steel columns braced with an OSB panel and an innovative technoprene slab infilled with plaster. Shear walls were tested following the quasi-static cyclic-loading protocol according to EN 12512 [4.19], to characterize the structural system in terms of strength, stiffness, ductility, and hysteresis behaviour. Numerical analyses were also performed to evaluate the dissipative capacity and to estimate the suitable intrinsic q-factor.

4.2 Evaluation of the seismic response of non-glued massive timber shear walls

The research presented in this section is partly available also at Springer via <http://dx.doi.org/10.1007/s10518-015-9765-7> [4.20]. Journal Bulletin of Earthquake Engineering is acknowledged as the original source of publication.

4.2.1 Description of the systems and experimental tests

4.2.1.1 Description of the specimens

Two massive wooden shear-wall systems are analysed in this section. The main difference with standard CLT system is the absence of glue to assemble the layers of timber boards.

The first is a Cross-laminated-stapled wall, hereafter called stapled wall, composed of crossed layers of timber boards assembled with ductile metal staples, Fig. 4.1a.

The second one is a layered wall with horizontal dovetail timber inserts, which provide in-plane shear stiffness to the vertically oriented boards thanks to precise carpentry joints, Fig. 4.1b.

These two innovative non-glued timber walls were tested at the Laboratory of Mechanical Testing, CNR-IVALSA, at San Michele all'Adige (Trento, Italy) [4.21]. These tests were part of two experimental campaigns, partly commissioned by private Companies for research and development projects. Test configurations and connection systems to the foundations (hold-downs and angle brackets, fastened with nails to the timber panels) were different for the two walls, since each Company adopted a specific connection system, as summarised in Table 4.1.

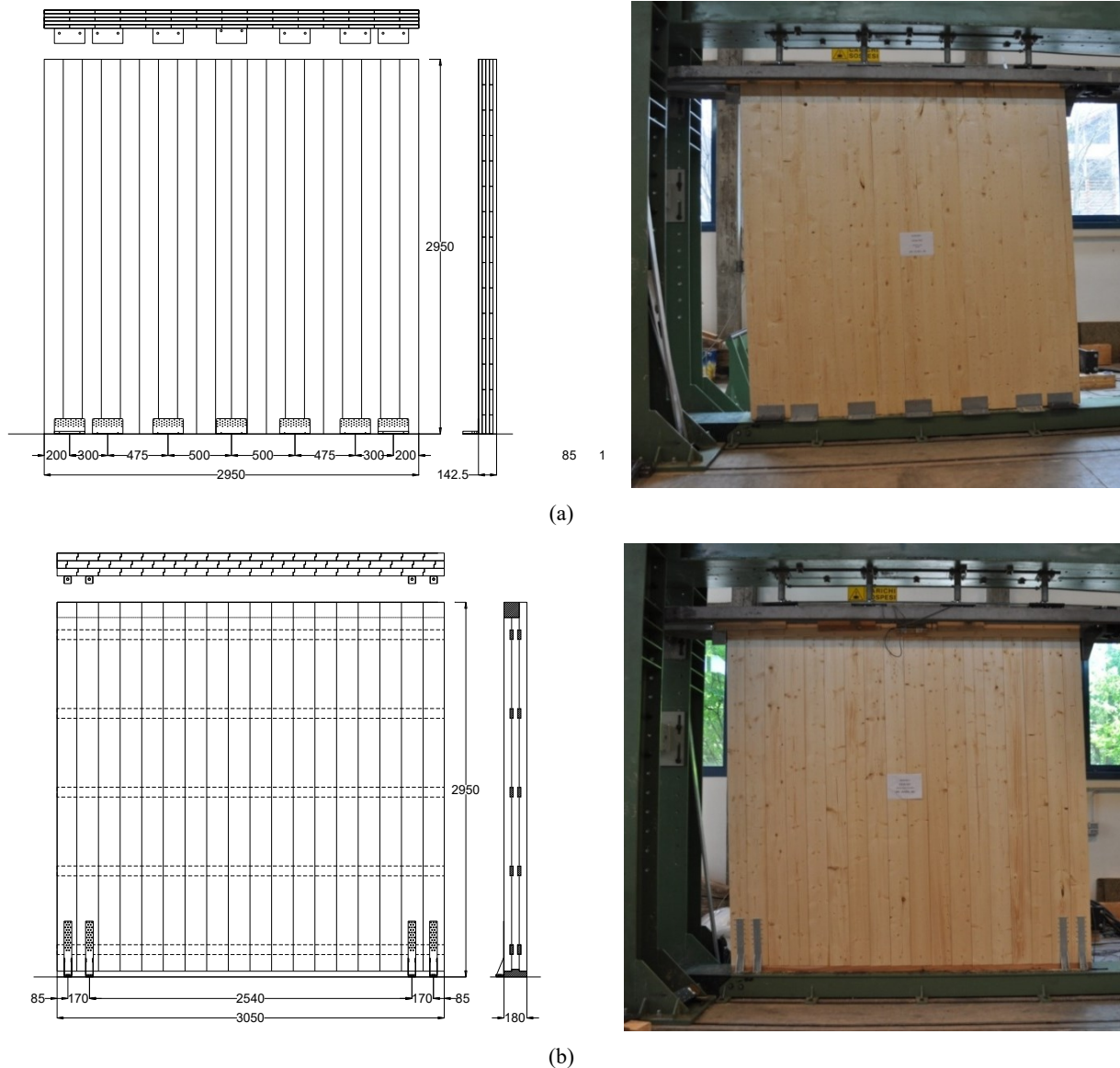


Fig. 4.1 – (a) Stapled wall; (b) layered wall. [4.20]

Table 4.1 – Scheme of the studied configurations. [4.20]

Specimen	Connectors		Anker type nails or screws	
	Type	No.	Size	No.
Stapled wall	Angle bracket - foundation	7	4x100	36
Layered wall	Hold-down - foundation	4	4x60	30
	Inclined screw - foundation	18 pairs	8x200	-

The stapled wall is made of five crossed layers of C24 spruce boards [4.22], with a nominal thickness 28.5 mm. The panel is 142.5-mm thick. The used boards have a width approximately equal to 200 mm. Layers are stapled to each other with six staples at each node of crosswise jointed layers of boards. This wall was fixed to the foundation with seven angular steel elements positioned as shown in Fig. 4.1a and two M16 bolts per element. The side connections acting as hold-downs have a thick steel plate between the bolt head and the angle bracket.

The layered wall is realized with three layers of vertical sawn spruce boards, nominal thickness 60 mm, coupled with five pairs of 26 x 90 mm horizontal dovetail spruce inserts. Both inserts and

timber vertical elements require a precise production by the use of CNC (computer numerical control) machine since no clearance is admitted between the two orthogonal timber elements. The timber panels are connected to a base larch beam with 18 pairs of cross-screws (HBS 8 mm × 200 mm), inclined 45° with respect to the vertical. This beam was previously fixed to the portal's foundation with seventeen 12-mm steel bolts. The panels were also connected directly to the foundation with two hold-downs on each side anchored with M16 bolts. Locally, the vertical timber boards were reinforced with 12 HBS 8 × 160 mm screws positioned at the sides of the hold-downs. An horizontal timber board (120 × 120 mm) was fixed to the upper side of the wall with cross-screws (HBS 8 mm × 200 mm) inclined 45° with respect to the vertical, to ensure uniform distribution of both vertical and horizontal loads.

4.2.1.2 Test results and comparison with CLT

The specimens were tested with quasi-static cyclic loading protocol. An identical test protocol recommended by EN 12512 [4.19] was adopted for both the walls, together with an applied vertical load of 18,5 kN/m. At the end of testing, both specimens did not show an evident failure (Fig. 4.1). Shear deformation and consequent sliding between boards occurred due to staple deformation for the stapled wall (Fig. 4.2a), and due to plastic deformation of the dovetail inserts subjected to compression perpendicular to the grain for the layered wall (Fig. 4.2b).

Performed quasi-static cyclic loading tests allowed to define elastic and post-elastic stiffness, yielding point, failure condition, and ductility ratio ([4.19];[4.23]). Thanks to the same testing protocol followed, a comparison with CLT system can be given in terms of hysteresis behaviour and seismic response. Two CLT specimens have been chosen for this comparison: wall A-2 (hereafter called un-jointed CLT wall) and wall C (hereafter called jointed CLT wall), whose geometrical and mechanical characteristics have already been described in section 2.2. These walls are representative of the CLT system: the un-jointed wall behaves almost as a rigid wall and deformation is concentrated in connections at the base; the jointed wall revealed rigid rotation of the two panels, which, subjected to large displacements, behaved independently.



Fig. 4.2 – Deformation of connections and panels: (a) stapled wall; (b) layered wall. [4.20]

Fig. 4.3 shows the recorded hysteresis cycles and the determination of elastic and post-elastic stiffness and yielding point. Various methods have been proposed to compute this point ([4.19];[4.24]). In this work, an equivalent-energy method with post-elastic hardening branch was

used [4.25]. Three limits of ultimate top displacements (i.e., inter-storey drift) were imposed, which correspond to three levels of increasing damage of the structure: 80 mm (2.67% - limit of the setup), 60 mm (2.00% - ultimate drift for the un-jointed CLT wall) and 40 mm (1.33%). For each limit, the proper evaluation of the yielding point is given in order to obtain the appropriate data as input for the numerical analyses and q-factor calculation. Table 4.2 to Table 4.4 list all values, which define the bi-linear curves, together with the evaluation of the ductility.

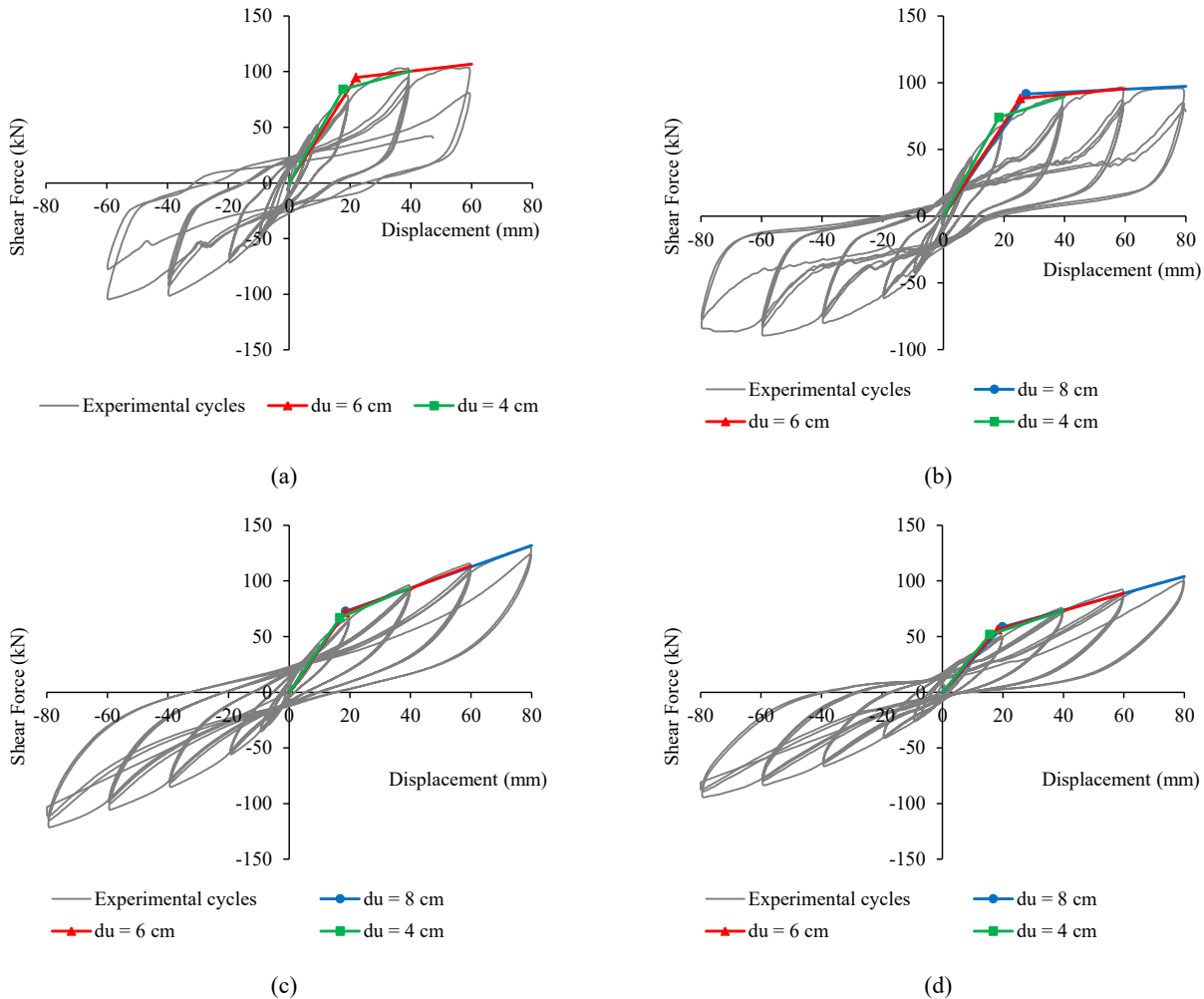


Fig. 4.3 – Recorded hysteresis cycles and evaluation of yielding points: (a) un-jointed CLT; (b) jointed CLT; (c) stapled wall; (d) layered wall. [4.20]

Table 4.2 – Analytical evaluation of test parameters for imposed ultimate displacement of 40 mm. [4.20]

Parameters, notations and units		Un-jointed CLT wall	Jointed CLT wall	Stapled wall	Layered wall
Elastic stiffness	K_e [kN/mm]	4.72	4.03	3.99	3.30
Hardening stiffness	K_{pl} [kN/mm]	0.74	0.72	1.17	0.89
Yielding displacement	d_y [mm]	17.8	18.4	16.8	15.7
Yielding force	F_y [kN]	84.1	74.0	66.9	51.7
Ductility ratio	$\mu = d_u / d_y$	2.25	2.18	2.38	2.55

Table 4.3 – Analytical evaluation of test parameters for imposed ultimate displacement of 60 mm. [4.20]

Parameters, notations and units		Un-jointed CLT wall	Jointed CLT wall	Stapled wall	Layered wall
Elastic stiffness	K_e [kN/mm]	4.30	3.48	3.87	3.09
Hardening stiffness	K_{pl} [kN/mm]	0.32	0.21	1.01	0.78
Yielding displacement	d_y [mm]	22.0	25.3	18.5	18.2
Yielding force	F_y [kN]	94.7	88.2	71.7	56.2
Ductility ratio	$\mu = d_u / d_y$	2.73	2.37	3.24	3.30

Table 4.4 – Analytical evaluation of test parameters for imposed ultimate displacement of 80 mm. [4.20]

Parameters, notations and units		Un-jointed CLT wall	Jointed CLT wall	Stapled wall	Layered wall
Elastic stiffness	K_e [kN/mm]	-	3.35	3.90	2.95
Hardening stiffness	K_{pl} [kN/mm]	-	0.11	0.96	0.75
Yielding displacement	d_y [mm]	-	27.4	18.7	19.9
Yielding force	F_y [kN]	-	91.7	72.8	58.7
Ductility ratio	$\mu = d_u / d_y$	-	2.92	4.29	4.02

The CLT walls showed a different response with respect to the stapled and layered walls. In detail, the two novel wall specimens revealed a quite marked hardening after yielding and higher ductility capacity, fixed a common ultimate displacement capacity of 80 mm, due to lower values of yielding displacements. Ultimate displacement capacity equal to 80 mm is a conservative estimation for the two not-glued walls: in fact from the analysis of the hysteresis cycles it can be noted that strength degradation at 80-mm displacement is only 10.2% for stapled wall and 7.5% for layered wall. While for the comparative CLT wall specimens 80 mm represents the actual ultimate displacement capacity. CLT walls exhibited less ductility than the other two walls and a mechanical behaviour characterised by an almost horizontal post-elastic branch. This elastic perfectly plastic behaviour is more evident for the jointed wall, due to the ductile behaviour of the joint, with plasticisation and deformation of fasteners.

Therefore, for the two novel systems (stapled and layered walls) higher q_0 -factors can be expected, due to higher ductility and “intrinsic” over-resistance (hardening behaviour). The estimation of expected q_0 -factors has been conducted by means of the numerical analyses reported in the following section.

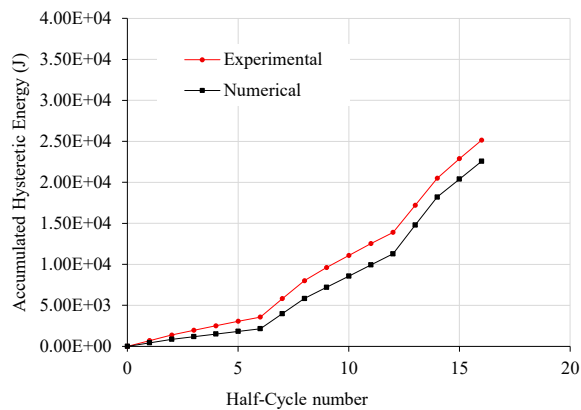
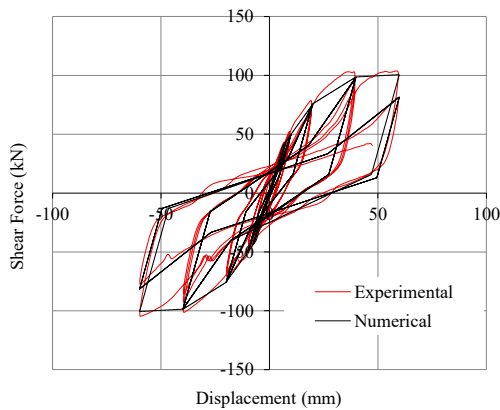
4.2.2 Numerical modelling of not-glued CLT shear walls and evaluation of q_0 -factor

4.2.2.1 Description and calibration of the models

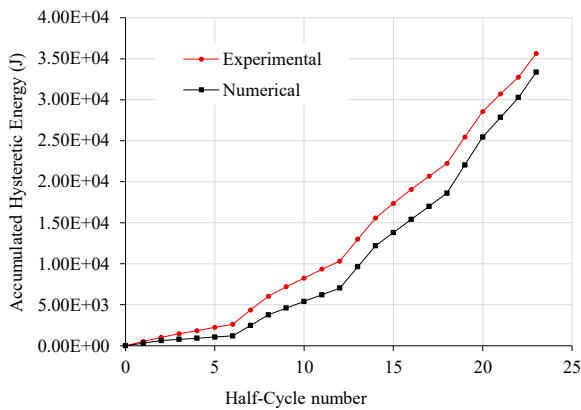
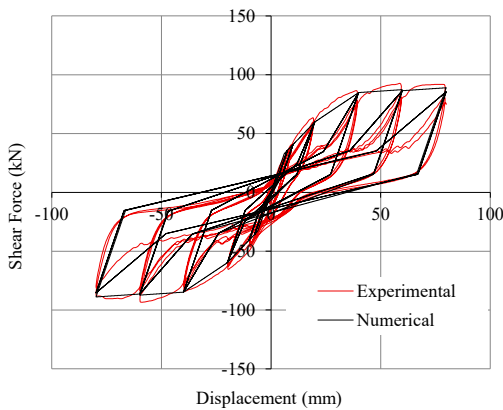
A simplified numerical model of the tested shear walls was performed. In detail, the shear walls were modelled with all non-linear deformations diffused in the bracing system, according to the “diffused non-linearity” approach described in section 1.2.2. The modelling of non-linear effects

exclusively in the equivalent diagonals is possible because of the analysis of simple case studies, with geometry equal to the tested specimens. This allows to replicate test behaviour faithfully. This modelling strategy is more appropriate for walls, whose deformation is mainly due to shear deformation of the wooden panel, whereas base connections are over-resistant and undergo negligible displacements (e.g., stapled and layered wall). To have consistency among studied models, the same modelling approach has been adopted also for comparative CLT walls.

The parameters of the non-linear diagonal springs were obtained by fitting the experimental cyclic behaviour under lateral loads. The research-oriented numerical code “Open System for Earthquake Engineering Simulation - OPENSEES” [4.26] was used for the analyses, modelling the non-linear elements with the Pinching 4 hysteresis model [4.27]. Each numerical model was calibrated on experimental results, reproducing the base shear force for each imposed top displacement according to the cyclic-loading protocol applied during tests [4.19]. Fig. 4.4 shows the numerical hysteresis cycles superimposed on the experimental ones and the total amount of dissipated energy at the end of each pushing and pulling phase (i.e. half-cycle) of the cyclic-loading procedure to demonstrate the reliability of the numerical model. It can be seen that the numerical model always gives a conservative estimation of the experimental values, in order to derive a conservative value of q_0 -factor.



(a)



(b)

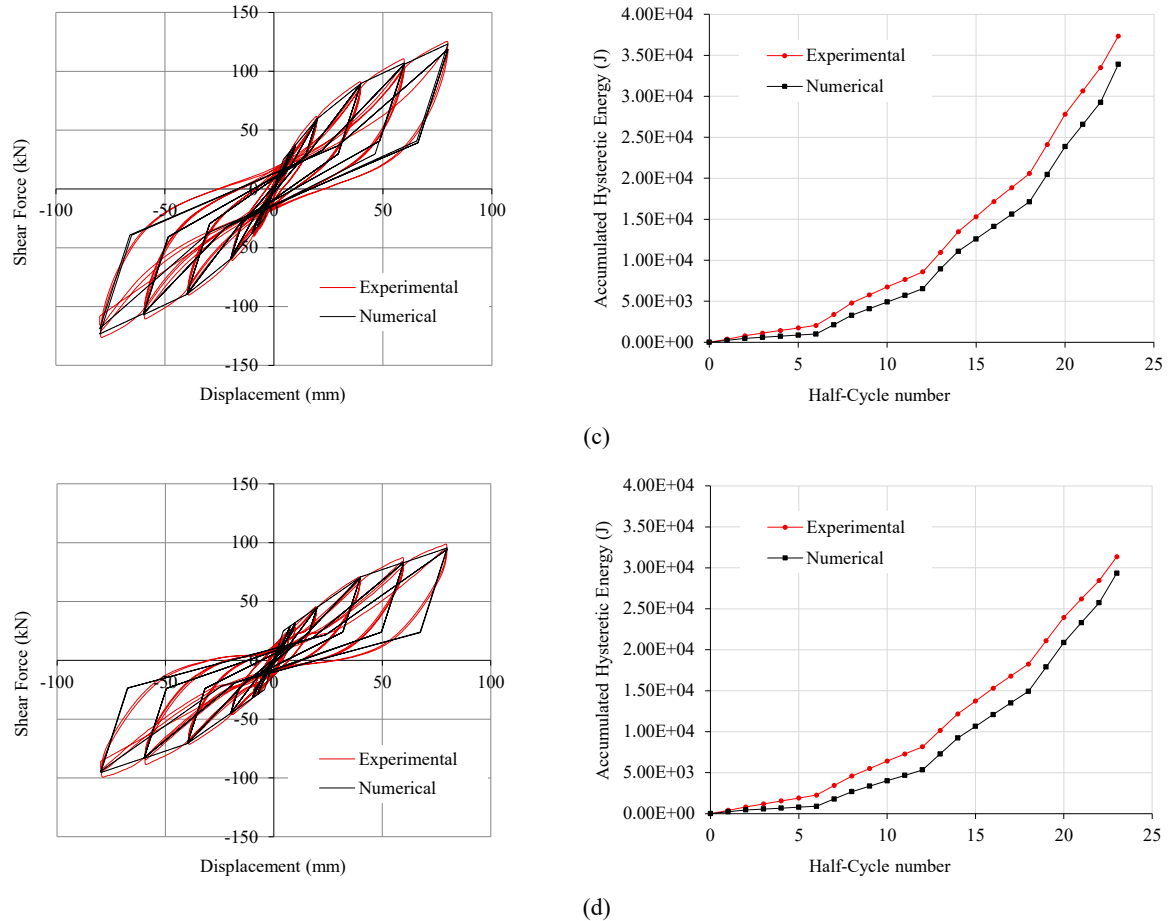


Fig. 4.4 – Calibration of the models: fitting of experimental hysteresis cycles and dissipated energy comparison: (a) glued CLT A.2 wall; (b) glued CLT C wall; (c) stapled wall, (d) layered wall.

4.2.2.2 Evaluation of the q_0 -factor

The q_0 -factor has been determined by applying the method proposed by Ceccotti and Sandhaas [4.28], described in section 2.3 and already used to evaluate the q_0 -factor for CLT wall systems (section 2.3.1) and CLT buildings (section 2.3.2). As already emphasized in §1.3, the applicability of such method requires additional details about the definition of the design and of the near-collapse condition. In fact, differences between design and modelling phase introduce uncertainties in the final values of q -factor that can be influenced mainly by design over-strength Ω . A correct evaluation of the q_0 -factor should take into account all intrinsic capacities of the system, i.e., dissipative capacity, ductility, redundancy, post-elastic hardening behaviour, and strength reserve. However, each over-resistance of walls induced by design criterion (e.g. safety level assumed by designers or simplified analytical methods adopted for design) should not influence this value and have to be accounted separately. Imposing the design condition coinciding with that of yielding of the structure allows to calculate the intrinsic value of the q -factor (q_0 -factor). It is clear that such design condition depends on the bi-linearization method adopted to evaluate the yielding limit from the experimental load-displacement curve. This approach is therefore: dependent on method used to define yielding and near-collapse conditions, independent of the design of the structure (e.g., over-design factors and safety level assumed) and of the adopted seismic codes for design (e.g., the factored resistances of materials).

The near-collapse condition of timber wall systems is defined in the modelling by assuming a criterion based on the maximum displacement capacity that the structure can reach before collapse. Various limits of near-collapse condition can be imposed, e.g., the first collapse of a connection element [4.29] or the achievement of an inter-storey drift, beyond which the structure is not more safe and suffers severe damage [4.1]. The choice of a near-collapse condition linked to the failure of a connection element is more suitable for structural systems characterized by rigid panels and deformable connection elements (fuses) (e.g., CLT system). Otherwise, a near-collapse condition based on the inter-storey drift is more general and suitable to describe the failure of structural systems characterized by deformable wooden panel and over-resistant connections. This definition is also adopted by codes [4.23] to define the DLS verification of a structure. In these analyses the inter-storey drift has been used as near-collapse condition and various limits have been imposed to evaluate the variation of q_0 -factor with the admissible damage level chosen.

A simplified numerical model of a shear wall of a three-storey building, formed by stacking three levels of the experimentally tested panels, was considered. Design earthquake forces on the case-study shear walls were calculated by means of an equivalent static analysis considering elastic response spectrum for building foundations resting on type A soil (rock soil, corresponding to $S=1.0$, $T_B=0.15s$, $T_C=0.4s$, $T_D=2.0s$), q -factor=1, and building importance factor $\gamma_I=1$, according to Eurocode 8 [4.23]. In order not to introduce effect of design over-strength in the evaluation of q -factor, the equivalence of the design base shear force to the experimentally evaluated yielding force (i.e., $PGA_d = PGA_y$) had to be imposed. Assuming the first mode period of each wall in the plateau range of the spectral responses and the first mode participating seismic mass equal to 14t, for all the shear walls, the PGA_y values were determined from the experimentally evaluated yielding shear force proper of each wall for each imposed drift, applying the equivalent linear static analysis [4.23], Fig. 4.5. Then the initial hypothesis that all first mode periods were in the plateau range was confirmed, since the fundamental periods of all shear walls resulted to be in the range between 0,36 and 0,40 s, i.e., between $T_B=0.15s$ and $T_C=0.4s$.

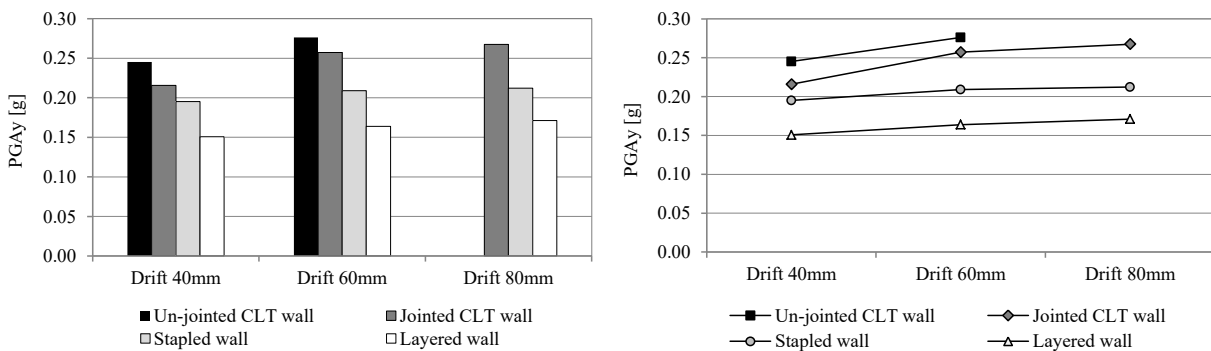


Fig. 4.5 – PGA_y values for the specimens for the three levels of drift: comparison and trend.

NLDAs were carried out considering 15 seismic shocks, artificially generated in order to meet the spectrum compatibility requirement with the design elastic spectra. Two types of software were used to generate the shock signals: SIMQKE_GR [4.30] and SeismoArtif [4.31]. Dynamic equilibrium equations were integrated with a not-dissipative Newton-Raphson scheme and time-steps of 0.001 s, introducing an equivalent Rayleigh viscous damping of 2%, according to Ceccotti [4.29]. By progressively increasing the magnitude of the applied seismic signals, the $PGA_{u,i}$ values, which lead to the three imposed ultimate levels of inter-storey drift, were evaluated for all 15 signals. Finally, the q_0 -factors for each shear wall and drift level were evaluated as the ratio between the $PGA_{u,i}$ values and the PGA_y value. Results are reported in Fig. 4.6 in terms of PGA_u

and Fig. 4.7 in terms of q_0 -factor. Table 4.5 lists maximum, minimum, mean and 5% characteristic ($q_{0,0.05}$) values, computed according to EN 1990 [4.32].

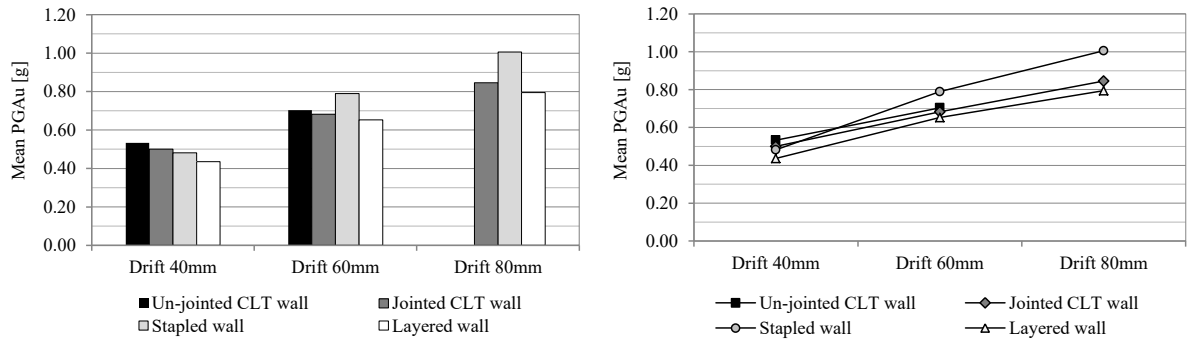
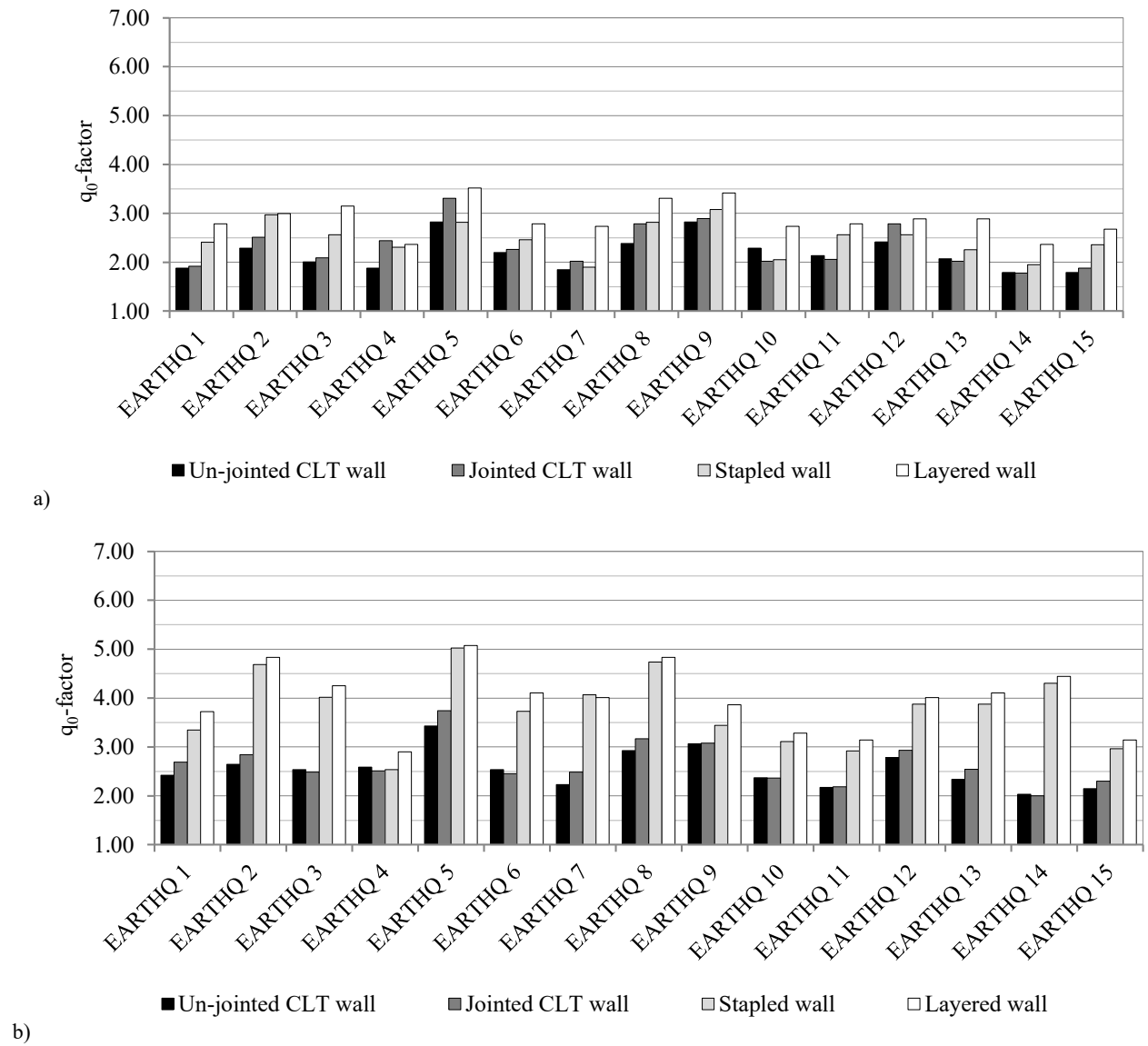
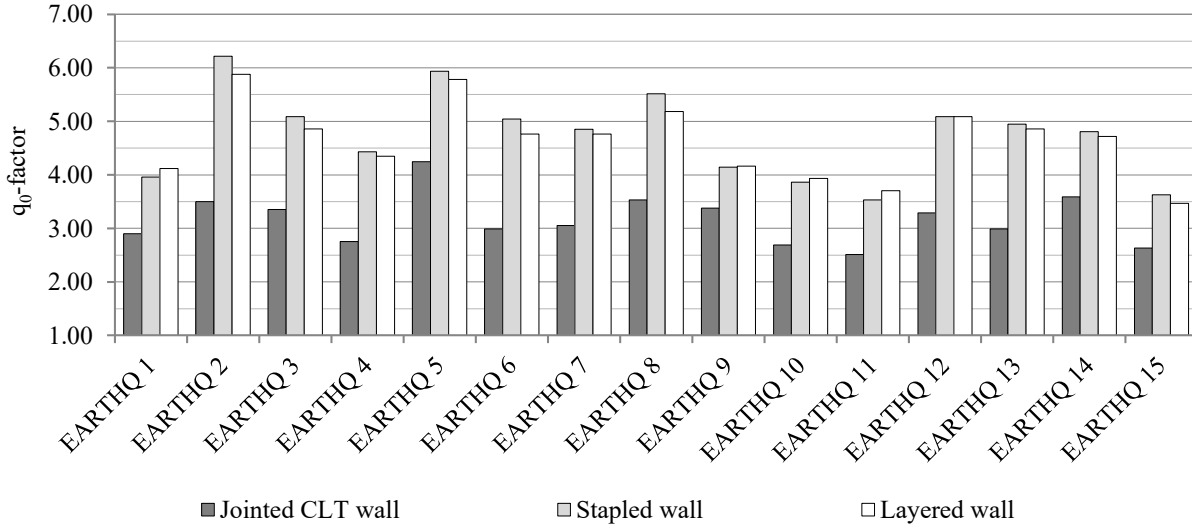


Fig. 4.6 – Mean PGA_u values: comparison and trend.





c)

Fig. 4.7 – Obtained q_0 -factor values: (a) drift 40 mm; (b) drift 60 mm; (c) drift 80 mm.

Table 4.5 – 1st mode periods and results in terms of q_0 -factor values.

	Un-jointed CLT wall			Jointed CLT wall			Stapled wall			Layered wall		
T_1 (s)	0.36			0.37			0.40			0.37		
DRIFT (mm)	40.0	60.0	80.0	40.0	60.0	80.0	40.0	60.0	80.0	40.0	60.0	80.0
Mean PGA_u (g)	0.53	0.70	-	0.50	0.68	0.85	0.48	0.79	1.01	0.44	0.65	0.79
Min q_0	1.79	2.03	-	1.78	2.00	2.51	1.90	2.54	3.53	2.36	2.90	3.47
Max q_0	2.82	3.43	-	3.31	3.74	4.25	3.08	5.02	6.22	3.52	5.07	5.88
Mean q_0	2.18	2.55	-	2.32	2.65	3.16	2.47	3.78	4.74	2.89	3.98	4.64
SD	0.34	0.38	-	0.45	0.44	0.46	0.35	0.73	0.81	0.34	0.66	0.70
$q_{0,0.05}$	1.55	1.85	-	1.49	1.84	2.31	1.83	2.44	3.25	2.26	2.77	3.35

The PGA_u values provide the first comparison among walls in terms of resistance to seismic actions because the walls have the same mass and geometry. Fig. 4.6 shows that the stapled wall guarantees the highest resistance. Also the un-jointed CLT wall shows a good behaviour for low drifts thanks to high strength and stiffness of the wall.

Q_0 -factor values obviously increase with the drift level, even if not proportionally. The significant value of q_0 -factor is that achieved at the real ultimate capacity of the walls, evidenced with bold characters in Table 4.5. The un-jointed CLT shear wall demonstrates the lowest dissipative and ductility capacity, whereas the other three panels have a greater ultimate drift capacity (2,67%), for which they assure higher q_0 -factors.

Fig. 4.8 shows a comparison among walls in terms of average q_0 -factor. The higher value for stapled and layered panels, if compared with CLT walls, is not only due to higher dissipative capacity, but also to the hardening behaviour of those two panels. Hardening post-elastic behaviour implies intrinsic strength reserve after yielding that increases the PGA_u value, and a lower PGA_y because of the lower yielding strength (Fig. 4.3). Both the increase of PGA_u and the decrease of PGA_y contribute to increase the q_0 -factor.

The comparison between the examined CLT walls shows that the un-jointed panel presents less displacement capacity and less ductility than the jointed one. Therefore, the jointed panel ensures a reserve of ductility and energy dissipation until reaching a state of near-collapse condition for a

greater drift, for which a greater q_0 -factor can be obtained (Table 4.5), despite an ultimate strength less than that of the un-jointed wall. The jointed CLT wall results more performant for use in seismic-prone areas, because of the reaching of higher displacements before failure and consequent increase of q_0 -factor. This result is consistent with conclusions obtained in Chapter 2.

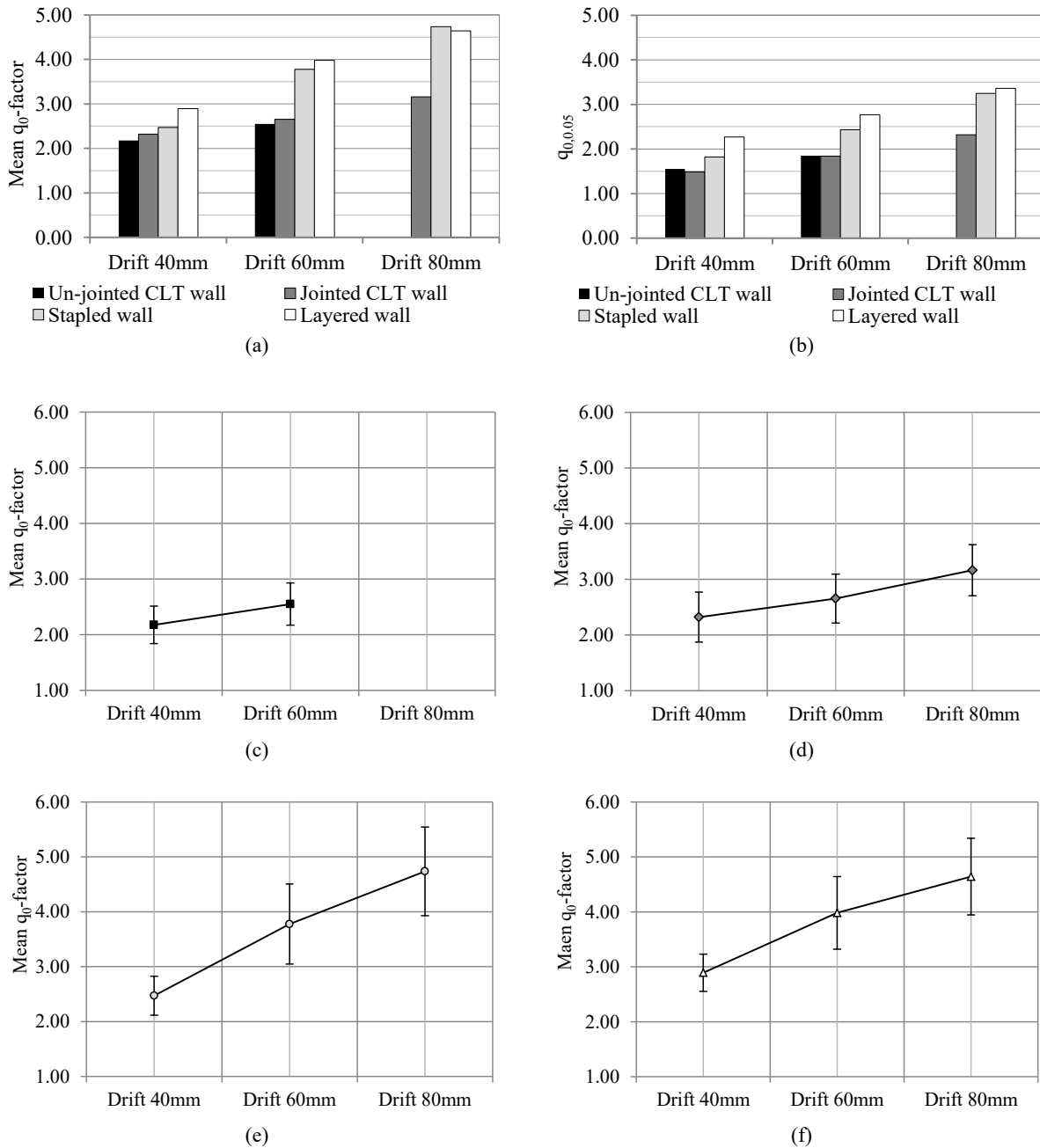


Fig. 4.8 – Mean values and standard deviation of q_0 -factors: (a) comparison of mean q_0 ; (b) comparison of characteristic $q_{0,0.05}$; (c) un-jointed CLT wall; (d) jointed CLT wall; (e) stapled wall; (f) layered wall.

The above reported remarks have been derived by comparing mean values of q_0 -factor. The standard deviation is however not the same among walls and for the three drift limits. It has to be noted that stapled and layered walls present higher dispersion of results for drift higher or equal than 6 cm. The consequence is that difference among the four examined walls in terms of characteristic q_0 values (e.g. 5th percentile) becomes lower (Table 4.5, Fig. 4.8b).

According to these results, it can be confirmed that a q_0 -factor in the range between 2.00 and 3.00 is suitable for glued CLT wall systems, depending on the assembling of the wall. For walls composed of various panels vertically jointed with metal ductile fasteners, the highest value can be properly adopted. This range is also consistent with values proposed in literature ([4.29];[4.33]) and with values obtained in Chapter 2. Application of formula (2.10) provides almost identical results, as demonstrated in Table 4.6. It has to be noted that the three-storey shear walls studied in this section are to be considered as irregular in elevation, according to the definition provided in section 2.6, since in numerical models timber panels and connections have been assumed the same at each storey. Therefore, for a correct comparison of numerical and analytical behaviour factor values, a k_R factor equal to 0.7 and 0.75 has to be assumed in the un-jointed CLT wall (considered as NVJ) and in the jointed CLT wall (considered as MVJ) respectively, according to Fig. 2.29, section 2.5.2.

Table 4.6 – Comparison between analytical and numerical q_0 -factors for un-jointed and jointed CLT walls.

Parameters	Units	Un-jointed CLT wall	Jointed CLT wall	Demonstration of analytical calculation via abacus representation
B	m	3.00	3.00	$q_0(\beta, \lambda) = \left(2.00 + \frac{\lambda}{2} \right) \cdot \sqrt[3]{\beta}$
H	m	9.00	9.00	
n	-	3.00	3.00	
m	-	0.00	1.00	
P ₀	m	30.00	39.00	
P	m	24.00	24.00	
β	-	1.25	1.625	
λ	-	3.00	3.00	
q_0 <i>analytical</i>	-	3.77	4.11	
k_R	-	0.70	0.75	
$q_0 \cdot k_R$ <i>analytical</i>	-	2.64	3.09	
$q_0 \cdot k_R$ <i>numerical</i>	-	2.55	3.16	
Relative Difference	-	-3.50%	+2.34%	

For the other two novel systems, characterized by a diffuse and greater shear deformability of the wooden panel, a post-elastic hardening stiffness and a higher dispersion of results, the adoption of q_0 -factor in the range between 3.00 and 4.00 represents a suitable and precautionary value.

Obtained results are consistent with initial assumptions about: (1) characteristics of tested specimens, (2) hypotheses assumed for the design, (3) chosen bi-linearization criterion that influences the PGA_y value, (4) choice of a design over-strength Ω equal to 1 (i.e. $PGA_d = PGA_y$).

It has to be recalled that above reported q_0 values do not account for over-strength Ω . Consequently, q -factors to be used for evaluation of seismic design forces are even greater.

Lastly, some considerations about the influence of the allowable near-collapse conditions on the q_0 -factor to be assumed in design are mandatory. Q_0 -factor should be correlated with the chosen design approach and the assumed admissible damage level. If more strict limitations to inter-storey drift are to be assumed in order to ensure reduced structural damage ([4.1];[4.23]), smaller values of the q_0 -factor than those above proposed are to be assumed. If no-damage criterion instead of life-safety requirement is to be chosen in ULS verification, mean q_0 -factors (or $q_{0,0.05}$ factors) obtained for drifts equal to 4.00 cm should be used.

4.3 Evaluation of the seismic performance of a new mixed steel-timber solution with an innovative bracing system

Research results presented in this section are partly available at MDPI via <http://dx.doi.org/10.3390/ma8115386> [4.34]. Journal Materials is acknowledged as the original source of publication.

In this section, an innovative timber frame for shear walls is presented. The system is based on the light-frame concept, modified with the addition of steel columns and a novel plastic bracing system, which works in parallel with a standard OSB panel. The multi-storey thin-box steel columns assure adequate resistance to vertical static loads and have the main advantages of reduced geometric tolerances and reduced on-site assembling time. Steel columns are fastened to the vertical panels, the foundations and the floors by means of steel brackets and self-tapping screws. The additional bracing system is obtained with a hot-moulded technoprene sheet infilled with plaster. This infilled slab improves not only the seismic behaviour but also the thermal and acoustic insulation properties of the wall. Two walls were analysed with quasi-static cyclic-loading tests [4.34], according to EN 12512 protocol [4.19]. Then, numerical simulations allowed to analyse the behaviour of a case-study building to provide an estimation of the suitable q_0 -factor. Main results are here reported and discussed.

4.3.1 Description of the system

The investigated system represents a modification of that described by Pozza et al. [4.35]. Now, the outer reinforced concrete skin is substituted by suitably shaped plastic panels infilled with plaster and the timber columns are replaced by steel ones.

Each structural element has proper function: steel columns support vertical loads, whereas the OSB panel and the external plastic slabs confer to the timber frame resistance against lateral loads and dissipation capacity during earthquake. The precast frame (Fig. 4.9) has modular dimensions: width is equal to 1080 mm and height is three times the width dimension. 15-mm thick OSB/3 panel conforming to EN 300 [4.36] is stapled to the timber frame, realized with 200x80-mm horizontal crosspiece beams and 100x80-mm vertical studs. Both beams and studs are made of C24 timber [4.37].

The innovative technoprene slab (polypropylene homopolymer reinforced with 18.5% chemically coupled glass fiber), hereafter called skin (Fig. 4.10), is infilled with plaster and acts as an additional bracing system, collaborating with the OSB panel to provide strength and dissipative capacity to the timber frame. The skin is a square slab of about 108.6 mm width, and thickness equal to 35 mm, including the plaster layer. It is connected to the frame with three 10x120-mm screws each side (steel class 8.8, according to ISO 898 [4.38]). The main advantages are: the lightweight panel facilitates the realization of the buildings; the special 3d shape improves the adherence with the plaster and allows the creation of a ventilation chamber between the OSB and the external layer (i.e., a continuous natural airflow from the ground level to the roof), improving the durability of the wooden parts and providing good insulation properties to the building.

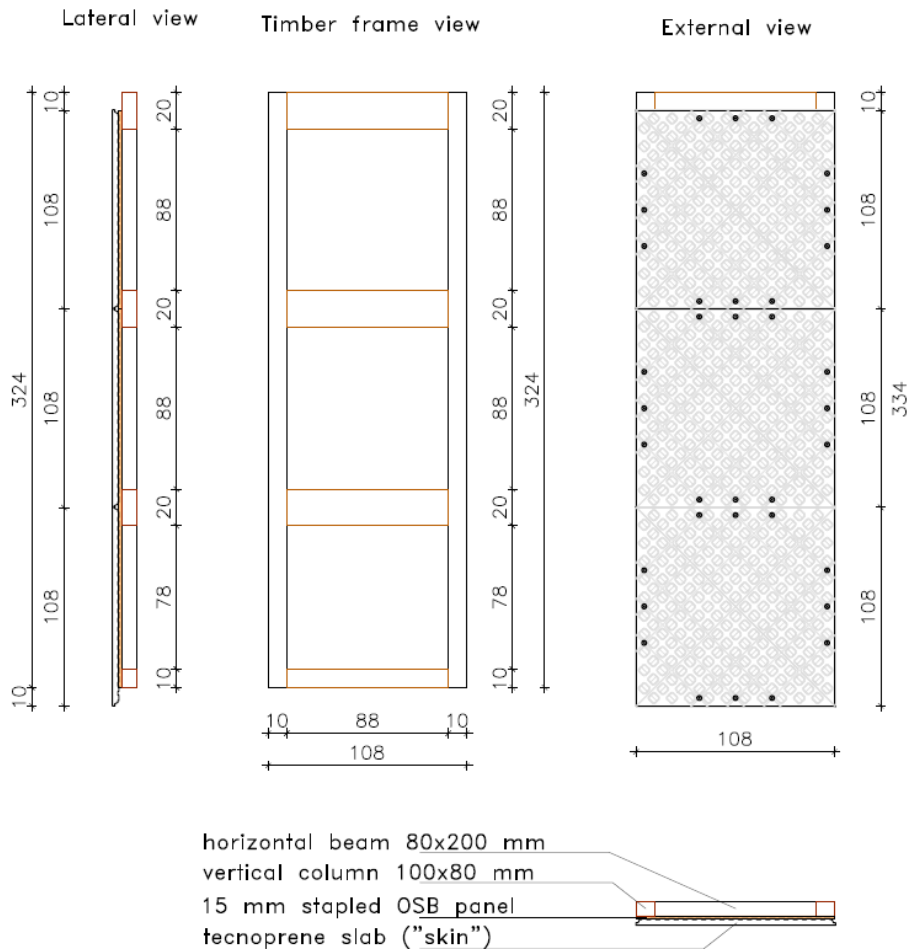


Fig. 4.9 – View of the modular shear wall (dimensions in cm).

The steel columns (Fig. 4.11) allow to speed-up the construction of the building because they are placed before the shear walls and can be continuous from the foundation to the roof (balloon system), for low- and medium-rise buildings. Columns are connected to the frame with 30x20x2-mm continuous press-belted L-profiles, which are jointed to the wooden side with 4x60-mm ring shank nails and to the steel side with 6.3x19-mm screws (self-tapping screws according to EN 15480 [4.39], steel class 9.8 according to ISO 898 [4.38]). The same column-to-frame L-profiles have the function of connecting two adjacent modular shear walls through a steel column acting as vertical joint.

Connection elements, made with steel brackets, are used for supporting floor and roof beams and connecting columns at foundation, in order to resist to uplift of the shear wall. These brackets are made of the same tubular element of the column, 2- or 3-mm thick, and are connected with 6.3x19-mm self-tapping screws to the column and with 20mm-diameter anchors to the foundation (Fig. 4.11). The resistance to base shear forces is provided mainly by three vertical 12x180-mm wood screws (class 4.8 according to DIN 571 [4.40]) fixed between the timber frame and the concrete foundation curb. Moreover, three horizontal 12x100-mm horizontal wood screws connect the bottom edge of the skin and the foundation curb. A vertical section of the system is shown in Fig. 4.12.

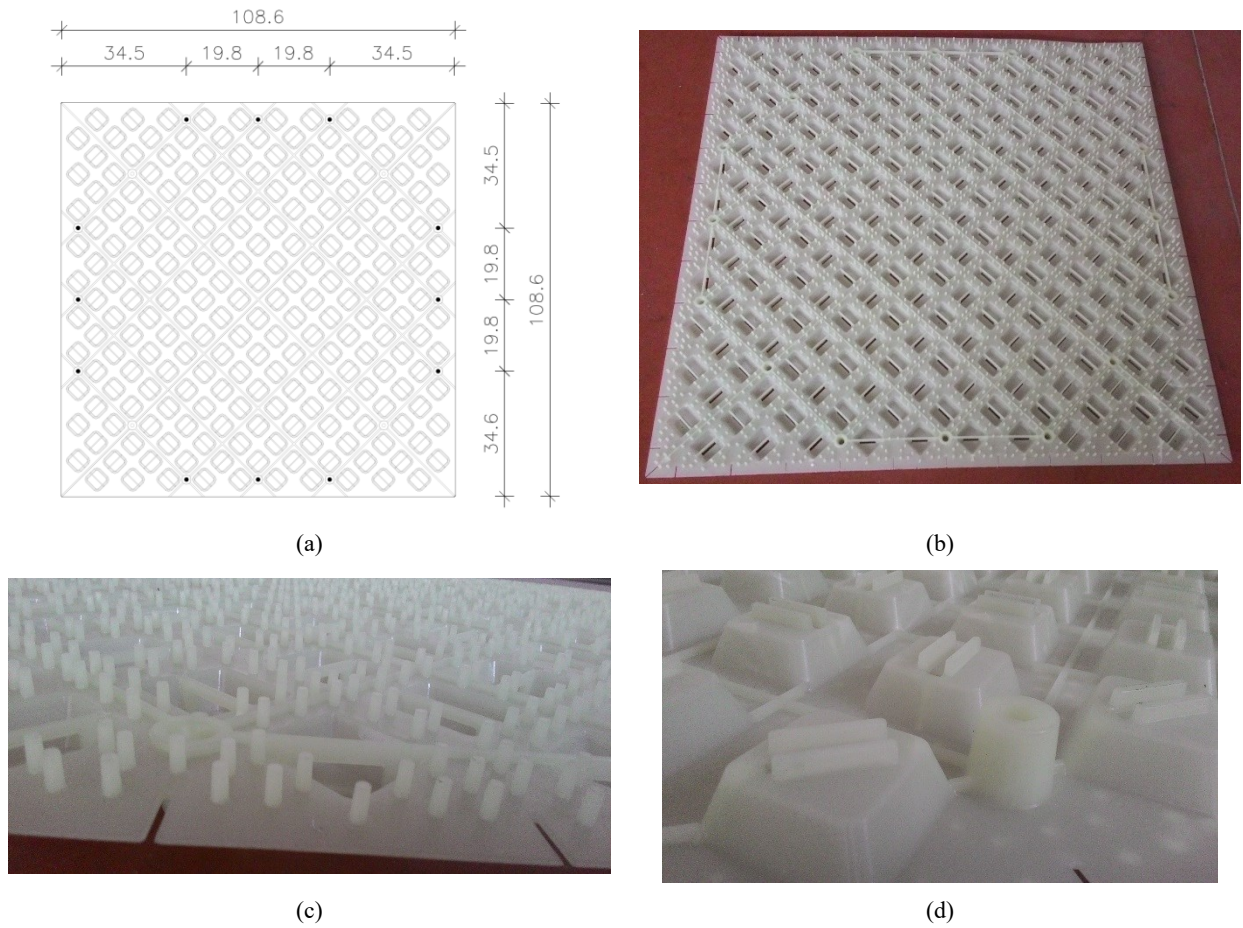
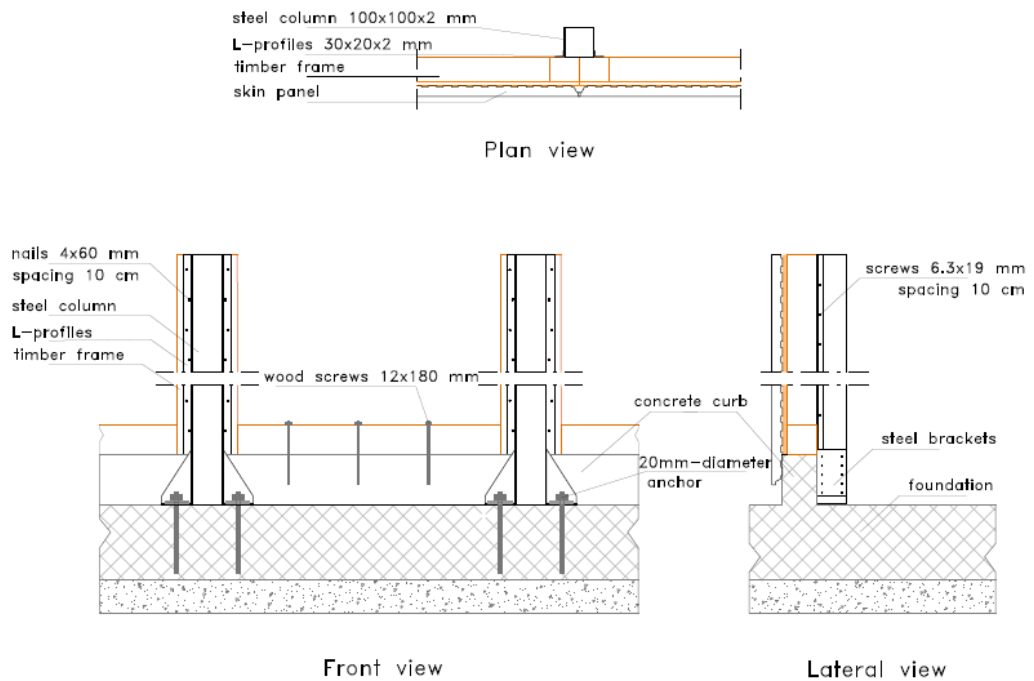


Fig. 4.10 – Skin: (a) geometry; (b) front view; (c) front-view detail; (d) back-view detail.



(a)



(b)



(c)



(d)

Fig. 4.11 – Steel columns and brackets: (a) geometric details of connection with foundation; (b) view of the modular walls assembled; (c) detail of connection with the foundation; (d) detail of connection with the floor.



Fig. 4.12 – Wall section: (from left to right) skin, OSB panel, timber stud, steel column.

4.3.2 Experimental tests

Quasi-static cyclic-loading tests were conducted according to EN 12512 [4.19] on two walls realized with the studied construction system, in order to assess the resistance of the system against lateral loads and to evaluate its seismic behaviour. The first wall tested (wall A) was realized with all the components of the system. In the second wall (wall B) the OSB panel was removed and only the skin acted as bracing system. In this way, the contribution of the skin to the global seismic response has been evaluated. Two adjacent panels were assembled to realize the walls, which are 3.24-m high and 2.16-m wide. A reinforced concrete foundation was realized to reproduce the base connection of the system. Fig. 4.13 shows the test set-up used for both the walls, which was chosen to be consistent with the previous experimental campaign, whose results are presented in [4.35]. A vertical load of 8.8 kN (reproducing gravitational loads at the first storey of a low-rise building with lightweight floors) was applied for each steel column by three hydraulic actuators. Lateral guides were positioned at top of specimen to avoid out-of-plane movement. Displacements of panels and connections were measured with transducers, placed as shown in Fig. 4.13: CH1, CH4 and CH5 measured the base uplift, CH3 the base slip, CH6 the panel-to-panel slip, CH2 the top displacement and LVDT applied and measured the top horizontal force and displacement. Fig. 4.14 shows the configuration before the test.

At the end of tests, no failure localization was evident, but diffuse yielding of fasteners between bracing systems and frame and between frame and steel L-profiles. Thin cracks at the perimeters of the skin panels were also observed. Fig. 4.15 demonstrates the formation of a plastic hinge in the 10x120 mm wood screws connecting skin to frame. Tests were stopped before the ultimate displacement of the walls was reached, due to limited allowable jacket elongation. Fig. 4.16 shows the hysteresis curves of the two specimens, i.e., the imposed top displacement vs. the corresponding applied force. Fig. 4.17 shows the walls at the end of the tests, at the maximum applied displacement.

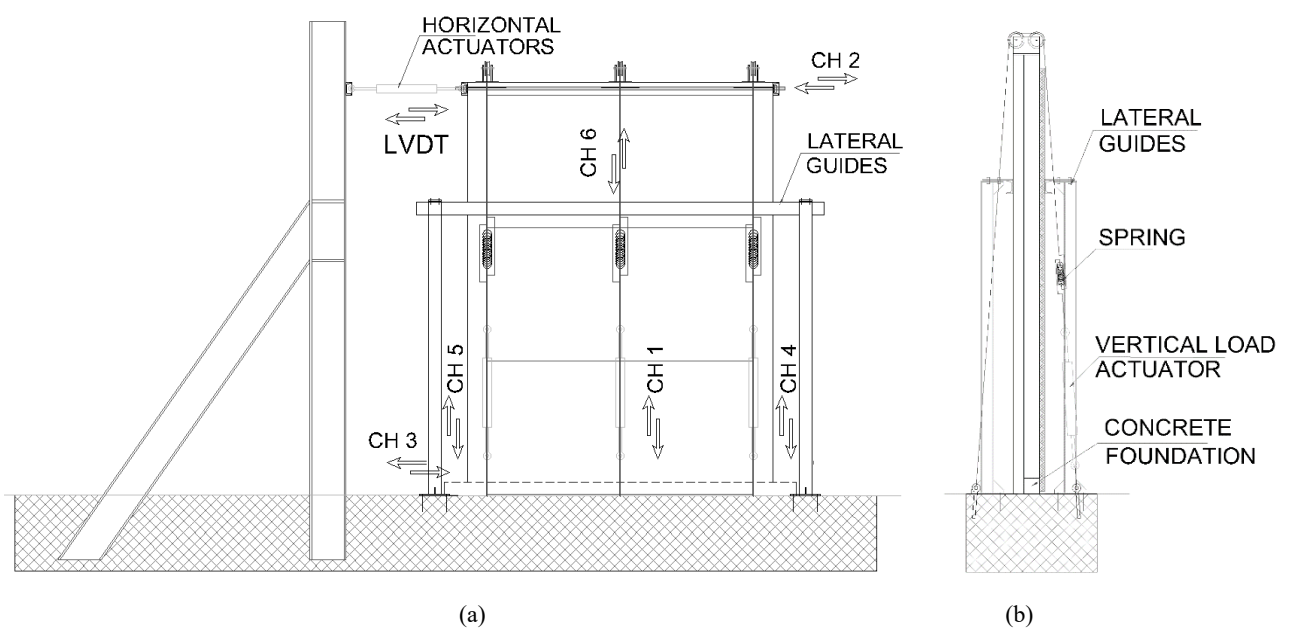


Fig. 4.13 – Test setup: (a) front view; (b) side view.



Fig. 4.14 – Experimental setup: (a) external view; (b) inner view.



Fig. 4.15 – Yielding of the 10x120 mm screws connecting skin to frame (single plastic hinge).

Wall A reached the maximum displacement without relevant failures or strength degradation phenomena (Fig. 4.16a). This specimen exhibited the hysteretic behaviour typical of timber structures, characterized by pinching phenomenon of steel-wood and wood-wood connections. Moreover, the skin and the OSB panel contributed to the hardening behaviour shown. The shear resistance of the system is limited by the weakest mechanism among the followings: (1) the in-plane shear resistance of skin and OSB panel and the shear resistance of the relative connectors; (2) the axial and shear resistance of the connections at foundation; (3) the shear resistance of frame-to-column joints. The main contributions to the ductility of the system are given by the shear deformation of the bracing system and the panel-to-panel relative slip (see Fig. 4.17a). Conversely, base connections should be over-designed due to their brittle behaviour and, therefore, small and almost elastic deformations are expected for them, according to the capacity design approach.

Fig. 4.16b allows to assess the contribution of the skin to the shear resistance of the whole system. In the cyclic tests for wall A and wall B the same displacements were reached with lower resistance for wall B. The hysteretic behaviour of this wall confirms also the contribution of the skin panel to the energy dissipation capability of the system: the pinching behaviour was reduced and the ductility was maintained. The comparison between Fig. 4.16a and Fig. 4.16b allows also to quantify this contribution in terms of strength: it can be stated that almost the 60% of in-plane shear resistance is given by the skin.

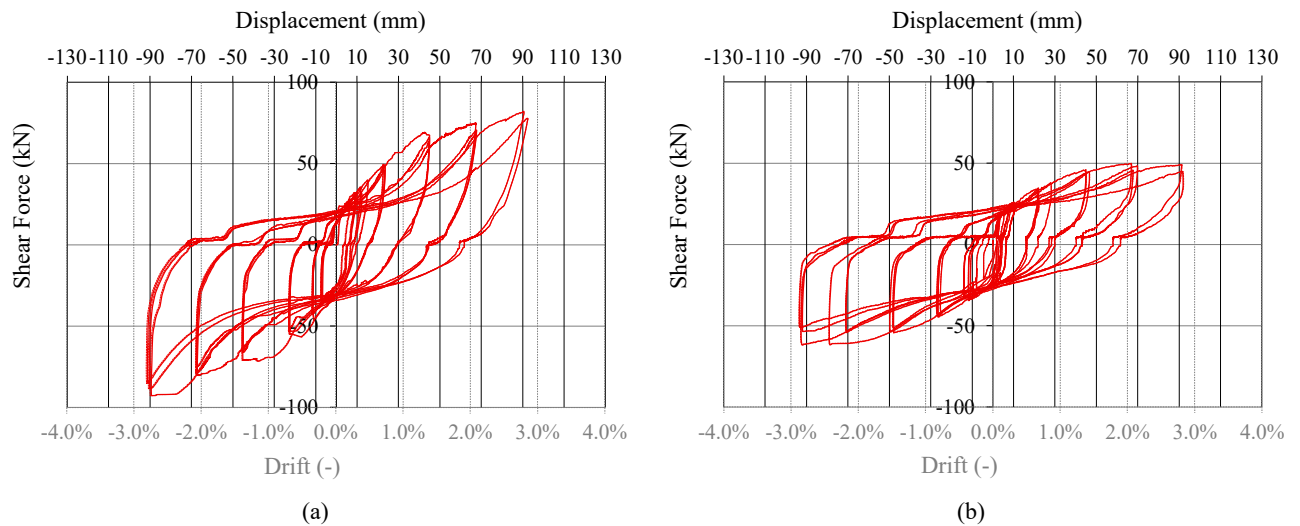


Fig. 4.16 – Hysteresis curves: (a) wall A; (b) wall B.



Fig. 4.17 – Wall configurations at the end of the cyclic loading tests: (a) wall A; (b) wall B.

4.3.2.1 Analysis of test results

Results obtained from the cyclic tests were analysed to define the main mechanical properties of this innovative system. This section discusses the evaluation of the following parameters: yielding point (d_y , F_y), maximum displacement and force reached (d_{max} , F_{max}), stiffness for the elastic and post-elastic branches (K_e , K_{pl}), ductility μ , strength degradation at different cycle amplitudes and viscous damping ratio ν_{eq} . Finally, the evaluation of the ductility class, according to design provisions [4.23] is reported.

Table 4.7 lists the yielding values and the main outcomes in terms of strength, stiffness and ductility according to different approaches. The envelope of the hysteresis curve was fitted using the analytical formulation proposed by Foschi and Bonac [4.41]. Then, the mechanical parameters were obtained applying the bi-linearization methods that better fit the envelope curve. In detail, results for wall A were fitted with method “a” of EN 12512 [4.19], EEEP method [4.42] and EEEH method [4.25]. To obtain a comparison with wall B in terms of stiffness and strength, only the EEEP method was applied due to its perfectly-plastic behaviour. Ductility ratios were evaluated assuming the maximum applied displacement as ultimate top displacement, i.e., 92 mm for wall A and 90 mm for wall B.

Table 4.7 – Test results and interpretation.

Parameters	Notations	WALL A			WALL B
		ENa	EEEH	EEEP	EEEP
Ultimate displacement	d_{max} (mm)	92.0	92.0	92.0	90.0
Ultimate force	F_{max} (kN)	86.0	86.0	65.9	47.4
Elastic stiffness	K_e (kN/mm)	7.5	5.0	4.5	4.1
Hardening stiffness	K_{pl} (kN/mm)	0.5	0.5	0.0	0.0
Yielding displacement	d_y (mm)	5.6	8.6	14.7	11.6
Yielding force	F_y (kN)	41.7	43.2	65.9	47.4
Ductility ratio	$\mu = d_{max}/d_y$	16.5	10.7	6.2	7.7

Obtained ductility is always higher than 6, which is the minimum value to be assured for the High Ductility Class (DCH), according to Eurocode 8 [4.23]. Comparing these ductility values with those obtained for massive wall systems presented in this dissertation (sections 2.2 and 4.2) it can be seen that the ductility of this novel system is higher.

Table 4.8 lists the strength degradation recorded between the first and third cycles of each displacement level of the tested walls and the equivalent viscous damping v_{eq} , defined according to EN 12512 [4.19]. These values demonstrate that the loss in strength increases with the cycle amplitude but is always less than 20%. Therefore, given the ductility higher than 6, the system can be classified into the DCH. Table 4.8 lists also the equivalent viscous damping v_{eq} values, which summarize the hysteretic dissipative capacity of the structural system. These values are constantly greater than 18%, confirming a good dissipative capability of this system. Moreover, it can be seen that the values of the equivalent viscous damping for wall B are higher than results for the entire system (wall A). These values confirm the contribution of the skin to the dissipative capability of the system and therefore its suitability for use in seismic areas.

Comparing the results with those obtained for the previous system [4.35], a slight improvement in terms of both strength reduction and equivalent viscous damping has been obtained.

Table 4.8 – Strength degradations and equivalent viscous damping at each cycle amplitude.

Cycle amplitude (mm)	Strength reduction (%)		v_{eq} (%)	
	WALL A	WALL B	WALL A	WALL B
20	5.9	3.4	23.8	31.2
40	5.9	4.9	20.9	24.3
60	7.6	8.9	19.6	24.9
80	11.4	16.2	18.6	25.8

4.3.3 Numerical modelling and simulations

4.3.3.1 Simulation of quasi-static test and validation of the model

A model of wall A has been performed to simulate numerically the test results and validate the calibration of non-linear elements. Then, the behaviour of a case-study building has been studied to evaluate the suitable q_0 -factor for a complete seismic characterization of the studied system.

In the studied shear-wall system, connection elements and bracing system are characterized by a hysteretic behaviour and show pinching behaviour and strength degradation under cyclic loading.

Therefore, a modelling for components with non-linear elements simulating the shear deformation of the bracing system and non-linear springs representing the connection elements has been adopted, according to section 1.2.2. Each finite-element module consists of a perimeter frame made with elastic trusses braced by diagonal nonlinear springs, which reproduce faithfully the in-plane cumulated response of stapled OSB panel, plastic skin and relative connectors (staples and screws). Inelastic springs are used also for hold-downs, base shear bolts and in-plane vertical joints between adjacent wall modules. Linear compression-only elements are coupled in parallel with hold-down springs in order to simulate the asymmetric behaviour of this component. Vertical loads and seismic masses are applied at upper nodes. In order to reproduce faithfully their actual response, the research-oriented numerical code “Open System for Earthquake Engineering Simulation–OPENSEES” [4.26] was used also in this case, with the hysteresis material model Pinching 4 [4.27].

After the calibration of the elementary nonlinear connections, the experimental cyclic test of wall A described above was reproduced with the numerical model by imposing the same horizontal top displacements (loading protocol according to EN 12512 - [4.19]) and vertical loads and recording displacements at the same position of test transducers (Fig. 4.13). A description of this procedure is summarized in section 2.3.1 (phenomenological model). Fig. 4.18 shows main recorded results superimposed on experimental cycles, i.e., lateral force vs. displacement at the top (Fig. 4.18a), vs. displacement at hold-downs (Fig. 4.18b) and vs. relative displacement at vertical joint (Fig. 4.18c). The good accuracy of the model was demonstrated by comparing the numerical data with test results in terms of accumulated dissipated energy (Fig. 4.19a) and dissipated energy computed separately for each pulling and pushing phase, i.e., half-cycle (Fig. 4.19b).

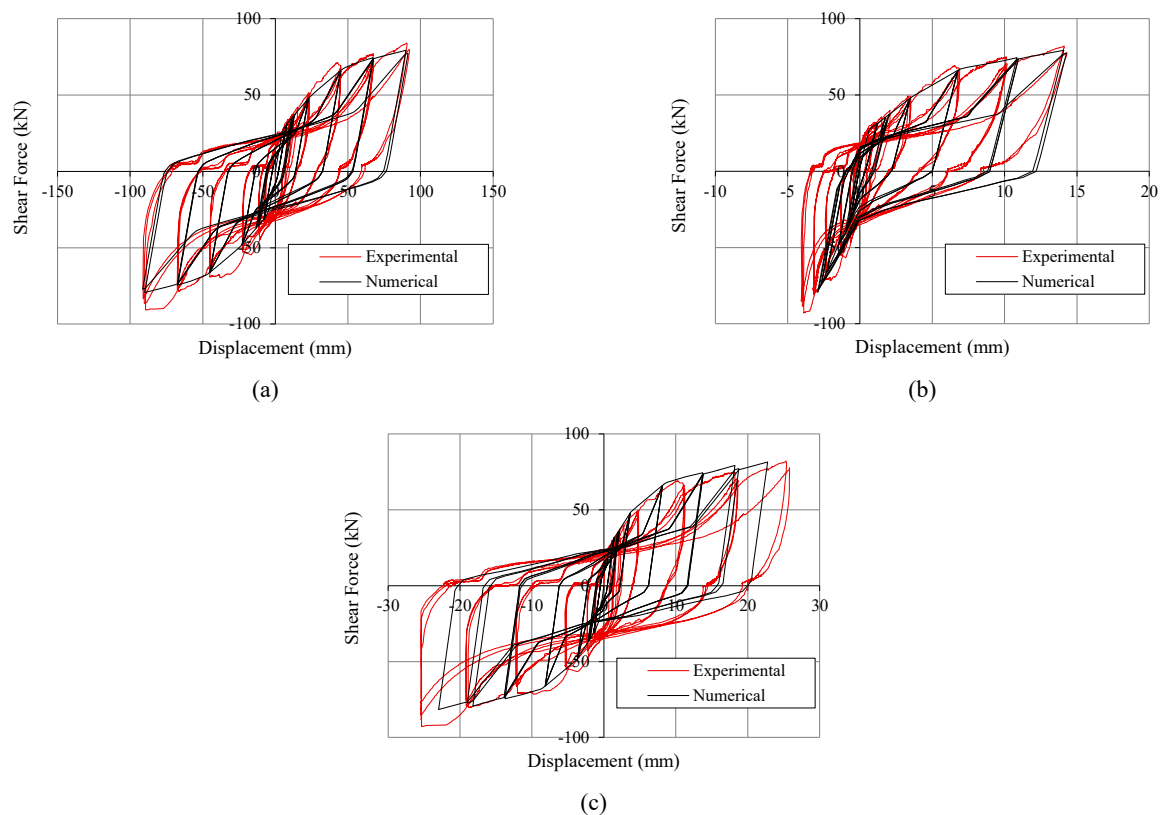


Fig. 4.18 – Hysteresis cycles of shear wall: (a) top displacement vs. lateral force; (b) displacement at hold-down vs. lateral force; (c) relative displacement at vertical joint vs. lateral force.

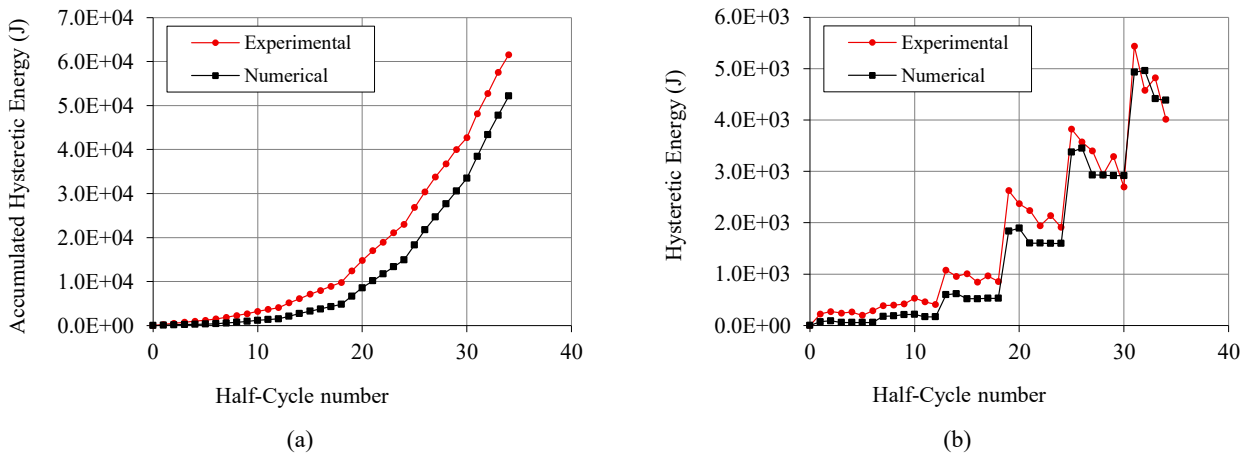


Fig. 4.19 – Energy comparison: (a) accumulated hysteresis energy up to the end of the test; (b) dissipated energy computed for each half-cycle.

4.3.3.2 Evaluation of the q_0 -factor for a case-study building

The three-storey CLT building tested on the shaking table during the SOFIE project ([4.29];[4.43]) was assumed as case study. A 2D model of the façade placed in X direction was analysed (evidenced within dashed box in Fig. 4.20). To allow a simplified 2D model of the structure, configuration with symmetric openings was chosen and rigid diaphragm assumption was made. The same precast modular panels subjected to the cyclic test and numerical calibration described above were used in the model to assemble the building (Fig. 4.21), conforming the resistance of the base connections to the seismic loads.

The PGA compatible with an elastic design of the case-study building (PGA_d) was evaluated according to the elastic response spectrum for building foundations resting on type A soil (rock soil, corresponding to $S = 1.0$, $T_B = 0.15$ s, $T_C = 0.4$ s, $T_D = 2.0$ s). Behaviour factor $q = 1$, and building importance factor $\gamma = 1$ were assumed [4.23]. The maximum spectral amplification factor F_o was assumed equal to 2.5. Then, the unit lateral load-bearing capacity of the shear wall was deduced from the experimental load-displacement curve, i.e., the force corresponding to the yielding of the shear wall (according to the EEEP bilinear model) was assumed to be the conventional design strength of the wall. Therefore, given the overall seismic mass equal to 25.2 t, the PGA_d compatible with an elastic design of the structure, without safety factors applied, was equal to 0.21g, assuming the fundamental period of the shear wall within the plateau range. The hypothesis that the first mode period was in the plateau range was confirmed by the frequency analysis, which provided the fundamental period of the building $T_1=0.36$ s.

The method proposed by Ceccotti and Sandhaas [4.28] was used to estimate the q -factor as the ratio between PGA_u and PGA_d . Also for this system, the yielding condition was assumed coincident with design condition (i.e., $PGA_d = PGA_y$), in order to evaluate correctly the intrinsic value of the q -factor, i.e., the q_0 -factor. Near-collapse limits were fixed as: a) vertical uplift 18 mm, b) inter-storey drift of bracing system of 2.0%.

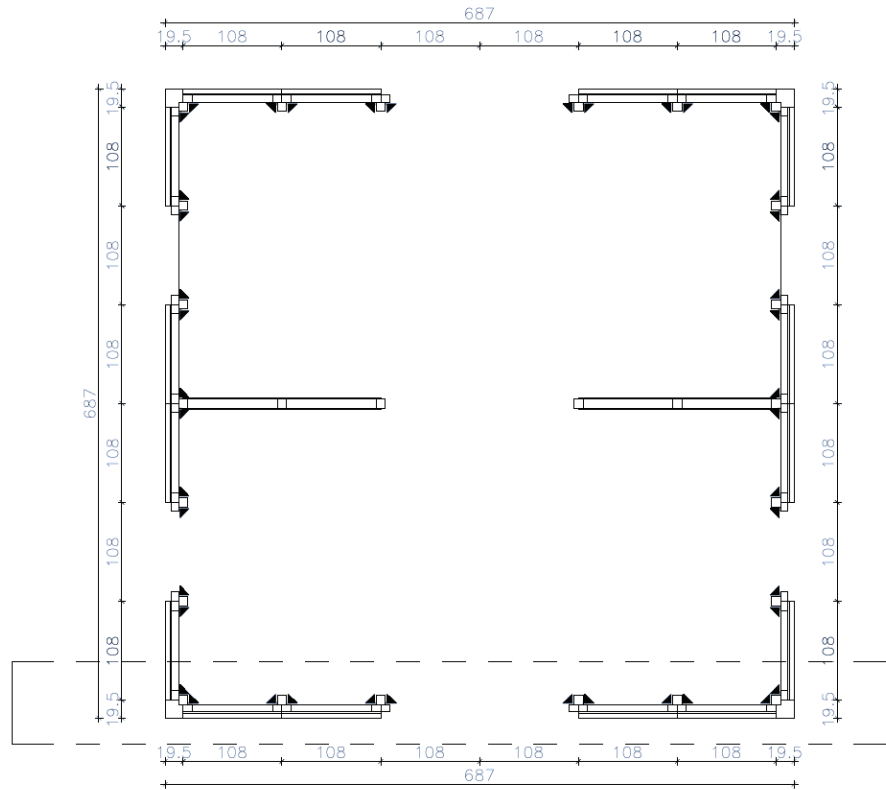


Fig. 4.20 – Case-study building. First-storey plan (dimensions in cm).

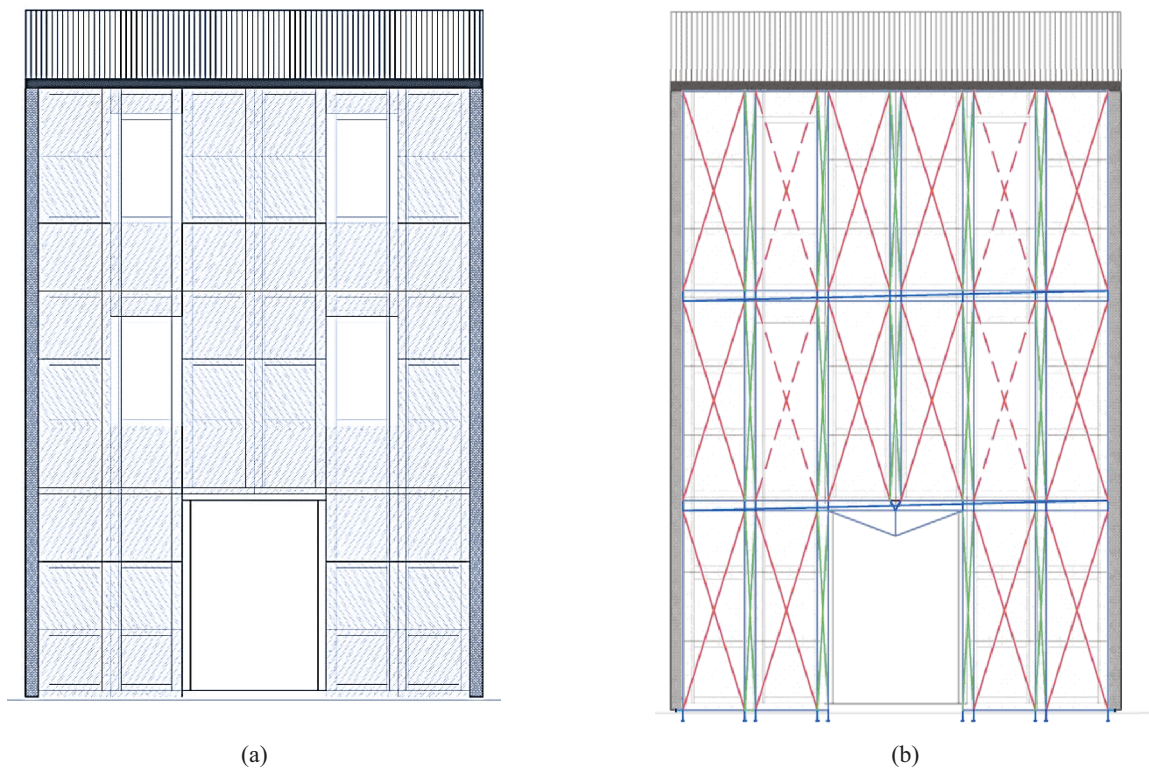


Fig. 4.21 – Case-study building. (a) View of the modelled façade; (b) numerical FE model (truss elements) superimposed on the façade: bracing system (in red); vertical joints (in green); base and inter-storey connections (in blue).

A capacity design approach was followed in order to avoid brittle failures and to obtain the maximum ductility of the building at the near-collapse condition. Consequently, the weakest components of the structure were the bracing system and the vertical joints, i.e., OSB panel-to-frame connections, skin-to-frame connections and frame-to-column connections, which in each test and analysis yielded before other seismic-resisting components, i.e., before yielding of other connections and failure of wooden and plastic components. Therefore, obtained values of q_0 -factor are consistent only with a correct capacity design of the building. Otherwise, the building could fail before reaching the maximum ductility and the PGA_u could be lower.

The NLDAs were carried out considering 8 seismic shocks, artificially generated with SIMQKE_GR [4.30] in order to meet the spectrum compatibility requirement with the design elastic spectrum. Dynamic equilibrium equations were integrated with a not-dissipative Newton–Raphson scheme and time-steps of 0.001 s, introducing an equivalent Rayleigh viscous damping of 2%, according to Ceccotti [4.29].

Results are reported in Table 4.9 in terms of average and 5th percentile of q_0 -factor ($q_{0.05}$) computed according to EN 1990 [4.32]. The obtained average q_0 -factor was 5.42, confirming the good dissipative capability of the tested system. $q_{0.05}$ value, equal to 4.62, could be used as conservative estimation of the intrinsic q -factor.

Table 4.9 – Obtained PGA_u and q_0 -factor values.

SEISMIC SIGNALS	PGA_u [g]	q_0 -factor [-]
EARTHQUAKE 1	1.10	5.2
EARTHQUAKE 2	1.15	5.5
EARTHQUAKE 3	1.15	5.5
EARTHQUAKE 4	1.10	5.2
EARTHQUAKE 5	1.30	6.2
EARTHQUAKE 6	1.05	5.0
EARTHQUAKE 7	1.20	5.7
EARTHQUAKE 8	1.05	5.0
AVERAGE	1.14	5.4
5th PERCENTILE	0.97	4.6

4.4 Conclusions

In this chapter, three innovative shear-wall systems have been presented, as alternative to more common CLT or light-frame systems.

Quasi-static cyclic-loading tests represent an essential step in the investigation of the static and seismic behaviour of newly developed wooden wall systems. Test results permit to define the main mechanical characteristics of the wall and ensure a proper calibration of the non-linear numerical model suitable to study the seismic behaviour of the shear-wall systems in terms of q_0 -factor and PGA_u . A proper choice of the yielding and of the failure limit ensures a reliable estimation of the intrinsic q -factor of the examined system. Moreover, by imposing the experimental yielding limit equal to the design condition (i.e., $PGA_d = PGA_y$), the design over-strength effects are avoided.

Results show that wall systems characterized by shear deformability are more efficient in terms of q_0 -factor than systems with rigid wooden panel. In the studied massive shear walls, the shear behaviour is due to staple deformation or deformation of timber inserts. In the hybrid system, this deformability is mainly guaranteed by the ductile fasteners used to connect skin and OSB panel to the frame. Conversely, for systems with low displacement capacity due to very stiff wooden panels, vertical joints can be introduced to subdivide the walls into narrow panels improving the ductility and energy dissipation capacity.

Another aspect here evidenced is the importance of adopting a rigorous capacity design approach. In detail, in system with rigid wooden panels, base connections and vertical joints should be the weakest component of the structure. Conversely, in light-frame systems all base connections and all brittle components (timber and plastic) must be over-resistant than the bracing system and the nails at vertical joints, which are the most ductile and dissipative components of the shear wall.

Results in terms of intrinsic behaviour factor for the two novel massive shear walls tested, show an improved dissipative capacity with respect to CLT walls, whose seismic response has been in depth studied in the previous chapters. This improvement has been obtained also for the light steel-timber frame tested, with respect to the traditional platform-frame system. In recent works concerning light timber-frame buildings values of q -factor equal to 2.5 [4.44] or in the range between 2.5 and 4.5 [4.45] were obtained. The innovative system here investigated assures higher values of q -factor due to the presence of staples and additional fasteners (skin-to-frame screws and frame-to-column nails), which diffusely yield, providing high ductility and dissipation capacity to the system.

The main conclusions are therefore that an intrinsic q -factor up to 3 can be used for the seismic design of massive shear walls with rigid wooden panel ($q \leq 2.5$ for un-jointed CLT wall and $q \leq 3$ for jointed CLT wall). Otherwise, an intrinsic q -factor of 4 is suitable for wall systems with deformable panel ($q \leq 4$ for both stapled and layered massive walls and $q \leq 4.5$ for the novel light-frame system). Such values are consistent only if a rigorous capacity design method is applied and should be modified using suitable design over-strength factors taking into account the design approach, the calculation methods and code guidelines.

Acknowledgments

Lignaconstruct, Soligno, TIS Innovation Park and CNR-IVALSA are acknowledged for the experimental results on stapled and layered walls, presented in section 4.2.

Polifar S.r.l. and Dese Stampi are acknowledged for the experimental results on the mixed steel-timber hybrid system and on skin, presented in section 4.3.

References – Chapter 4

- [4.1] Schädle P., and Blaß, H.J. (2010). "Earthquake behaviour of modern timber construction systems". In Proceedings of the 11th World Conference on Timber Engineering WCTE, Riva del Garda, Italy.

- [4.2] Bedon, C., Fragiaco, M., Amadio, C., and Battisti, A. (2014). "A buckling design approach for 'Blockhaus' timber walls under in-plane vertical loads". In Proceedings of 1st International Network on Timber Engineering Research (INTER), Bath, United Kingdom.
- [4.3] Bedon, C., Rinaldin, G., and Fragiaco, M. (2015). "Non-linear modelling of the in-plane seismic behaviour of timber *Blockhaus* log-walls". *Engineering Structures*, **91**:112-124, doi: 10.1016/j.engstruct.2015.03.002.
- [4.4] Iqbal, A., Smith, T., Pampanin, S., Fragiaco, M., Palermo, A., and Buchanan, A.H. (2015). "Experimental Performance and Structural Analysis of Plywood-Coupled LVL Walls". *Journal of Structural Engineering*, ASCE, doi: 10.1061/(ASCE)ST.1943-541X.0001383.
- [4.5] Karacabeyli, E., and Ceccotti, A. (1997). "Seismic force modification factor for design of multi-storey wood-frame platform construction". In Proceedings of the Meeting 30 of the Working Commission W18-Timber Structures, CIB, Vancouver, Canada. Paper CIB-W18/30-15-3.
- [4.6] De la Roche, I., Dangerfield, J.A., and Karacabeyli, E. (2003). "Wood Products and Sustainable Construction". *New Zealand Timber Design Journal* **12(1)**:9-13.
- [4.7] Khorasani, Y. (2011). "Feasibility study of hybrid wood steel structures". Master Thesis, Faculty of Graduate Studies, University of British Columbia, Vancouver.
- [4.8] Stiemer, S., Tesfamariam, S., Karacabeyli, E., and Propovski, M. (2012). "Development of steel-wood hybrid systems for buildings under dynamic loads". In Proceedings of the 7th International Specialty Conference on Behaviour of Steel Structures in Seismic Areas (STESSA), Santiago, Chile.
- [4.9] Dickof, C., Stiemer, S.F., Bezabeh, M.A., and Tesfamariam, S. (2014). "CLT–Steel Hybrid System: Ductility and Overstrength Values Based on Static Pushover Analysis". *J. Perform. Constr. Facil.*, doi:10.1061/(ASCE)CF.1943-5509.0000614.
- [4.10] Zhang, X., Fairhurst, M., and Tannert, T. (2015). "Ductility Estimation for a Novel Timber–Steel Hybrid System". *Journal of Structural Engineering*, ASCE, Doi: 10.1061/(ASCE)ST.1943-541X.0001296.
- [4.11] Li, Z., He, M., Lam, F., Li, M., Ma, R., and Ma, Z. (2014). "Finite element modeling and parametric analysis of timber–steel hybrid structures". *The Structural Design of Tall and Special Buildings* **23(14)**:1045-1063.
- [4.12] He, M., Li, Z., Lam, F., Ma, R., and Ma, Z. (2013). "Experimental investigation on lateral performance of timber-steel hybrid shear wall systems." *Journal of Structural Engineering*, ASCE, Doi: 10.1061/(ASCE)ST.1943-541X.0000855.
- [4.13] Uang, C., and Gatto, K. (2003). "Effects of finish materials and dynamic loading on the cyclic response of woodframe shearwalls". *Journal of Structural Engineering*, ASCE, **129(10)**:1394-1402.
- [4.14] Zisi, N. (2009). "The influence of brick veneer on racking behavior of light frame wood shear walls". Doctoral Thesis, University of Tennessee, Knoxville.
- [4.15] Zisi, N.V., and Bennett, R.M. (2010). "Shear behavior of corrugated tie connections in anchored brick veneer–wood frame wall systems". *Journal of Materials in Civil Engineering* **23(2)**:120-130.
- [4.16] Van De Lindt, J. (2004). "Evolution of wood shear wall testing, modeling, and reliability analysis: Bibliography". *Practice Periodical on Structural Design and Construction* **9(1)**:44-53.
- [4.17] Ellingwood, B.R., Rosowsky, D.V., and Pang, W. (2008). "Performance of light-frame wood residential construction subjected to earthquakes in regions of moderate seismicity". *Journal of Structural Engineering*, ASCE, **134(8)**:1353-1363.

- [4.18]Kirkham, W.J., Rakesh G., and Thomas H.M. (2013). "State of the art: Seismic behavior of wood-frame residential structures". *Journal of Structural Engineering*, ASCE, DOI: 10.1061/(ASCE)ST.1943-541X.0000861.
- [4.19]EN 12512 (2001). "Timber structures—test methods—cyclic testing of joints made with mechanical fasteners". CEN. Brussels, Belgium.
- [4.20]Pozza, L., Scotta, R., Trutalli, D., and Polastri, A. (2015). "Behaviour factor for innovative massive timber shear walls." *Bulletin of Earthquake Engineering*, 13(11):3449-3469. Springer. DOI 10.1007/s10518-015-9765-7.
- [4.21]Pozza, L., Scotta, R., Trutalli, D., Pinna, M., Polastri, A., and Bertoni, P. (2014). "Experimental and Numerical Analyses of New Massive Wooden Shear-Wall Systems." *Buildings* 4(3):355-374. MDPI. DOI: 10.3390/buildings4030355.
- [4.22]EN 338 (2009). "Structural timber—Strength classes". CEN. Brussels, Belgium.
- [4.23]EN 1998-1-1 Eurocode 8 (2004). "Design of structures for earthquake resistance, part 1: general rules, seismic actions and rules for buildings". CEN. Brussels, Belgium.
- [4.24]Muñoz, W., Mohammad, M., Salenikovich, A., and Quenneville, P. (2008). "Need for a harmonized approach for calculations of ductility of timber assemblies". In *Proceedings of Meeting 41 of the Working Commission W18-Timber Structures*, St Andrews, Canada, paper CIB-W18/41-15-1.
- [4.25]Pozza, L., Scotta, R., Polastri, A., and Ceccotti, A. (2012). "Seismic behaviour of wood-concrete frame shear-wall system and comparison with code provisions". In *Proceedings of Meeting 45 of the Working Commission W18-Timber Structures*, Växjö, Sweden.
- [4.26]"OpenSees. Open System for Earthquake Engineering Simulation" (2009). Pacific Earthquake Engineering Research Center, University of California, Berkeley. Available at <http://opensees.berkeley.edu>.
- [4.27]Lowes, L.N., and Altoontash, A. (2003). "Modeling reinforced-concrete beam-column joints subjected to cyclic loading". *Journal of Structural Engineering*, **129**:1686–1697.
- [4.28]Ceccotti, A., and Sandhaas, C. (2010). "A proposal for a standard procedure to establish the seismic behaviour factor q of timber buildings." In *proceedings of the 11th World Conference on Timber Engineering WCTE*, Riva del Garda, Italy.
- [4.29]Ceccotti, A. (2008). "New technologies for construction of medium-rise buildings in seismic regions: the XLAM case". *Structural Engineering International* **18(2)**:156-165.
- [4.30]Gelfi, P. (2012). "SIMQKE_GR", Version 2.7. University of Brescia, Italy. Available online: <http://dicata.ing.unibs.it/gelfi>.
- [4.31]Seismosoft (2013). *SeismoArtif v2.1*. (Software).
- [4.32]EN 1990 Eurocode (2002). "Basis of structural design". CEN, Brussels, Belgium.
- [4.33]Pozza, L., and Scotta, R. (2014). "Influence of wall assembly on behaviour of cross-laminated timber buildings". *Proceedings of the ICE - Structures and Buildings* **168(4)**:275-286.
- [4.34]Scotta, R., Trutalli, D., Fiorin, L., Pozza, L., Marchi, L., and De Stefani, L. (2015). "Light steel-timber frame with composite and plaster bracing panels. *Materials*, **8(11)**:7354-7370. MDPI. DOI 10.3390/ma8115386
- [4.35]Pozza, L., Scotta, R., Trutalli, D., Polastri, A., and Ceccotti, A. (2015). "Concrete-Plated Wooden

Shear Walls: Structural Details, Testing, and Seismic Characterization.” Journal of Structural Engineering. ASCE. DOI 10.1061/(ASCE)ST.1943-541X.0001289.

- [4.36]EN 300 (2006). “Oriented Strand Boards (OSB) – Definitions, classifications and specifications”. CEN, Brussels, Belgium.
- [4.37]EN 338 (2009) “Structural timber—Strength classes”. CEN, Brussels, Belgium.
- [4.38]EN ISO 898 (2013). “Mechanical properties of fasteners made of carbon steel and alloy steel - Part 1: Bolts, screws and studs with specified property classes - Coarse thread and fine pitch thread (ISO 898-1:2013)”. CEN, Brussels, Belgium.
- [4.39]EN 15480 (1999). “Hexagon washer head drilling screws with tapping screw thread”. CEN, Brussels, Belgium.
- [4.40]DIN 571. Hexagon head wood screws. 2010.
- [4.41]Foschi, R.O., and Bonac, T. (1977). “Load slip characteristic for connections with common nails”. Wood. Sci. Technol. **9(3)**:118-123.
- [4.42]Foliente, G.C. (1996). “Issues in seismic performance testing and evaluation of timber structural systems”. Proceedings of the International Timber Engineering Conference. Vol. **1**:29–36.
- [4.43]Ceccotti, A., Sandhaas, C., Okabe, M., Yasumura, M., Minowa, C. and Kawai, N. (2013). “SOFIE project – 3D shaking table test on a seven-storey full-scale cross-laminated timber building”. Earthquake Engineering & Structural Dynamics **42(13)**: 2003-2021.
- [4.44]Germano, F., Metelli, G., and Giuriani, E. (2015). “Experimental results on the role of sheathing-to-frame and base connections of a European timber framed shear wall”. Construction and Building Materials **80**:315–328.
- [4.45]Gattesco, N., and Boem, I. (2015). “Seismic performances and behavior factor of post-and-beam timber buildings braced with nailed shear walls”. Engineering Structures **100**:674–685.

Chapter 5 Conclusions and future works

The primary findings presented in this thesis lead to following conclusions that resume the original outcomes of the work.

- The design and modelling of timber shear-wall buildings must take into account correctly the deformation mechanisms that occur during earthquake and their actual stiffness and strength. These mechanisms have to be the result of elastoplastic deformations concentrated or diffused in ductile components, i.e., semi-rigid metal joints. This behaviour can be reached only applying correctly the capacity design rules and using suitable connection elements designed to deform cyclically with high ductility and reduced strength degradation.
- The design and modelling of timber shear walls can be inaccurate if proper attention is not paid to evaluate and represent the stiffness of the deformable parts of the structure. Stiffness values should be evaluated with tests, or, only if no experimental results are available, with code provisions. Moreover, assumed stiffness for ductile components has to be made consistent with their strength via an iterative design procedure. Otherwise, incorrect sizing of structural elements and/or inaccurate prediction of inter-storey drifts can occur.
- The definition of the behaviour factor as product between two sub-factors, allows to separate the contributions of intrinsic energy dissipation and design over-strength in the reduction of forces obtained from a linear analysis. The first contribution is proper of the structural system and characterizes its dissipative capacity. The second one is due to design and factored resistances assumed. This enables to classify each timber shear-wall system with its dissipative capacity without considering all external contributions to over-resistance. Furthermore, a third factor is needed to account for both plan and elevation irregularities.
- Quasi-static cyclic-loading tests are an essential step in the investigation of the static and seismic behaviour of newly developed timber wall systems. Test results permit to define the main mechanical characteristics of the wall and ensure a proper calibration of the non-linear numerical model suitable to study the seismic behaviour of the shear-wall system in terms of q_0 -factor and ultimate PGA. A proper choice of the yielding and of the failure limit

is fundamental to ensure a reliable estimation of the intrinsic q_0 -factor of the structural system.

- Timber shear-wall systems characterized by diffuse yielding and increased shear deformability of the panel are more efficient in terms of dissipative capacity than systems adopting glued rigid panels. These features can be obtained using ductile fasteners as panel-to-frame connections (in platform frame system) or as connection among layers of timber elements (in massive shear walls). For construction systems using stiff glued wooden panels (e.g., cross-laminated timber), vertical joints should be introduced to subdivide the walls into narrow panels to improve ductility and energy dissipation capacities.
- For cross-laminated timber (CLT) systems different seismic responses can be expected, depending on design, slenderness, irregularity, number of storeys, number of vertical joints and width of the panels used to assemble buildings. In detail, the dissipative capacity increases with number of connections and slenderness of the building. An analytical formulation to account for effect of subdivision into small panels and geometrical proportion of shear walls on q_0 -factor has been proposed.
- The definitions provided by Eurocode 8 for structural regularity are not adequate for CLT buildings and should be modified. In particular, the in-elevation regular CLT buildings should be characterized by an almost constant ratio between the actual storey resistance to the design forces from the analysis at each storey of the building. This means that strength, and consequently stiffness, of connections should decrease from foundation to roof in order to ensure simultaneous yielding of connections at each floor. The same definition of elevation regularity is consistent also with timber-frame buildings.
- The realization of tall CLT buildings is mainly impeded by excessive uplift forces in the hold-downs anchoring shear walls to foundations. Up-lift forces can be properly reduced with adoption of higher behaviour factor values but this makes DLS verifications more significant, in particular for regular buildings.
- Plastic slabs infilled with plaster jointed to the frame with ductile fasteners can be used as additional bracing in innovative platform-frame system, coupled with standard timber panels. If correctly designed and conceived, bracing plastic slabs improve both the resistance to lateral loads and dissipative capacity of the basic system, without particular increase of the weight of the structure. This innovative skin also provides other advantages to the structure, as acoustic insulation properties and a natural ventilation of the façade useful to improve lifetime of timber components.

Future works may extend these researches and provide additional information on the seismic response of timber shear-wall systems. In particular, the study of the seismic behaviour of CLT systems in function of the several construction variables can be further extended. Moreover, the implementation of three-dimensional numerical models would allow to evaluate the response of in-plan irregular buildings.

Future studies could also be planned to compare the innovative systems studied in this work with other shear-wall systems and to propose analytical methods to compute the lateral load resistance.

The numerical simulations may be extended also to other case-study buildings varying geometry, number of storeys and slenderness.

The research on high-rise CLT buildings could be continued performing non-linear analyses on different case-study buildings. Furthermore, it is necessary to focus attention on development of special high-capacity anchoring systems for CLT walls or techniques to decrease the high up-lift forces at the base.

Finally, the study of the suitable design over-strength value for traditional or novel timber shear-wall systems is of great importance to correlate clearly the behaviour factor value with the applied design code and analytical method to compute the resistance of the system. Other studies could also emphasize the correlation between the behaviour factor and a correctly applied capacity design method.

List of Figures

Fig. 1.1 – 5-storey pagoda in Horyu-ji Temple (Japan). [1.7].....	2
Fig. 1.2 – Typical hysteresis behaviour of a connection with metal fasteners. [1.12].....	3
Fig. 1.3 – Comparison between residential buildings in 1999 in millions of m ³ . [1.13].....	3
Fig. 1.4 – Log-house system. (a) Example of building [1.14]; (b) assembly of orthogonal walls [1.15].....	4
Fig. 1.5 – Cross-laminated timber system. (a) Example of building [1.16]; (b) cross-lamination technique [1.17].....	4
Fig. 1.6 – Platform-frame system. (a) Example of building [1.18]; (b) bracing of light frame [1-19].....	5
Fig. 1.7 – Quasi-static tests according to EN 12512 [1.22]. (a) Setup of a test of a connection element for CLT structures [1.23]; (b) setup of a test on a timber structural system [1.24].....	6
Fig. 1.1 – Example of brittle failures in timber shear-wall systems. (a) Failure of bracing panel in light-frame system [1.3]; (b) brittle failure of an hold-down and an angle bracket in CLT system [1.4]; (c) failure of timber lintel in CLT system [1.5].	12
Fig. 1.2 – Definition of capacity design and over-strength factor.	13
Fig. 1.3 – Deformability of a timber shear wall.	14
Fig. 1.4 – Iterative scheme for the seismic design of connection elements.	15
Fig. 1.5 – Seismic-design procedure for timber shear-wall buildings based on linear modelling.	16
Fig. 1.6 – Estimation of connection stiffness from cyclic tests of single elements [1.25].	17
Fig. 1.7 – Table 7.1 of Eurocode 5 [1.26]. Slip modulus k_{ser} per shear plane per fastener in N/mm in timber-to-timber and wood-based panel-to-timber connections.	17
Fig. 1.8 – Numerical models of timber shear walls: (a) diffused non-linearity; (b) modelling for components (suitable for stiff panels as CLT); (c) modelling for components (suitable for deformable panels as light-frame system).	18
Fig. 1.9 – Other strategies to model the in-plane behaviour of a timber wall: (a) linear shell elements [1.25]; (b) rotational springs [1.28]; (c) diffused springs [1.21].	19
Fig. 1.10 – Example of a CLT building: connections designed with over-strength, which can be modelled as rigid [1.16].	20
Fig. 1.11 – Examples of linear FE models of CLT buildings. (a) 5-storey building with vertical joints; (b) 5-storey building without vertical joints [1.25].	20
Fig. 1.12 – Table 8.1 of Eurocode 8 [1.15]. Behaviour factor values for timber structures.	21
Fig. 1.13 – (a) Bi-linearization of envelope curve and estimation of q_0 ; (b) bi-linearization of envelope curve and estimation of Ω and q . [1.45]	23
Fig. 1.14 – Definition of q-factor.	23
Fig. 2.1 - Shake-table tests: (a)(b) SOFIE project [2.14][2.17] and (c) Timber Buildings project [2.26].....	29
Fig. 2.2 - Traditional connections for CLT structures: (a) angle brackets loaded in shear; (b) hold-down loaded in tension; (c) panel-to-panel vertical joint loaded in shear. [2.42]	30
Fig. 2.3 - Innovative connections for CLT structures: (a) [2.44]; (b) [2.46]; (c) [2.48].	30

Fig. 2.4 – Geometric arrangement, hysteresis cycles, and envelope and bilinear curves of specimens: (a) A-1; (b) A-2; (c) B-1; (d) B-2; (e) C. [2.51].....	34
Fig. 2.5 – (a) Specimen A-1: large deformation of angle brackets, lateral yielding of hold-downs; (b) Specimen A-2: major deformation concentrated at hold-downs, and deformation of angle brackets; (c) Specimen B-1: predominant sliding and uplift of wall; (d) Specimen B-2: sliding, uplift and relative displacement of CLT plates; (e) Specimen C: pull-out of screws and nails missing due to shear failure. [2.51]	36
Fig. 2.6 - Definition and calculation of shear resistance F_A and uplift resistance F_{HD} . [2.51]	37
Fig. 2.7 – Results in terms of q , q_0 and Ω	40
Fig. 2.8 – Calibration process adopted for modelling of the CLT shear walls.	43
Fig. 2.9 – Top displacement vs. lateral force: (a) Wall A-1; (b) wall A-2; (c) wall B-2.	44
Fig. 2.10 – Calibration of non-linear springs: (a) angle bracket loaded in shear; (b) hold-down loaded in shear; (c) hold-down loaded in tension; (d) angle bracket loaded in tension. (Tests: [2.30];[2.34]).....	45
Fig. 2.11 – Comparison of the two modelling strategies: (a) tested specimen; (b) phenomenological model; (c) detailed model.	45
Fig. 2.12 – Simulation of test on case-study wall: (a) phenomenological model; (b) detailed model.....	46
Fig. 2.13 – Simulation of test on case-study wall with detailed model: (a) hold-down shear resistance neglected; (b) angle-bracket tension resistance neglected.	47
Fig. 2.14 – Assembling of large horizontal panels [2.63]: (a) façade panel; (b) floor.	50
Fig. 2.15 – Assembling of small jointed panels [2.64].	50
Fig. 2.16 –Scheme of numerical model for case-study A3H.	53
Fig. 2.17 – Comparison of results from NLSA and NLDA for building configuration A3M.	54
Fig. 2.18 – Obtained q_0 -factor values and normal distribution of results.	54
Fig. 2.19 – Definition of actual (left) and reference (right) joint indexes.	56
Fig. 2.20 – Histograms and normal distributions of q_0 -factors for two ranges of slenderness.	58
Fig. 2.21 – Histograms and normal distributions of q_0 -factors for three ranges of β	58
Fig. 2.22 – Abacus representations for q_0 -factor estimation: (a) first formulation; (b) second formulation.	59
Fig. 2.23 – Comparison between average numerical results and analytical prediction with scatter plots: (a) first formulation; (b) second formulation.	60
Fig. 2.24 – Comparison among average numerical results and analytical prediction with residual plots: (a) first formulation; (b) second formulation.	60
Fig. 2.25 – Abacus representation for the approximate formulation.....	61
Fig. 2.26 – NEES-Soft project. Collapse of a wood-frame building due to “soft-storey” mechanism. [2.71]...	62
Fig. 2.27 – Consequences of structural regularity in seismic analysis and design [2.50].	62
Fig. 2.28 – Normal distribution of obtained k_R coefficients.	66
Fig. 2.29 – Normal distribution of obtained k_R coefficients, grouped according to vertical joint density.....	66
Fig. 3.1 – (a) Murray Grove, 9 storeys, London, 2009 ([3.15];[3.16]). (b) Bridport House, 8 storeys, London, 2011 [3.17].	74
Fig. 3.2 – Forte Living, 10 storeys, Melbourne, 2012 ([3.18];[3.19]).....	75
Fig. 3.3 – Cenni di cambiamento, 9 storeys, Milano, 2013 ([3.19];[3.20]).	75
Fig. 3.4 – High-strength IVALSA hold-downs [3.21].	76
Fig. 3.5 – Modelled case-study buildings [3.9].	78
Fig. 3.6 – Numerical models of case-study buildings (3B, 5B and 8B).	79
Fig. 3.7 – Main numerical results and comparisons.	81
Fig. 3.8 – Comparison between results obtained with q -factor from code and from proposed formulation. ...	83
Fig. 4.1 – (a) Stapled wall; (b) layered wall. [4.20]	92
Fig. 4.2 – Deformation of connections and panels: (a) stapled wall; (b) layered wall. [4.20]	93
Fig. 4.3 – Recorded hysteresis cycles and evaluation of yielding points: (a) un-jointed CLT; (b) jointed CLT; (c) stapled wall; (d) layered wall. [4.20]	94
Fig. 4.4 – Calibration of the models: fitting of experimental hysteresis cycles and dissipated energy comparison: (a) glued CLT A.2 wall; (b) glued CLT C wall; (c) stapled wall, (d) layered wall.....	97
Fig. 4.5 – PGA_y values for the specimens for the three levels of drift: comparison and trend.	98
Fig. 4.6 – Mean PGA_u values: comparison and trend.	99
Fig. 4.7 – Obtained q_0 -factor values: (a) drift 40 mm; (b) drift 60 mm; (c) drift 80 mm.....	100

Fig. 4.8 – Mean values and standard deviation of q_0 -factors: (a) comparison of mean q_0 ; (b) comparison of characteristic $q_{0,0.05}$; (c) un-jointed CLT wall; (d) jointed CLT wall; (e) stapled wall; (f) layered wall. 101

Fig. 4.9 – View of the modular shear wall (dimensions in cm). 104

Fig. 4.10 – Skin: (a) geometry; (b) front view; (c) front-view detail; (d) back-view detail. 105

Fig. 4.11 – Steel columns and brackets: (a) geometric details of connection with foundation; (b) view of the modular walls assembled; (c) detail of connection with the foundation; (d) detail of connection with the floor. 106

Fig. 4.12 – Wall section: (from left to right) skin, OSB panel, timber stud, steel column. 106

Fig. 4.13 – Test setup: (a) front view; (b) side view. 107

Fig. 4.14 – Experimental setup: (a) external view; (b) inner view. 108

Fig. 4.15 – Yielding of the 10x120 mm screws connecting skin to frame (single plastic hinge). 108

Fig. 4.16 – Hysteresis curves: (a) wall A; (b) wall B. 109

Fig. 4.17 – Wall configurations at the end of the cyclic loading tests: (a) wall A; (b) wall B. 109

Fig. 4.18 – Hysteresis cycles of shear wall: (a) top displacement vs. lateral force; (b) displacement at hold-down vs. lateral force; (c) relative displacement at vertical joint vs. lateral force. 111

Fig. 4.19 – Energy comparison: (a) accumulated hysteresis energy up to the end of the test; (b) dissipated energy computed for each half-cycle. 112

Fig. 4.20 – Case-study building. First-storey plan (dimensions in cm). 113

Fig. 4.21 – Case-study building. (a) View of the modelled façade; (b) numerical FE model (truss elements) superimposed on the façade: bracing system (in red); vertical joints (in green); base and inter-storey connections (in blue). 113

List of Tables

Table I.1 – Effectiveness of the use of timber, comparison with traditional materials (data from [I.1]).....	1
Table 1.1 – Modelling strategies for complete building superstructures.	20
Table 2.1 - Type and number of wall connectors. (see also [2.35];[2.51])	34
Table 2.2 - Design values of lateral load resistance F_d . [2.51]	39
Table 2.3 - Results of analysis of test data to obtain q_0 and Ω , based on $F_{d,nail} = 2.22$ kN. [2.51].....	39
Table 2.4 - Dependence of q-factor on $F_{d,nail}$. [2.51].....	41
Table 2.5 – $q_{0,i}$ values from numerical analysis.....	48
Table 2.6 – Summary of results from numerical analysis.....	49
Table 2.7 – Building configurations studied.....	51
Table 2.8 – Obtained q_0 -factor values for case-study building with $B=17.50$ m.....	54
Table 2.9 – Obtained q_0 -factor values for case-study building with $B=8.75$ m.....	55
Table 2.10 – Indexes and q_0 -factor values for buildings with $B=17.50$ m.....	57
Table 2.11 – Indexes and q_0 -factor values for buildings with $B=8.75$ m.....	57
Table 2.12 – Obtained k_R coefficients for case-study building with $B=17.50$ m.	65
Table 2.13 – Obtained k_R coefficients for case-study building with $B=8.75$ m.	65
Table 3.1 – Scheme of the studied configurations.	77
Table 3.2 – Design spectra for L'Aquila (Italy) according to Italian Regulation [3.35].....	78
Table 3.3 – Analytical and experimental values of connection stiffness [3.9].	80
Table 3.4 – Computation of q-factor according to equation (2.10).	82
Table 4.1 – Scheme of the studied configurations. [4.20]	92
Table 4.2 – Analytical evaluation of test parameters for imposed ultimate displacement of 40 mm. [4.20]....	94
Table 4.3 – Analytical evaluation of test parameters for imposed ultimate displacement of 60 mm. [4.20]....	95
Table 4.4 – Analytical evaluation of test parameters for imposed ultimate displacement of 80 mm. [4.20]....	95
Table 4.5 – 1 st mode periods and results in terms of q_0 -factor values.	100
Table 4.6 – Comparison between analytical and numerical q_0 -factors for un-jointed and jointed CLT walls.	102
Table 4.7 – Test results and interpretation.	110
Table 4.8 – Strength degradations and equivalent viscous damping at each cycle amplitude.....	110
Table 4.9 – Obtained PGA_u and q_0 -factor values.	114

List of Publications

International journals

Pozza, L., Scotta, R., Trutalli, D., Polastri, A., and Smith, I. (2016). "Experimentally based q-factor estimation of cross-laminated timber walls." Proceedings of the Institution of Civil Engineers - Structures and Buildings. DOI: 10.1680/jstbu.15.00009. Available online: <http://dx.doi.org/10.1680/jstbu.15.00009>.

Scotta, R., Trutalli, D., Fiorin, L., Pozza, L., Marchi, L., and De Stefani, L. (2015). "Light steel-timber frame with composite and plaster bracing panels". Materials, **8(11)**:7354-7370. MDPI. DOI 10.3390/ma8115386. Available online: <http://dx.doi.org/10.3390/ma8115386>.

Pozza, L., Scotta, R., Trutalli, D., and Polastri, A. (2015). "Behaviour factor for innovative massive timber shear walls." Bulletin of Earthquake Engineering, **13(11)**:3449-3469. Springer. DOI 10.1007/s10518-015-9765-7. Available online: <http://dx.doi.org/10.1007/s10518-015-9765-7>.

Pozza, L., Scotta, R., Trutalli, D., Polastri, A., and Ceccotti, A. (2015). "Concrete-Plated Wooden Shear Walls: Structural Details, Testing, and Seismic Characterization." Journal of Structural Engineering. ASCE. DOI 10.1061/(ASCE)ST.1943-541X.0001289. Available online: [http://dx.doi.org/10.1061/\(ASCE\)ST.1943-541X.0001289](http://dx.doi.org/10.1061/(ASCE)ST.1943-541X.0001289).

Pozza, L., Scotta, R., Trutalli, D., Pinna, M., Polastri, A., and Bertoni, P. (2014). "Experimental and Numerical Analyses of New Massive Wooden Shear-Wall Systems." Buildings **4(3)**:355-374. MDPI. DOI: 10.3390/buildings4030355. Available online: <http://dx.doi.org/10.3390/buildings4030355>.

Conference proceedings

Scotta, R., Pozza, L., Trutalli, D., Marchi, L. and Ceccotti, A. (2015). "Dissipative connections for squat or scarcely jointed CLT buildings. Experimental tests and numerical validation." In proceedings of International Network on Timber Engineering Research (INTER), meeting 2015, 24-27 August, Šibenik, Croatia.

Marchi, L., Pozza, L., Scotta, R., and Trutalli, D. (2015). "Design and testing of a dissipative connection for XLam buildings." In proceedings of XVI ANIDIS, 13-17 September 2015, L'Aquila, Italy.

De Stefani, L., Fiorin, L., Marchi, L., Pozza, L., Scotta, R., and Trutalli, D. (2015). "Seismic characterization of steel-timber shear walls with innovative bracing system." In proceedings of XVI ANIDIS, 13-17 September 2015, L'Aquila, Italy.

Pozza, L., Scotta, R., Trutalli, D., Polastri, A., and Ceccotti, A. (2014). "Effects of design criteria on an experimentally-based evaluation of the behaviour factor of novel massive wooden shear walls." In proceedings of International Network on Timber Engineering Research (INTER), meeting 2014, 01-04 September, Bath, United Kingdom.

Polastri, A., Pozza, L., Trutalli, D., Scotta, R., and Smith, I. (2014). "Structural characterization of multi-storey buildings with CLT cores." In proceedings of the World Conference on Timber Engineering (WCTE), 10-14 August 2014, Quebec City, Canada.

Pozza, L., Scotta, R., Trutalli, D., Ceccotti, A., and Polastri, A. (2013). "Analytical formulation based on extensive numerical simulations of behavior factor q for CLT buildings." In proceedings of meeting 46 of the Working Commission W18-Timber Structures, CIB, 26-29 August 2013, Vancouver, Canada. Paper CIB-W18/46-15-5.

Pozza, L., Trutalli, D., Polastri, A., and Ceccotti, A. (2013). "Seismic design of CLT buildings: definition of the suitable q -factor by numerical and experimental procedures." In proceedings of the Second International Conference ICSEA, 24-26 July, Guimaraes, Portugal. Structures and Architecture **9**:90–97. Print ISBN: 978-0-415-66195-9, DOI: 10.1201/b15267-13. Available online: <http://dx.doi.org/10.1201/b15267-13>.

Pozza, L., Trutalli, D., Scotta, R., Polastri, A., and Ceccotti, A. (2013). "Proposal of an analytical-experimental procedure for determining the q -factor of timber building systems." In proceedings of XV ANIDIS, 30 June – 04 July 2013, Padova, Italy.